



UNIVERSITÀ DEGLI STUDI DI MILANO

Ph.D. GRADUATE SCHOOL IN
Land, Environment and Biodiversity

DEPARTMENT OF
*Agricultural and Environmental Science – Production, Landscape and
Agroenergy*

COURSE IN
Agricultural Ecology – cycle XXVIII

The interplay between photorespiration and iron deficiency

DISCIPLINARY SCIENTIFIC FIELD
- AGR/13 -

DOCTORAL CANDIDATE
Fabio Marco Casiraghi

DOCTORAL ADVISOR
Prof. Graziano Zocchi

Ph.D. SCHOOL COORDINATOR
Prof. Graziano Zocchi

A.A. 2015-2016

Activities carried out during the three-year Ph.D.

Common Courses of the Ph.D. Graduate School *Land, Environment and Biodiversity*

- **Microscopy School** – prof. Franco Faoro – Dr. Marco Saracchi – Università degli Studi di Milano 16, 17, 18 April 2013
- **Corso online “formazione generale dei lavoratori”** – sicurezza sul lavoro, Università degli Studi di Milano, 22 October 2013

International Ph.D. School

- **BIONUT - International Ph.D. Summer school “Biochemical and Genetic dissection of control of plant mineral nutrition**
Università degli Studi di Milano – Gargnano (BS) 23-27 June 2012
- **International Ph.D. winter school, Rhizosphere at work: soil-plant-microbes interactions, from plant nutrition to soil remediation.** Società Italiana di Chimica Agraria, Piacenza, Italy 17-20 February 2014
- **International Ph.D. winter school, Feeding the world: the contribution of research in agricultural chemistry to sustainable development Soil, plant and biomasses in a changing environment** Società Italiana di Chimica Agraria, Piacenza (PC) 9-12 February 2015

Scientific experience in National Research Institutions

- Dipartimento di Scienze Agrarie, Alimentari e Agro-ambientali - Università di Pisa – Pisa. *In vivo* determination of chlorophyll fluorescence, gas exchange measurements, *in vivo* determination of photorespiration- April/May - September 2015

Scientific experience in International Research Institutions

- Consejo Superior de Investigaciones Científicas (EEAD-CSIC) - Estación Experimental de Aula Dei -Zaragoza, Spain. Proteomic characterization of peroxisome and mitochondria- June-July - September 2015.

National Congress

- XXXII Convegno Nazionale - Società Italiana di Chimica Agraria – “Il potenziale biologico del sistema pianta-microrganismi-suolo come chiave della sostenibilità e qualità delle produzioni” - Libera Università di Bolzano – Bolzano 7-9 September 2014

International Congress

- FISV 2014 XIV Congress Università di Pisa – Pisa, 24-27 September 2014

International Publications (ISI)

Vigani G., Bashir K., Ishimaru Y., Lehmann M., **Casiraghi F.M.**, Nakanishi H., Seki M., Geigenberger P., Zocchi G. and Nishizawa N.K.; Knocking down Mitochondrial Iron Transporter (MIT) reprograms primary and secondary metabolism in rice plants, manuscript accepted, Journal of Experimental Botany.

National and International poster presentation

- **F.M. Casiraghi**, G. Vigani, K. Bashir, Y. Ishimaru, L. Tato, H. Nakanishi, N.K. Nishizawa and G. Zocchi; Metabolic reprogramming of rice mutant plants knocking-down in the Mitochondrial Iron Transporter (MIT) expression; International Ph.D. winter school, Piacenza, Italy 17-20 February 2014

- **F.M. Casiraghi** and G. Zocchi, The interplay between photorespiration and iron deficiency: a preliminary study in *Cucumis sativus* L.; International Ph.D. winter school, Società Italiana di Chimica Agraria, Piacenza (PC) 9-12 February 2015
- **F.M. Casiraghi** and G. Zocchi, The interplay between photorespiration and iron deficiency: a preliminary investigation; FISV 2014 XIV Congress Università di Pisa – Pisa, 24-27 September 2014
- **F.M. Casiraghi** and G. Zocchi, Studio degli effetti della carenza di ferro sull'attività foto respiratoria; XXXII Convegno Nazionale - Società Italiana di Chimica Agraria – Bolzano 7-9 September 2014

National and international oral presentation

- **F.M. Casiraghi**, G. Vigani, K. Bashir, Y. Ishimaru, L. Tato, H. Nakanishi, N.K. Nishizawa and G. Zocchi; Metabolic reprogramming of rice mutant plants knocking-down in the Mitochondrial Iron Transporter (MIT) expression; International Ph.D. winter school, Piacenza, Italy 20 February 2014
- **F.M. Casiraghi**, G. Zocchi. The interplay between photorespiration and iron deficiency, a preliminary investigation; Estacion Experimental De Aula Dei – CSIC - Zaragoza, Monday, 29 th June 2015

Seminar presentation on progress research activity during Ph.D.

- L'effetto della Fe-carenza sull'efficienza dei processi fotosintetici – Università degli Studi di Milano – 27-Nov-13
- L'effetto della Fe-carenza sull'efficienza dei processi fotosintetici – Università degli Studi di Milano – 27-Nov-14

- The interplay between photorespiration and iron deficiency: a preliminary investigation – Università degli Studi di Milano – 22 Oct 2015

Participation to Seminars

- *Application of molecular techniques to study accumulation of health promoting compounds in fruits* - Prof. Laura Jaakola - Department of Arctic and Marine Biology, University of Tromsø - Università degli studi di Milano 23-Jan-13
- *Genetic dissection of peach fruit quality traits* – Dr. Raul Pirona – Plant Genomics Group, Parco Tecnologico Padano -Università degli studi di Milano 27-Feb-13
- *Photoperiodical flowering in rice* - Università degli studi di Milano 06-mar-13
- *The importance of rhizosphere in a changing environment* - Prof. George Gobran – Swedish University of Agricultural Sciences - Università degli studi di Milano 29-Apr-13
- *Assessment of Genetic Diversity among Portuguese Grapevine*- Prof. I. Castro - Università degli studi di Milano 15-Jan-14
- *Imaging and Cytometry Tools for Cell Structure and Function analysis – practical session “bring your samples and try EVOS cell imaging systems* – Workshop -Università degli Studi di Milano 23-May-14
- *Structure and function of voltage-gated proton channels*, Università degli Studi di Milano 03-Jun-14
- *Domesticating unicellular algae for increase light use efficiency towards biofuel production* Prof. Roberto Bassi – Dipartimento di Biotecnologie Università di Verona – Università degli Studi di Milano – 04-Jun-14
- *Microscale thermophoresis workshop (some like it hot: biomolecule analytics using microscale thermophoresis)* Università degli Studi di Milano, 11-Jun-14
- *Paddy field agriculture and water conservation: monitoring and SWAT model application* – Università degli Studi di Milano 20-Jun-2014

- *Current status of Grapevine phytoplasmas in vineyards in Turkey* – Università degli Studi di Milano – 8-Jul-14
- *A mechanism of DNA double-strand break repair mediated by transcript RNA* – Università degli Studi di Milano – 16-Dec-14
- *Sustainability of food supply chains* Università degli Studi di Milano 16-Dec-14
- *Physiological and molecular basis of plant responses to mineral stress: from acid to calcareous soils* Prof. Miroslav Nikolic University of Belgrade – Università di Bologna – Alma mater studiorum- Dipartimento di Scienze Agrarie – 15-Jan-15.
- *The role of silicon on nutrient utilization by crops under stressful environment.* Prof. Miroslav Nikolic University of Belgrade – Università di Bologna – Alma mater studiorum- Dipartimento di Scienze Agrarie- 15-Jan-15.
- *The agriculture of tomorrow. Growing with less – the research activities of the Volcani center.* Prof J. Kalpunik Volcani Centre – Israel – Università degli Studi di Milano – 24 Feb-15
- *The science behind feeding the world healthily: the ultimate gxe challenge* (Workshop cost action FA1106) – Polo didattico Zanutto – Università degli Studi di Verona

Teaching activity

- 2013, October (4 hours): General Biology Course -Agricultural Faculty - Università degli Studi di Milano
- 2014, October (4 hours): General Biology Course - Agricultural Faculty - Università degli Studi di Milano
- 2015 October (4 hours): General Biology Course -Agricultural Faculty - Università degli Studi di Milano

M.Sc. Fabio Marco Casiraghi attended the three year PhD studies with diligence, perseverance and responsibility. He has shown great interest in the topics addressed demonstrating ability in critical analysis towards the issues faced during the research activities. He has acquired a very good knowledge of the eco-physiological basis inherent the issue studied as well as the physiological and biochemical techniques for their study. He has independently set collaborations with other research groups in order to investigate specific aspects of the research, thus acquiring new analytical techniques. He spent a short period at the Dipartimento di Scienze Agrarie, Alimentari e Agro-ambientali – Università di Pisa – Italy under the supervision of Prof. Lucia Guidi applying the *in vivo* determination of chloropyll fluorescence, gas exchange measurements and *in vivo* determination of photorespiration and abroad at the Consejo Superior de Investigaciones Científicas (EEAD-CSIC) - Estación Experimental de Aula Dei, Zaragoza (ES) under the supervision of Dr. Javier Abadia, where he try to perform the Proteomic characterization of peroxisome and mitochondria. Therefore I express an excellent opinion regarding the work carried out by Fabio Marco Casiraghi.

to my parents, who give me my roots

to Maria Grazia, who give me my wings...

ABSTRACT

Iron (Fe) is an essential micronutrient for plants as it takes part in major metabolic pathways such as photosynthesis and respiration and is linked to many enzymes that accomplish many other cellular functions (DNA synthesis, nitrogen fixation, hormone production). Fe deficiency reduces crop yields worldwide but particularly in plants grown on calcareous soils, which represent almost the 30% of the earth land surface. In the near future to cope with the increasing demand of food caused by a strong increase in world's population (FAO estimates in 9 billion people by 2050), agriculture must be extended to marginal areas, many of which include calcareous soils.

The most evident effect of Fe deficiency in plant leaves is a marked chlorosis caused by a decrease in chlorophyll biosynthesis, which may result in a reduction in CO₂ assimilation rate. In these conditions leaves have low photosynthetic activity but they absorb more light energy per chlorophyll molecule than required for photosynthesis, especially under high radiation. This results in a high risk for photoinhibitory and photooxidative damages in Fe-deficient leaves. The photorespiratory cycle can be considered in these circumstances as an energy dissipating cycle, operating between chloroplasts, peroxisomes, mitochondria and cytosol, which helps to protect chloroplasts from photoinhibition and plants from excessive accumulation of reactive oxygen species.

We suggest that Fe deficiency leads to a strong impairment of the photosynthetic apparatus at different levels: an increase in the rate of CO₂ assimilation in many biological repetition (+29%) was observed, suggesting a possible induction of photorespiratory metabolism. However, the variation was not significant and so further analysis must be required in order to reduce the variability among the repetition to get more reliable results. In addition, the reduction of CO₂ assimilation can be also attributable to a reduced stomatal conductance or to a mesophyll-reduced utilization of CO₂.

Iron deficiency affects also amino acid (aa) metabolism since the concentration of Ser and Gly, two aa involved in the photorespiratory metabolism, increased in leaves (+94% and +160%, respectively). Resupply of iron to Fe-deficient plants led to an increase in the concentration of some divalent cations other than Fe like Ca and Mn, whilst Na, Mg, Cu, Zn decrease as Fe sufficient condition are restored. On the other hand, as Fe deficiency proceeds during time, we observed a significant increase in Na, Mg, Zn, Mn content. These alterations suggest that Fe deficiency induces a metabolic imbalance in which other divalent cations are absorbed by unspecific transporter, due to their similar characteristics to Fe.

Under our experimental conditions, ROS accumulation detected in cucumber plants

grown in the absence of Fe could be attributable to an increase in the activity of enzymes involved in their formation or to a reduced detoxification. We observed a slight induction in the activity of Cu/Zn-SOD isoform whereas a reduction in Fe- and also in Mn-SOD isoforms activity was also recorded. At the same time, the concentration of H₂O₂ in the leaves of Fe-deficient plants was significantly higher (+40%). This overproduction could lead to an onset of oxidative stress which can lead to further cell damage at different levels also with the involvement of the photosynthetic apparatus. Fe deficiency also induces alterations in peroxisomes at different levels indicating modifications in the photorespiratory metabolism. The complete lack of Fe results in a strong inhibition of catalase activity (-35%). Nevertheless, we detect higher levels of catalase in Fe-deficient plants compared to the control condition. In Fe-sufficient condition the total activity of hydroxypyruvate reductase was fully attributable to the peroxisomal isoform (HPR1), while we recorded an equal distribution of the activity between the two isoforms, peroxisomal and cytosolic (HPR2) in plants grown under conditions of Fe deficiency.

Moreover, the characterization of rice mutant plants defective in mitochondrial Fe importer allow us to investigate the involvement of this organelle in the photorespiratory metabolism during Fe deficiency. The partial loss of function of MIT (*mit-2*) affects the mitochondrial functionality by decreasing the respiratory chain activity. Furthermore, the transcriptome and the metabolome strongly change in rice mutant plants, in a different way in roots and shoot. Biochemical characterization of purified mitochondria from rice roots showed alteration in the respiratory chain of *mit-2* compared to wild type plants. In particular, proteins belonging to the type II alternative NAD(P)H dehydrogenases strongly accumulated in *mit-2* plants, indicating that *mit-2* mitochondria activate alternative pathways to keep the respiratory chain working.

The data obtained and exposed in this doctorate thesis, in agreement with what widely previously reported in literature, allow us to state that the absence or the low Fe bioavailability during the growth of the plants results in several alterations more or less reversible at different levels of the overall metabolic plant system.

ACKNOWLEDGMENTS

I would like to express my special appreciation and thanks to my mentor, advisor and supervisor Professor Dr. Graziano Zocchi. I would like to thank him for encouraging my research and for allowing me to grow as a research scientist. His advice on both research as well as on my career have been priceless.

I would also like to thank the members of my research group, Dr. Patrizia De Nisi, for her advice, the laughs and for the good time we spend during these years. I am totally grateful to Dr. Marta Dell'Orto for her inestimable help. She always provided me with valuable and thought-provoking opinion. I would also like to thank Dr. Silvia Donnini for her constant urge me to never give up in the face of adversity and, in particular, I would like to express my sincere thanks to Dr. Gianpiero Vigani that most of all encouraged and persuaded me to take this path three-year work. Thanks to everyone for your brilliant comments and suggestions.

I would especially thank Dr. Javier Abadía for giving me the opportunity to join his group to perform part of the work carried out during my Ph.D., Dra. Ana Álvarez-Fernández and all the people of the stress physiology lab, especially Laura Ceballos and Adrián Luis Villarroya for the help they gave me and for the time we spent together during my stay in the wonderful Zaragoza.

I would also thank Prof. Lucia Guidi and Dr. Marco Landi for their precious cooperation and hospitality.

A very special thanks to ALL my family. Words cannot express how grateful I am to Mamma e Papà: for all of the sacrifices that you've made on my behalf. Your prayer for me was what sustained me thus far. A special thank goes to my brother Davide, my sister-in-law Barbara and my niece Emma, the apple of my life.

I would also like to thank all of my friends Stacey and Luca, Simone, Lorenzo, Fabrizio, Matteo who supported me and incited me to strive towards my goals.

I would like to thank also Marino Valtorta and prof. Francesco Paoletti, for the invaluable contribute to my personal and human

growth and for their advice on my careers.

A special thanks also to Antonio, Mimma and Roberta, recently become a kind of "second" family to me . I'm really happy to be part of this.

In the end, most important, I would like express again appreciation to my beloved Maria Grazia who spent sleepless nights with me in writing this thesis and was always my support in the moments when there was no one to answer my queries.

“I have not failed. I've just found 10,000 ways that won't work.”

Thomas A. Edison

*“...And all that is now
All that is gone
All that's to come
And everything under the sun is in tune
But the sun is eclipsed by the moon”
(Pink Floyd - Eclipse - The dark side of the moon)*

TABLE OF CONTENTS

ABSTRACT	8
AKNOWLEDGEMENTS.....	10
CHAPTER I. General Background: Ecophysiology of iron plant nutrition..	17
Iron in the soil.....	23
Iron in plant physiology.....	28
Iron acquisition in dycotiledoneous plants: the Strategy I	31
Reduction of Fe(II) chelates: a pre-condition to Fe acquisition	32
Fe(II) transport inside the root cell	34
Acidification of the rhizosphere; the proton pump H ⁺ -ATPase	37
The role of the rhizosphere in Fe acquisition	43
Plant-soil interaction.....	47
Morphological changes induced by Fe deficiency	50
Iron deficiency and photosynthesis	52
Iron deficiency in crops	56
An overview on human health and dietary	60
References	62
CHAPTER II. In vivo photosynthesis performance and gas exchange alterations induced by iron deficiency in <i>Cucumis sativus</i> L. .	80
Highlights	81
Abstract	81
Introduction.....	84
Materials and methods	87
Results	93
Discussion.....	101
References	102

CHAPTER III. Iron deficiency alters the amminoacid content and the ion composition in the leaves of cucumber plants.	106
Highlights	107
Abstract	107
Introduction.....	108
Materials and methods	110
Results	112
Discussion.....	118
References	121
CHAPTER IV. Iron deficiency induces ROS accumulation in cucumber plants linked to an imbalance in the antioxidant machinery ..	124
Highlights	125
Abstract	125
Introduction.....	127
Materials and methods	138
Results	141
Discussion.....	143
References	145
CHAPTER V. Iron deficiency induces alterations in the photorespiratory peroxisome metabolism.....	154
Highlights	155
Abstract	155
Introduction.....	157
Materials and methods	173
Results	179
Discussion.....	184
References	187

CHAPTER VI

Knocking down Mitochondrial Iron Transporter (MIT) reprograms

primary and secondary metabolism in rice plants197

Highlights 198

Abstract 198

Introduction..... 199

Materials and methods202

Results206

Discussion.....216

References223

CHAPTER VII.223

APPENDIX A243

CHAPTER I

General background: Ecophysiology of plant iron nutrition

One of the greatest challenges in modern agriculture is increasing biomass production, while improving plant product quality, in a sustainable way. This requires increasing productivity and improving product quality within the confines of a changing global climate with increasing average CO₂ concentrations and temperatures. Mineral nutrients are major actors in this new scenario. They are essential both for plant productivity and for the quality of their products, and they can affect the environment through the application of fertilizers. Among minerals, iron (Fe) plays a major role in this process because it is essential for plant life and productivity, and also for the quality of production. As a transition element, Fe is characterized by the relative ease by which it may change its oxidation state:



and by its ability to form octahedral complexes with various ligands. Depending on the ligand, the redox potential of Fe(II/III) varies widely. This variability explains the importance of Fe in biological redox systems. Due to the high affinity for various ligands (e.g. organic acids or inorganic phosphate) ionic Fe³⁺ or Fe²⁺ do not play a direct role in short or long-distance transport in plants. In aerobic systems many low-molecular-weight Fe chelates, and free Fe in particular (either Fe³⁺ or Fe²⁺), produce reactive oxygen species (ROS) such as superoxide radical and hydroxyl radical (Halliwell and Gutteridge, 1986; Halliwell, 2009) and related compounds, for example:

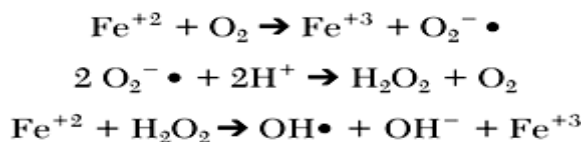


Figure 1.1. Haber-Weis-Fenton sequence. Fe(II) can react with O₂ to form hydroxyl radicals and other reactive oxygen species.

These radicals are highly toxic and responsible for peroxidation of polyunsaturated fatty acids of membrane lipids and proteins. To prevent oxidative cell damage, Fe has to be either tightly bound or incorporated into structures (e.g., heme and non-heme proteins), which allow controlled reversible oxidation–reduction reactions.

Clearly, the properties of Fe are unique and irreplaceable, and cells spend a large amount of energy to acquire Fe from the environment and handle it safely inside the cell. Due to all these reasons Fe is an essential element readily incorporated for use in biological processes where Fe ions play a key role in metabolic pathways such as DNA synthesis, nitrogen and hormone production. A wide number of cellular enzymes depend also on Fe for their biological function, (Curie and Briat, 2003; Briat et al., 2007). (Thomine and Vert, 2013). Furthermore, Fe is required for the proper functionality of the photosynthetic and the respiratory chain, which are respectively located in chloroplasts and mitochondria. These processes are responsible for the energetic support of the cell and therefore of the whole plant life. A shortage of Fe results in strong impairments of these organelles determining an energetic emergency in the cell which results in reduced growth of the entire plant and so in a lower crops yield (Vigani et al, 2012). Fe also plays an important role in the scavenging of reactive oxygen species (ROS) as a constituent of the heme moiety of antioxidant enzymes such as catalase (CAT), unspecific peroxidases (POD), and ascorbate peroxidase (APX) and as a metal cofactor of Fe-superoxide dismutase (Fe-SOD; Briat and Lobreaux, 1997).

Despite its geologic abundance (it is the second most abundant metal in the earth's crust after aluminium) Fe is

often a growth limiting factor in the environment (Quintero-Gutiérrez et al., 2008). This apparent paradox is due to the fact that in contact with oxygen Fe forms oxides, which are highly insoluble, and thus Fe is not readily available for uptake by living organisms. In aerated systems in the physiological pH range, the concentrations of ionic Fe^{3+} and Fe^{2+} are below 10^{-15} M due to formation of Fe hydroxides, oxyhydroxides and oxides (Lemanceau et al., 2007). Chelates of Fe(III) and occasionally of Fe(II) are therefore the dominant forms of soluble Fe in the soil and in the nutrient solutions. Although Fe is a ubiquitous element in neutral and well oxygenated environments it is found mostly in Fe(III) oxidized forms that have very low solubility and are not readily bioavailable for plants.

A further limitation for Fe availability occurs in calcareous soils, which account for about 30% of world-cultivated lands where Fe deficiency is a common nutritional disorder in crops. In these environments high pH decrease even more dramatically the Fe solubility. It was also reported that the presence of high levels of bicarbonate negatively affects either the FCR activity and/or IRT (Lucena et al. 2007).

As a consequence, plants have evolved two main strategies to acquire Fe: a reduction-based strategy (Strategy I) present in dicotyledonous and monocotyledonous non *poacea* plants and a chelation strategy (Strategy II) in graminaceous ones.

Strategy I plants are able to take up only Fe(II) from the soil, so they are forced to reduce Fe(III) before carrying it inside the cell. This reduction-based mechanism hand over the combined function of three plasma membrane proteins: H^+ -ATPase, Fe-chelate reductases (FCR) and Iron Regulated Transporter (IRT). Fe deficiency induces the activation of these root plasmalemma enzymes/ion transporter as well as many

other morphological and physiological responses at root level aiming at facilitate the mobilization of Fe (Schmidt, 2003; Marschner et al. 1986).

A major gap in our understanding of Strategy I has been the potential role of phenolic compounds secreted by the roots (Morrissey and Guerinot, 2009). The release of small molecules into the rhizosphere is an important component of a plant's response to fluctuations in the abiotic and biotic environment (Badri and Vivanco, 2009). Root exudates can, for instance, function as allelochemicals or alter the surrounding substrate. It is well documented that phenolic compounds including flavonoids comprise a large fraction of the root exudates of Strategy I plants under Fe deficiency (Cesco et al., 2010). They have been hypothesized to mobilize apoplastically bound Fe(III) for uptake into the symplast. Studies on red clover showed that removal of secreted phenols from the roots led to Fe deficiency of the shoot even though acidification and ferric reductase activity were enhanced (Zheng et al., 2003). These observations suggested a crucial role for secreted phenols in Fe acquisition independent of established Strategy I processes. The exact mechanisms underlying the mobilization of Fe(III) are unknown. Phenolic compounds including flavonoids have been discussed both as chelators of Fe(III) and as reductants (Cesco et al., 2009; Romheld and Marschner, 1986; Tomasi et al., 2008). Until recently, neither specific information on the activity of particular compounds nor direct genetic evidence for the importance of phenol secretion in Fe acquisition by non-graminaceous plants was available. Rodriguez-Celma et al. (2013) then showed that secretion of phenolics is critical for *A. thaliana* Fe acquisition from low bioavailable sources.

On the other hand, Strategy II is used by grasses only. It is based on the solubilization of ferric precipitates through the secretion of strong Fe(III)-chelating phytosiderophores. These molecules belong to the mugineic acid family and are released into the rhizosphere by efflux transporters such as TOM1 (Nozoye et al., 2011). Uptake of Fe(III)-phytosiderophore complexes into the symplast is mediated by YS1/YSL-transporters (Santi and Schmidt, 2009). Rice, which is a particular exception, employs both Strategy I and Strategy II (Kobayashi and Nishizawa, 2012), the efflux transporter PEZ1 was recently described as an integral component of Strategy I (Ishimaru et al., 2011). It mediates the secretion of compounds such as caffeic acid and is essential for the solubilization of apoplastic Fe oxides. Rice absorbs iron also through a ferrous iron transporter OsIRT1 and the Fe(III)-phytosiderophore based uptake using OsYSL15 (Inoue et al., 2009; Ishimaru et al., 2006; Lee et al., 2009). Rice roots however display very low ferric reductase activity (Ishimaru et al., 2009). Rice thus appear to have evolved and adapted to its growth habitat where oxygen is low due to flooding, thus favoring the existence of iron into its Fe(II) form.

Whatever is the Strategy adopted for Fe absorption, once inside the cell the accumulation of Fe(II) may catalyzes the generation of hydroxyl radicals that are potent oxidation agents resulting in oxidative damage of cellular components such as DNA and lipids. Thus, plants have to cope with this dual effect of Fe: on one hand the metal reduced form Fe(II) is essential for life, but on the other hand free Fe(II) is toxic. Therefore, to secure Fe acquisition and preventing toxicity, plants have to tightly control uptake, utilization, and storage of Fe, in a word homeostasis, in response to its environmental availability.

Furthermore, plants are the primary dietary source of Fe for

humans therefore a decrease in the amount of Fe in the agricultural products has important implications for human health. Understanding the mechanisms of Fe uptake and regulation provide useful insights for producing plants tolerant to low Fe availability and able to increase their Fe content.

Iron in the soil

Fe can exist in a wide range of oxidation states, from -2 to $+6$, but the most commons are Fe(II) (ferrous iron) and Fe(III) (ferric iron). In soils three main sources of Fe can be recognized:

- ✓ Fe contained in minerals
- ✓ Fe in soil solution
- ✓ Fe bound to organic matter.

Fe availability in soils depends on a complex relation of the above components.

In primary minerals Fe can be found mostly as ferromagnesian silicates like augite, biotite, hornblend and olivine (Schwertmann and Taylor, 1989). Those minerals release Fe(II) and Fe(III) through weathering processes of dissolution and oxidation. In the presence of atmospheric oxygen and water Fe(II) is rapidly oxidized to Fe(III). Furthermore, free Fe forms a range of oxides, hydroxides and oxyhydroxides such as ferrihydrite, goethite and hematite. Most soils are oxic environments so Fe is mainly found as Fe(III) oxides that confer to the soil typical colors varying from brown to yellow-red. Fe(III) oxides are stable and have extremely low solubility. Conversely, soluble Fe(II) oxides forms are found in anoxic and reducing environments. In an aqueous or moist environment exposed to Earth's atmosphere oxygen, Fe(II) has a half-life of several minutes as it rapidly

oxidizes to Fe(III) (Stumm and Morgan 1996).

The result of the equilibrium between dissolution and precipitation processes strictly defines Fe oxides solubility. The hydrolysis of Fe oxides is fully dependent on the solution pH. As show in figure 1.2 concentration of all Fe species at a physiological pH (6-7) is far below the amount of Fe required by plant for optimal growth that ranges from 10^{-4} to 10^{-9} M (Guerinot and Yi, 1994).

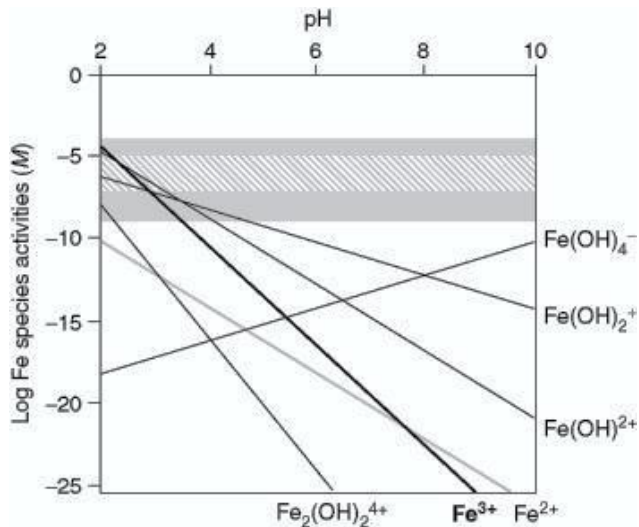


Figure 1.2. Solubility diagram of the different Fe(III) species obtained by hydrolysis an Fe oxide (goethite) as a function of pH. Black lines indicates Fe(III) species, while the grey line designates Fe(II). On the top grey bands indicates the range of concentration require for optimal growth of plants. Dashed area represents the optimal concentration for microbes. (from Robin et al., 2008)

As shown in Figure 1.2:

- Fe solubility is inversely related to the pH of the soil solution;
- total soluble Fe from different species reaches a minimum at about pH 8, a value close to that found in calcareous soils;
- for each increase in the pH value of one unit, the solubility decreases from hundred to thousand fold in most Fe form
- Fe concentration for optimal plant growth would be met at a very acidic condition (pH value of 3.5)

Many other factors as redox conditions, humic substances, mineral particle size, chelating agent's content and the presence of bicarbonate influence Fe solubility.

Under oxidizing conditions the activity of the readily available Fe(II) species are higher than the Fe(III) species at physiological pH. However, when the *redox* potential (*pe*) drops by 1 unit Fe(II) hydroxides concentration increases by two orders of magnitude. As mentioned before, the Fe species concentrations are anyway too low to supply available Fe to plants (Lindsay and Schwab, 1982). On the other hand, under reducing conditions (i.e. flooded soils), where *pe* is very low the concentration of soluble Fe(II) increases reaching high levels and becomes toxic.

The particle size of Fe minerals greatly affects its solubility: smaller is the size of the particles greater is the solubility of the Fe species. This is important because in well-oxygenated environments nanometric particle of Fe main minerals are very abundant (Cornell and Schwertmann, 2003). Moreover particle sizes strongly affect the kinetic of dissolution of Fe oxides (Schwertmann, 1991) also in the presence of organic ligands (Kraemer, 2004).

In addition, the presence of organic matter in the soil

considerably influences Fe solubility by complexation or chelation of Fe(III). Organic ligands are molecules that are able to bind to metals and form a stable complex with them. These molecules are called chelators or chelating agents while the metal complex is called chelate. Chelating agents usually originate from the activity of soil microorganisms, plants exudates and humic substance. Many organic molecules containing unsaturated bonds, oxygen, nitrogen or sulphur, are likely to play the role of chelators of transition metals. Van Hess and Lundström (2000) have reported that more than 95% of Fe in the soil solution was found to be organically bound. Compounds of very different nature act as chelating agents from low molecular weight organic compounds such as citric acid to more complex substance like polyphenols or humic acids. Chelating agents play an important role in providing available Fe for plants through increasing its mobilization and bioavailability.

Although salinity and high percentage of exchangeable Na (sodic soils) are alkaline, the soils dominated by HCO_3^- are the most alkaline ones (Läuchli and Grattan, 2012). The concentration of Fe expressed both on a dry weight leaf basis or on the amount of Fe per leaf frequently decreases in chlorotic leaves, although the Fe concentration can sometimes be the same or even higher in chlorotic leaves as compared with green ones (Fe chlorosis paradox) (Morales *et al.*, 1998; Römheld, 2000; Nikolic and Römheld, 2002).

The presence of free soil carbonate promotes the formation of poorly soluble Fe phosphates impairing so the availability of Fe. The solubilization of CaCO_3 forms in calcareous soil solution leads to a high concentration of HCO_3^- ions. It has been reported for sunflower, soybean and cucumber that addition of HCO_3^- at neutral pH could result in an inhibition of the activity of the key plasmalemma enzyme (FCR) involved

in Fe uptake (Toulon et al., 1992). On the contrary it was demonstrate that Fe reducing capacity increases when HCO_3^- was added at high pH values (Dofing et al., 1989; Romera et al., 1992). Despite contrasting findings that have been obtained for different species it is clear that between HCO_3^- and Fe uptake mechanism an interaction occurs. Thus, in calcareous soil Fe unavailability is not only due to high pH and buffering conditions but also to an interaction between HCO_3^- ion and the cell biochemistry.

In Harmsen et al. (2005) bioavailable Fe has been defined “as the portion of total Fe that can be easily assimilated by living organisms.” As mentioned above Fe bioavailability depends on many different factors that include inorganic and organic chemical processes, physical and biological processes. Furthermore, it must be taken into account that different organisms vary in their acquisition pathways and capabilities, other than usually performing strategies to inhibit the growth of other species limiting nutrient competition (allelopathy). Variation among organisms may also result in differences of the soil areas in which each organism interacts with its environment, the so-called bioinfluenced zone, thereby altering the availability of the nutrient. For plants, this bio-influenced zone typically corresponds to the rhizosphere (Harmsen et al., 2005). Soil microbial activity plays a key role in favouring plant Fe uptake. Typically soil microbes produce siderophores that is relatively small molecules that have high affinity and chelate Fe. These effective chelators increase Fe bioavailability for plants. In fact, it has been widely reported that Fe bioavailability depends on the plant/microbe mutualistic interactions.

Through root exudation plants provide a plenty of organic substances into rhizosphere that can be used by microbial communities that produce siderophores as nutrient. A quite

complex interaction settled among plants and microorganisms lies in the equilibrium between competition for Fe, since plant and microorganism need it for growing, and the improvement of Fe bioavailability (Lemanceau et al., 2009). Recent studies have suggested that in Fe deficiency treatments the number of microbes that produce siderophores increase as a result of the enhanced root exudation of phenolic compounds by the plants (Jin et al., 2007).

Iron in plant physiology

The biological importance of Fe relies on its electronic structure, which can undergo reversible changes of its oxidation state in a widespread range of redox potentials (*pe*). This aptitude confers to Fe a central role in all those biochemical reactions that comprise transfer of electrons and variations of redox potential together with binding in a reversible way many different ligands. The common biological ligands for Fe are oxygen, nitrogen and sulfur with which it forms coordination complexes. For all this features Fe is also required as cofactor of many enzymes that belong to several metabolic processes.

The major classes of Fe-containing proteins are:

- Fe-containing heme proteins: heme is a prosthetic group composed of a porphyrin ring structure with a central Fe²⁺ atom. In heme, Fe is coordinated in a tetrapyrrole ring with four nitrogen as ligands. Heme is a flat, rigid structure that is highly stable. The function of Fe in heme depends on the axial ligands perpendicular to the tetrapyrrole ring. If one axial ligand is unoccupied, Fe can bind oxygen and serve as an oxygen carrier, as in hemoglobin and myoglobin. Heme is also found in cytochromes of the respiratory and photosynthetic chains, catalases, superoxide dismutase, oxidase and peroxidases that are involved in detoxification of Reactive

Oxygen Species (ROS) (Balk and Schaedler, 2014).

- Fe-S proteins that are characterized by the presence of Fe-S clusters. In these clusters Fe is bound to S in different arrangements (Fe-S, 2Fe-2S, 4Fe-4S, 3Fe-4S) that are special redox centers. These proteins participate in various oxidation-reduction reactions. Fe-S proteins could achieve also catalytic functions (e.g. aconitase which catalyzed the transformation of citrate in isocitrate).

- Proteins for Fe storage; Ferritin is a globular nanobox protein composed, from bacteria to plants, by 24 subunit of the same type, thus they have 24 catalytic sites that concur to the formation of one or two Fe cores per molecule that can store from 2000 to 4500 atoms of Fe(III) (Arosio and Levi, 2002). It is almost ubiquitous and tightly regulated by the metal. Biochemical and structural properties of the ferritins are largely conserved from bacteria to man, although the role in the regulation of Fe trafficking varies in the different organisms (Arosio and Levi, 2002).

Fe is almost absent in its free form inside the cell as it catalyzes the generation of hydroxyl radicals that are strong oxidation agents resulting in oxidative damage of cellular components such as DNA and lipids. Thus, plants have to deal with a dual effect of Fe: on one hand the metal reduced form Fe(II) is essential for life, but on the other hand free Fe(II) is toxic. Therefore, to ensure Fe acquisition and avoiding toxicity, plants have to tightly control uptake, utilization, and storage of Fe in response to its homeostasis mechanism. Once absorbed by epidermal or cortical root cells it must be complexed with organic acids (mainly citric and malic) or with other organic molecules, which prevents Fe precipitation and avoid oxidative damages. In fact, once inside the cell, the redox capabilities of Fe can also be the basis of potential toxicity resulting from the Haber-Weiss-Fenton sequence that

leads to the generation of hydroxyl radical (OH^\bullet) subsequent to the formation of superoxide ($\text{O}_2^{\bullet-}$) following the one-electron reduction of dioxygen (O_2) by ferrous Fe. The accumulation and transport of ionic Fe is also improbable because Fe has a low solubility at physiological pH. The acquisition of Fe starts in the apoplast of the root epidermal cells. Fe inside the apoplast must undergo a reduction step before being transported through the plasma membrane. It has been observed that as much as 75% of Fe in the roots is precipitated in the apoplast as hydroxide or phosphate salts (Bienfait et al. 1985) forming an apoplastic Fe pool. In addition to this, Fe is attached to the apoplast since the negatively charged carboxyl groups of the cell walls serve as a cation sink. This Fe pool becomes important under Fe shortage. It has been shown that apoplastic Fe decreases when plants are grown under Fe starved conditions suggesting also the involvement of root exudates in facilitating Fe mobilization (Zhang et al. 1991, Jin et al. 2007).

Once inside the cell Fe is bound by chelating agents to avoid its oxidation and as a consequence its precipitation and generation of hydroxyl radicals. Even if many organic acids and amino acids are potentially Fe chelators, NA seems to have a favored function as Fe-chelator (Hell and Stephan, 2003). Fe-chelator complexes then move through the symplast into the stele along the diffusion gradient. At the pericycle, Fe is loaded into the xylem, and moves towards the shoot through the transpiration stream. When Fe is released into the xylem it is generally agreed that it is reoxidized to Fe(III) and it is probably transported in the xylem as Fe(III)-citrate complex (Rellán-Álvarez et al. 2011). The mechanism by which Fe is unloaded from the xylem to the leaf tissues has not been clearly elucidated yet, but it is probably mediated by transporters (Fe-citrate, Na-Fe or other complexes). The

photoreduction of the Fe-transporters also seems to play an important role in this (Bienfait and Scheffers 1992). In leaves the plasmalemma activity of FCR has been demonstrated supporting the opinion of an enzymatic Fe reduction. The distribution of Fe in leaf cells is again most likely mediated by NA. To prevent the toxic effect of overload Fe in the leaf, Fe is usually stored in ferritin.

Different groups of plants have very different optimum requirements of Fe from 0.5 to 50 ppm. The general Fe content of green plant tissues is about 2 $\mu\text{mol g}^{-1}$ of dry matter (Marschner 1995) which is quite lower in comparison of macronutrients, but represents the highest quantity among micronutrients.

Iron acquisition in dicotyledonous plants: the Strategy I

As pointed out before to cope with the problem of acquiring Fe dicotyledonous and monocotyledonous non-poaceae plants activate a reduce-based mechanism performed by the so-called Strategy I.

In general, Strategy I encompasses physiological, developmental and metabolic reactions that let the plant adapt to mutable levels of bio-available Fe. In this, two main specific processes are involved: the reduction of Fe(III) chelates at the root surface and the transport of the released Fe(II) ion across the root plasma membrane, as these plants can only take up Fe(II). Other less specific mechanisms involved in Strategy I are the extrusion of H^+ and the exudation of organic acids and phenolics into the rhizosphere. Moreover, depending on Fe bioavailability, morphological and architectural root changes complemented the activation of the previously described mechanism.

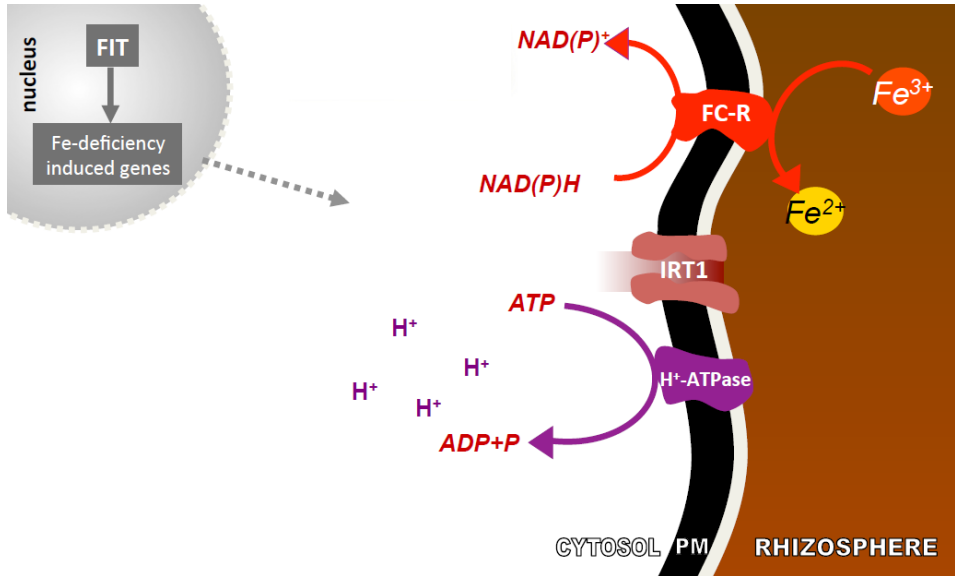


Figure 1.3. Schematic representation of Strategy I mechanisms for Fe acquisition. IRT1= Iron Regulated Transporter; FC-R= ferric-chelate reductase; H⁺-ATPase= ATP-dependent proton pump; Image courtesy of G. Vigani.

Reduction of Fe(III) chelates: a pre-condition to Fe acquisition.

All plants investigated so far shown FCR activity increase in response to Fe starvation, as much as 10-20 fold respect to plants grown in complete nutritive substrates (López-Millán et al. 2000 and references therein). The transmembrane FCR acts transferring electrons through the plasma membrane to reduce Fe(III) to Fe(II) in the apoplast thus allowing its transport into the cell.

As shown in figure 1.3, a FCR activity responsible of the reduction step of Fe(III) to Fe(II) has been elucidated from the identification of the gene, *FRO2*, in *Arabidopsis thaliana* (Yi and Guerinot, 1994; Robinson et al. 1999). *FRO2* belongs to a superfamily of flavocytochromes that transport electrons

across membranes.

FCR is constituted by eight transmembrane helices, four of which present structural homology with the flavocytochrome b family. An important water-soluble domain is localized between helices VIII and IX inside the membrane and contains NADPH, FAD and oxidoreductase activity. Between helices V and VII probably two heme groups are bind to conserved histidines. The structural homology with flavocytochrome b suggests a similar mechanism of electron transport: NAD(P)H is oxidized in the cytoplasm and electrons are transported through a flavine up to heme groups, when electrons arrive to the external surface of the membrane the reduction of Fe(III) to the Fe(II) occurs.

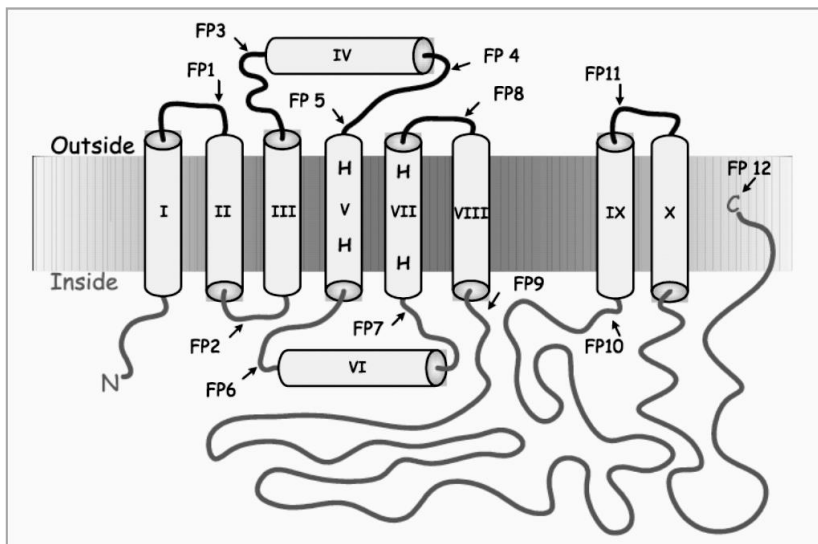


Figure 1.4. Topology model of FRO2 taken from Schagerlöf et al. (2006). Arrows indicate the localization of different fusion points.

In *Arabidopsis* other genes encoding isoforms of FCR were identified. Eight genes have shown conserved domain where

FAD and NADPH are bound. Each isoforms seems to be expressed preferentially at different levels in the plant. These isoforms do not compensate from one another. *FRO2* is responsible for Fe reduction at root level and mutants that lack in *FRO2* gene do not show any FCR activity induced in other isoforms. Genes encoding for FCR has also been identified in other Strategy I species as pea, tomato and cucumber; their expression varies among species suggesting that FROs may have roles in Fe distribution in the plant (Jeong and Connolly, 2009 and references therein).

In agreement with the idea that reduction of Fe is the rate-limiting step in Fe uptake by Strategy I plants (Grusak 1990), overexpression of *FRO2* confers tolerance to growth on low Fe media. Moreover, overexpression of *Arabidopsis FRO2* in soybean resulted in enhanced root ferric reductase activity and tolerance to Fe deficiency induced chlorosis (Vasconcelos et al. 2006).

Fe(II) transport inside the root cell.

Once reduced Fe(II) is transported into the root by means of an IRT generally localized at the plasmalemma. The IRT was first discovered as an homolog of a wide family of multigene metal transporters (ZIP, Zn-regulated transporter Fe-regulated transporter like protein) in *Arabidopsis* (*IRT1*), and even if it can also transport other divalent metals like Mn, Zn, and Cd, it shows a high affinity for Fe (Kobayashi and Nishizawa, 2012). *IRT1* plays a pivotal role in the regulation of plant Fe homeostasis, as demonstrated by the severe chlorosis and lethality of an *irt1-1* knockout mutant (Vert et al. 2002, Henriques et al. 2002). Consistently, *IRT1* gene is highly expressed in epidermal cells and the underlying cortex of Fe starved roots. Hence the Fe absorption dependent on *IRT1* allows proper growth and development under Fe limited conditions (Vert et al. 2002).

The Zip family transporters in *Arabidopsis* contain 15 members (including IRT1) that can be divided in four groups according to the alignment of the predicted amino acid sequences. The high variety of transporters in *Arabidopsis* have been explained as a consequence of the high number of different membranes that cations have to cross to be allocated through the plant, suggesting that different ZIP protein could have different localizations and specific functions. Furthermore, it is not to be rejected that many ZIP proteins could exhibit functional redundancy (Mäser et al. 2001). IRT2, for example, is very similar to IRT1 in its aminoacidic sequence and it is also expressed in the external layer cells of Fe starved roots. However, it was observed that up-regulation of *irt2* gene in knockout mutants of *irt1* under Fe deficiency conditions was not enough to recover from the chlorotic phenotype (Vert et al. 2002).

The predicted topology of most ZIP transporters has eight transmembrane domains and a similar orientation such that the amino and carboxy terminal ends are located on the extracellular surface. The difference among the various proteins is due to different lengths of the loop region (called variable region) between domains III and IV (Eide and Guerinot 1998). ZIP transporters have no similarities to other families of metal transporters.

Plants induce or repress various genes related to Fe homeostasis in response to Fe deficiency or Fe surplus. The molecular control expression mechanism of *IRT1* has been elucidated quite recently. The expression of IRT1 in root epidermis is induced by a transcription factor named FIT (Fe-deficiency-induced transcription factor) in *Arabidopsis* and by FER in tomato (Colangelo and Guerinot 2004, Ling et al. 2002). FIT/FER play a decisive role in positively regulating various Fe deficiency inducible genes, including *IRT1* and

FRO2. Since *FIT* overexpression did not induce downstream genes under Fe sufficiency conditions it was suggested the existence of interacting partners that are expressed or activated during Fe deficiency response (Colangelo and Guerinot 2004, Jakoby et al. 2004). It was also observed that Fe deficiency responses are transcriptionally regulated by a coexpression of different genes with *FIT*.

Furthermore, *IRT1* and *FRO2* expression showed a post-transcriptional regulation as the restoration of a Fe sufficiency medium induced a decrease in IRT1 protein accumulation and FRO2 activity in roots (Connolly et al. 2002). It was moreover reported that monoubiquitination of IRT1 at two lysine residues controls its subcellular localization, vacuolar sorting and degradation (Barberon et al. 2011). Many other studies have reported a large variability in genes involved during Fe deficiency depending on the specific response, function and localization. Other transcription factors identified are POPEYE (PYE) and BRUTUS (BTS) that play an important role in root morphology and growth level. Both PYE and BTS may act inversely: PYE regulates positively growth; elongation and swelling while on the contrary BTS may repress them (Long et al. 2010).

Other transporters belonging to the NRAMP (natural resistance-associated macrophage protein) family of integral membrane proteins was found in *Arabidopsis*. It was demonstrated the involvement of AtNRAMP proteins in divalent metal transport (Curie et al. 2000) and their localization either in the plasma membrane and intracellular vesicles (Kobayashi and Nashizawa, 2012).

Fe regulation and homeostasis involves so a large number of genes that expressed themselves at different localizations and with different ways (e.g. multiple pathway signaling and negative feed-backs loops). This complexity might confer the

necessary flexibility to cope with a constantly changing environment.

Acidification of the rhizosphere: the proton pump H⁺-ATPase

In strategy I plants, Fe deficiency is generally associated with an increased extrusion of protons mediated by plasmalemma H⁺-ATPases. In *Arabidopsis* twelve isoforms of H⁺-ATPase are known. From them AHA2 is involved in rhizosphere acidification whereas AHA7 seems to be related with radical hairs development.

The active extrusion of H⁺ is implicated in mineral nutrition among many other physiological functions such as control of the stomatal aperture, cell elongation, plant development, organ movement and intracellular pH homeostasis, although evidence for the direct involvement of H⁺-ATPases in some of these roles is uncommon (Sondergaard et al. 2004). In particular, regarding Fe nutrition the activation of this enzyme constitutes a key mechanism to Fe uptake by non-graminaceous plants and it is tightly correlated with the processes described in the previous paragraphs.

The plasma membrane H⁺-ATPase is a universal electrogenic H⁺ pump, which uses ATP as energy source to pump H⁺ across the plasma membranes into the immediate vicinity of root surface (apoplast and rhizosphere). In general, the key function of this enzyme is to keep pH homeostasis of plant cells and so generate an H⁺ transmembrane electrochemical gradient. This provides the driving force for the active flux of ions and metabolites across the plasma membrane. This ATP-dependent proton pumps thus drive the uptake of cations into plant cells. The resulting proton motive force typically embraces a membrane potential of about -150 mV, and a pH difference of 2 units (which contributes to another -120 mV to the proton motive force) (Mäser et al. 2001).

As protons accumulate outside the cell, the pH of the apoplast decreases to values of 5–6, markedly more acidic than the cytoplasmic pH (Palmgren 2001). This acidification of the apoplast and the rhizosphere is an essential step in Strategy I species since the solubility of Fe increases up to 1000-fold for each pH unit decrease. Thus, this process can have a huge impact on Fe activity in the close proximity of the roots (Olsen et al. 1981). The extrusion of H⁺ promotes the solubilization of Fe(III) and also balances the negative charges of the cell wall preventing repulsions of chelates. The H⁺ extrusion has also been associated to morphological changes in roots (López-Millán et al. 2000).

Plasma membrane H⁺-ATPases are found throughout the plant in all kind of cell type investigated so far. However, certain cell types have higher concentrations of H⁺-ATPases than others. In general, cell types with abundant H⁺-ATPases are specialized in active uptake of solutes from their surroundings. In some strategy I species the increased acidification of the rhizosphere under Fe deficiency conditions occurs as an increase in protein abundance that are predominantly localized in epidermal cells being differentiated as transfer cells (Dell'Orto et al. 2002).

Plant plasma membrane H⁺-ATPases is a single polypeptide of about 100 kDa that belongs to the large P-type H⁺-ATPases of cation pumps (Palmgren 2001). The enzyme has about 20% of its mass in the membrane, less than 10% is facing the non-cytoplasmic side and the largest mass is in four cytosolic domains, overall accounting for about 70% of the total mass of the protein itself (Palmgren and Harper 1999).

The primary structure of *Arabidopsis* AHA2 allows a prediction of ten transmembrane helices (figure 1.5). In the cytoplasmic region there are 3 well distinct domains: A- the actuator domain; P- the phosphorylation domain and N- the

nucleotidic binding domain that is fused with the P domain and contains the ATP binding site. Furthermore, there is a C-terminal domain (R) that yields a post-translational auto-inhibitory regulation. In the inactive state the R-domain might indeed be close to or partially folded on the membrane. The activation of the enzyme depends on the phosphorylation of the last but one Thr residue and the subsequent binding of 14-3-3 proteins that causes the displacement of the domain, so removing the inhibition.

The H⁺-ATPases are encoded by a gene family of about 10 members in *Arabidopsis thaliana* and other species (Arango et al. 2003). Depending on the gene, expression is either restricted to particular cell types or widespread in the plant. One gene can also be expressed in a given cell type at the same developmental stage, thus excluding the characterization of a single isoform from plant material. A study carried out in cucumber has shown a transcriptional regulation of a root plasma membrane H⁺-ATPase (Santi et al. 2005).

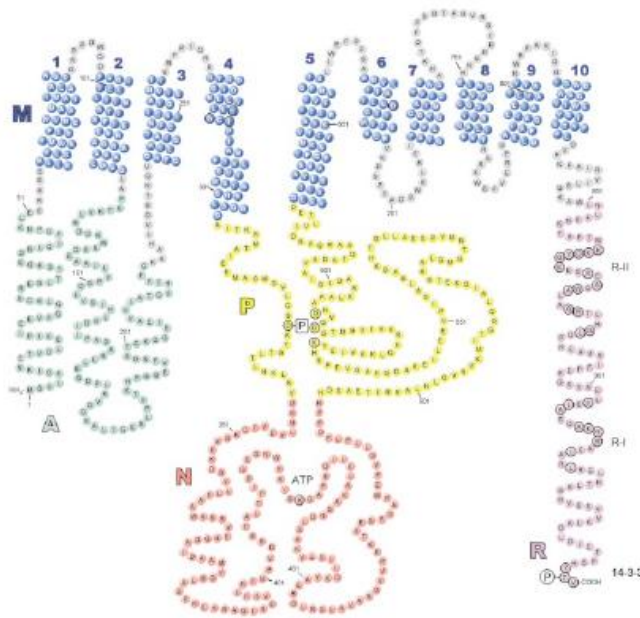


Figure 1.5. Schematic presentation of the AHA2 plasma membrane H⁺-ATPase. The various domains (A, P, N, and R) of the enzyme are indicated by colored residues (from Palmgren 2001).

Not all Strategy I species perform a high acidification (Zocchi et al, 2007) and in those species in which acidification is very scarce the response depends on many factors such as the balance of cation/anion uptake, the composition of root exudates and the type of nitrogen nutrition.

In conclusion, plants contain a complex regulation network of genes, which encode for the uptake, chelation, transport, sub-cellular distribution and storage of Fe. Understanding these processes is the essential prerequisite for their manipulation in order to breed in the future high-quality nutritious crops.

Iron acquisition in grasses: The Strategy II

The Strategy II response relies on biosynthesis and secretion of mugineic acids derivatives (MAs), which are specific to

graminaceous plants. Nine types of MAs have been identified to date, all of which are synthesized through a conserved pathway from S-adenosyl-L-methionine (Bashir et al., 2006, Kim et al., 2006, Mori and Nishizawa, 1987, Shojima et al., 1990; Ueno et al., 2007). This pathway comprises three sequential enzymatic reactions mediated by nicotianamine synthase (NAS), nicotianamine aminotransferase (NAAT), and deoxymugineic acid synthase (DMAS) (Bashir et al., 2006, Takahashi et al., Higuchi et al., 1999), generating 2'-deoxymugineic acid (DMA), the precursor of all other MAs. In restricted species, such as barley and rye, DMA is further hydroxylated to other MAs by dioxygenases, such as Fe deficiency-specific clone 2 (IDS2) and IDS3 (Kobayashi et al., 2001; Nakanishi et al., 2000). Fe deficiency strongly induces the expression of genes encoding these biosynthetic enzymes. To supply methionine for the successive production of MAs, a set of recycling reactions called the methionine cycle or Yang cycle is employed (Ma et al., 1995). Genes encoding the enzymes involved in this cycle were deduced from sequence comparison with corresponding genes in bacteria and yeast (Kobayashi et al., 2005; Suzuki et al., 2006). All of these candidate genes were inducible in response to Fe deficiency (Kobayashi et al., 2005; Suzuki et al., 2006), and the enzyme activities of most of the encoded proteins have recently been demonstrated (Pommerrenig et al., 2011, Rzewuski et al., 20007, Sauter et al., 2004, 2005).

The secretion of MAs follows a diurnal pattern with a vertical peak in the morning (Takagi et al., 1984. Certain vesicles observed in Fe deficient root cells are swollen in the early morning but shrink by the evening (Negishi et al., 2004; Nishizawa and Mori, 1987). The NAS enzyme is localized on the membrane of these vesicles, whereas NAAT is present within the vesicles itself (Nishizawa et al., 2000; S. Nagasaka,

unpublished results), suggesting that these vesicles are the sites of MA biosynthesis. Just recently, Nozoye et al. (2011) identified the transporter of mugineic acid family phytosiderophores 1 (OsTOM1) from rice and *HvTOM1* from barley, revealing the final piece in the mechanism. The MAs secreted into the rhizosphere solubilize Fe(III), and the resulting Fe(III)-MA complexes are taken up into root cells by the YELLOW STRIPE 1 (YS1) and YELLOW STRIPE 1-like (YSL) transporters (Curie et al., 2001, Inoue et al., 2009, Lee et al., 2009, Murata et al., 2006).

Rice, despite being a Strategy II plant, possesses a ferrous transporter, *OsIRT1*, that allows this crop to absorb directly Fe(II) (Ishimaru et al., 2006) in addition to its Strategy II-based Fe(III)-DMA uptake by the *OsYSL15* transporter (Inoue et al., 2009, Lee et al., 2009). In contrast to Strategy I plants, however, rice has very low ferric-chelate reductase activity on the root surface (Ishimaru et al., 2006), suggesting that it has adapted to directly take up Fe(II), which is abundant in submerged and anaerobic conditions.

There are many reports on other divalent metal transporters in both non-graminaceous and graminaceous plants. The ZIP (zinc-regulated transporter, iron-regulated transporter-like protein) family was first discovered as an homolog of *Arabidopsis* *IRT1*: it transports various divalent metals, including Fe(II), zinc (Zn^{2+}), manganese (Mn^{2+}), cadmium (Cd^{2+}), nickel (Ni^{2+}), and cobalt (Co^{2+}) (Guerinot, 2000; Korshunova et al., 1999; Nakanishi et al., 2006; Pedas et al., 2008). Another family of transporters, NRAMP (natural resistance-associated macrophage protein), also transports similar divalent metals. IRT transporters generally localize to the plasma membrane, whereas NRAMP transporters localize either to the intracellular vesicles or at the plasma membrane depending on the species of the protein (Calliate et al., 2010;

Lanquar et al., 2005; Takahashi et al., 2011; Thomine et al., 2003). Members of these transporter families in the plasma membrane of the root epidermis/exodermis are thought to be responsible for the uptake of essential metal elements from the rhizosphere (Calliate et al., 2010, Pedeas et al., 2008). Fe deficiency-induced expression of these members, such as Arabidopsis IRT1 and rice OsIRT1, is thought to be a major route for accumulation of harmful metals, including Cd under Fe deficiency (Morrissey et al., 2009; Nakanishi et al. 2006, Schaaf et al., 2006).

In graminaceous plants, MAs are also involved in the chelation and uptake of non-Fe metals, including Zn as a form of Zn(II)-MAs (Suzuki et al., 2006). In contrast, chelate formation of Cd(II)-DMA is reportedly much weaker than that of Fe(III)-DMA and Zn(II)-DMA, and thus DMA should not function in Cd uptake (Meda et al., 2007).

The role of the rhizosphere in Fe acquisition.

The rhizosphere is defined as the soil volume influenced by root activity (Hinsinger, 1998). This small and particular soil part is characterized by fluxes and gradients of both organic and inorganic compounds that are fundamental to rhizosphere processes. These latter, in turn, are able to influence considerably the transformations and flows of nutrients from soil to plant (Mimmo et al., 2014). For all these reasons, and because they are the linkage between soil and plant, these compounds are generally considered the bottleneck of nutrient mobilization in soil and subsequent acquisition by plants and, therefore, of crop yield.

Rhizosphere processes and the rhizosphere effects on plants are governed mainly by the release from roots, in a complex mixture, of low- and high-molecular-weight substances (such as protons, carbohydrates, organic acids, amino acids,

phytosiderophores (PS), phenolics and enzymes; Dakora & Phillips, 2002), able to induce fundamental changes in the chemical, physical and biological characteristics of this part of soil closely surrounding the roots. These substances are involved in important pedogenic and rhizospheric processes involving fundamental functions such as (i) modulation of nutrient availability (Fe, P, Zn; Dakora & Phillips, 2002), (ii) root protection against toxic metals (Al, Zn, Cd; Jones, 1998) or pathogens (Bais et al., 2004) and (iii) attraction and/or repulsion of microorganisms (Bais et al., 2004). In this context, soil microorganisms along with fungi hyphae by enhancing or restricting these rhizosphere processes, can play an important role in determining nutrient availability for plants in the rhizosphere.

Physical, chemical and biological processes in soil are largely connected with Fe (Les et al., 2006) and, in turn, with its availability for the soil-growing microorganisms and plants. Plant organic exudates operate through Fe complexation mechanisms as well as low-molecular-weight Fe-binding molecules (microbial siderophores, MSs) (Lemanceau et al., 2009), released by microorganisms in the rhizosphere.

Higher plants and microorganisms can release significant amounts of assimilated carbon (70% of the carbon in the root; Neumann and Römheld 2007) as organic compounds of high and low molecular weight into the rhizosphere as a response to Fe deficiency. For instance, it has been recently reported that maize releases up to 166 kg C ha⁻¹ as rhizo-deposited carbon (C) in the soil, 50% of which was recovered in the upper 10 cm (Pausch et al., 2013).

In addition to high-affinity ligands, microorganisms and plants also produce a range of lower-affinity ligands such as phenolics and organic acids (Jones et al., 1996; Reichard et

al., 2005; Robin et al., 2008). Organic compounds derived from soil organic matter decomposition can also contribute to Fe dynamics in the rhizosphere (Mimmo et al., 2014). The quantity and quality of ROCs varies largely on the specie, the age of an individual plant and external factors like biotic and abiotic stress. The composition of root exudates can be complex, and often ranges from mucilage, root border cells, extracellular enzymes, simple and complex sugars, phenolics, amino acids, vitamins, organic acids, nitrogenous macromolecules such as purines and nucleosides to inorganic or gaseous molecules such as HCO_3^- , OH^- , H^+ , CO_2 and H_2 (Mimmo et al., 2014). Many of these compounds have metal reductant or/and chelating abilities and can enhance Fe availability in the apoplast and rhizosphere (Ohwaki and Sugahara, 1997, Jin et al. 2007, Cesco et al. 2010, Rodríguez-Celma et al. 2011, Mimmo et al. 2012). The main ROCs are (i) carboxylates, such as citrate and malate, which originate from the primary metabolism, and (ii) many compounds such as phenolics and flavins, which are produced by secondary metabolism (Cesco et al., 2010, 2012; Vigani et al., 2012; Tato et al., 2013).

These root exudates are considered as one of the main root products, which are well known to influence nutrient solubility and uptake when plants are subject to stress. They are involved in plant nutrition through direct or indirect mechanisms. In the first case, some compounds act directly on nutrients making them more available while, in the second case, exudates act on soil microbial communities generating mutualistic associations and determining the structure of microbial community in its area of influence.

Root exudation of various chemical molecules into the rhizosphere is largely dependent on the nutritional status of the plant, with some species exuding organic acid anions in

response to P and Fe deficiency. The accumulation of low molecular weight organic acids (LOAs) has been recorded in many species as a response to Fe deficiency and may be involved in solubilization of Fe from the soil.

In Fe deficiency conditions it has been demonstrated that dicots accumulate and exude organic acids, mainly malate and citrate (de Vos et al. 1986, López-Bucio et al. 2000, Abadía et al. 2002). Due to their carboxylic groups, these organic acids can chelate metals from the soil solution and thus are involved in mobilization and uptake of nutrients such as P and Fe. Moreover, when soil pH is high, as in calcareous soils, mobilization of Fe(III) by malate and citrate are very slow since the chelates they form are quite unstable (Jones et al. 1996). However, in these conditions it was suggested a coordinate action between organic acids and the acidification performed by the H⁺-ATPase (Jones, 1998). Several reports show that cations were also simultaneously released during the excretion of organic acids from roots. For example, wheat and lupin released K⁺ (Ryan et al. 1995) and H⁺ (Neumann and Römheld 1999) during the excretion of malate and citrate, respectively. Cation transport might be necessary for maintaining a transmembrane electrical potential difference during the release of organic acids (anion).

Many phenolic compounds have been identified in root exudates (Dakora and Phillips 2002, Jin et al. 2007, Cesco et al. 2010). Lan et al. (2011) has recently observed in a proteomic analysis a strong induction in phenylpropanoid pathways in *Arabidopsis* under Fe deficiency conditions. Also *Parietaria judaica*, a spontaneous plant well adapted to calcareous environments, demonstrates a high metabolic flexibility in response to Fe starvation. Plants grown under low Fe availability conditions showed a strong accumulation of phenolics in roots as well as an improved secretion of root

exudates. *P. judaica* exhibits enhanced enzymatic activities of phenylpropanoid pathways (Tato et al., 2013). These compounds exhibited multiple functions in root exudates. Regarding Fe nutrition, Jin et al. have demonstrated their role in mobilization of Fe apoplastic deposits (Jin et al. 2007).

Plant–soil interaction

Under limited Fe availability, the metabolic reprogramming of plants to take up more Fe from soil represents not only a survival mechanism for the plant but is responsible for the production of large amounts of metabolites that are exuded (ROCs) into the rhizosphere. In addition to the role played in the rhizosphere, carboxylates act also within plants as Fe-chelates, aiding transport of Fe inside the plant, and play a central role in metabolism (Vigani et al., 2013). Under Fe deficiency the phosphoenolpyruvate carboxylase (PEPC) activity is strongly increased and produces more oxaloacetic acid (OAA) and in turn malate, by malate dehydrogenase activity (Zocchi, 2006). It has also been

a
et al., 2002), (ii) reducing equivalents for ferrioxalate reductase (FCR) through the cytosolic NADP⁺ dependent isocitrate dehydrogenase (ICDH) activity and (iii) 2-oxoglutarate, which contributes to nitrogen metabolism (Zocchi, 2006; Borlotti et al., 2012). The citrate and malate accumulated in Fe deficient plants can be released by roots to facilitate acquisition of Fe from the soil or transported to the shoot via the xylem.

On the other hand, phenolic compounds can act both as

antioxidant compounds and as Fe-ligands in plant tissues and play a critical role in aiding the reutilization of apoplastic Fe in roots (Jin et al., 2007). Moreover, these compounds can be increased or synthesized de novo, not only under Fe-deficient conditions, but also as a response to other nutrient deficiencies. Under these stressed conditions carbohydrates can be sidetracked into secondary metabolism to produce phenols (Donnini et al., 2012; Vigani et al., 2012; Tato et al., 2013). The activation of such processes permits the production and accumulation of phenols in plants allowing their release into the rhizosphere.

In addition to this, the oxidative pentose phosphate pathway and Calvin cycle can also provide carbon skeleton in the form of erythrose-4-P, which, with phosphoenolpyruvate (PEP) formed during glycolysis, can be used as a precursor for phenylpropanoid metabolism via the shikimic acid pathway (Herrmann, 1995). These pathways convert carbohydrates into aromatic amino acids (such as phenylalanine), which are the first substrate for the phenylpropanoid pathway and thus precursors for the synthesis of various phenolic compounds (Herrmann, 1995). Some enzymes belonging to the shikimate pathway, such as shikimate kinase (SK) and shikimate dehydrogenase (SDH), increased their activities under Fe deficiency in different plants along with the phenylalanine ammonia lyase (PAL) (Vigani et al., 2012).

In addition, the accumulation and the extrusion into rhizosphere of some flavin compounds such as riboflavins (Rbfl) have been observed (Siso-Terraza et al., 2015;

- lvarez et al., 2010). The exact role of accumulating flavins under Fe deficiency is still unknown and it has been hypothesized that flavin accumulation in the roots may be an integral part of the Fe-reducing system of Strategy I plants (FCR is a flavin-containing protein).

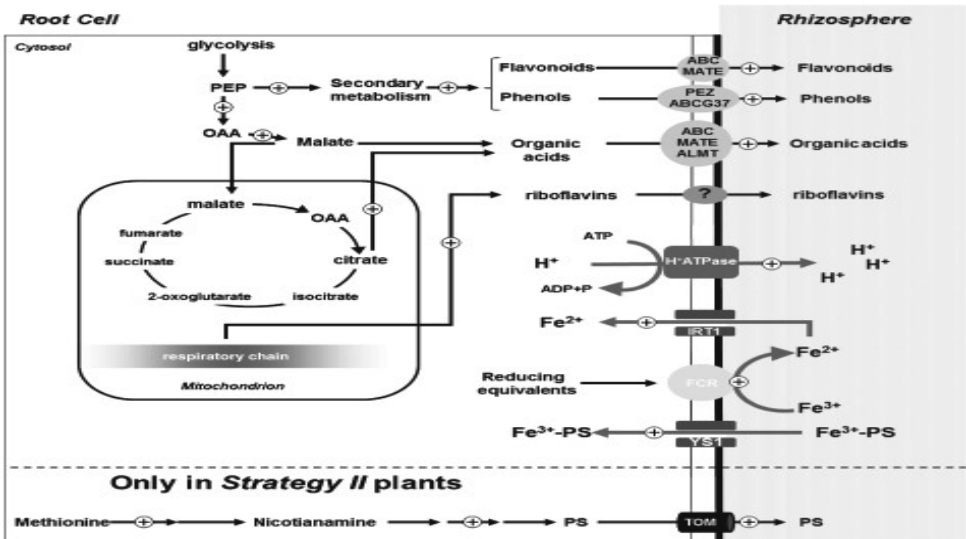


Figure 1.6 Schematic representation of the root exudation and main metabolic changes occurring in plants under Fe deficiency. The Fe shortage determines a strong mitochondrial alteration characterized by a reduction in the activity of the respiratory chain as well as an increase of organic acid biosynthesis (mainly citrate and malate). To support energetically the mechanism of Fe acquisition the activity of glycolysis is strongly induced. There is an increase of secondary metabolism pathways leading to an accumulation of phenolic compounds. The phenols, together with the organic acids and the unused riboflavins, are released from the root (see text for more details). Below the dashed line the pathway of synthesis and exudation of phytosiderophores occurring only in Strategy II plants grown under Fe-deficiency is also summarized (From Mimmo et al., 2014).

All these findings suggest that root exudates are synthesized by cellular metabolism both as a specific response to mobilize Fe outside the cell and as unused/accumulating compounds in the cell, which result from metabolism influenced by Fe deficiency.

Despite root cells can produce and release exudates quickly in response to mainly abiotic or biotic stresses, the processes involved in their release and regulation are still poorly known (Mathesius & Watt, 2011).

Recently the transporter involved in the release of PSs has been isolated and characterized in rice and barley (Nozoye et al., 2011). The protein named TOM1 catalyzes the release of DMA from these plant species. It is a component of the major facilitator superfamily (MFS), which is a large family of membrane proteins that act as uniporters, cotransporters or antiporters. Finally, other transport systems might be involved in the exudate release from roots of Fe-deficient plants, and highly lipophilic compounds might be able to diffuse across the lipid bilayer; however, most root exudates are too polar to simply diffuse through membranes, especially when it is considered that they are often glycosylated, acylated or hydroxylated (Weston et al., 2012). Further, some volatiles such as ethylene and NO might be directly released by roots, but it has been hypothesized that even in this case some specific transport systems might be involved (Dudareva et al., 2004). The exocytosis of compounds via a subcellular vesicle transport system is often proposed in response to stress or for the release of mucilage from the root cap, but clear evidence confirming the presence of vesicular root exudation is still missing (Badri and Vivanco, 2009).

Morphological changes induced by Fe deficiency.

The study of root system architecture (RSA) modifications provides interesting inputs regarding the tight relationship between root development and soil resource. Its importance in plant productivity lies in the fact that major soil resources are heterogeneously distributed in the soil, so the spatial disposition of roots will substantially determine the ability of a plant to ensure nutrient resources. Therefore, studies revealing the extent and nature of the genetic variation of RSA have profound implications for improving water- and nutrient-use efficiency of crops or for enhancing their productivity under abiotic stresses or suboptimal soil conditions.

The bioavailability of nutrients in the soil solution so influences root growth, root proliferation and specific functional responses that in part depend on the nutrient status of the plant. Nitrogen (N), phosphorus (P), iron (Fe) and sulfur (S) are among the nutrients that have been reported to alter post-embryonic root developmental processes. Changes in root architecture can mediate the adaptation of plants to soils in which nutrient availability is limited by increasing the total absorptive surface of the root system. The development of root systems is usually highly asymmetric and reflects the ability of roots to adjust their growth and development to environmental factors (Forde and Lorenzo 2001). Furthermore, even if a general trend could be drawn the variability among the morphological response in different species can be very high.

Low Fe availability induces morphological changes both at macroscopic and microscopic level. Changes observed in root epidermal cell under Fe deficiency comprise increase in root hair by modulating their length, position and abundance. Root hairs are the extensions of single epidermal cells and embrace as much as 77% of the total root surface area of cultivated crops, forming the major point of contact between the plant and the rhizosphere (Parker et al. 2000). It was also reported that during Fe deficiency root hairs occupied zones that did not have this structures in Fe sufficient conditions (Schmidt et al. 2000).

Changes in root elongation and in the number of lateral roots were also observed in Fe deficient roots. In a recent work on *Arabidopsis* it was point out that symplastic content of Fe triggers the local elongation of lateral roots by inducing an auxin promoter. The changes in root morphology are directly related with hormone regulation.

All of the root modifications previously pointed out are

concerned with increasing the contact surface of the root with the soil, its primary source of nutrients.

Iron deficiency and photosynthesis

The most noticeable effect of Fe deficiency in plant leaves is the typical yellowing of top leaves in the interveinal blade zones, known as chlorosis, caused by a decrease in the concentration of chlorophyll (Chl; *Chen and Barak, 1982; Abadía et al., 1989*). Fe deficiency symptoms manifest themselves in the younger leaves due to the relative immobility of Fe in the plants. Crop chlorosis is generally a result of both limited Fe bioavailability and cultivation of susceptible genotypes (*Hansen et al. 2006*). When Fe nutritional deficiency persists the leaves yellowing extends to the veins and the new leaves appear completely yellow. Fe in fact is required as an essential cofactor for various enzymes, which belong to the biosynthetic pathway of chlorophyll, in particular for the synthesis of δ -aminolevulinic acid. Under Fe deficiency, leaves generally have low photosynthetic activity due to several reasons discussed below; but they absorb more light energy per chlorophyll molecule than required for photosynthesis, especially under high radiation (*Abadía et al., 1999*). This results in a high risk for photoinhibitory and photooxidative damages and may also cause a reduction in CO₂ assimilation rate in Fe-deficient leaves, leading to substantial agricultural losses and decreases in nutritional quality of many crops of great economic interest.

In addition, under these conditions of supra-optimal light, photoinhibition of photosynthesis occurs due to over-excitation of chloroplast membranes, generation of reactive oxygen species (ROS) which may induce an alteration in the cellular redox state with the onset of oxidative stress and further damage of photosystem II (PSII) and sometimes

photosystem I (PSI) (Andersson and Aro, 2001; Ohad et al. 2000). More in details, PSI proteins are largely reduced, but the stoichiometry of the antenna composition of PSI is not compromised. On the contrary, PSII proteins were less affected by the stress, but the specific antennae Lhcb4 and Lhcb6, Lhcb2 and its isoform Lhcb1.1 are all reduced, whilst the concentration of Lhcb3 increase (Timperio et al., 2007). Fe deficiency is also known to cause a reduction in the number of granal and stromal lamellae per chloroplast (Platt-Aloia et al., 1983) and decrease in the amount of many thylakoid membrane components, including proteins, electron carriers and lipids (Terry and Abadia, 1986). Several studies (Yadavalli et al., 2014; Guikema and Sherman, 1983; Pakrasi et al., 1985, Timperio et al., 2007) showed that in *Chlamydomonas* and in higher plants the amount of large complexes and supercomplexes are decreased in Fe-deficient conditions, indicating that aggregation of small complexes into higher ordered structures is also affected by this nutritional disorder and a new re-arrangement could take place. As stressors can modify the partitioning of absorbed light energy in leaves, analysis of the contribution of different routes for excitation energy utilisation/dissipation in PSII complexes is of huge importance to study the regulatory mechanisms involved in responses of the photosynthetic apparatus (Korniyev and Hendrickson, 2007) Plants have different ways to release the pressure of excessive redox equivalents of chloroplasts and to minimize the damage caused by photoinhibition, including thermal dissipation capacity, the xanthophyll cycle, adjustment of chlorophyll antennae size, the water-water cycle, PSI cyclic electron transport and rapid turnover of the D1 protein of PSII (Niyogi, 1999, Andersson and Aro, 2001, Kato et al., 2003).

Photorespiration, as well, might be an important protective

mechanism to prevent photoinhibition. The photorespiratory cycle can therefore be considered in this as an energy dissipating cycle, operating between chloroplasts, peroxisomes, mitochondria and cytosol, which helps to protect chloroplasts from photoinhibition and plants from excessive accumulation of reactive oxygen species (Tolbert 1985, Wingler et al. 2000).

In a functional sense, the photorespiratory carbon cycle is an indispensable ancillary metabolic process that allows the Calvin-Benson cycle and hence photosynthesis to occur in oxygen containing environments. Biochemically, photorespiration starts at the enzyme by which all oxygenic phototrophs assimilate CO_2 to form sugar phosphates and subsequently all other organic molecules. This key catalyst of the global carbon cycle, ribulose 1,5-bisphosphate (RuBP) carboxylase/oxygenase (Rubisco), can also oxygenate RuBP, generating one molecule each of 3-phosphoglycerate (3PGA) and 2-phosphoglycolate (2PG). 2PG is the most important by-product of Rubisco in normal air concentrations of O_2 and CO_2 , and it is produced in large amounts every day. Before it can re-enter the CB cycle, it needs to be recycled by the photorespiratory cycle into 3PGA. This is the central function of photorespiratory metabolism. In higher plants, this pathway comprises at least eight core enzymes and several auxiliary enzymes localized to four different cellular compartments, the chloroplast, the peroxisome, the mitochondrion and the cytosol, which are all in close proximity to each other (Figure 1.7). Photorespiratory metabolite flow thus requires many membrane passage steps; however, transporters of the photorespiratory core cycle are not yet exactly known. By contrast, transporters involved in the re-assimilation of photorespiratory ammonia (NH_3) were identified. One of these, the chloroplastic 2-

sugar or reducing equivalents. Many recent research (Boldt et al., 2005; Timm et al., 2102, Hasunuma et al., 2010; Keerberg et al., 2011, Araujo et al., 2012, Fernie et al., 2012 and references therein) revealed that this important pathway originated as a partner of oxygenic photosynthesis billions of years ago is multiply linked to other pathways of central metabolism of contemporary land plants. Photorespiration is now also appreciated as an important part of stress responses in green tissues for preventing ROS accumulation. Photorespiratory reactions can also dissipate excess reducing equivalents and energy either directly (using ATP, NAD(P)H and reduced ferredoxin) or indirectly (e.g., via alternative oxidase (AOX) and providing an internal CO₂ pool). In addition, this metabolic pathway is also a source of H₂O₂ that is possibly involved in signal transduction, resulting in modulation of gene expression. (Voss et al. 2012).

Iron deficiency in crops

According to FAO 39% of rural land areas are affected by mineral deficiency and low fertility that constrain crop production (Cramer et al., 2011). Fe deficiency is a problem in crop production worldwide but particularly in plants grown on calcareous soils (Vose, 1982). Calcareous soils represent almost the 30% of the earth land surface. Their total extent has been estimated by FAO at 800 million hectares worldwide, 57 million of which in Europe. In the near future to cope with the increasing demand of food caused by a strong increase in world's population (FAO estimates in 10 billion people by 2050), agriculture must be extended to marginal areas, many of which include calcareous soils.

Many differences in genotypic characteristic exist among crop species, and also among varieties of the same species, regarding their responses to low Fe availability. These

differences are mainly based on the capacity to mobilize and acquire Fe from the rhizosphere.

Crop Fe deficiencies have been reported for many plant species and geographical regions. The most frequent problems correspond to the cultivation of sensitive crop species in arid and semi-arid regions with calcareous soils for crop such as soybean (*Glycine max*), peanut (*Arachis hupogaea*), dry bean (*Phaseolus vulgaris*), sorghum (*Sorghum bicolor*) and rice (*Oryza sativa*). Fe deficiencies have also been reported in corn (*Zea mays*), wheat (*Triticum aestivum*) and oat (*Avenae sativa*) but only in particular conditions. The following crops have been also found to be especially responsive to Fe low bioavailability: alfalfa, asparagus, barley, beans (white), beets, broccoli, brussel sprouts, cabbage, cauliflower, celery, citrus, pear, kiwifruit, grapevine, grass, oats, peach, peanuts, rye, strawberry, sudangrass and turf.

Fe is a limiting factor for biomass production: phytoplankton primary productivity in 30–40% of the oceans is also limited by Fe availability (Martin and Fitzwater, 1988). More recently Fe was shown to be a limiting factor for biomass and seed yield in *Arabidopsis* (*Arabidopsis thaliana*) (Ravet et al., 2009, 2012) and in crops including tomato (*Solanum lycopersicum*) (Jin et al., 2009), spinach (*Spinacia oleracea*) (Jin et al., 2013), and rice (*Oryza sativa*) (Takahashi et al., 2011). In the case of phytoplankton and *Arabidopsis*, the Fe-storage protein ferritin (Briat et al. 2010) is necessary to buffer transiently the fertilizing Fe in a safe form (Ravet et al., 2009; Marchetti et al., 2009) revealing that Fe-dependent biomass production requires the control of Fe homeostasis.

Mesoscale Fe-addition experiments have demonstrated that Fe supply limits biomass production in one-third of the oceans by controlling the dynamics of plankton blooms (Boyd et al.,

2009). Photosynthesis is the engine of this process, and Fe fertilization of the oceans leads to a nine fold increase in the chlorophyll concentration of phytoplankton, which results in doubling their maximum quantum yield of photosynthesis (Hiscock et al., 2008). Fe deficiency is known to alter both chloroplast structure and photosynthetic rate in higher plants (Eberhard et al., 2008), but our knowledge of the impact of Fe homeostasis on photosynthesis efficiency, and therefore on biomass production, is still very limited. As described above, from a functional point of view, Fe deficiency alters chlorophyll synthesis (Tottey et al. 2003) (explaining the interveinal yellowing of leaves known as chlorosis (see also figure 2.1). It also modifies electron transport in both PSI and PSII from dicotyledonous (Msilini et al., 2011, 2013) and monocotyledonous (Sharma, 2007) plants. Adaptation to Fe deficiency involves remodelling of the electron transfer chain (Vigani et al., 2012). The plasticity of the thylakoid membranes in response to Fe deficiency is evidenced by comparative proteome analysis of chloroplast thylakoids (Andaluz et al., 2006; Laganowsky et al., 2009). These studies report that the protein contents of electron transfer chain components (including the core and light-harvesting components of the PSI and PSII complexes), and of cytochrome b6/f, decrease in response to Fe deficiency, with PSI being the most affected. In addition, a transient decrease in trimeric and dimeric organization of the light-harvesting complex (LHC) of PSII from Fe-deficient spinach illustrates an impact on supercomplex organization, a likely adaptive response to energy dissipation in Fe-deficient plants (Timperio et al. 2007). In rice, probing the PSI core and Lhca1– Lhca4 proteins of LHC1 has been used to assess the kinetics of PSI subunit degradation in response to Fe deficiency (Yadavalli et al., 2012). PsaA and PsaB are stable under Fe deficiency, whereas the levels of PsaC, PsaD, Lhca1, and Lhca2 decrease

by 40–50%, and PsaE, Lhca3, and Lhca4 are fully degraded. In addition, several proteins are post-translationally modified; in particular the PSII oxygen-evolving complex is phosphorylated in Fe-deficient plants, whereas it remains unphosphorylated in Fe-replete plants (Laganowsky et al., 2009). The biological meaning of such modifications is so far unknown. Furthermore, Fe homeostasis controls the circadian clock rhythm – the mechanism that living organisms employ to adjust their metabolism in anticipation of environmental fluctuations – revealing another key regulatory factor controlling photosynthetic efficiency (Tissot et al., 2014). Fe nutrition and CO₂ interactions impact upon plant biomass production. Atmospheric CO₂ concentrations have increased by 38% since the start of the industrial era, and could double by the end of the 21st century (Feely et al., 2009). About 25% of this CO₂ has been absorbed by the ocean owing to phytoplankton photosynthetic activity that is known to be Fe-dependent (Boyd et al., 2009).

In areas where Fe deficiency is manifested, the deficiencies generally occur in patches rather than uniformly through a field. Chlorotic patches often arise in fields where high soil pH is homogeneous, indicating that alkalinity is not the only factor controlling the bioavailability and uptake of Fe (Hansen et al. 2006).

Many interactions exist between different mineral especially between P and Fe. In fact the manifestation of chlorosis depends on the P/Fe ratio rather than the single amounts of one or another nutrient.

Because plants are a primary food source for humans, the nutritional state of plants is also of central importance to human health. In particular, Fe content in plants becomes important in those populations whose diet is primarily vegetal.

Understanding of Fe homeostasis has been successfully applied to generate crops that are tolerant to Fe deficiency or whose edible parts are more nutritious. Creating crops with enhanced nutrient uptake could also aid agriculture to reduce the need for fertilizer application decreasing consistently the managing costs of agriculture.

An overview on human health and dietary.

Since plants are the primary source of Fe for humans a decrease in the amount of Fe in agricultural products has important implications for human health. Understanding the mechanisms of Fe uptake and regulation will provide useful insights for producing plants tolerant to low Fe availability and able to increase their Fe content.

Like in the plants, Fe mainly exists in the human body in complex bound to protein (hemoprotein) as heme compounds (haemoglobin or myoglobin), heme enzymes, or non-heme compounds (flavin-Fe enzymes, transferrin, and ferritin) (McDowell et al., 2003). The body requires Fe for the synthesis of its oxygen transport proteins, in particular haemoglobin and myoglobin, and for the formation of heme enzymes and other Fe-containing enzymes involved in electron transfer and oxidation-reduction reactions (Hurrell et al., 1997; McDowell et al., 2003) Almost two-thirds of the body Fe is found in the haemoglobin present in circulating erythrocytes, 25% is contained in a readily mobilizable Fe store, and the remaining 15% is bound to myoglobin in muscle tissue and in a variety of enzymes involved in the oxidative metabolism and many other cell functions (Washington DC Institute of Medicine, 2001).

Fe is the most commonly deficient micronutrient in the

human diet, and this deficiency affects an estimated 2 billion people all over the world. The highest probability of suffering Fe deficiency is found in those parts of a population that have inadequate access to foods rich in absorbable Fe during stages of high Fe demand. These groups correspond usually to children, adolescents, and women in the reproductive age, in particular during pregnancy (Dallman et al., 1990; FAO/WHO, 2004). The primary causes of Fe deficiency include: (i) low intake of bioavailable Fe; (ii) increased Fe requirements as a result of rapid growth, pregnancy, menstruation, and excess blood loss caused by pathologic infections, such as hook worm and whipworm causing gastrointestinal blood loss (Cooper et al., 1987; WHO, 1995; Crampton et al., 2002; Larocque et al., 2005;) and impaired absorption of Fe (Zimmermann et al., 2007). The most significant and common cause of anaemia is Fe deficiency (De Benoist et al., 2008). If Fe intake is limited or inadequate due to poor dietary intake, anaemia may occur as a result. This is called Fe deficiency anaemia. Fe deficiency anaemia can also occur when there are stomach ulcers or other sources of slow, chronic bleeding (colon cancer, uterine cancer, intestinal polyps, haemorrhoids, etc.) (Johnson-Wimbley et al., 2011).

For many years, nutritional interest in Fe focused only on its role in haemoglobin formation and oxygen transport (Underwood et al., 1999). Nowadays, although low Fe intake and/or bioavailability are responsible for most anaemia in industrialized countries, they account for only about half of the anaemia in developing countries (Allen et al. 2006), where infectious and inflammatory diseases (especially malaria), blood loss from parasitic infections, and other nutrient deficiencies (vitamin A, riboflavin, folic acid, and vitamin B12) are also important causes (Brabim et al., 2001).

In this context, Fe biofortification may be one of the possible

ways to feed humans safely with sufficient Fe directly within their diet (Lieu et al., 2001). Reaching such a goal requires an integrated knowledge of the establishment and control of Fe homeostasis (Guerinot, 1994; Askwin et al., 1998; Miur et al. 1983).

References

- Abadía J., López-Millán A.F., Rombolà A., Abadía A., (2002). Organic acids and Fe deficiency: a review, *Plant and Soil*, 241:75–86
- Allen L., de Benoist B., Dary O., Hurrell R., editors. Geneva: WHO and FAO; (2006). WHO. *Guidelines on food fortification with micronutrients*; p. 236.
- Andaluz, S. et al. (2006) Proteomic profiles of thylakoid membranes and changes in response to iron deficiency. *Photosynth. Res.* 89, 141–155
- Arango M., Gévaudant F., Oufattole M., Boutry M., (2003). The plasma membrane proton pump ATPase: the significance of gene subfamilies, *Planta*, 216(3): 355-65
- Arosio P. And Levi S., Ferritin, iron homeostasis and oxidative damage, *Free Radical Biology & Medicine*, Vol. 33, No. 4, pp. 457–463, 2002
- Askwith C, Kaplan J. Iron and copper transport in yeast and its relevance to human disease. *Trends Biochem Sci.* (1998); 23:135–8. [PubMed: 9584616]
- Badri DV, Vivanco JM (2009) Regulation and function of root exudates. *Plant Cell Environ* 32: 666–681. doi: 10.1111/j.1365-3040.2009.01926.x
- Barberon M., Zelaznya E., Robert S., Conéjéro G., Curie C., Frim J., Verta G., (2011). Monoubiquitin-dependent endocytosis of the IRON-REGULATED TRANSPORTER 1 (IRT1) transporter controls iron uptake in plants, *PNAS*,108(32):E450-E458

- Bashir K, Inoue H, Nagasaka S, Takahashi M, Nakanishi H, et al. 2006. Cloning and characterization of deoxymugineic acid synthase genes from graminaceous plants. *J. Biol. Chem.* 43:32395–402
- Bauwe H., Hagemann M., Fernie A.R.; Photorespiration: players, partners and origin; *Trends in Plant Science* 15 (2010) 330–336
- Bauwe H., Hagemann M., Kern R. and Timm S.; Photorespiration has a dual origin and manifold links to central metabolism; *Current Opinion in Plant Biology* 2012, 15:269–275
- Bienfait H.F., de Weger L.A., Kramer D., (1987). Control of the development of iron-efficiency reactions in potato as a response to iron deficiency is located in the roots, *Plant Physiology*, 83:244–247
- Bienfait H.F., Scheffers M.R., (1992). Some properties of ferric citrate relevant to the iron nutrition of plants, *Plant and Soil*, 143:141–144
- Bienfait H.F., van den Briel W., Mesland-Mul N.T., (1985). Free Space Iron Pools in Roots, *Plant Physiology*, 78(3): 596–600
- Boyd, P.W. et al. (2007) Mesoscale iron enrichment experiments 1993–2005: synthesis and future directions. *Science* 315, 612–617
- Brabin BJ, Premji Z, Verhoeff F. An analysis of anemia and child mortality. *J Nutr.* (2001); 131:636–45S.
- Briat, J.F., Curie C., Gaymard F., Iron utilization and metabolism in plant, *Current Opinion in Plant Biology* (2007), 10:276–282
- Briat, J.F. et al. (2010) Ferritins and iron storage in plants. *Biochim. Biophys. Acta* 1800, 806–814.
- Calliatte R, Schikora A, Briat JF, Mari S, Curie C. 2010. High-affinity manganese uptake by the metal transporter NRAMP1 is essential for *Arabidopsis* growth in low manganese conditions. *Plant Cell* 22:904–17
- Cesco S., Neumann G., Tomasi N., Pinton R., Weisskopf L., (2010). Release of plant-borne flavonoids into the rhizosphere and their role in plant nutrition, *Plant Soil*, 329:1–25

Colangelo E.P., Guerinot M.L., (2004). The Essential Basic Helix-Loop-Helix Protein FIT1 Is Required for the Iron Deficiency Response, *The Plant Cell*, 16(12):3400-3412

Connolly E.L., Campbell N.H., Grotz N., Prichard C.L., Guerinot M.L., (2003). Overexpression of the FRO2 ferric chelate reductase confers tolerance to growth on low iron and uncovers posttranscriptional control, *Plant Physiology*, 133:1102–1110

Connolly E.L., Fett J.P., Guerinot M.L., (2002). Expression of the IRT1 metal transporter is controlled by metals at the levels of transcript and protein accumulation, *Plant Cell*, 14:1347–1357

Cooper ES, Bundy DA. Trichuriasis. *Ballieres Clin Trop Med Commun Dis.* (1987); 2:629–43.

Cornell R.M., Schwertmann U., (2003). The iron oxides: Structure, Properties, Reactions, Occurrences and Uses, Wiley-VCH, Weinheim, New York

Curie C., Alonso J.M., Le Jean M., Ecker R., Briat J-F., (2000). Involvement of NRAMP1 from Arabidopsis thaliana in iron transport, *Biochemical Journal*, 347:749–755

Curie C., Panaviene Z., Loulergue C., Dellaporta S.L., Briat J.F., Walker E.L.. 2001. Maize *yellow stripe 1* encodes a membrane protein directly involved in Fe(III) uptake. *Nature* 409:346–49

Crompton DW, Nesheim MC. Nutritional impact of intestinal helminthiasis during the human life cycle. *Annu Rev Nutr.* (2002); 22:35–99. [PubMed: 12055337]

Dallman P. Iron. In: Brown ML, editor. Present Knowledge in Nutrition. 6th ed. Washington DC: Nutrition Foundation; (1990). pp. 241–50.

De Benoist B, McLean E, Egli I, Cogswell M, editors. Geneva: WHO Press, World Health Organization; (2008). WHO/CDC. Library Cataloguing-in-Publication Data. Worldwide prevalence of anaemia 1993-2005: WHO global database on anaemia; p. 40.

de Vos C.R., Lubberding H.J., Bienfait H.F., (1986). Rhizosphere Acidification as a Response to Iron Deficiency in Bean Plant, *Plant*

Physiology, 81(3):842-846

Dell'Orto M., Pirovano L., Villalba J.M., Gonzales-Reyes J.A., Zocchi G, (2002). Localization of the plasma membrane H⁺-ATPase in Fe-deficient cucumber roots by immunodetection, *Plant and Soil*, 241:11-17

Dell'Orto M., Santi S., De Nisi P., Cesco S., Varanini Z., Zocchi G., Pinton R., (2000). Development of Fe-deficiency responses in cucumber (*Cucumis sativus* L.) roots: involvement of plasma membrane H⁺-ATPase activity, *Journal of Experimental Botany*, 51:695-701

Dofing S.M., Penas E.J., Maranville J.W., (1989). Effect of bicarbonate on iron reduction by soybean roots, *Journal of Plant Nutrition*, 12(6): 797-802

Donnini S., De Nisi P., Gabotti D., Tato L., Zocchi G., Adaptive strategies of *Parietaria diffusa* (M.&K.) to calcareous habitat with limited iron availability, *Plant, Cell and Environment*, 35(6):1171-1184

Eberhard, S. et al. (2008) The dynamics of photosynthesis. *Annu. Rev.Genet.* 42, 463-515

Eide D.J., Guerinot M.L. (1998). The ZIP Genes: a Family of Eukaryotic Metal Ion Transporters, 5th Internet World Congress for Biomedical Sciences, Ontario-Canada, december 7-16

FAO/WHO. 2nd ed. Bangkok: (2004). Expert Consultation on Human Vitamin and Mineral Requirements, Vitamin and mineral requirements in human nutrition: Report of joint FAO/WHO expert consultation; p. 341.

Feely, R.A. et al. (2009) Ocean acidification: present conditions and future changes in a high-CO₂ world. *Oceanography* 22, 36-47

Forde B., Lorenzo H., 2001. The nutritional control of root development, *Plant Soil*, 232:51-68

Grusak M.A., Welch R.M., Kochian L.V., 1990. Does iron deficiency in *Pisum sativum* enhance the activity of the root plasmalemma iron transport protein?, *Plant Physiology*, 94:1353-1357

Guerinot M.L., Microbial iron transport. *Annu Rev Microbiol.* 1994; 48: 743–72. [PubMed: 7826025]

Guerinot M.L. 2000. The ZIP family of metal transporters. *Biochim. Biophys. Acta* 1465:190–98

Guerinot M.L., Yi Y., 1994. Iron: Nutritious, Noxious, and Not Readily Available, *Plant Physiology*, 104:815-820

Hansen, N.C., Hopkin B.G., Ellsworth, J.W., Jolley V.D., (2006). Iron nutrition in field crops, in L. L. Barton and J. Abadía (eds.), *Iron Nutrition in Plants and Rhizospheric Microorganisms*, Springer, 23–59

Harmsen J., Rulkens W.H. and Eiasakers H.J.P. (2005). Bioavailability, concept for understanding to tool for predicting? *Land Contamination and reclamation*, 13(2):161-171

Higuchi K., Suzuki K., Nakanishi H., Yamaguchi H., Nishizawa N.K., Mori S. 1999. Cloning of nicotianamine synthase genes, novel genes involved in the biosynthesis of phytosiderophores. *Plant Physiol.* 119:471–79

Hell R., Stephan U.W., (2003). Iron uptake, trafficking and homeostasis in plants, *Planta*, 216:541–551

Henriques R., Jásik J., Klein M., Martinoia E., Feller U., Schell J., Pais M.S., Koncz C., (2002). Knock-out of Arabidopsis metal transporter gene IRT1 results in iron deficiency accompanied by cell differentiation defects, *Plant Molecular Biology*, 50:587–597

Hindt, M.N. and Guerinot, M.L. (2012) Getting a sense for signals: regulation of the plant iron deficiency response. *Biochim. Biophys. Acta* 1823, 1521–1530

Hiscock, M.R. et al. (2008) Photosynthetic maximum quantum yield increases are an essential component of the Southern Ocean phytoplankton response to iron. *Proc. Natl. Acad. Sci. U.S.A.* 105

Houtz R.L., Stanley K. Ries and N. E. Tolbert, Effect of Triacontanol on *Chlamydomonas* II. Specific Activity of Ribulose-Bisphosphate Carboxylase/Oxygenase, Ribulose-Bisphosphate Concentration, and Characteristics of Photorespiration; *Plant Physiology* (1985) vol.

79 no. 2 365-370.

Hurrell RF. Bioavailability of iron. *Eur J Clin Nutr.* (1997); 51: S4–8. [PubMed: 9023471]

Inoue H., Kobayashi T., Nozoye T., Takahashi M., Kakei Y., Suzuki K., Nakazono M., Nakanishi H., Mori S., Nishizawa N.K. Rice OsYSL15 is an iron-regulated iron(III)-deoxymugineic acid transporter expressed in the roots and is essential for iron uptake in early growth of the seedlings *J Biol Chem*, 284 (2009), pp. 3470–3479

Ishimaru Y., Suzuki M., Tsukamoto T., Suzuki K., Nakazono M., Kobayashi T., Wada Y., Watanabe S., Matsushashi S., Takahashi M., et al. Rice plants take up iron as an Fe³⁺-phytosiderophore and as Fe²⁺ *Plant J*, 45 (2006), pp. 335–346

Ishimaru Y, Kakei Y, Shimo H, Bashir K, Sato Y, et al. (2011) A rice phenolic efflux transporter is essential for solubilizing precipitated apoplasmic iron in the plant stele. *J Biol Chem* 286: 24649–24655.

Ivanov, R. et al. (2012) Fitting into the harsh reality: regulation of iron-deficiency responses in dicotyledonous plants. *Mol. Plant* 5, 27–42

Jakoby M., Wang H.Y., Reidt W., Weisshaar B., Bauer P., (2004). FRU (BHLH029) is required for induction of iron mobilization genes in *Arabidopsis thaliana*, *FEBS Letters*, 577(3):528–534

Jin C.W., You G.Y., He Y.F., Tang C., Wu P., Zheng S.J., (2007). Iron Deficiency-Induced Secretion of Phenolics Facilitates the Reutilization of Root Apoplastic Iron in Red Clover, *Plant Physiology*, 144(1):278–285

Jin, C.W. et al. (2009) Elevated carbon dioxide improves plant iron nutrition through enhancing the iron-deficiency-induced responses under iron-limited conditions in tomato. *Plant Physiol.* 150, 272–280

Jin C.W., Li G.X., Yu X.H., Zheng S.J., (2010). Plant Fe status affects the composition of siderophore-secreting microbes in the rhizosphere, *Annals of Botany*, 105: 835–841.

- Jin, C.W. et al. (2013) Mild Fe-deficiency improves biomass production and quality of hydroponic-cultivated spinach plants (*Spinacia oleracea* L.). *Food Chem.* 138, 2188–2194
- Johnson-Wimbley TD, Graham DY. Diagnosis and management of iron deficiency anemia in the 21st century. *Ther Adv Gastroenterol.* (2011); 4:177–84. [PMCID: PMC3105608]
- Jones D.L., (1998). Organic acids in the rhizosphere – a critical review, *Plant and Soil*, 205:25–44
- Jones D.L., Darah P.R., Kochian L.V., (1996). Critical evaluation of organic acid mediated iron dissolution in the rhizosphere and its potential role in root iron uptake, *Plant and Soil*, 180(1):57-66
- Julian G., Cameron J., Olsen R.A., (1983). Role of chelation by ortho di hydroxy phenols in iron absorption by plant roots, *Journal of Plant Nutrition*, 6:163–75
- Kim S.A., Punshon T., Lanzirotti A., Li L., Alonso J.M., et al. 2006. Localization of iron in Arabidopsis seed requires the vacuolar membrane transporter VIT1. *Science* 314:1295–98
- Kobayashi T., Nakanishi H., Takahashi M., Kawasaki S., Nishizawa N.K., Mori S. 2001. In vivo evidence that *Ids3* from *Hordeum vulgare* encodes a dioxygenase that converts 2'-deoxymugineic acid to mugineic acid in transgenic rice. *Planta* 212:864–71
- Kobayashi T., Suzuki M., Inoue H., Itai R.N., Takahashi M., et al. 2005. Expression of iron-acquisition- related genes in iron-deficient rice is coordinately induced by partially conserved iron-deficiency-responsive elements. *J. Exp. Bot.* 56:1305–16
- Kobayashi T., Nishizawa N.K., (2012). Iron Uptake, Translocation, and Regulation in Higher Plants, *Annual Review of Plant Biology*, 63:131-152
- Kochian U., Lucas W.J. (1991). Do plasmalemma oxidoreductases play a role in plant mineral ion transport?, In: Crane FU, Morre DJ, Low HE (eds.) Oxidoreduction at the plasma membrane: relation to growth and transport, Madison, Wisconsin, USA: *Soil Science Society of America*, 189–205

Korshunova Y.O., Eide D., Clark W.G., Guerinot M.L., Pakrasi H.B. 1999. The IRT1 protein from *Arabidopsis thaliana* is a metal transporter with a broad substrate range. *Plant Mol. Biol.* 40:37–44

Kraemer, S.M., (2004). Iron oxide dissolution and solubility in the presence of siderophores, *Aquatic Science*, 66:3-18

Laganowsky, A. et al. (2009) Hydroponics on a chip: analysis of the Fe deficient *Arabidopsis* thylakoid membrane proteome. *J. Proteomics* 72, 397–415

Lan P., Li W., Wen T.-N., Shiao J.-Y., Wu Y.C., Lin W., Schmidt W., (2011). iTRAQ Protein Profile Analysis of *Arabidopsis* Roots Reveals New Aspects Critical for Iron Homeostasis, *Plant Physiology*, 155(2):821-834

Landsberg, E.C., (1981). Organic acid synthesis and release of hydrogen ions in response to Fe-deficiency stress of mono - and dicotyledonous plant species, *Journal of Plant Nutrition*, 3:579–91

Lanquar V., Lelievre F., Bolte S., Hames C., Alcon C., et al. 2005. Mobilization of vacuolar iron by AtNRAMP3 and AtNRAMP4 is essential for seed germination on low iron. *EMBO J.* 24:4041–51

Larocque R, Casapia M, Gotuzzo E, Gyorkos TW. Relationship between intensity of soil-transmitted helminth infections and anemia during pregnancy. *Am J Trop Med Hyg.* (2005); 73:783–9. [PubMed: 16222026]

Läuchli A., Grattan S.R., (2012). Soil pH extreme, in Shabala S. (ed.), *Plant stress physiology*, CAB International, UK

Lee S., Chiecko J.C., Kim S.A., Walker E.L., Lee Y., Guerinot M.L., An G., Disruption of OsYSL15 leads to iron inefficiency in rice plants *Plant Physiol*, 150 (2009), pp. 786–800

Lemanceau P., Expert D., Gaymard F., Bakker P.A.H.M., Briat J.-F., (2009). Role of Iron in Plant–Microbe Interactions, *Advances in Botanical Research*, 51:491–549

Lieu PT, Heiskala M, Peterson PA, Yang Y. The roles of iron in health and disease. *Mol Aspects Med.* (2001); 2: 1–87. [PubMed: 11207374]

Lindsay W.L., Schwab A.P., (1982). The chemistry of iron in soils and its availability to plants, *Journal of Plant Nutrition*, 5(4-7):821-840

Ling H.-Q., Bauer P., Bereczky Z., Keller B., Ganai M., (2002). The tomato fer gene encoding a bHLH protein controls iron-uptake responses in roots, *PNAS*, 99(21): 13938–13943

Long T. A., Tsukagoshi H., Busch W., Lahner B., Salt D.E., Benfey P.N., The bHLH Transcription Factor POPEYE Regulates Response to Iron Deficiency in Arabidopsis Roots, *The Plant Cell*, 22(7):2219-2236

López-Bucio J., Nieto-Jacobo M.F., Ramírez-Rodríguez V., Herrera-Estrella L., (2000). Organic acid metabolism in plants: from adaptive physiology to transgenic varieties for cultivation in extreme soils, *Plant Science*, 160(1): 1–13

López-Millán A.F., Morales F., Abadía A., Abadía J., (2000). Effects of Iron Deficiency on the Composition of the Leaf Apoplastic Fluid and Xylem Sap in Sugar Beet. Implications for Iron and Carbon Transport, *Plant Physiology*, 124(2):873-884

Lucena C., Romera F.J., Rojas C.L., García M.J., Alcántara E., Pérez-Vicente R., (2007). Bicarbonate blocks the expression of several genes involved in the physiological responses to Fe deficiency of Strategy I plants, *Functional Plant Biology*, 34(11): 1002–1009

Ma J.F., Shinada T., Matsuda C., Nomoto K. 1995. Biosynthesis of phytosiderophores, mugineic acids, associated with methionine cycling. *J. Biol. Chem.* 270:16549–54

Ma J.F., Taketa S., Chang Y.C., Iwashita T., Matsumoto H., et al. 1999. Genes controlling hydroxylations of phytosiderophores are located on different chromosomes in barley (*Hordeum vulgare* L.). *Planta* 207:590– 96

Marchetti, A. et al. (2009) Ferritin is used for iron storage in bloom-forming marine pennate diatoms. *Nature* 457, 467–470

Marschner H., Römheld V., Kissela M., 1986. Different strategies in higher plants in mobilization and uptake of iron, *Journal of Plant Nutrition*, 9(3-7):695-713

Marschner H., (1995). Mineral nutrition of higher plants, *Academic Press*, London

Martin, J.H. and Fitzwater, S. (1988) Iron deficiency limits phytoplankton growth in the north-east Pacific subarctic. *Nature* 331, 341–343

Mäser P., Thomine S., Schroeder J.I., Ward J.M., Hirschi K., Sze H., Talke I.N., Amtmann A., Maathuis F.J.M., Sanders D., Harper J.F., Tchieu J., Gribskov M., Persans M.W., Salt D.E., Kim S.A., Gueriot M.L., (2001). Phylogenetic Relationships within Cation Transporter Families of Arabidopsis, *Plant Physiology*, 126(4): 1646-1667

McDowell LR. 2nd ed. Amsterdam: Elsevier Science; (2003). *Minerals in Animal And Human Nutrition*; p. 660.

Meda A.R., Scheuermann E.B., Prechsl U.E., Erenoglu B, Schaaf G, et al. 2007. Iron acquisition by phytosiderophores contributes to cadmium tolerance. *Plant Physiol.* 143:1761–73

Mimmo T., Terzano R., Medici L., Lettino A., Fiore S., Tomasi N., Pinton R., Cesco S., (2012). Interaction of root exudates with the mineral soil constituents and their effect on mineral weathering, EGU General Assembly, 22-27 April Vienna - Austria., p.11494

Morales F., Grasa R., Abadía A., Abadía J., (1998). Iron chlorosis paradox in fruit trees, *Journal of Plant Nutrition*, 21:815-825

Mori S, Nishizawa N. 1987. Methionine as a dominant precursor of phytosiderophores in Graminaceae plants. *Plant Cell Physiol.* 28:1081–92

Morrissey J, Gueriot ML (2009) Iron uptake and transport in plants: the good, the bad, and the lonome. *Chem Rev* 109: 4553–4567. doi: 10.1021/cr900112r

Morrissey J., Baxter I.R., Lee J., Li L., Lahner B., et al. 2009. The ferroportin metal efflux proteins function in iron and cobalt homeostasis in Arabidopsis. *Plant Cell* 21:3326–38

Msilini, N. et al. (2011) Inhibition of photosynthetic oxygen evolution and electron transfer from the quinone acceptor QA to QB by iron deficiency. *Photosynth. Res.* 107, 247–256

Msilini, N. et al. (2013) How does iron deficiency disrupt the electron flow in photosystem I of lettuce leaves? *J. Plant Physiol.* 170,1400–1406

Muir A, Hopfer U. Regional specificity of iron uptake by small intestinal brush-boarder membranes from normal and iron deficient mice. *Am J Physiol.* (1985); 248:G376–9. [PubMed: 3976894]

Müller M., Schmidt W., (2004). Environmentally induced plasticity of root hair development in Arabidopsis, *Plant Physiology*, 134:409–419

Murata Y., Ma J.F., Yamaji N., Ueno D., Nomoto K., Iwashita T. 2006. A specific transporter for iron(III)-phytosiderophore in barley roots. *Plant J.* 46:563–72

Murgia, I. et al. (2012) Biofortification for combating ‘hidden hunger’ for iron. *Trends Plant Sci.* 17, 47–55

Nakanishi H., Yamaguchi H., Sasakuma T., Nishizawa N.K. , Mori S. 2000 Two dioxygenase genes, *Ids3* and *Ids2*, from *Hordeum vulgare* are involved in the biosynthesis of mugineic acid family phytosiderophores. *Plant Mol. Biol.* 44:199–207

Nakanishi H., Ogawa I., Ishimaru Y., Mori S., Nishizawa N.K., 2006. Iron deficiency enhances cadmium uptake and translocation mediated by the Fe²⁺ transporters OsIRT1 and OsIRT2 in rice. *Soil Sci. Plant Nutr.* 52:464–69

Neumann G., Römheld V., (1999). Root excretion of carboxylic acids and protons in phosphorus-deficient plants, *Plant and Soil*, 211:121–130

Neumann G., Römheld V., (2001). The Release of Root Exudates as Affected by the Plant's Physiological Status, in: Willig S., Varanini Z., Nannipieri P. (eds), *The Rhizosphere: Biochemistry and Organic*

Substance at the Soil-Plant Interface, Marcel Dekker, New York, pp. 41-93

Negishi T, Nakanishi H, Yazaki J, Kishimoto N, Fujii F, et al. 2002. cDNA microarray analysis of gene expression during Fe-deficiency stress in barley suggests that polar transport of vesicles is implicated in phytosiderophore secretion in Fe-deficient barley roots. *Plant J.* 30:83-94

Nikolic M., Roemheld V., (2002). Does high bicarbonate supply to roots change availability of iron in the leaf apoplast?, *Plant Soil*, 241:67-74

Nishizawa N., Mori S. 1987, The particular vesicle appearing in barley root cells and its relation to mugineic acid secretion. *J. Plant Nutr.* 10:1013-20

Nishizawa N.K., Negishi T., Higuchi K., Takahashi M., Itai R., et al. 2000. The secretion and biosynthesis of mugineic acid family phytosiderophores (MAs) in iron deficient barley roots. Abstr. 10th Int. Symp. Iron Nutr. Interact. Plants, Houston, p. 40 (Abstr.)

Nozoye T, Nagasaka S, Kobayashi T, Takahashi M, Sato Y, et al. (2011) Phytosiderophore efflux transporters are crucial for iron acquisition in graminaceous plants. *J Biol Chem* 286: 5446-5454.

Ohwaki Y., Sugahara K., (1997). Active extrusion of protons and exudation of carboxylic acids in response to iron deficiency by roots of chickpea (*Cicer arietinum* L.), *Plant and Soil* 189: 49-55, 1997

Olsen R.A., Clark R.B., Bennett J.H., (1981). The Enhancement of Soil Fertility by Plant Roots, *American Scientist*, 69(4): 378-384

Palmgren M.G., (2001). Plant Plasma Membrane H⁺-ATPases: Powerhouses for Nutrient Uptake, *Annual Review of Plant Physiology and Plant Molecular Biology*, 52:817-45

Palmgren M.G., Harper J.F., (1999). Pumping with plant P-type ATPases, *Journal of Experimental Botany*, 50:883-893

Parker J.S., Cavell A.C., Dolan L., Roberts K., Grierson C.S., (2000). Genetic interactions during root hair morphogenesis in Arabidopsis,

The Plant Cell, 12:1961–1974

Pedas P., Ytting C.K., Fuglsang A.T., Jahn T.P., Schjoerring J.K., Husted S. 2008. Manganese efficiency in barley: identification and characterization of the metal ion transporter HvIRT1. *Plant Physiol.* 148:455–66

Pommerrenig B., Feussner K., Zierer W., Rabinovych V., Klebl F., et al. 2011. Phloem-specific expression of Yang cycle genes and identification of novel Yang cycle enzymes in *Plantago* and *Arabidopsis*. *Plant Cell* 23:1904–19

Quintero-Gutiérrez A.G., González-Rosendo G., Sánchez-Muñoz J., Polo-Pozo J., Rodríguez-Jerez J.J. Bioavailability of heme iron in biscuit filling using piglets as an animal model for humans. *Int J Biol Sci.* (2008); 4:58–62.

Ravet, K. et al. (2009) Ferritins control interaction between iron homeostasis and oxidative stress in *Arabidopsis*. *Plant J.* 57, 400–412

Ravet, K. et al. (2012) Iron and ROS control of the DownStream mRNA decay pathway is essential for plant fitness. *EMBO J.* 3

Rellán-Álvarez R., El-Jendoubi H., Wohlgemuth G., Abadía A., Fiehn O., Abadía J., Álvarez-Fernández A., 2011. Metabolite Profile Changes in Xylem Sap and Leaf Extracts of Strategy I Plants in Response to Iron Deficiency and Resupply, *Frontiers Plant Science*, 2: 66

Robin A., Vansuyt G., Hinsinger P., Meyer J.M., Briat J.F., Lemanceau P., (2008). Iron Dynamics in the Rhizosphere: Consequences for Plant Health and Nutrition, in: Sparks D.L. (ed), *Advances in Agronomy*, 99:183-225

Robinson N.J., Procter C.M., Connolly E.L., Guerinot M.L., (1999). A ferric-chelate reductase for iron uptake from soils, *Nature*, 397:694-697

Rodríguez-Celma J., Lattanzio G., Grusak M.A., Abadía A., Abadía J., López-Millán A.F., (2011). Root Responses of *Medicago truncatula*

Plants Grown in Two Different Iron Deficiency Conditions: Changes in Root Protein Profile and Riboflavin Biosynthesis, *Journal of Proteome Research*, 10(5):2590–2601

Römheld V., (2000). The chlorosis paradox: Fe inactivation as a secondary event in chlorotic leaves of grapevine, *Journal of Plant Nutrition*, 23:1629-1643

Römheld V, Marschner H (1986) Mobilization of iron in the rhizosphere of different plant species. *Adv Plant Nutr* 2: 155–204.

Romera F.J., Alcántara E., de la Guardia M.D., (1992). Effects of bicarbonate, phosphate and high pH on the reducing capacity of Fe-deficient sunflower and cucumber plants, *Journal of Plant Nutrition*, 15(10):1519-1530

Ryan P.R., Delhaize E., Randall P.J., (1995). Malate Efflux From Root Apices and Tolerance to Aluminium Are Highly Correlated in Wheat, *Australian Journal of Plant Physiology*, 22(4): 531-536

Rzewuski G., Kornell K.A., Rooney L., Burstenbinder K., Wirtz M., et al. 2007. OsMTN encodes a 5'-methylthioadenosine nucleosidase that is up-regulated during submergence-induced ethylene synthesis in rice (*Oryza sativa* L.). *J. Exp. Bot.* 58:1505–14

Santi S., Cesco S., Pinton V.Z.R., (2005). Two plasma membrane H⁺-ATPase genes are differentially expressed in iron-deficient cucumber plants, *Plant Physiology and Biochemistry*, 43:287–292

Santi S., Schmidt W., (2008). Laser microdissection-assisted analysis of the functional fate of iron deficiency-induced root hairs in cucumber, *Journal of Experimental Botany*, 59:697–704.

Santi S, Schmidt W (2009) Dissecting iron deficiency-induced proton extrusion in Arabidopsis roots. *New Phytol* 183: 1072–1084.

Sauter M., Cornell K.A., Beszteri S., Rzewuski G. 2004. Functional analysis of methylthioribose kinase genes in plants. *Plant Physiol.* 136:4061–71

Sauter M., Lorbiecke R., OuYang B., Pochapsky T.C., Rzewuski G. 2005. The immediate-early ethylene response gene OsARD1 encodes an acireductone dioxygenase involved in recycling of the ethylene

precursor S-adenosylmethionine. *Plant J.* 44:718–29

Schaaf G., Honsbein A., Meda A.R., Kirchner S., Wipf D., von Wiren N. 2006. *AtIREG2* encodes a tonoplast transport protein involved in iron-dependent nickel detoxification in *Arabidopsis thaliana* roots. *J. Biol. Chem.* 281:25532–40

Schagerlöf U., Wilson G., Hebert H., Al-Karadaghi S., Hägerhäll C., (2006). Transmembrane topology of FRO2, a ferric chelate reductase from *Arabidopsis thaliana*, *Plant Molecular Biology*, 62:215–221

Schikora A., Schmidt W., (2002). Formation of transfer cells and H⁺-ATPase expression in tomato roots under P and Fe deficiency, *Planta*, 215:304–311

Schmidt W., (2003). Iron solutions: acquisition strategies and signaling pathways in plants, *Trends in Plant Science*, 8(4): 188–193

Schmidt W., Michalke W., Schikora A., (2003). Proton pumping by tomato roots. Effect of Fe efficiency and hormones on the activity and distribution of plasma membrane H⁺-ATPase in rhizodermal cells, *Plant, Cell and Environment*, 26:361–370

Schmidt W., Tittel J., Schikora A., (2000). Role of hormones in the induction of iron deficiency responses in *Arabidopsis* roots, *Plant Physiology*, 122:1109-1118

Schwertmann U., Taylor R.M., (1989). Iron oxides, in: Dixon J.B, Weed S.B., Mineral in soils Environments, *Soil society of America*, 379-438

Sharma, S. (2007) Adaptation of photosynthesis under iron deficiency in maize. *J. Plant Physiol.* 164, 1261–1267

Shojima S., Nishizawa N.K., Fushiya S., Nozoe S., Irifune T., Mori S. 1990. Biosynthesis of phytosiderophores: in vitro biosynthesis of 2'-deoxymugineic acid from L-methionine and nicotianamine. *Plant Physiol.* 93:1497–503

Sondergaard T.E., Schulz A., Palmgren M.G., (2004). Energization of Transport Processes in Plants. Roles of the Plasma Membrane H⁺-

ATPase, *Plant Physiology*, 136(1):2475-2482

Stumm, W., Morgan, J.J., (1996). *Aquatic Chemistry, Chemical Equilibria and Rates in Natural Waters*, John Wiley & Sons, New York, NY

Suzuki M., Takahashi M., Tsukamoto T., Watanabe S., Matsuhashi S., et al. 2006. Biosynthesis and secretion of mugineic acid family phytosiderophores in zinc-deficient barley. *Plant J.* 48:85–97

Takagi S., Nomoto K., Takemoto S. 1984. Physiological aspect of mugineic acid, a possible phytosiderophore of graminaceous plants. *J. Plant Nutr.* 7:469–77

Takahashi, M. et al. (2001) Enhanced tolerance of rice to low iron availability in alkaline soils using barley nicotianamine aminotransferase genes. *Nat. Biotechnol.* 19, 466–469

Takahashi R., Ishimaru Y., Senoura T., Shimo H., Ishikawa S., et al. 2011. The OsNRAMP1 iron transporter is involved in Cd accumulation in rice. *J. Exp. Bot.* 62:4843–50

Taylor K.G., Konhauser K.O., (2011). Iron in Earth Surface Systems: A Major Player in Chemical and Biological Processes, *Elements*, 7:83-88

Timperio, A.M. et al. (2007) Proteomics, pigment composition, and organization of thylakoid membranes in iron-deficient spinach leaves. *J. Exp. Bot.* 58, 3695–3710

Tissot, N. et al. (2014) Iron around the clock. *Plant Sci.* 224, 112–119

Thomine S., Lelievre F., Debarbieux E., Schroeder J.I., Barbier-Brygoo H. 2003. AtNRAMP3, a multispecific vacuolar metal transporter involved in plant responses to iron deficiency. *Plant J.* 34:685–95

Thomine, S.; Vert G., Iron transport in plants: better be safe than sorry, *Current Opinion in Plant Biology* 2013, 6:322–327

Takahashi M., Yamaguchi H., Nakanishi H., Shioiri T., Nishizawa N.K., Mori S. 1999. Cloning two genes for nicotianamine

aminotransferase, a critical enzyme in iron acquisition (Strategy II) in graminaceous plants. *Plant Physiol.* 121:947–56

Tomasi N, Weisskopf L, Renella G, Landi L, Pinton R, et al. (2008) Flavonoids of white lupin roots participate in phosphorus mobilization from soil. *Soil Biol Biochem* 40: 1971–1974.

Toulon V., Sentenac H., Thibaud J.B., Davidian J.C., Moulineau C., Grignon C., (1992). Role of apoplast acidification by the H⁺pump, *Planta*, 186 (2):212-218

Tottey, S. et al. (2003) Arabidopsis CHL27, located in both envelope and thylakoid membranes, is required for the synthesis of protochlorophyllide. *Proc. Natl. Acad. Sci. U.S.A.* 100, 16119–16124

Ueno D., Rombola A.D., Iwashita T., Nomoto K., Ma J.F. 2007 Identification of two new phytosiderophores secreted by perennial grasses. *New Phytol.* 174:304–310

Underwood EJ, Suttle NF. 3rd ed. Wallingford: CABI International Publishing; (1999). The mineral nutrition of livestock; p. 614

van Hees P.A.W., Lundström U.S, (2000). Equilibrium models of aluminium and iron complexation with different organic acids in soil solution, *Geoderma*, 94(2–4):201–221

Vasconcelos M., Eckert H., Arahana V., Graef G., Grusak M.A., Clemente T., (2006). Molecular and phenotypic characterization of transgenic soybean expressing the Arabidopsis ferric chelate reductase gene, FRO2, *Planta*, 224:1116–1128.

Vert G., Grotzb N., Dédaldéchamp F., Gaymard F., Guerinot M.L., Briat J.-F., Curie C., (2002). IRT1, an Arabidopsis transporter essential for iron uptake from the soil and for plant growth, *Plant Cell*, 14:1223–1233.

Vose P.B., (1982). Rationale of selection for specific nutritional characters in crop improvement with *Phaseolus vulgaris* L. as a case study, *Plant and Soil*, 72 (2-3):351-364

Washington, DC: National Academy Press; (2001). IOM. Institute of Medicine. iron. In: Dietary Reference Intakes for Vitamin A, Vitamin K, Arsenic, Boron, Chromium, Copper, Iodine, iron, Manganese,

Molybdenum, Nickel, Silicon, Vanadium, and Zinc; pp. 290–393.

Wingler A. , Lea P.J. , Quick P.W. and Leegood R.C.; Photorespiration: metabolic pathways and their role in stress protection, *Phil. Trans. R. Soc. Lond. B* (2000) 355, 1517-1529

World Health Organization, Geneva; (1995). WHO. Report of the WHO informal consultation on hookworm infection and anaemia in girls and women; p. 46.

Yadavalli, V. et al. (2012) Differential degradation of photosystem I subunits under iron deficiency in rice. *J. Plant Physiol.* 169, 753–759 28

Yi Y., Guerinot M.L., (1996). Genetic evidence that induction of root Fe(III) chelate reductase activity is necessary for iron uptake under iron deficiency, *The Plant Journal*, 10(5):835–844

Zhang F., Römheld V., Marschner H., (1991). Role of the Root Apoplasm for Iron Acquisition by Wheat Plants, *Plant Physiology*, 97(4): 1302–1305

Zhang W.-H., Ryan P.R., Tyerman S.D., (2004). Citrate-Permeable Channels in the Plasma Membrane of Cluster Roots from White Lupin, *Plant Physiology*, 136:3771-3783

Zheng S.J., Tang C., Arakawa Y., Masaoka Y., The responses of red clover (*Trifolium pratense* L.) to iron deficiency: a root Fe(III) chelate reductase, *Plant Science* 164 (2003) 679/687

Zimmermann MB, Hurrell RF. Nutritional iron deficiency. *Lancet.* (2007); 370:115–20.

CHAPTER II

***In vivo* photosynthesis performance and gas exchange alterations induced by iron deficiency in *Cucumis sativus* L.**

Highlights

The characteristic iron (Fe) deficiency marked chlorosis of the leaf is largely caused by a decrease in the concentration of chlorophyll and may result in a reduction in CO₂ assimilation rate. In these conditions leaves generally have low photosynthetic activity but they absorb more light energy per chlorophyll molecule than required for photosynthesis, especially under high radiation. This results in a high risk for photoinhibitory and photooxidative damages in Fe-deficient leaves. We suggest that Fe deficiency leads to a strong impairment of the photosynthetic apparatus at different levels: an increase in the rate of CO₂ assimilation rate in many biological repetition (+29%) was observed, suggesting a possible induction of photorespiratory metabolism. However, the variation is not significant and so further analysis are strictly required in order to reduce the variability among the repetition to get a more get a more reliable result form. In addition, the reduction of CO₂ assimilation can be also attributable to a reduced stomatal conductance, but also to an altered activity of the mesophyll.

Abstract

The most evident effect of Fe deficiency in plant leaves is a marked internervous chlorosis caused by a decrease in the concentration of chlorophyll (Chen and Barak, 1982; Abadía et al., 1989), which may result in a reduction in CO₂ assimilation rate. In addition to the synthesis of this photosynthetic pigment, high amount of Fe are strictly required for the structural and functional integrity of the thylakoid membranes, explaining the particular sensitivity of chloroplasts in general, and the thylakoids in particular, to Fe deficiency (Helch-Buchholz et al., 1986). As a general rule, Fe deficiency has less effect on leaf growth, cell number per unit

area, or number of chloroplasts per cell than on the size of the chloroplasts and protein content per chloroplast. Under Fe deficiency, leaves generally have low photosynthetic activity due to several reasons, but they absorb more light energy per chlorophyll molecule than required for photosynthesis, especially under high radiation (Abadía *et al.*, 1999). This results in a high risk for photoinhibitory and photooxidative damages in Fe-deficient leaves, leading to substantial agricultural losses and decreases in nutritional quality of many crops of great economic interest.

Cucumber plants shows a significant increase of C_i , whereas stomatal conductance and values of apparent electron transport rate decrease after 10 days of Fe deficiency. Interestingly, we observe a remarkable decrease of P_n , which appears to be negative. Further *in vivo* analysis allows us to determine the chlorophyll *a* fluorescence. In particular a decrease in the F_v/F_m ratio, in the quantum yield of PSII (Φ_{PSII}) and in the photochemical quenching was observed, on the contrary, we see an increase in the non-photochemical quenching (Q_{np}). In the Fe-sufficient plants, a significant increase in photoassimilation of CO_2 was recorded, indicating that photorespiration contributes 43% to the decrease of CO_2 assimilated. In Fe deficiency condition we recorded an increase in the rate of CO_2 assimilation rate in many biological repetition (+29%). However, further analysis are strictly required in order to reduce the variability among the repetition. In addition, the rate of CO_2 assimilation was significantly reduced (-84%). This was probably attributable to stomatal closure but also to an altered activity of the mesophyll.

Taken all together, our data allow us to suggest that Fe deficiency leads to a strong impairment of the photosynthetic

apparatus at different levels. It appears clear that the reaction centers of PS-II are largely inactive. Performed Chl-fluorescence analysis revealed a general increase in nonphotochemical quenching (qNP) in chlorotic leaves, indicating the activation of photoprotective mechanisms which however are not sufficient to prevent photoinhibition, as indicated by a significant reduction in maximal PSII photochemistry (F_v/F_m) and photochemical quenching (qp). In Fe deficiency condition we recorded an increase in the rate of CO_2 assimilation rate in many biological repetition (+29%), suggesting a possible induction of photorespiratory metabolism. However, the variation is not significant and so further analysis are strictly required in order to reduce the variability among the repetition to get a more complete form. In addition, the reduction of CO_2 assimilation can be also attributable to a reduced stomatal conductance, but also to an altered activity of the mesophyll. The results obtained from the chlorophyll fluorescence analysis seem to validate these latter hypothesis.

Introduction.

The most evident effect of Fe deficiency in plant leaves is a marked internerval chlorosis caused by a decrease in the concentration of chlorophyll (Chl; Chen and Barak, 1982; Abadía et al., 1989), which may result in a reduction in CO₂-assimilation rate.

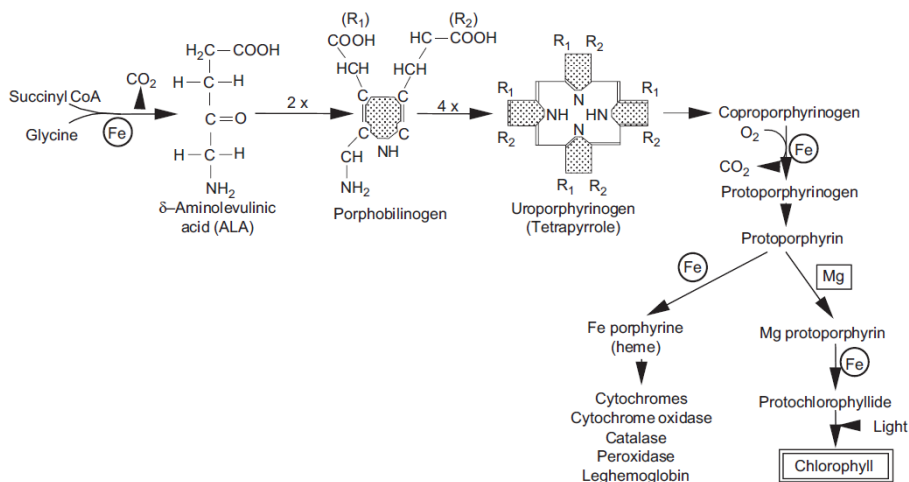


FIGURE 2.1 Role of Fe in the biosynthesis of heme coenzymes and chlorophyll (From Marschner Mineral Nutrition).

As a general rule, Fe deficiency has less effect on leaf growth, cell number per unit area, or number of chloroplasts per cell than on the size of the chloroplasts and protein content per chloroplast (Terry et al., 1980). The element is required for protein synthesis, and the number of ribosomes actually decreases in Fe-deficient leaf cells (Lin and Stocking, 1978). In sugar beet leaves, Fe is important for RNA synthesis and a decrease in Fe concentration is associated with a strong decrease in protein synthesis (Nishio et al., 1985). Decreases in leaf protein content under Fe deficiency are particularly

pronounced for the Rubisco protein that represents nearly 50% of the chloroplast soluble proteins (Ellis, 1979; Larbi et al., 2006).

In the thylakoid membranes, about 20 Fe atoms are directly involved in the electron transport chain. Photosystem I (PS-I) is a strong sink for Fe due to its higher Fe content (12 atoms of Fe per complex) compared to photosystem II (PS-II) (3 atoms of Fe per complex) and the Cyt b_f complex (5 atoms of Fe per complex) (Raven et al., 1999). The high Fe requirement for the structural and functional integrity of the thylakoid membranes, and the additional Fe requirement for ferredoxin and the biosynthesis of chlorophyll explain the particular sensitivity of chloroplasts in general, and the thylakoids in particular, to Fe deficiency (Helch-Buchholz et al., 1986).

More in details, Chlorophyll is formed in higher plants starting from δ -amino-levulinic acid (ALA), a precursor for both heme and chlorophyll formation, which may be synthesized through a 5-carbon substrate, such as a ketoglutarate or glutamate. This primary pathway may be activated by Fe, related to aconitase activity and/or the formation of ferredoxin (Fd). Ferredoxin could be necessary to activate the ALA-synthesizing enzyme. With plants that are Fe-stressed, Fd would be limiting and directly affect Chl biosynthesis (Miller et al., 1984). Decrease in photosynthetic activity induced by Fe deficiency is also associated with a further decrease in the concentration of light-harvesting complexes (LHCs) and electron-transport carriers (Terry, 1980; Abadía et al., 1989; Pérez et al., 1995; Donnini et al., 2009). In particular, a decrease in thylakoid protein was observed in chlorotic leaves, with the result that PS-I appeared more affected than cytochrome b_6f , which in turn was more sensitive than PS-II (Soldatini et al., 2000). On the other hand, a reduction in Chl

concentration diminished the number of photosynthetic units per unit leaf area (Spiller and Terry, 1980).

In Fe-deficient leaves, however, not all photosynthetic pigments and components of the electron transport chain decrease to the same extent (Pushnik and Miller, 1989). Carotenoids such as β -carotene and neoxanthin also show significant decreases, whereas lutein and the three xanthophylls (violaxanthin, antheraxanthin, and zeaxanthin) involved in the xanthophyll cycle seem to be less affected (Morales et al., 1994; Donnini et al. 2003, 2009). When Fe is resupplied to Fe-deficient plants, they recover progressively from Fe deficiency and the photosynthetic pigments and the components of photosystems are gradually resynthesized (Nishio et al., 1985; Hecht-Buchholz and Ortmann, 1986; Pushnik and Miller, 1989). López-Millán et al. (2001) showed that Fe resupply to Fe-deficient sugar beet increased first leaf Fe concentration and later, after a short lag-phase, the Chl concentration.

Chlorophyll (Chl) fluorescence is a non-invasive technique employed to measure photosynthesis in leaves, widely used to study plant's response to abiotic stresses. In fact, Chl fluorescence parameters can be efficiently used to evaluate changes in photosystem II photochemistry, linear electron transport rate and CO₂ assimilation *in vivo* (Guidi et al., 2012). Determination of Chl fluorescence has been widely used to study photosynthetic performance in different species subjected to Fe deficiency, such as sugar beet (Belkhodia et al., 1998), pear (Morales et al., 2000), peach (Molassiotis et al., 2006), poplar (Solti et al., 2008) and cucumber (Donnini et al., 2013). Chl-fluorescence analysis in pear (Morales et al., 2000), tomato (Donnini et al., 2003), peach (Molassiotis et al., 2006), and pea (Jelali et al., 2011) revealed a general increase

in nonphotochemical quenching (qNP) in chlorotic leaves, indicating the activation of photoprotective mechanisms which, however, are not sufficient to prevent photoinhibition, as indicated by a significant reduction in maximal PSII photochemistry (Fv/Fm) and photochemical quenching (qp). The actual quantum yield of PSII (Φ_{PSII}) and the intrinsic PSII efficiency (Uexc) showed the same behavior of qp and Fv/Fm ratio. Interestingly, Morales et al. (2000) showed that only extreme Fe-deficient leaves exhibited a decrease in PSII efficiency after dark adaptation, while moderate chlorotic leaves appeared generally little affected.

Materials and Methods

Plant material and growth conditions

Seeds of cucumber (*Cucumis sativus* L. cv. Marketmore '76) were surface-sterilized and sown in Agriperlite, watered with 0.1 mM CaSO₄, allowed to germinate in the dark at 26°C for 3 d, and then transferred to a nutrient solution with the following composition: 2 mM Ca(NO₃)₂, 0.75 mM K₂SO₄, 0.65 mM MgSO₄, 0.5 mM KH₂PO₄, 10 μM H₃BO₃, 1 μM MnSO₄, 0.5 μM CuSO₄, 0.5 μM ZnSO₄, 0.05 μM (NH₄)₂MoO₇ and 0.1 mM Fe(III)-EDTA (when added). The pH was adjusted to 6.2 with NaOH. Aerated hydroponic cultures were maintained in a growth chamber with a day:night regime of 16:8 h and a photosynthetic photon flux density (PPFD) of 200 μmol m⁻² s⁻¹ photosynthetically active radiation (PAR) at the plant level. The temperature was 18°C in the dark and 24°C in the light. For the time-course experiments, 3 d-old plants grown in the nutrient solution were transferred, after removal of cotyledons, to 10 L of the same solution without Fe (Fe-deprived plants). Roots of these plants were carefully washed

with 0.5 mM CaSO₄ and rinsed with distilled water before being transferred. Other 3-day-old plants grown in the nutrient solution without Fe were transferred of the complete solution (Fe-resupplied plants). Sampling was performed after 0, 1, 3 and 7 days following induction/removal of Fe deficiency and 4 h after onset of the photoperiod. For clarity, plants previously grown in the presence/absence of Fe for 3 d and then transferred to a Fe-free/complete solution are hereby referred to as 0 throughout the text.

Fe-deficient plants showed the typical Fe deficiency morphological responses (development of leaf Fe deficiency chlorosis, stunted growth and appearance of lateral roots) and the increase in the specific activities (Fe³⁺-chelate reductase and H⁺-ATPase) proper of Strategy I plants (data not shown).

Photosynthesis measurements

Leaf gas exchange measurements were taken during 7 days of the experiment to characterize photosynthesis performance and gas exchange measurements with a portable photosynthesis system (CIRAS-2, PP System, USA). Measurements were carried on fully expanded, intact leaves of Fe sufficient and Fe deficient plants. Net CO₂ assimilation rate and transpiration were assessed at a concentration of 330 μmol CO₂, ambient relative humidity, 28° C chamber temperature and a photon flux density of 1500 μmol m⁻²s⁻¹. The instrument was stabilized according to manufacturer guidelines.

Gas exchanges measurements

Gas exchanges were measured in intact leaves using a portable infrared gas analyzer (LI-6400; Li-Cor, Lincoln, NE, USA). Measurements were performed at increasing light from

0 to 2500 $\mu\text{mol m}^{-2} \text{s}^{-1}$ PPFD (photosynthetic photon flux density) at leaf temperature of 25 °C, either with air (21% of O_2) or a synthetic air mixture containing <2% O_2 where O_2 was replaced by N_2 . In both the cases, the air flow ($300 \mu\text{mol s}^{-1}$) was humidified by bubbling it in water whose temperature was maintained lower than that of the leaf surface. When the synthetic air with <2% O_2 was utilized, O_2 from the bubbling solution was carefully removed by blowing the same synthetic air mixture for 10 min. Photosynthesis (A), stomatal conductance (G_s), and the intercellular CO_2 concentration (C_i) were calculated using the LI-6400 software. Quantum yield for CO_2 uptake was determined as the slope of the linear regression of CO_2 assimilation versus light intensity above 100 $\mu\text{mol photons m}^{-2} \text{s}^{-1}$. Responses of A to changes in C_i were measured at a PPFD of 1000 $\mu\text{mol m}^{-2} \text{s}^{-1}$ and $[\text{CO}_2]$ increasing from 50 to 1800 $\mu\text{mol mol}^{-1}$. Measurements started with the lowest $[\text{CO}_2]$ to remove stomatal limitations of Pn (Centritto et al., 2003). Gas exchange parameters obtained from A/ C_i curves were calculated with the equation reported in von Caemmerer and Farquhar (1981).

Analysis of the chlorophyll a fluorescence

Chlorophyll fluorescence measurements were performed with a modulated light fluorimeter (PAM-2000 Walz, Effeltrich, Germany), which differs from the conventional fluorimeters as the source which excites the fluorescence, and the one that causes the photosynthesis (actinic light) are separated to avoid interference with the light of the external environment. The F_0 were recorded in a dark-adapted state of leaves for 40 min. The frequency of the light pulses was programmed at 600 Hz for the determination of F_0 or 20000 Hz for the recording of the kinetics of induction of fluorescence. The maximum fluorescence yield, F_m , was determined with a saturating pulse

of $8000 \mu\text{mol m}^{-2} \text{s}^{-1}$ PAR for 1-2 s. F_0 and F_m were subtracted and divided $[(F_m - F_0)/F_m]$ to draw the maximum quantum efficiency of PSII photochemistry F_v/F_m . The current fluorescence yield (F_t) and the maximum light adapted fluorescence (F_m') were determined in the presence of an actinic illumination of $400 \mu\text{mol m}^{-2} \text{s}^{-1}$, then Φ_{PSII} was computed as the quotient $[(F_m' - F_t)/F_m']$ (Genty et al. 1989). The coefficients of photochemical quenching, q_p , was calculated as $QP = (F_m' - F_t)/(F_m' - F_0')$ according to Schreiber et al. (1986). NPQ was calculated as $NPQ = (F_m - F_m')/F_m$ as reported by Bilger and Björkman (1990). The apparent electron transport rate (ETR) was determined as $0.5 \times \Phi_{\text{PSII}} \times \text{PAR} \times 0.84$ where 0.5 accounted for the excitation of both PSII and PSI and 0.84 represented the average value for leaf absorbance.

The fluorometer was linked with a claw (2030-B Heinz Walz, Germany), which was inserted in an optical tri-forked fiber, which collected the receiving fluorescence. The optical fiber was positioned in the clamp with an angle of 60° to the plane of the sample in order to minimize the so-called "shadow effect" and its distance from the sample could be varied to allow adjustment intensity of light gradient. Furthermore the claw bears a thermocouple (temperature sensor) and a device for the measurement of PAR (Photosynthetically Active Radiation), both located in the interface where the leaf was placed. To record the kinetics of fluorescence induction this tool was connected to an IBM compatible computer. The data processing was done through a specific software supplied from the Waltz (DA-2000).

Fluorescence was excited with modulated very weak red light ($\lambda=650\text{nm}$) emitted by diodes (LED). Before reaching the sample to be analyzed, the light passed through a filter ($\lambda < 670$

nm), while the fluorescence emitted from the leaf was monitored by a photo detector protected by another filter which let pass the wavelength light $\lambda=700\text{nm}$.

Inside the main control device there were five other diodes that emit red actinic light, unfiltered and with a peak at $\lambda=655\text{nm}$ and another LED for emitting light in the "red-far", with a peak at $\lambda=735\text{nm}$. A halogen lamp was used to generate pulses saturating and lighting continues to actinic light white.

Kinetics of induction of fluorescence

For the determination of F_0 , F_m , F_v , the leaves were kept in the dark for about 60 minutes in order to allow the complete oxidation of the primary acceptor PSII (Qa) and initially exposed to an intensity of low modulated light (about $0.4 \text{ mol m}^{-2}\text{s}^{-1}$) that cause the emission of F_0 but not activate the electron transport chains. Subsequently exposure to a saturating white light ($15000\mu\text{mol m}^{-2} \text{ s}^{-1}$ for 0.8 s) causing the complete reduction of Qa and thus allow the determination of F_m . From the parameters thus determined it was obtained the F_v/F_m ratio ($F_v = F_m - F_0$), which represents the quantum optimal yield of PSII.

Quenching analysis measurements was performed by the method of the pulses of saturant light as described before (Schreiber et al., 1986), which is based on the complete reduction of the primary acceptor of PSII (Qa) during steady state of photosynthesis, maintaining the leaf in continuous actinic light ($150 \text{ mol m}^{-2} \text{ s}^{-1}$) and then overlapping the light intermittent pulses ($15000\mu\text{mol m}^{-2} \text{ s}^{-1}$ for 0.8 s): this cause the complete reduction of Qa. Complete removal of the photochemical quenching (qP) brings to an increase of the fluorescence varies from F_v to F_m (which corresponds to the value of the maximum fluorescence for the sample adapted to

light) and each remaining shape of quenching was thus assumed to be the type not photochemical (QNP). Since background fluorescence (F_0) is frequently suppressed during exposure to intense light, the calculation of the components of quenching was performed using F_0' (the value of the minimal fluorescence for a sample adapted to light). F_0' was determined by the exposure of the leaf for 3 seconds to “far-red” light, which excites especially the PSI, and then, indirectly, causes oxidation of PSII primary acceptor allowing thus to determine the minimal fluorescence emitted by the latter.

More in details, the components of the quenching were calculated following the formulas described by Schreiber et al. (1986):

$$qP = (F_m' - F_t) / (F_m' - F_0')$$

$$QNP = 1 - (F_m' - F_0') / (F_m - F_0)$$

Another illustration of nonphotochemical quenching is given by the parameter NPQ, calculated through equation:

$$NPQ = (F_m - F_0') / F_m$$

The choice between QNP and NPQ depends on the applications: the NPQ stands out that part of the non-photochemical quenching that reflects the excitation energy dissipation into heat in the antenna systems and does not require knowledge of F_0' , but it is not very sensitive to the fraction correlated with the energization of the thylakoid membranes.

Other important parameters associated with the analysis of the quenching and correlated with photosynthesis, are the effective quantum yield of PSII (ϕ_{psII}) and excitation efficiency of PSII (ϕ_{exc}). The first parameter was calculated as the ratio

$\Delta F_m'$ (where $D_f = F_m' - F_t$) and can be considered the most important information obtained from the instrument used, since its value closely related to the quantum yield of photosynthesis.

The other important parameter, the excitation efficiency of PSII, which measures the efficiency of photons absorption by open PSII-HLC distribution centers, is calculated as the ratio between F_v' and F_m' ($F_v' = F_m' - F_0'$) (Donnini et al., 2003).

Results.

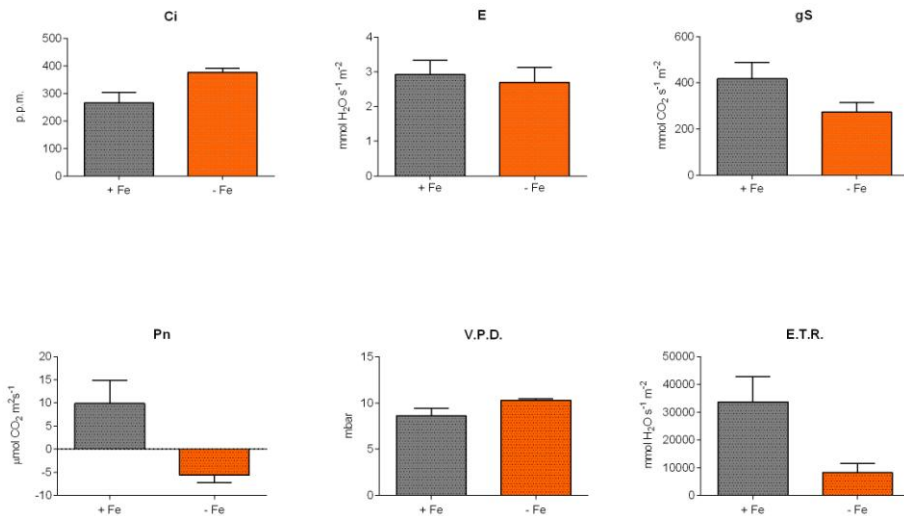


Figure 2.2 *In vivo* measurement of photosynthetic parameters, carried out on plants grown for 10 d in the presence or absence of Fe (50-0 mM) for 10 d. CIRAS-2 (PP system) FMS-2 (Hansatec).

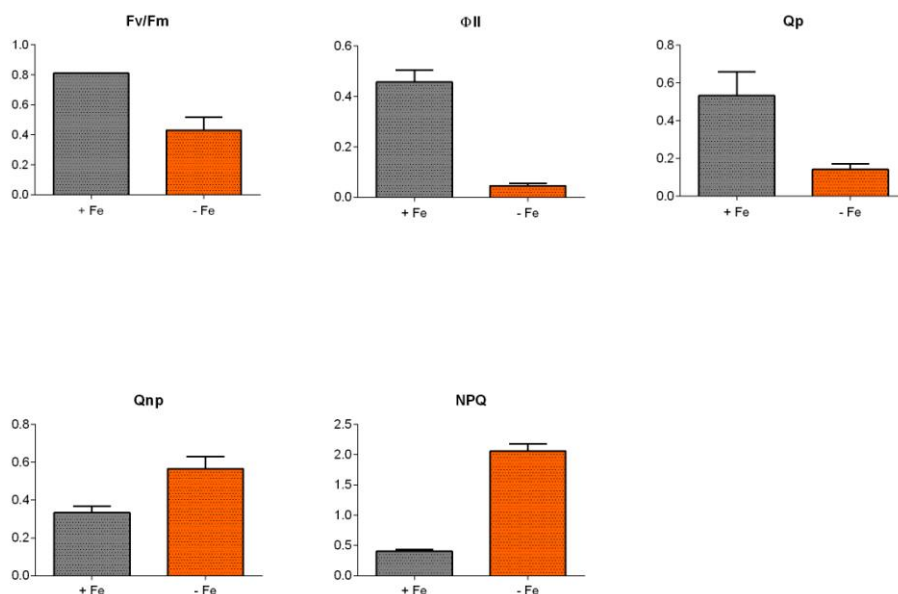


Figure 2.3 *In vivo* measurement of chlorophyll fluorescence parameters, carried out on plants grown for 10 d in the presence or absence of Fe (50-0 mM). PAM-2000 (Waltz, Effelrtich).

As described in Figure 2.2, after 10 days of Fe deficiency cucumber plants shows *in vivo* alterations of photosynthetic parameters, such as internal [CO₂] (Ci), net photosynthesis (Pn), stomatal conductance (Gs) and apparent electron transport rate (E.T.R.). More in details, the deficiency of this element results in a significant increase of Ci, whereas stomatal conductance and values of apparent electron transport rate decrease. Interestingly, we observe a remarkable decrease of Pn, which appears to be negative. No further significant variations are observed regarding evaporation/transpiration (E) and vapor pressure deficit (V.P.D.).

Further *in vivo* analysis allows us to determine the chlorophyll

a fluorescence. In particular, after 10 days of Fe deficiency, cucumber plants show a decrease in the Fv/Fm ratio, in the quantum yield of PSII (Φ PSII) and in the photochemical quenching. On the contrary, we see an increase in the non-photochemical quenching (Qnp), and also in the component that reflects the excitation energy dissipation into heat from the antenna systems (NPQ).

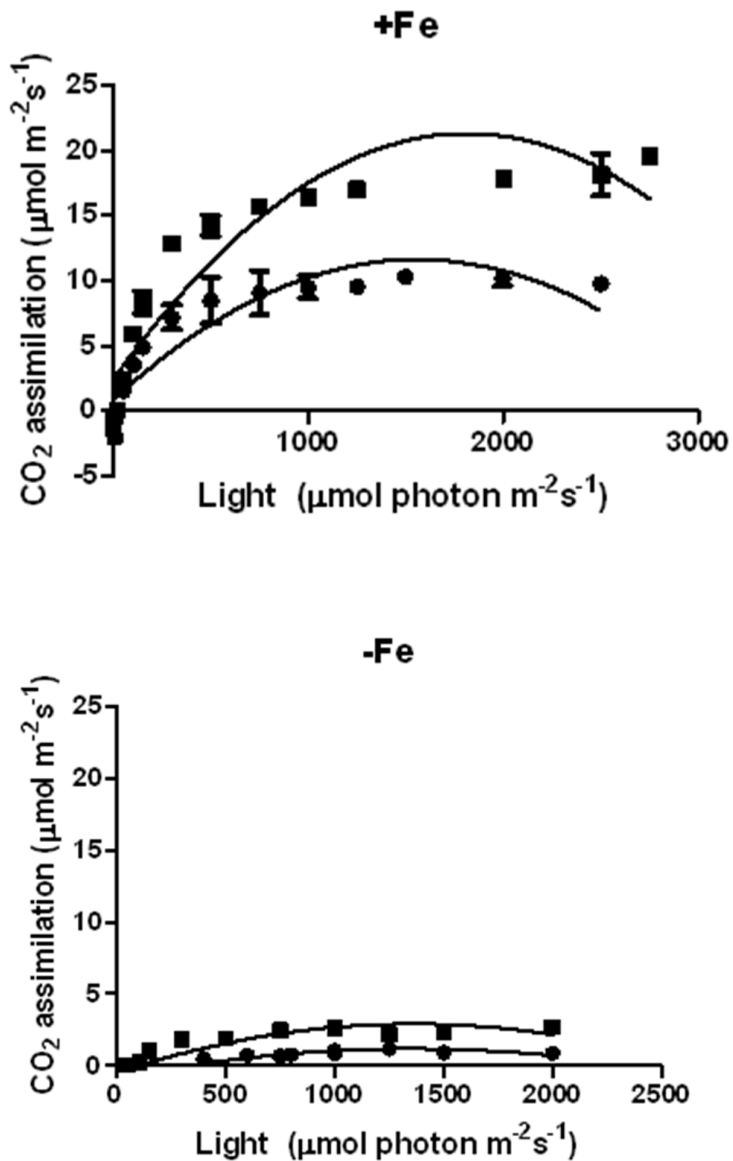


Figure 2.4 Response curve of the photosynthetic activity according to the light under conditions of 21% O₂ (round symbol) and in the absence of O₂ (square symbol). Plants were grown hydroponically for 10 d, in the presence (50mM, up sheet) or absence of Fe (0mM, down).

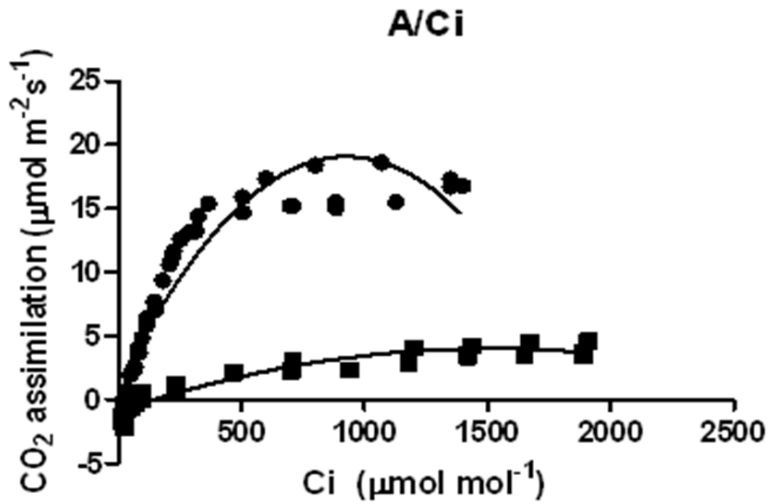


Figure 2.5 Response curve of the photosynthetic activity according to the intercellular concentration of CO₂ in leaves of control plants (round) and Fe deficiency (square).

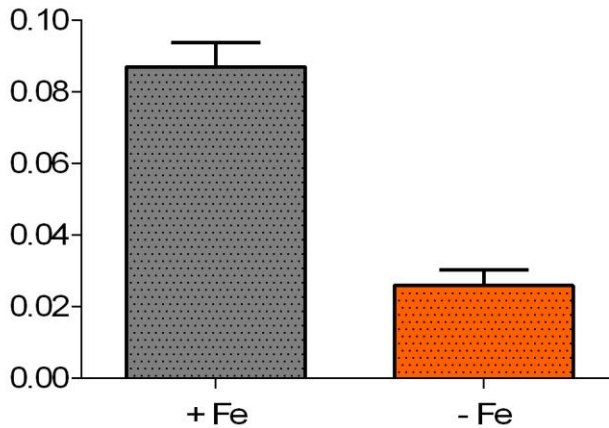


Figure 2.6 *In vivo* carboxylase activity of Rubisco. This data was calculated starting from the response curve of the photosynthetic activity according to the intracellular concentration of CO₂, as reported in figure 2.5.

VARIABLES	+Fe +O ₂	+Fe -O ₂	-Fe +O ₂	-Fe -O ₂
R_d ($\mu\text{mol CO}_2 \text{ m}^{-2} \text{ s}^{-1}$)	1.6 (0.7) a	1.2 (0.7) a	1.2 (0.2) a	1.2 (0.2)a
A_{390} ($\mu\text{mol CO}_2 \text{ m}^{-2} \text{ s}^{-1}$)	10.4 (0.2) b	18.2 (1.5) a	1.7 (0.7) c	2.4 (0.2) c
g_s ($\text{mmol H}_2\text{O}_2 \text{ m}^{-2} \text{ s}^{-1}$)	233.8 (22.4) a	253.0 (15.6) a	110.5 (3.5) b	158.5 (14.9) b
C_i ($\mu\text{mol CO}_2 \text{ mol}^{-1} \text{ air}$)	283.5 (13.1) b	247.5 (10.0) c	367.0 (1.4) a	354.5 (0.7) a
Φ_{CO_2} ($\mu\text{mol CO}_2 \mu\text{mol}^{-1} \text{ photons}$)	0.05 (0.01) a	0.07 (0.01) a	0.008 (0.004) a	0.012 (0.002) a
V_{cmax} ($\mu\text{mol CO}_2 \text{ m}^{-2} \text{ s}^{-1}$)	0.087 (0.007) a	0.026 (0.004) b		

Table 2.1. Gas Exchange parameters variations determined in normal condition or in a low [O₂] atmosphere. R_d : dark respiration; A_{max} : assimilation of CO₂ under saturating light; G_s : stomatal conductance to CO₂; C_i : intercellular concentration CO₂; Φ_{CO_2} : quantum yield of the assimilation of CO₂; V_{Cmax} : carboxylative efficiency of Rubisco. Standard deviation is reported between round brackets.

The estimation of photorespiration is determined in conditions of absence of oxygen (<2%), results are reported in table 2.1. In the control plants, a significant increase in photoassimilation of CO₂ was recorded to indicate that in these plants photorespiration contributes 43% to the decrease of CO₂ assimilated. The measurement of the CO₂ treated in conditions of absence of oxygen did not shows any significant increase in the rate of CO₂ assimilation in plants grown in Fe deficiency both in aerobic conditions that anaerobiosis. However, further analysis are strictly required in order to reduce the variability among the repetition: in Fe deficiency condition we recorded an increase in the rate of CO₂ assimilation rate in many biological repetition (+29%).

In addition, the rate of CO₂ assimilation is significantly reduced in Fe deficient plants (-84%). This was probably attributable to stomatal closure (g_s passes from 234 to 110 $\text{mmol H}_2\text{O m}^{-2}\text{s}^{-1}$) but also to an altered activity of the

mesophyll whereas the there in Fe deficient plants increased significantly. In these plants the reduction in stomatal aperture restricts the entry of CO₂. However, the increase in the level indicates that there was a mesophyll reduced utilization of CO₂. On the other hand the V_{Cmax} was significantly reduced, indicating a reduced activity of this carboxylative enzyme (-70%), as reported also in fig. 2.6.

The reduced ability of assimilation of Fe deficient plants was evident both in light conditions that saturating light conditions limiting. In fact, the ΦCO₂ is significantly reduced, indicating a poor efficiency of the use of CO₂ per mole of absorbed photons.

VARIABLES	+Fe +0 ₂	-Fe +0 ₂	<i>P</i>
F_0	196 (12)	330 (24)	***
F_m	993 (14)	550 (38)	***
F_v/F_m	0.81 (<0.01)	0.43 (0.09)	***
ETR (μmol electron m ⁻² s ⁻¹)	110.7 (26.4)	13.5 (1.7)	***
Φ_{PSII}	0.46 (0.05)	0.05 (<0.01)	***
q_P	0.53 (0.13)	0.14 (0.03)	***
q_{NP}	0.33 (0.04)	0.57 (0.07)	***
NPQ	0.41 (0.03)	2.06 (0.12)	***

Table 2.2. Chlorophyll fluorescence parameters variations F₀: minimal fluorescence determined in dark conditions; F_m: maximal fluorescence determined in dark conditions; F_v/F_m: potential quantum yield of PSII; ETR: rhythm of electronic transport; ΦPSII: current efficiency of PSII (in light conditions); q_P coefficient of photochemical quenching; QNP: coefficient of non-photochemical quenching; NPQ: non-photochemical quenching. Standard deviation is reported between round brackets.

As determined by the gas exchange parameters, the reduction

of CO₂ assimilation was probably attributable, to a reduced stomatal conductance, but also to an altered activity of the mesophyll. The results obtained from the chlorophyll fluorescence analysis seem to validate this hypothesis (see table 2.2). In fact, the photochemical efficiency of PSII in conditions of light significantly decreased in Fe-deficient plants reaching activity values practically negligible. The inevitable consequence of the reduced activity of PSII photochemistry was highlighted by the pronounced reduction in the rate of electron transport (ETR). In the Fe-deficient plants it was also evident a significant increase in the NPQ parameter, closely linked with the energy excess dissipating mechanism in the PSII antenna systems. The NPQ presents a main component determined by qE, namely the mechanisms of dissipation of the excess energy associated with the formation of the gradient of trans-thylakoid membrane. This mechanism is connected with the conversion of the reaction centers from active form to inactive. The precise site of NPQ formation is not yet known but certainly involves carotenoids and, specifically, the xanthophylls, lutein and neoxanthin. The results obtained also shows that the mechanisms described above induce a significant reduction in maximum efficiency of PSII (Fv/Fm) attributable to the increased value of the minimum chlorophyll fluorescence F₀. The increase of this value indicates that in the antenna centre, most of the energy absorbed is dissipated and not used for the photosynthetic process. With the data obtained it was not possible to identify whether the reduction in the efficiency of PSII photochemistry was reversible or not. What appears certain is that much of the reaction centers of PSII are strongly inactivated (significant increase in the qP).

Discussion

From the data obtained in our experiments, it appears clear that Fe-deficiency strongly impairs the photosynthetic machinery at different levels. This is probably attributable first to a lack in the biosynthesis of chlorophyll. In fact Fe is strictly required as cofactor from many enzymes involved in this metabolic pathway. Further damage can be induced since in thylakoids, about 20 Fe atoms are directly involved in the electron transport chain. Photosystem I (PS-I) is also a strong sink for Fe due to its higher Fe content (12 atoms of Fe per complex) compared to photosystem II (PS-II) (3 atoms of Fe per complex) and the Cyt b_f complex (5 atoms of Fe per complex) (Raven et al., 1999). The high Fe requirement for the structural and functional integrity of the thylakoid membranes, and the additional Fe requirement for ferredoxin and the biosynthesis of chlorophyll explain the particular sensitivity of chloroplasts in general, and the thylakoids in particular, to Fe deficiency (Helch-Buchholz et al., 1986). Taken all together, our data allow us to suggest that Fe deficiency leads to a strong impairment of the photosynthetic apparatus at different levels. It appears clear that the reaction centers of PS-II are largely inactive. Performed Chl-fluorescence analysis revealed a general increase in nonphotochemical quenching (qNP) in chlorotic leaves, indicating the activation of photoprotective mechanisms which, however, are not sufficient to prevent photoinhibition, as indicated by a significant reduction in maximal PSII photochemistry (F_v/F_m) and photochemical quenching (qp). These findings are in agreement with previous in other species, pear (Morales et al., 2000), tomato (Donnini et al., 2003), peach (Molassiotis et al., 2006), and pea (Jelali et al., 2011). In Fe deficiency condition we recorded an increase in the rate of CO_2 assimilation rate in many biological

repetition (+29%), suggesting a possible induction of photorespiratory metabolism. However, the variation is not significant and so further analysis are strictly required in order to reduce the variability among the repetition to get a more get a more reliable result. In addition, the reduction of CO₂ assimilation can be also attributable to a reduced stomatal conductance, but also to an altered activity of the mesophyll. The results obtained from the chlorophyll fluorescence analysis seem to validate these latter hypothesis.

References

- Abadía, A., Le Moine, Y., Trémolières, A., Ambard-Bretteville, F., Rèmej, R. (1989): Iron deficiency I in pea: Effects on pigment, lipid and pigment-protein complex composition of thylakoids. *Plant Physiol. Biochem.* 27, 679–687.
- Abadía, J., Morales, F., Abadía, A. (1999): Photosystem II efficiency in low chlorophyll, iron-deficient leaves. *Plant Soil* 215, 183–192.
- Belkhodja, R., Morales, F., Quilez, R., Lopez-Millan, A. F., Abadia, A., Abadia, J. (1998): Iron deficiency causes changes in chlorophyll fluorescence due to the reduction in the dark of the Photosystem II acceptor side. *Photosynth. Res.* 56, 265–276.
- Centritto M., Loreto F., Chartzoulakis K.; (2003) The use of low [CO₂] to estimate diffusional and non-diffusional limitations of photosynthetic capacity of salt stressed olive saplings. *Plant, Cell & Environment*, 26: 585-594.
- Chen, Y., Barak, P. (1982): Iron nutrition of plants in calcareous soils. *Adv. Agron.* 35, 217–240.
- Donnini S., Castagna, A., Guidi, L., Zocchi, G., Ranieri, A. (2003): Leaf responses to reduced iron availability in two tomato genotypes: T3238FER (iron efficient) and T3238fer (iron inefficient). *J. Plant Nutr.* 26, 2137–2148.

Donnini S., Castagna, A., Ranieri, A., Zocchi, G. (2009): Differential responses in pear and quince genotypes induced by Fe deficiency and bicarbonate. *J. Plant Physiol.* 166, 1181–1193.

Donnini S., Guidi L., Degl'Innocenti E. and Zocchi G., Image changes in chlorophyll fluorescence of cucumber leaves in response to iron deficiency and resupply. *J. Plant Nutr. Soil Sci.* 2013, 176, 734–742.

Guidi, L., Degl'Innocenti, E. (2012). Chlorophyll a fluorescence in abiotic stress. In *Crop Stress and its Management: Perspectives and Strategies* (pp. 359-398). Springer Netherlands.

Hecht-Buchholz, C. H., Ortmann, U. (1986): Effect of foliar iron application on regreening and chloroplast development in iron chlorotic soybean. *J. Plant Nutr.* 9, 647–659.

Jelali, N., Salah, I. B., M'sehli, W., Donnini, S., Zocchi, G., Gharsalli, M. (2011): Comparison of three pea cultivars (*Pisum sativum*) regarding their responses to direct and bicarbonate-induced iron deficiency. *Sci. Hort.* 129, 548–553.

Larbi, A., Abadía, A., Abadía, J. and Morales, F. (2006). Down co-regulation of light absorption, photochemistry, and carboxylation in Fe-deficient plants growing in different environments. *Photosynth. Res.* 89, 113–126.

Lin, C. H. and Stocking, C. R. (1978). Influence of leaf age, light, dark and iron deficiency on polyribosome levels in maize leaves. *Plant Cell Physiol.* 19, 461–470.

López-Millán, A. F., Morales, F., Abadía, A., Abadía, J. (2001): Changes induced by Fe deficiency and Fe resupply in the organic acid metabolism of sugar beet (*Beta vulgaris* L.) leaves. *Physiol. Plant.* 112, 31–38.

Miller G.W., Pushnika J.C., Welkiea G.W. Iron chlorosis, a worldwide problem, the relation of chlorophyll biosynthesis to iron; *Journal of Plant Nutrition Volume 7, Issue 1-5, 1984 Special Issue: Iron Nutrition and Interactions in Plants*

Molassiotis, A., Tanou, G., Diamantidis, G., Patakas, A., Therios, I. (2006): Effects of 4-month Fe deficiency exposure on Fe reduction

mechanism, photosynthetic gas exchange, chlorophyll fluorescence and antioxidant defense in two peach rootstocks differing in Fe deficiency tolerance. *J. Plant Physiol.* 163, 176–185.

Morales, F., Abadía, A., Belkhodja, R., Abadía, J. (1994): Iron deficiency induced changes in the photosynthetic pigment composition of field grown pear (*Pyrus communis* L.) leaves. *J. Plant Nutr.* 17, 1153–1160.

Morales, F., Belkhodja, R., Abadía, A., Abadía, J. (2000): Photosystem II efficiency and mechanisms of energy dissipation in iron-deficient, field grown pear trees (*Pyrus communis* L.). *Photosynth. Res.* 63, 9–21.

Nishio, J. N., Abadía, J., Terry, N. (1985): Chlorophyll-proteins and electron transport during iron nutrition-mediated chloroplast development. *Plant Physiol.* 78, 269–299.

Pérez, C., Val, J., Monge, E. (1995): Effects of iron deficiency on photosynthetic structures in peach (*Prunus persica*) leaves, in Abadía, J. (ed.): Iron Nutrition in Soil and Plants. Kluwer Academic Publishers, Dordrecht, The Netherlands, pp. 183–189.

Pushnik, J. C., Miller, G. W. (1989): Iron regulation of chloroplasts photosynthetic function: Mediation of PS I development. *J. Plant Nutr.* 12, 407–421.

Raven, J. A., Evans, M. C. W. and Korb, R. E. (1999). The role of trace metals in photosynthetic electron transport in O₂-evolving organisms. *Photosynth. Res.* 60, 111–149.

Soldatini, G. F., Tagliavini, M., Baldan, B., Castagna, A., Ranieri, A. (2000): Alterations in thylakoid membrane composition induced by iron starvation in sunflower plants. *J. Plant Nutr.* 23, 1717–1732.

Solti, A., Gaspar, L., Meszaros, I., Szigeti, Z., Levai, L., Sarvari, E. (2008): Impact of iron supply on the kinetics of recovery of photosynthesis in Cd-stressed poplar (*Populus glauca*). *Ann. Bot.* 102, 771–782.

Spiller, S., Terry, N. (1980): Limiting factors in photosynthesis. Iron stress diminishes photochemical capacity by reducing the number of photosynthetic units. *Plant Physiol.* 65, 121–125.

Terry, N. (1980): Limiting factors in photosynthesis. Iron stress mediated changes in light-harvesting and electron transport capacity and its effects on photosynthesis *in vivo*. *Plant Physiol.* 71, 885–860.

Von Caemmerer S., Farquhar G.D.; (1981) Some relationships between the biochemistry of photosynthesis and the gas exchange of leaves. *Planta* (1981) 153: 376-387.

CHAPTER III

Iron deficiency alters the amminoacid content and the ion composition in the leaves of cucumber plants.

Highlights

Iron (Fe) deficiency affect amminoacid (aa) metabolism since the concentration of Ser and Gly, two aa involved in the photorespiratory metabolism, increased in leaves (+94% and +160%, respectively) while it decreased in root during the evolution of Fe deficiency in time. Resupply of iron to Fe deficient plants led to an increase in the concentration of some divalent cations like Fe, Ca and Mn, whilst Na, Mg, Cu, Zn decrease as Fe sufficient condition are restored. On the other hand, as Fe deficiency proceeds during time, we observed a significant decrease in Fe, Mo, Cu concentration and an increase in Na, Mg, Zn, Mn content.

Abstract

Fe deficiency is a well-documented problem affecting crop production worldwide, in particular in calcareous soils of Mediterranean basin countries (Pestana et al., 2004). Fe-deficient plants are characterized by the development of a pronounced chlorosis occurring first on the youngest leaves and causing various morphological and physiological changes in plants. However, like many others abiotic stresses Fe deficiency, do not result in uniform symptoms. Among other effects, the lack of Fe strongly impairs photosynthetic processes by affecting the structure, development and function of the entire photosynthetic apparatus (Terry and Abadía, 1986 and Abadía et al., 1999). Its reduced bioavailability also strongly prejudices mitochondrial respiration. These two processes are responsible for the energetic support of the cell and therefore of the whole plant life. A shortage of Fe so determine an energetic emergency in the cell which results in reduced growth of the entire plant and so in a lower yield of crops.

Since this deficiency alters two important physiological processes like photosynthesis and photorespiration, we decided to perform a series of analysis on leaf tissues of Fe-deficient leaves in order to fill out the general form of the metabolic changes. Fe deficiency strongly affected amino acid (aa) metabolism. Especially, the concentration of Ser and Gly, two aa involved in the photorespiratory metabolism, increased in leaves (+94% and +160%, respectively) while it decreased in root, during the evolution of Fe deficiency in time. Resupply of iron to Fe-deficient plants led to an increase in the concentration of some divalent cations like Fe, Ca and Mn, whilst Na, Mg, Cu, Zn decrease as Fe sufficient condition are restored. No significant variations are observed in these experimental conditions for Mo, K and Pb. On the other hand, as Fe deficiency proceeds during time, we observed a significant decrease in Fe, Mo, Cu concentration and an increase in Na, Mg, Zn, Mn content. In these conditions, no significant variations were detected in the concentration of Pb and K.

These data, together with previous, allow us to suggest that Fe deficiency strongly affected aa metabolism. The accumulation of Ser and Gly might be due to an alteration in the photorespiratory metabolism at the GDC-SHMT1 cycle in the mitochondria of the -Fe plant. The alterations in the concentrations of metals suggest that Fe deficiency induces a metabolic imbalance in which other divalent cations are absorbed by unspecific transporter, due to their similar characteristics to Fe, this can affect the metabolism of the plant at different levels.

Introduction

Fe deficiency is a well-documented problem affecting crop production worldwide, in particular in calcareous soils of

Mediterranean basin countries (Pestana et al., 2004). Fe-deficient plants are characterized by the development of a pronounced chlorosis occurring first on the youngest leaves and causing various morphological and physiological changes in plants. Among other effects, the lack of Fe strongly impairs photosynthetic processes by affecting the structure, development and function of the entire photosynthetic apparatus (Terry and Abadía, 1986 and Abadía et al., 1999). It has been shown that Fe deficiency leads to a decrease in the light-harvesting pigments, particularly chlorophylls (Morales et al., 2000), and promotes antenna disconnection in PSII (Morales et al., 2001, Moseley et al., 2002). Additionally, Fe-deficient leaves show lower actual PSII efficiency (ϕ_{II}) and a decrease in the proportion of open PSII reaction centers (qp) (Larbi et al., 2006). However, many abiotic stresses, including also Fe deficiency, do not result in uniform symptoms, but rather on patches of visible injuries on leaf surfaces, more drastic in mesophyll leaf areas than in midrib and veins in the case of this deficiency. It was also shown that Fe-deficient leaves accumulated more Fe in the midrib and veins, with lower Fe concentration in mesophyll leaf areas (Jiménez et al., 2009 and Tomasi et al., 2009). Thus, this heterogeneous distribution of photosynthetic pigments and Fe in leaves could equally affect the photosynthetic efficiency.

Various authors reported that Fe resupply to deficient plants restores many plant functions. For instance, it leads within a few days to an increase in chlorophyll concentration and photosynthetic activity in several annual species, including sugar beet (Nishio et al., 1985 and Larbi et al., 2004), soybean (Hecht-Buchholz and Ortman, 1986) and tobacco (Pushnik and Miller, 1989). It was also recorded that tolerance to Fe deficiency may vary between different varieties of the same species, and the capacity to recover from this stress was

related with sensitivity to the deficiency (Mahmoudi et al., 2007). However, knowledge on the responses of chlorotic plants to Fe resupply is still scarce, although it may provide crucial information to optimize Fe-fertilization strategies (Abadía et al., 2011 and Pestana et al., 2012). The lack of Fe may also results in alterations of the photorespiratory metabolism, as we can infer from the data showed in the previous chapter of this work (for further details see chapter II).

Since this deficiency alters two important physiological processes like photosynthesis and photorespiration, we decided to perform a series of analysis on leaf tissues of Fe-deficient leaves in order to fill out the general form of the metabolic changes. For this purpose, we decided to investigate the metabolism of amino acids and determine the mineral content of the leaf tissues.

Materials and Methods

Plant growing conditions

Seeds of cucumber (*Cucumis sativus* L. cv. Marketmore '76) were surface-sterilized and sown in Agriperlite, watered with 0.1 mM CaSO₄, allowed to germinate in the dark at 26°C for 3 d, and then transferred to a nutrient solution with the following composition: 2 mM Ca(NO₃)₂, 0.75 mM K₂SO₄, 0.65 mM MgSO₄, 0.5 mM KH₂PO₄, 10 µM H₃BO₃, 1 µM MnSO₄, 0.5 µM CuSO₄, 0.5 µM ZnSO₄, 0.05 µM (NH₄)₆Mo₇O₂₄ and 0.1 mM Fe(III)-EDTA (when added). The pH was adjusted to 6.2 with NaOH. Aerated hydroponic cultures were maintained in a growth chamber with a day:night regime of 16:8 h and a photosynthetic photon flux density (PPFD) of 200 µmol m⁻² s⁻¹ photosynthetically active radiation (PAR) at the plant level.

The temperature was 18°C in the dark and 24°C in the light. For the time-course experiments, 3 d-old plants grown in the nutrient solution were transferred, after removal of cotyledons, to 10 L of the same solution without Fe (Fe-deprived plants). Roots of these plants were carefully washed with 0.5 mM CaSO₄ and rinsed with distilled water before being transferred. Other 3-day-old plants grown in the nutrient solution without Fe were transferred of the complete solution (Fe-resupplied plants). Sampling was performed after 0, 1, 3 and 7 days following induction/removal of Fe deficiency and 4 h after onset of the photoperiod. For clarity, plants previously grown in the presence/absence of Fe for 3 d and then transferred to a Fe-free/complete solution are hereby referred to as 0 throughout the text.

Iron-deficient plants showed the typical Fe deficiency morphological responses (development of leaf Fe deficiency chlorosis, stunted growth and appearance of lateral roots) and the increase in the specific activities (Fe³⁺-chelate reductase and H⁺-ATPase) proper of Strategy I plants (data not shown).

Amino acid analysis

Amino acid (aa) analysis was performed on 0, 1, 3, 7-d plants. Leaves and roots were harvested separately. Free aa were extracted from fresh tissues at 4°C, first in 80% ethanol over night, then in 60% ethanol for 1 h and finally in distilled water for 24 h. The supernatants of each sample were pooled, aliquoted and kept at -20°C. Free aa were determined by HPLC as described before (Muller and Touraine, 1992).

Mineral content determination in leaves

The concentration of metals in the tissue of cucumber plants was determined by ICP-MS spectroscopy (Varian, Fort Collins,

CO, USA) after mineralization in HNO₃ at 100-120°C as described previously (Vigani et al., 2009).

Protein determination

Total protein concentration was determined by using the dye-binding method of Bradford (Bradford, 1976), using serum albumin as a standard.

Statistical analysis

All statistical analyses were conducted with Sigma-Stat® 3.1. Means were compared by Student's t test at the P≤0.05 level in all cases.

Results

Figure and table 3.1 reports the amino acid (aa) concentration in roots and leaves of plants during the progression of Fe deficiency. The analysis of aa closely related to glycolysis, photorespiration and to Krebs cycle, like, glutamate (Glu), glutamine (Gln), aspartate (Asp), asparagine (Asn), arginine (Arg), glycine (Gly), and serine (Ser) was chosen. In general, it is possible to note that aa concentration decreased in Fe-deficient roots, while it increased in leaves, as the Fe deficiency goes forward, with the sole exception of the Arg (see table 3.1).

Table 3.1 reports for all the aa determined the differences between 0 d and 7 d. In particular the concentration of Ser and Gly, two aa involved in the photorespiratory process, increased in leaf while they decreased in root, as Fe deficiency condition proceed in time. However, the Ser decrease in root was only significant after 3 days since Fe starvation was induced (-38%), while Gly decreased in root by about 25% after 7 d of Fe deficiency. At the same time both Ser and Gly

strongly increased in leaves (+94% and +160%, respectively). Interestingly, only the Arg showed a significant decreased concentration at d 7 in both roots (-96%) and leaves (-35%). Furthermore, Asp showed a decrease in Fe-deficient roots (-49%) while it increased in Fe-deficient leaves (+125%). The Asn concentration differed at leaf level where the increase was about 13-fold at 7 d of -Fe condition compared to the control, while it did not show any difference in the roots (Table 3.1). The variation of Glu and Gln was very similar, but, in Fe-deficient tissues, Gln decreased more in root (-64%) and increased more in leaf (3-fold) when compared with Glu (-52% and +138%, in roots and leaves, respectively).

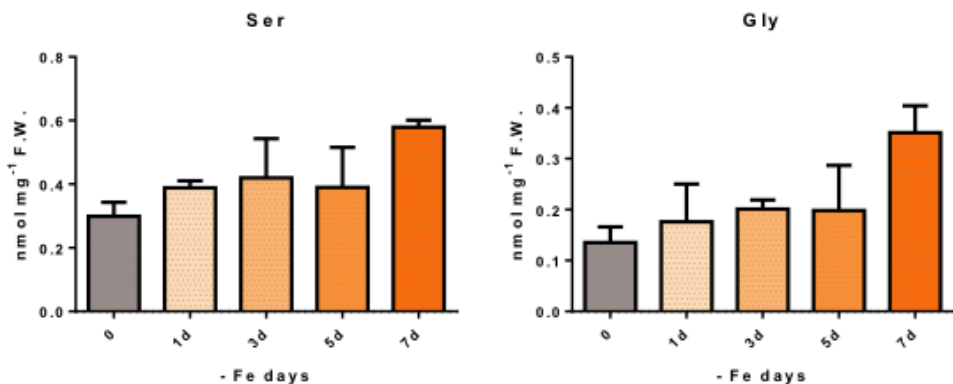


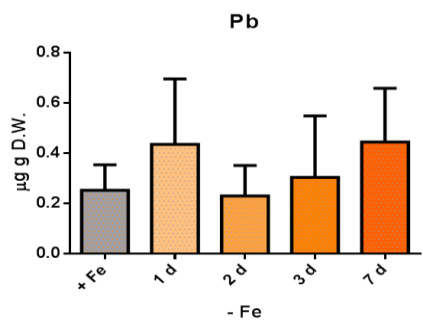
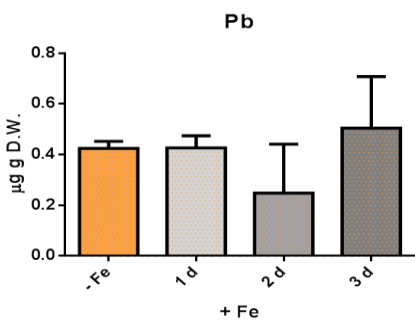
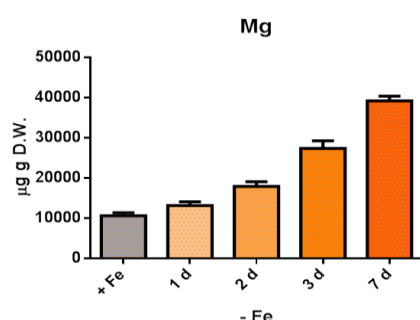
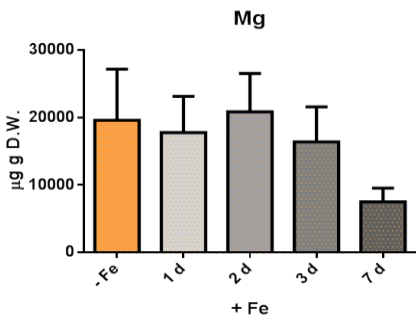
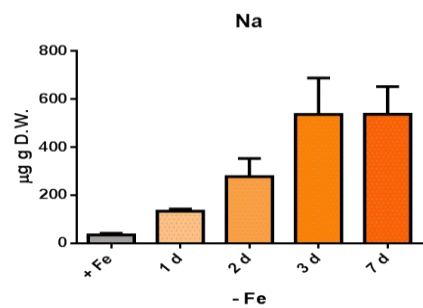
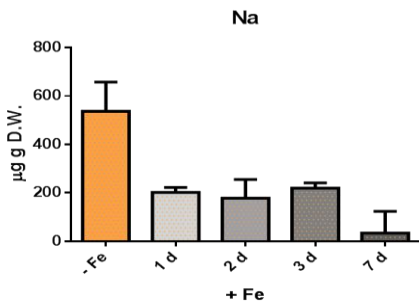
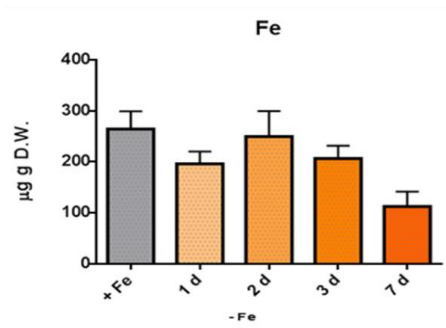
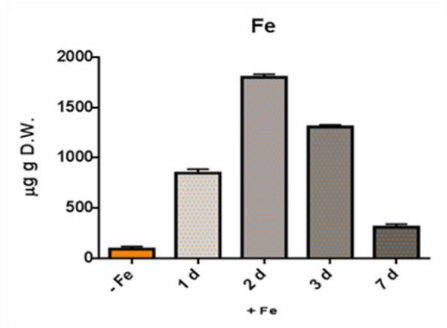
Figure 3.1 Concentration of Ser (a) and Gly (b) in leaf tissues during the evolution of Fe-deficiency in time. In both cases, plants were grown in conditions of Fe sufficiency for 6 d, and subsequently Fe deprived (1). HPLC. Values were determined between 0 and 7 days of treatment

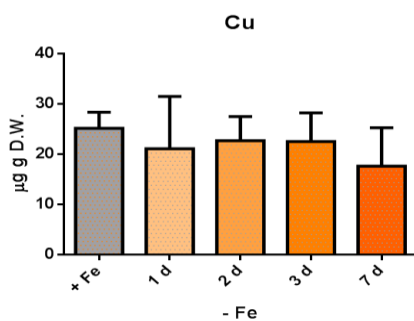
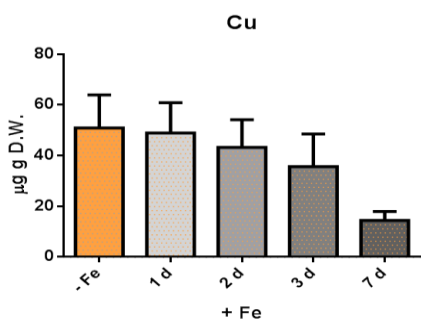
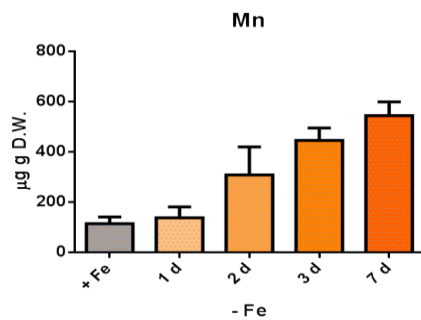
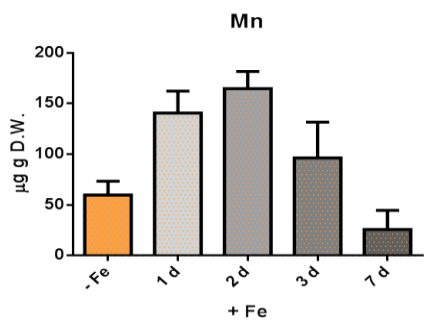
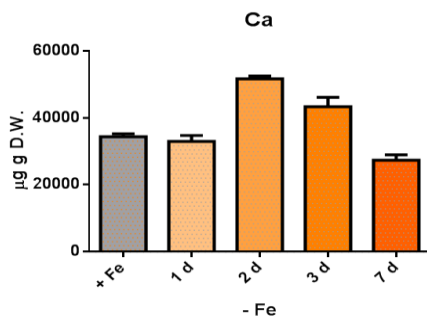
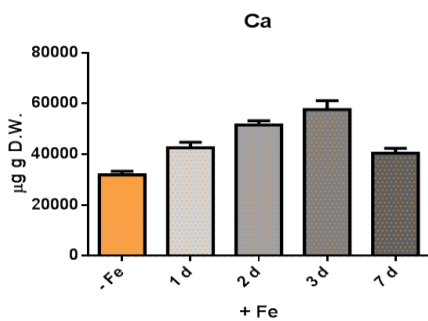
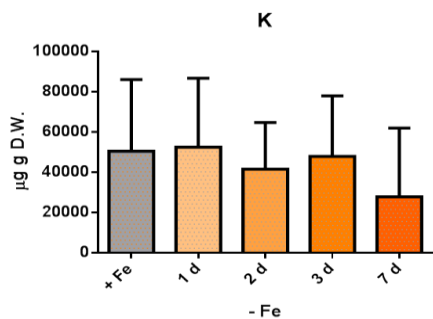
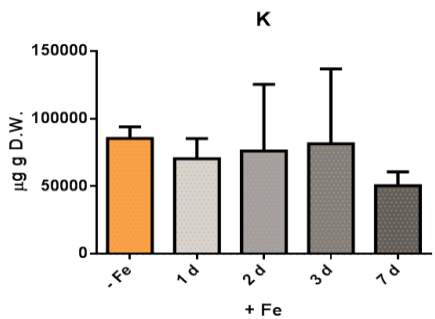
	+Fe (0d)/-Fe(7d)	
	Roots	Leaves
Asp	- 49	+ 125
Asn	0	+ 1.263
Gln	- 64	+ 350
Glu	- 53	+ 138
Gly	- 25	+ 160
Ser	- 12	+ 94
Arg	- 96	- 35

Table 3.1 Changes in amino acid concentration (%) in roots and leaves of cucumber plants, as determined by Borlotti et al., 2012. Values are the ratio determined between 0 and 7 days of treatment.

Figure 3.2 reports the variations of metals concentration in the leaves of cucumber plants, as Fe deficiency proceed during time, and over the restoration of Fe-sufficient conditions. In general, resupply of iron to Fe-deficient plants led to a increase of the concentration of some divalent cations like Fe, Ca and Mn, whilst Na, Mg, Cu, Zn verge to decrease as Fe sufficient condition are restored. No significant variations are observed in this experimental condition for Mo, K and Pb. On the other and, as Fe deficiency proceeds during time, we observed a significant decrease in Fe, Mo, Cu concentration and an increase in Na, Mg, Zn, Mn concentration. In these conditions, no significant variations were detected in the concentration of Pb and K. More in details, Fe concentration strongly increase after 2 d of Fe resupply in the nutrient solution, showing an almost 18 fold increase. This so strong response of accumulation is weakening later to recover, after 7 days, Fe concentrations similar to those observed in Fe sufficient plants. Fe deprivation, on the other hand, lead to a progressive reduction of the concentration of this element during the proceeding of the time (with the exception of day 2 after the induction of Fe deficiency). Interestingly Mn shows a quite similar, but less intensive (3 fold ater 2 d), trend in the plants during the Fe resupply condition. The concentration of this element increases in our plants in the first 2 days and

then diminishes constantly after 3d and 7d (the concentration after 7 d was however lower than those found in Fe sufficient plant). Conversely, induction of Fe deficiency leads to a gradual increase of the concentration of Mn during the time. The concentration of Na decrease immediately after the resupply of Fe in the nutrient solution and no other significant variations were observed in the following days during the restoration of Fe-sufficient conditions. The induction of Fe deficiency, contrariwise, results in a gradual increase on Na concentration for the first three days, and then the concentration was stable at day 7. Furthermore, the content of Mg, was significantly reduced only after 7 days in the Fe-resupplied plants, whereas we saw a gradual and constant accumulation of this element in the Fe-deprived plants. A similar, but different, behavior was observed for Zn, which decreases constantly throughout the days after the resupply of Fe, and increases continuously after the induction of Fe deficiency. Moreover, the concentration of Ca was increased during the first three days of Fe resupply, showing an 1,5-fold increase for the first two days and a 2-fold increase at day 3, after this the concentration decreases significantly and was comparable with the one observed at day 1. The induction of Fe deficiency leads to a first increase in Ca concentration, significant after 2 days, an increase, which fades with the progress of the time, when the concentrations return to levels found at the beginning of the experiment. In this condition, after 7 days, the concentration of Ca was also comparable with the -Fe plants. In addition, Cu concentration decreases in the Fe resupply experiment, showing a significant 5-fold decrease after 7 d. We also observed a lower concentration of Mo in the Fe resupply plants after 7 d from the resupplying of Fe in the nutrient solution. No significant variation was observed in our experiments in the concentration of Pb in leaves tissue.





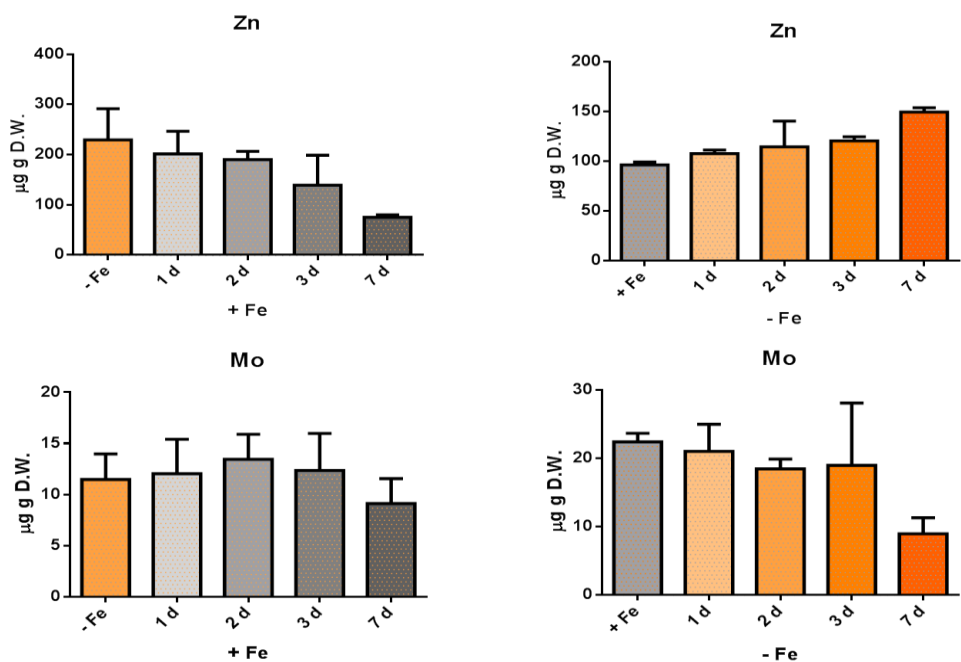


Figure 3.2. Variations in metal concentration in the leaves during the evolution of Fe bioavailability in time. On the left, concentration of Fe in leaves of plants grown in the total absence of Fe for 6 d, and subsequently resupplied with Fe. On the right, concentration of Fe in Fe-sufficient leaves of plants grown for 6 d and subsequently Fe-deprived. Samplings were performed after 1, 2, 3 and 7 d from the change of Fe availability. ICP-MS.

Discussion

The general decrease in aa content observed in Fe-deficient roots could be caused by different factors: (i) a major utilization of aa in the protein synthesis, (ii) an increase in their translocation to the leaves and (iii) a degradation and/or recycling of aa (Borlotti et al., 2012). Direct evidences supporting the first hypothesis have been documented in Fe-deficient cucumber root (Pontiggia et al., 2003). Concerning the second hypotheses, an increase in the total aa concentration in the xylem sap was observed during the

progression of Fe deficiency (Borlotti et al., 2012)). Considering that the transpiration rate (E) determined did not change during this progression (see chapter II and also Rombolà et al., 2005) it would mean that the aa concentration in the xylem sap increased under Fe deficiency accordingly with the decrease of aa in roots. Concerning the last hypothesis it remains speculative, being supported only by indirect evidence. An increase in roots but not in leaves in the activity of two enzymes involved in the recycling of aa, alanine-aminotransferase (ALT) and aspartate-aminotransferase (AST) was already showed by Borlotti et al. These data are also supported by proteomic studies conducted on cucumber (Donnini et al., 2010) and *Medicago truncatula* (Rodriguez-Celma et al., 2011). Among all those aa variations, we focus our attention mainly on the variations showed by Gly and Ser, due to their involvement in the photorespiratory metabolism. In particular, the strong accumulation of these two aa in leaves (+94% Ser and +160% Gly) might suggest an alteration in the mitochondrial activity of the Glycine decarboxylase complex-Serine hydroxymethyltransferase cycle (GDC-SHMT1 cycle), that converts glycine into serine within the mitochondria, with the involvement of methylene tetrahydrofolate and complex I of the respiratory chain, in a process decoupled from the ATP synthesis.

ICP-MS analysis allows us to determine the concentration of metals inside the leaves of Fe-deprived and Fe-resupplied plants. Interestingly, we observe a similar trend in the concentration of Fe and Mn during all experimental conditions, suggesting that these two elements might share the uptake mechanisms and the regulation pathway. It is well established that IRTs are unspecific transporter and even if they can also transport other divalent metals like Mn, Zn, and Cd, they show a high affinity for Fe (Kobayashi and Nishizawa,

2012). IRT1 so plays a pivotal role in the regulation of plant Fe homeostasis, as demonstrated by the severe chlorosis and lethality of an *irt1-1* knockout mutant (Vert et al. 2002, Henriques et al. 2002). Hence the Fe absorption dependent on IRT1 allows proper growth and development under Fe limited conditions (Vert et al. 2002). The strong increase in Fe concentration for three days and the subsequent decrease after the resupply of this element in the nutrient solution suggests that the Fe deficiency response is maintained active for a certain period of time after the element returns to be bioavailable and then subsequently attenuated. Discerning the behavior of the other elements, we can assume that in the absence of Fe, non-specific transporters instead of Fe may absorb other divalent cations.

In conclusion, these data, together with previous, allow us to suggest that Fe deficiency strongly affected aa metabolism. It has been proposed that it occur by limiting NR activity and by increasing GS/GOGAT in both root and leaf (Borlotti et al., 2012). Nevertheless under Fe deficiency root and leaf showed some important differences: the aa content in root decreased while in leaf it increased, and this changes might match the opposite NR gene expression. Additionally, the different aa distribution in Fe-deficient plants might be due the a major translocation (together with other metabolites) via xylem from root to leaf (Borlotti et al., 2012). Thus, under Fe deficiency, root seems to respond more efficiently sustaining the whole plant by furnishing metabolites (i.e. aa, organic acids) to the leaves, in which the whole metabolism is inferred by a decreased photosynthetic activity. The accumulation of Ser and Gly might also be due to an alteration in the photorespiratory metabolism at the GDC-SHMT1 cycle in the mitochondria of the -Fe plant.

The alterations in the concentrations of metals suggest that Fe deficiency induces a metabolic imbalance in which other divalent cations are absorbed by unspecific transporter, due to their similar characteristics to Fe, this can affect the metabolism of the plant at different levels. Other metabolic variations induced by Fe-deficiency were detected in *Oryza sativa* and are reported in this work (see Chapter V).

References

Abadía J., F. Morales F., A. Abadía, Photosystem II efficiency in low chlorophyll, iron-deficient leaves; *Plant Soil*, 215 (1999), pp. 183–192.

Abadía J., S. Vázquez, R. Rellán-Álvarez, H. El-Jendoubi, A. Abadía, A. Álvarez-Fernández, A.F. López-Millán; Towards a knowledge-based correction of iron chlorosis; *Plant Physiol. Biochim.*, 49 (2011), pp. 471–482

Bradford MM: A rapid and sensitive method for the quantization of micrograms quantities of protein utilizing the principle of protein-dye binding. *Anal Biochem* 1976, 72:248–254.

Borlotti et al.: Iron deficiency affects nitrogen metabolism in cucumber (*Cucumis sativus* L.) plants. *BMC Plant Biology* 2012 12:189.

Donnini S, Prinsi B, Negri AS, Vigani G, Espen L, Zocchi G: Proteomic characterization of iron deficiency response in *Cucumis sativus* L. roots. *BMC Plant Biol* 2010, 10:268.

Hecht-Buchholz C.H., U. Ortmann; Effect of foliar iron application on greening and chloroplast development in iron chlorotic soybean; *J. Plant Nutr.*, 9 (1986), pp. 647–659.

Jiménez S., F. Morales, A. Abadía, J. Abadía, M.A. Moreno, Y. Gogorcena; Elemental 2-D mapping and changes in leaf iron and chlorophyll in response to iron re-supply in iron-deficient GF 677

peach–almond hybrid, *Plant Soil*, 315 (2009), pp. 93–106.

Larbi A., A. Abadía, F. Morales, J. Abadía, Fe resupply to Fe deficient sugar beet plants leads to rapid changes in the violaxanthin cycle and other photosynthetic characteristics without de novo chlorophyll synthesis. *Photosynth. Res.*, 79 (2004), pp. 59–69.

Larbi A., A. Abadía, J. Abadía, F. Morales; Down co-regulation of light absorption, photochemistry, and carboxylation in Fe-deficient plants growing in different environments; *Photosynth. Res.*, 89 (2006), pp. 113–126.

H. Mahmoudi, N. Labidi, R. Ksouri, M. Gharsalli, C. Abdelly; Differential tolerance to iron deficiency of chickpea varieties and Fe resupply effects; *C.R. Biol.*, 330 (2007), pp. 237–246

Morales F., R. Belkhodja, A. Abadía, J. Abadía, Photosystem II efficiency and mechanisms of energy dissipation in iron-deficient, field-grown pear trees (*Pyrus communis* L.), *Photosynth. Res.*, 63 (2000), pp. 9–21.

Morales F., N. Moise, R. Quílez, A. Abadía, J. Abadía, I. Moya; Iron deficiency interrupts energy transfer from a disconnected part of the antenna to the rest of Photosystem II; *Photosynth. Res.*, 70 (2001), pp. 207–220.

Moseley J.F., T. Allinger, S. Herzog, P. Hoerth, E. Wehinger, S. Merchant, M. Hippler; Adaptation to Fe-deficiency requires remodelling of the photosynthetic apparatus; *EMBO J.*, 21 (2002), pp. 6709–6720.

Muller B, Touraine B: Inhibition of NO₃⁻ uptake by various phloemtranslocated amino acids in soybean seedlings. *J Exp Bot* 1992,43:617–623.

Nishio J.N., J. Abadía, N. Terry; Chlorophyll-proteins and electron transport during iron nutrition-mediated chloroplast development; *Plant Physiol.*, 78 (1985), pp. 269–299.

Pestana M., A. de Varennes, E.A. Faria; Lime-induced iron chlorosis in fruit trees, in: R. Dris, S.M. Jain (Eds.), *Production Practices and Quality Assessment of Food Crops, Plant Mineral Nutrition and*

Pesticide Management, 1-4020-1699-9, 2, Kluwer Academic Publishers, Dordrecht, The Netherlands (2004), p. 171.

M. Pestana, P.J. Correia, T. Saavedra, F. Gama, A. Abadía, A. de Varennes; Development and recovery of iron deficiency by iron resupply to roots or leaves of strawberry plants; *Plant Physiol. Biochim.*, 53 (2012), pp. 1–5.

Pontiggia A, De Nisi P, Zocchi G: Effect of iron deficiency on RNA and protein syntheses in cucumber roots. *J Plant Nutr* 2003, 26:2177–2186.

Pushnik J.C., G.W. Miller; Iron regulation of chloroplasts photosynthetic function: mediation of PS I development; *J. Plant Nutr.*, 12 (1989), pp. 407–421

- n AF: Root responses of *Medicago truncatula* plants grown in two different iron deficiency conditions: changes in root protein profile and riboflavin biosynthesis. *J Prot Res* 2011, 10:2590–2601.

a J: Iron deficiency-induced changes in carbon fixation and leaf elemental composition of sugar beet (*Beta vulgaris*) plants. *Plant Soil* 2005, 271: 39–45.

Terry N., Abadía J., Function of iron in chloroplasts, *J. Plant Nutr.*, 9 (1986), pp. 609–646.

Tomasi N., C. Rizzardo, R. Monte, S. Gottardi, N. Jelali, R. Terzano, B. Vekemans, M. De Nobili, Z. Varanini, R. Pinton, S. Cesco; Micro-analytical, physiological and molecular aspects of Fe acquisition in leaves of Fe-deficient tomato plants re-supplied with natural Fe-complexes in nutrient solution; *Plant Soil*, 325 (2009), pp. 25–38

Vigani G, Maffi D, Zocchi G. 2009. Iron availability affects the function of mitochondria in cucumber roots. *New Phytologist* 182, 127-136.

CHAPTER IV

Iron deficiency induces ROS accumulation in cucumber plants linked to an imbalance in the antioxidant machinery

Highlights

Adverse environmental conditions are reported to induce oxidative stress in plants as a consequence of reactive oxygen species (ROS) overproduction. Under our experimental conditions, reactive oxygen species accumulation detected in cucumber plants grown in the absence of Fe could be attributable to an increase in the activity of enzymes involved in the formation of these species, or due to a simultaneous reduced activity of enzymes involved in their detoxification. We observed a slight induction in the activity of Cu/Zn-SOD isoform whereas, in the same experimental conditions, a reduction in Fe- and also in Mn-SOD isoforms activity was also recorded. At the same time, the concentration of H₂O₂ in the leaves of Fe-deficient plants, was significantly higher (+40%) in the absence of Fe. All the data obtained in our experiments allow us to speculate that Fe deficiency can induce in the leaves of cucumber plants imbalances in the metabolism of reactive oxygen species. This overproduction could lead to an onset of oxidative stress which can lead to further cell damage at different levels also with the involvement of the photosynthetic apparatus.

Abstract

Adverse environmental conditions are reported to induce oxidative stress in plants as a consequence of reactive oxygen species (ROS) overproduction (Foyer et al. 1997). Plants have well-developed defence systems against ROS, involving both limiting their formation as well as instituting their removal (Ogawa et al., 1996, Alscher et al., 2002; Culotta et al., 2006). Iron (Fe) is either a constituent or a cofactor of many antioxidant enzymes and, at the same time, can act as a prooxidant through the Fenton reaction (Halliwell and Gutteridge 1984). In its role as an enzyme constituent, Fe is

part of catalase (CAT, EC 1.11.1.6), non-specific peroxidases (POD, EC 1.11.1.7), ascorbate peroxidase (APX, EC 1.11.1.11) and Fe superoxide dismutase (Fe-SOD, EC 1.15.1.1). These enzymes constitute the first line of defence against ROS. (McCord et al., 1969; Alscher et al. 2002, Blokhina et al. 2003, Culotta et al. 2006).

Under our experimental conditions, reactive oxygen species accumulation detected in cucumber plants grown in the absence of Fe could be linked to an imbalance in this antioxidant machinery. We observed a slight induction in the activity of Cu/Zn-SOD isoform whereas, in the same experimental conditions, a reduction in Fe- and also in Mn-SOD isoforms activity was recorded. These findings are in accordance with studies already performed on plants grown in Fe-deprived conditions (Iturbe-Ormaeste et al. 1995, Molassiotis et al. 2006, Donnini et al., 2012). At the same time, the concentration of H₂O₂ in the leaves of Fe-deficient plants, was significantly higher (+40%) in the absence of Fe. Nevertheless, it is remarkably that this increase of H₂O₂ could be also triggered by rise in other enzymatic activities, such as NAD(P)H oxidases (Romero-Puertas et al. 2004), pH-dependent PODs (Bestwick et al. 1998), as previously suggested by Donnini et al. (2012). The concentrations of H₂O₂ might play an important role in the Fe deficiency response signalling processes, which should be further investigated also considering the increasingly important role of this molecule as a messenger involved in the processes of adjustment of cell expansion during leaf development (Lu et al., 2014), which is effectively reduced in Fe deficient plants.

Taken together, all the data obtained in our experiments allow us to speculate that Fe deficiency can induce in the leaves of cucumber plants imbalances in the metabolism of reactive

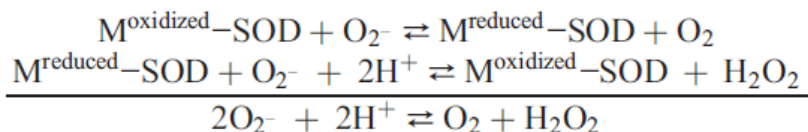
oxygen species, either attributable to an increase in the activity of enzymes involved in the formation of these species, or due to a simultaneous reduced activity of enzymes involved in their detoxification. This overproduction of reactive oxygen species, if not properly handled by the cell, could lead to an imbalance in the cellular homeostasis of the ROS, resulting in an onset of oxidative stress which can lead to further cell damage at different levels, also with the involvement of the photosynthetic apparatus.

Introduction

Reactive O₂ species (ROS) are produced in both unstressed and stressed cell. Adverse environmental conditions are reported to induce oxidative stress in plants as a consequence of reactive oxygen species (ROS) overproduction (Foyer et al. 1997). Plants have well-developed defence systems against ROS, involving both limiting their formation as well as instituting their removal (Ogawa et al., 1996, Alscher et al., 2002; Culotta et al., 2006). Plants generally react to a rise in ROS concentration that the defence system is unable to remove with increased enzymatic and/or non-enzymatic antioxidant process (Alscher and Hess, 1993), but the mechanism underlying these processes are not fully understood yet. More in detail, relatively little information is available on the relationships between Fe deficiency and secondary oxidative stress, and some data remain controversial (Iturbe-Ormaeste et al. 1995, Ranieri et al. 2001, Lombardi et al. 2003, Chouliaras et al. 2004, Molassiotis et al. 2005). Fe is either a constituent or a cofactor of many antioxidant enzymes and, at the same time, can act as a prooxidant through the Fenton reaction (Halliwell and Gutteridge 1984). In its role as an enzyme constituent, Fe is part of catalase (CAT, EC 1.11.1.6), non-specific peroxidases

(POD, EC 1.11.1.7), ascorbate peroxidase (APX, EC 1.11.1.11) and Fe superoxide dismutase (Fe-SOD, EC 1.15.1.1).

Superoxide radical (O_2^-) is produced at any location where an electron transfer is present and thus in every compartment of the cell. Superoxide dismutases are ubiquitous components of cellular antioxidant systems. These enzymes constitute the first line of defence against ROS by catalysing the disproportionation of superoxide anion to oxygen and hydrogen peroxide in different plant species under several stress conditions, (McCord et al., 1969; Alscher et al. 2002, Blokhina et al. 2003, Culotta et al. 2006). All known SODs require a redox active transition metal in the active site in order to accomplish the catalytic breakdown of superoxide anion. A generic mechanism for the metalloenzyme-dependent dismutation steps is described below.



The metal cofactors catalyse both a one-electron oxidation (see first step) and a one-electron reduction of (second step) separate superoxide anions to give the overall disproportionation reaction. These reactions typically do not require external source of redox equivalents and are thus self-contained components of the antioxidant machinery. This allows SODs to function in a variety of intracellular and extracellular environments. Superoxide dismutases are typically soluble secreted or cytosolic proteins but are also found in a number of subcellular compartments such as the cell envelope of gram-negative bacteria, the mitochondria of eukaryotic cells and chloroplasts, as well as the extracellular

environment (Alscher et al., 2002). Based on the metal co-factor used by the enzyme, SODs are classified into three main groups: iron SOD (Fe-SOD), manganese SOD (Mn-SOD) and copper-zinc SOD (Cu/Zn-SOD), and all these SODs are located in different compartment of the cell.

Comparison of deduced amino acid sequences from these three different type of SODs suggest that Mn and Fe-SOD are the most ancient type of SODs and these enzymes might probably have arisen from the same ancestral enzyme, whereas Cu/Zn-SOD have probably evolved separately in eukaryotes (Kanematsu and Asada, 1990; Smith and Doolittle, 1992). The evolutionary reason for the separation of SODs with different metal requirements is probably related to the different availability of soluble transition metal compounds in the biosphere in relation to the O₂ content of the atmosphere in different geological eras (Bannister et al., 1991). While there is no similarity in sequence or structure between Cu/Zn-SOD and Mn/Fe-SOD families, these metalloproteins do share some intriguing properties. For instance, both are quite stable relative to most proteins found in mesophilic organisms (Culotta et al., 2006). Members of these families of enzymes are found across the continuum of life: examples are known in prokaryotes, archea and eukaryotes. The Cu/Zn-SODs and Mn-SOD, are the only forms found in yeast and mammals. Excellent overviews of the prokaryotic nickel and Fe-SODs can be found (Barondeau et al., 2004; Wintjens et al., 2004).

Intracellular Cu/Zn-SOD in mammals and *S. cerevisiae* is mainly localized in cytosol with a smaller fraction in the intermembrane space of mitochondria (Weiseger et al., 1973; Lindeau et al., 2000; Sturtz et al., 2001; Okado-Matsumoto et al., 2002; Field et al., 2003;). It has also been reported in nuclei, lysosomes and peroxisomes using

immunocytochemical methods (Chang et al., 1988). While superoxide is produced in cytosol by several enzymes such as xanthine oxidase (Moriwaki et al., 1993), respiratory components in mitochondria are thought to be a major source of O_2^- generation (Cadenas et al., 2000). In fact, in mammals, more than 95% of consumed daily oxygen is reduced to water in the respiratory chain, and 1– 2% of it has been estimated to be converted to O_2^- by proteins in the electron transport chain in mitochondria. Most of mitochondrial O_2^- is disproportionate by high levels of Mn-superoxide dismutase (1.1×10^{-5} M) (Tyler, 1975) in the mitochondrial matrix. While the presence of intracellular Cu/Zn-SOD in the mitochondrial matrix is a controversial issue (Vijayvergiya et al., 2005), its localization in the inter-membrane space (IMS) is now well established (Weisiger et al., 1973; Sturtz et al., 2001; Han et al., 2001; Okado-Matsumoto et al., 2002; Field et al., 2003). Cu/Zn-SODs are important for survival of prokaryotes in relatively late/stationary phase and contributes to the ability to grow aerobically (St John et al., 1996). The periplasmic sources of O_2^- have not yet been characterized but it is likely that Cu/Zn-SOD protects components of this compartment against both endogenous and exogenous sources of O_2^- , for instance those arising from host pathogen responses.

Cu/Zn-SOD is quite strong with respect to physical or chemical denaturation; enzymatic activity was observed in the presence of stringent denaturants such as 10 M urea or 4% SDS, and activity in standard buffers is also observed at 80 °C (Hottinger et al., 1997; Bertini et al., 1998;). While thermal (non-enzymatic) dismutation of O_2^- to O_2 and H_2O_2 is somewhat fast under typical conditions (5×10^5 $M^{-1} s^{-1}$), Cu/Zn-SOD catalyzed dismutation is accelerated by four orders of magnitude and approaches the diffusion-controlled limit (1.6×10^9 $M^{-1} s^{-1}$). It is important to note that the rate of

disproportionation by these enzymes is very similar to that of buffer solutions containing transition metal salts. This observation led to a significant amount of debate concerning the actual function of SOD. Recent *in vitro* and *in vivo* studies strongly support a model for the inorganic physiology of the cytosol in which intracellular free Zn and Cu ion concentrations are vanishingly small under normal aerobic growth (Outten et al., 2001; Rae et al., 2001; Changela et al., 2003; Finney et al., 2003; Tottey et al., 2005). This is consistent with a selection process favouring organisms that elaborate a means of localizing transition metal catalyst for superoxide dismutation to different parts of the cell, depending upon the origin and nature of the oxidative stress. Free Fe, on the other hand, has been proposed to be more available (Srinivasan et al., 2000)

The sequence and structure of Cu/Zn-SOD is highly conserved from prokaryotes to eukaryotes (Bordo et al., 1994). This protein associates to form a dimer with a dissociation constant of $1.0 \times 10^{-10} \text{ M}^{-1}$ (Khare et al., 2004), and each subunit has an immunoglobulin-like fold that provides an active site with one copper and one zinc ion. One remarkable feature is the intra-subunit disulphide bond, which is stable and observed in most if not all Cu/Zn-SOD structures published to date. It has long been known that the apo-form of Cu/Zn-SOD can be generated *in vitro* and then reconstituted with the native copper and zinc ions or with other metals (Bertini et al., 1998). Most cells do not leave the insertion of Cu to diffusion reactions and employ an accessory protein known as the Cu chaperone for Cu/Zn-SOD (CCS) to facilitate this process. CCS docks with and transfers the metal ion to the disulphide-reduced apo-SOD1 (Rae et al., 2001; Culotta et al., 1997). An intrasubunit disulphide is observed in all structurally characterized forms of native Cu/Zn-SOD

published to date. The disulphide reduced form of the yeast Cu/Zn-SOD protein can accumulate in the cell under anaerobic conditions or in the absence of CCS (Furukawa et al., 2004; Brown et al., 2004). This immature state of the protein is important for the physiology of Cu/Zn-SOD: only the disulphide reduced and apo-form of the polypeptide can be imported into the IMS of mitochondria (Field et al., 2003). Several studies have shown that the disulphide is essential for SOD activity and provide initial insights into how the Cu loaded form of CCS might catalyse the oxidation of SOD to its disulphide form [Furukawa et al., 2004, 2006; Brown et al., 2004; Arnesano et al., 2004].

The Cu/Zn-SODs play important, but not necessarily essential, roles in protecting components of the bacterial cell envelope or many compartments of the eukaryotic cells. In addition, there is accumulating evidence that copper dependent SODs play roles in signal transduction pathways (Leopold et al., 2005). The products of superoxide dismutation, i.e. hydrogen peroxide and oxygen, may also play direct signalling roles in the intracellular environment as well (Immenschuh et al., 2005). With these more complex SOD functions in mind, it is not surprising that numerous post-translational mechanisms for regulating SOD activity in response to physiological signals are beginning to emerge (Brown et al., 2004). Intriguingly, metal insertion, proteolytic processing and disulphide formation are important post-translational modifications that alter Cu/Zn-SOD activity. Three isozymes of Cu/Zn-SOD have been isolated from spinach: one was found in intact chloroplast (Kanematsu and Asada, 1990) The other two isozymes are considered “cytosolic” isozymes, because they could not be found in intact chloroplast but were major isoforms in non-photosynthetic tissues (Kanematsu and Asada, 1990). Immunogold-electron

microscopic analyses of spinach leaves done with the antibody specific for “cytosolic” Cu/Zn-SOD indicates that SODs are localized in the apoplast, in the nucleus and in, or near, the tonoplast (Ogawa et al., 1995). The association of Cu/Zn-SOD with the nucleus indicates it has a role in preventing fatal mutation caused by ROS. The localizing site of Cu/Zn-SOD in the apoplastic region of spinach leaf tissues corresponds to that of the accumulation of lignin. In spinach hypocotyl “cytosolic” Cu/Zn-SOD is localized in vascular tissues where lignification and the generation of superoxide respectively were shown by the phloroglucin-HCl reaction and formation of formazane from nitroblue tetraziolium. Because hydrogen peroxide is required for lignification via the peroxidase-catalysed reaction, the Cu/Zn-SOD in the apoplast appears to function in the biosynthesis of lignin by causing rapid disproportionation of the superoxide anion radical prior to its interaction with cellular components and peroxidase (Ogawa et al., 1996).

The family of MnSOD or FeSOD enzymes first discovered by Fridovich [11,16] has been well conserved throughout evolution. Across various phyla of archae, eubacteria and eukaryotes, the family of Mn/Fe SODs is comprised of dimers or tetramers of ≈ 21 kDa subunits with considerable sequence homology and well conserved protein folds (for review, see Wintjens et al., 2004 and reference therein). Within each subunit, a single Mn or Fe atom bound at the active site serves to catalyse the disproportionation of superoxide to oxygen and hydrogen peroxide. Based on the close homology of Mn and Fe SODs, one might expect easily metal co-factor substitution. Indeed, it has been shown that the Mn-SOD of *E. coli* binds Fe with affinities equal to that of Mn (Mizuno et al., 2004). Metal mis-incorporation with bacterial Mn-SODs has also been observed *in vivo*. Mn-SOD of *E. coli* is expressed as a

mixture of Mn and Fe bound forms (Beyer et al., 1991), and Fe binding to Mn-SOD increases during anaerobic conditions and when extracellular Fe is abundant (Privalle et al., 1992; Whittaker et al., 2003;).

In eukaryotes, the manganese form of SOD generally exists in the matrix of the mitochondria. Rare exceptions include the cytosolic Mn-SODs of the fungi *C. albicans* (Lamarre et al., 2001) and crustaceans (Brouwer et al., 2003;). The mechanism by which these cytosolic enzymes acquire their Mn cofactor is still unknown.

In all plant species examined to date, it is inferred that Fe-SODs are located in the chloroplast. Fe-SOD has also been localized in the chloroplast in *N. luteum* and a potential chloroplastic targeting sequence was found in soybean Fe-SOD. Three Fe SODs were reported in *Arabidopsis thaliana* (Kliebenstein et al., 1998). The absence of Fe-SOD in animals has given rise to the proposal that the Fe-SOD gene originated in the plastid and moved to the nuclear genome during the evolution. Support for this theory comes from the existence of several conserved regions that are present in plant and cyanobacterial Fe-SOD sequences, but absent in non-photosynthetic bacteria (Bowler et al., 1994).

There are two distinct groups of Fe-SOD. The first group is a homodimer formed from two identical 20KDa subunit proteins, with 1-2 gram atom of Fe in the active centre. This group was found in *Ginkgo biloba*, *Brassica calpestris* and *Nuphar luteum* (Salin and Bridges, 1980). The second Fe-SOD group, found in most of higher plants, is a tetramer of four equal subunits with a molecular weight of 80-90 KDa. Member of this group contain 2-4 gram atoms of Fe in the active centre.

Mn-SODs occur in mitochondria and peroxisomes and carry only one metal atom per subunit. These enzymes cannot function without the Mn atom present in the active site. Even though Mn and Fe SODs have a high similarity in their primary, secondary and tertiary structure, these enzymes have diverged sufficiently that Fe (II) could not restore the activity of Mn-SOD and vice versa (Fridovich, 1986).

Mn-SOD is either a homodimeric or a homotetrameric enzyme with one Mn(III) atom per subunit. The enzyme is not inhibited by potassium cyanide (KCN) or inactivated by H₂O₂ and is present in both eukaryotes and prokaryotes. Plant Mn SODs have approximately 65% sequence similarity to one another, and these enzymes also have high similarities to bacterial Mn-SODs (Bowler et al., 1994). Although SOD is known as the mitochondrial enzyme of eukaryotes, a Mn containing SOD has also been located in the peroxisomes. The presence of one peroxisomal and one mitochondrial Mn-SOD was shown by using immunolocalization assays in watermelon (del Rio et al., 1992). Four genes that encode Mn-SOD were reported in maize (*Zea mays*) (Zhu and Scandalios, 1993). Deduced amino acid sequences from these four isoenzymes have a mitochondrial targeting sequence, indicating that all are located in the mitochondria.

In all known cases of Mn-SOD, the polypeptide is encoded by a nuclear gene and is imported into the mitochondrial matrix. The enzyme is synthesized as a precursor polypeptide containing, at its N-terminus, a pre-sequence for mitochondrial targeting that is subsequently cleaved in mitochondria. Mitochondrial import of the precursor has shown to be necessary for co-factor insertion. During co-translational import of Mn-SOD into mitochondria, the polypeptide may remain sufficiently unfolded to facilitate Mn insertion (Culotta

et al., 2006). Alternatively, an accessory factor may contain Mn-SOD in the unfolded state during import to allow rapid manganese insertion prior to enzyme folding (Luk et al., 2005).

In contrast to the Cu/Zn-requiring SODs, the Mn containing SODs of the mitochondria plays an essential role in oxidative stress protection. Complete loss of the enzyme results in neonatal lethality in mice (Lebovitz et al., 1996) and is also critical for growth and viability of other eukaryotic organisms (Kirby et al., 2002; Duttaroy et al., 2003;). It is generally accepted that high Fe causes oxidative stress mainly through Fe catalysed Fenton chemistry, however, analyses of mitochondrial SOD suggest a new component to Fe toxicity: inactivation of important mitochondrial anti-oxidant enzymes (Culotta et al., 2006).

Finally, the studies on the various metal containing SODs raise questions about the evolution of SOD catalysts. It is quite possible that environmental metal ion availability and cell physiology have played important roles in determining the nature of the specific metal ion and SOD-type used in scavenging toxic superoxide anion (Culotta et al., 2006).

In addition to SOD activity, other enzymes, the most important being CAT and PODs control the intracellular level of H₂O₂. Peroxidases, by means of their hydroxylic or peroxidative activity, can regulate both ROS production and scavenging in numerous cell compartments and thus they can be involved in many plant processes, such as growth and biotic/abiotic stress responses (Passardi et al. 2005). In the cell wall, PODs are present as soluble, ionically and covalently bound forms and they can catalyse cross-linking reactions, building a rigid cell wall, or produce ROS-generating wall-loosening reactions, to make it more flexible (Lewis and

Yamamoto 1990, Polle et al. 1994, Schweikert et al. 2000). Additionally, PODs are enzymes directly involved in lignin biosynthesis by assembling lignin units through oxidative polymerization (Lewis and Yamamoto 1990). Several works have well documented that some growth conditions are responsible for the increase in cell-wall lignification, which, by reducing cell growth, may represent a plant's adaptation to adverse conditions (Jbir et al. 2001, Lee et al. 2007). With regard to plants grown under Fe deficiency, POD isoforms are differently affected. Ranieri et al. (2001) showed, in Fe-deficient sunflower, a preferential reduction in the activity of those isoforms involved in H₂O₂ detoxification, rather than in the maintenance of cell-wall structure.

According to Molassiotis et al. (2006), increased POD activity may be an important attribute linked to chlorosis tolerance in peach rootstocks. Furthermore, the occurrence of a overproduction of reactive oxygen species and, at the same time, of a scarce capacity to detoxifying them, may lead to alterations in organ growth through cell-wall modifications (Donnini et al. 2008, 2012). In particular, in a pear genotype tolerant to lime-induced chlorosis, treatment with bicarbonate results in an increase in non-specific POD activity, confirming its higher level of protection in particular against H₂O₂ accumulation. In a quince genotype susceptible to lime-induced chlorosis the presence of ROS in root apoplast under bicarbonate supply was correlated to lignin deposits in external layers and endodermis as a consequence of the shift of PODs towards a lignification role (Donnini et al., 2012). The possibility based on the idea that cell wall modifications underlying organ growth are affected by ROS production was supported by several previous reports (Schopfer, 2001; Liskay et al., 2004; Passardi et al., 2005).

Materials and Methods

Plant growing conditions

Seeds of cucumber (*Cucumis sativus* L. cv. Marketmore '76) were surface-sterilized and sown in Agriperlite, watered with 0.1 mM CaSO₄, allowed to germinate in the dark at 26°C for 3 d, and then transferred to a nutrient solution with the following composition: 2 mM Ca(NO₃)₂, 0.75 mM K₂SO₄, 0.65 mM MgSO₄, 0.5 mM KH₂PO₄, 10 μM H₃BO₃, 1 μM MnSO₄, 0.5 μM CuSO₄, 0.5 μM ZnSO₄, 0.05 μM (NH₄)₂MoO₇ and 0.1 mM Fe(III)-EDTA (when added). The pH was adjusted to 6.2 with NaOH. Aerated hydroponic cultures were maintained in a growth chamber with a day:night regime of 16:8 h and a photosynthetic photon flux density (PPFD) of 200 μmol m⁻² s⁻¹ photosynthetically active radiation (PAR) at the plant level. The temperature was 18°C in the dark and 24°C in the light. For the time-course experiments, 3 d-old plants grown in the nutrient solution were transferred, after removal of cotyledons, to 10 L of the same solution without Fe (Fe-deprived plants). Roots of these plants were carefully washed with 0.5 mM CaSO₄ and rinsed with distilled water before being transferred. Other 3-day-old plants grown in the nutrient solution without Fe were transferred to the complete solution (Fe-resupplied plants). Sampling was performed after 0, 1, 3 and 7 days following induction/removal of Fe deficiency and 4 h after onset of the photoperiod. For clarity, plants previously grown in the presence/absence of Fe for 3 d and then transferred to a Fe-free/complete solution are hereby referred to as 0 throughout the text.

Iron-deficient plants showed the typical Fe deficiency morphological responses (development of leaf Fe deficiency

chlorosis, stunted growth and appearance of lateral roots) and the increase in the specific activities (Fe³⁺-chelate reductase and H⁺-ATPase) proper of Strategy I plants (data not shown).

Protein determination

Protein content was determined by the Bradford (1976) procedure using the Bio-Rad reagent and bovine serum albumin as a protein standard.

SOD extraction and activity assay

Root samples were ground in liquid N₂ with 10% (w/w) polyvinylpyrrolidone (PVPP) and homogenized in a medium containing: 50 mM K-phosphate buffer (pH 7.00), 1 mM EDTA, 0.05% (v/v) Triton X-100, 1 mM dithiothreitol (DTT), 1 mM Na-ascorbate and 0.50 mM phenylmethylsulphonyl fluoride (PMSF). After centrifugation at 12,000g for 30 min at 4 °C, the supernatant was collected and dialysed overnight at 4 °C against 1:50 (v/v) diluted buffer. Superoxide dismutase activity was assayed according to the method of Scebba et al. (2003) at 560 nm, based on the enzyme's ability to inhibit the photoreduction of nitrobluetetrazolium (NBT). One enzyme unit was defined as the amount of enzyme inhibiting 50% of NBT photoreduction.

Native PAGE and SOD isoform visualization

Superoxide dismutase isoforms were separated by 12.5% native polyacrylamide gel electrophoresis (PAGE) at 100 V using the method described by Beuchamp and Fridovich (1971). Pre-treatment of the gels with 5 mM H₂O₂ and 3 mM KCN before SOD staining allowed us to characterize SOD isoforms as Cu/Zn-SOD, Fe-SOD or Mn-SOD. Mn-SOD is resistant to both inhibitors, Fe-SOD is resistant to KCN and

inhibited by H_2O_2 , and both inhibitors inhibit Cu/Zn-SOD.

Native PAGE and CAT activity assay

Electrophoresis was performed on 7.5% polyacrylamide gels electrophoresis (PAGE) at 100 (V) as described previously by Clare et al. (1984). Gel was soaked first for 45' min in the potassium phosphate buffer 50 mM, pH 7.0 containing horseradish peroxidase (50 μ g/ml). H_2O_2 was then added to a concentration of 5 mM and soaking was continued for 10 min. Higher levels of H_2O_2 reduce the sensitivity of this activity stain both by inactivating the catalase and by preventing the complete decomposition of H_2O_2 at the position of bands of catalase. Gels were then rapidly rinsed twice with distilled water and placed into 0.5 mg/ml of *O*-diaminobenzidine in the phosphate buffer, until staining was completed.

H₂O₂ content evaluation

H_2O_2 content was measured following the method reported by Ranieri et al. (2001) based on the formation of titanium-peroxide complex. The leaf samples, homogenized in cold 100% acetone (1:2; w:v), were centrifuged at 10000g for 10 min and 20% $TiCl_4$ in concentrated HCl was added to supernatant aliquots to give a final titanium concentration of 4%. After addition of NH_4OH (0,2 ml for each ml of sample) to precipitate the titanium-peroxide complex, samples were centrifuged at 10000 g for 5 min and the resulting pellet was washed five times in acetone and then resuspended in 2 N H_2SO_4 . The absorbance of the solution was read at 415 nm against a blank containing H_2O instead of extracts. H_2O_2

content was calculated using a standard curve of H_2O_2 of known concentrations from 0.1 to 1 mM.

Results

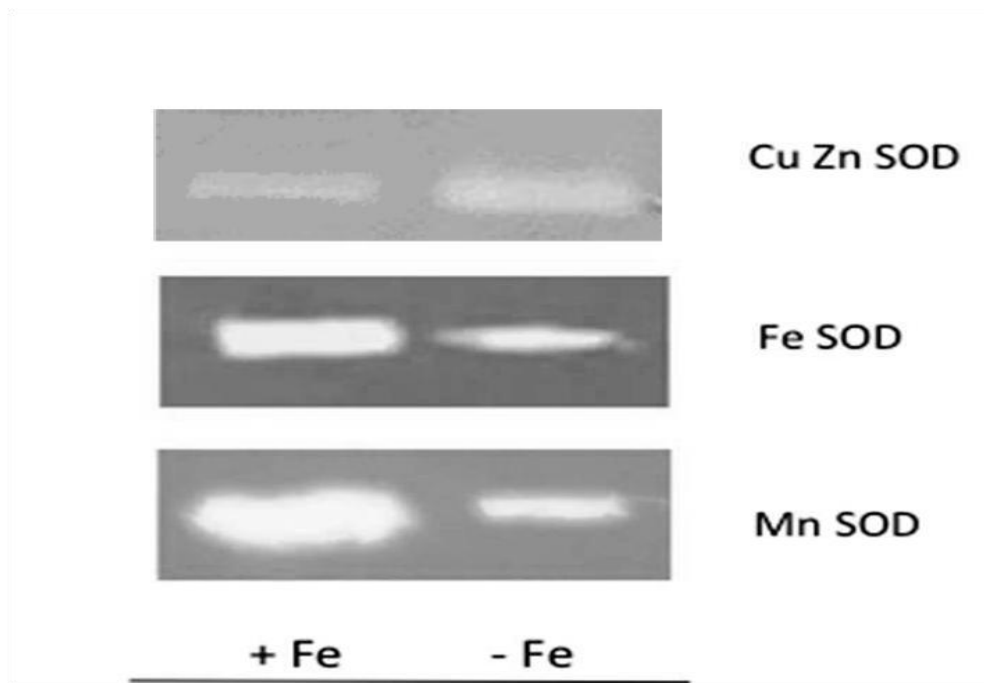


Figure 4.1 SOD isoforms activity assay on PAGE native electrophoresis: plants grown in the presence or absence of Fe (50-0 mM Fe) for 10 d. Discrimination among isoforms was performed using KCN, H_2O_2 or both as inhibitors; 12 ug protein x lane.

SOD isoform activities, performed on native PAGE, are showed in fig. 4.1. The pre-treatment of the gels with H_2O_2 and KCN as inhibitors before SOD activity staining allowed us to characterize SOD isoforms as Cu/Zn-SOD, Fe-SOD or Mn-SOD. Plants grown in the presence of Fe showed a higher activity of the Fe-SOD and Mn-SOD isoforms, whereas the activity of Cu/Zn-SOD was lower. On the contrary, the lack of

Fe results in a slightly increased activity of Cu/Zn SOD isoform, whilst we observed a reduced activity of the Fe-SOD and Mn-SOD isoforms, as expected. We then perform native PAGE in order to determine the activity of catalase during Fe deficiency. As shown in figure 4.2, Fe deficiency induces a reduction in the activity of catalase in the leaves of cucumber plants. The reduction of catalase activity in Fe-deficient plants is also confirmed by enzymatic analysis (for further details see chapter V). In the light of all these findings we decide to determine the concentration of hydrogen peroxide in the leaves. As shown in figure 4.3, the concentration was significantly higher (+40%) in the absence of Fe, and this datum is quite in accordance with the measured reduction of catalase activity in Fe-deficient plants, determined by enzymatic activity assay (-35%).

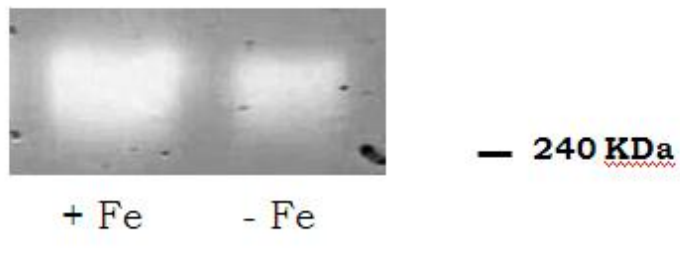


Figure 4.2. CAT activity assay on PAGE native electrophoresis: plants grown in the presence or absence of Fe (50-0 mM Fe) for 10 d; 10 μ g protein x lane.

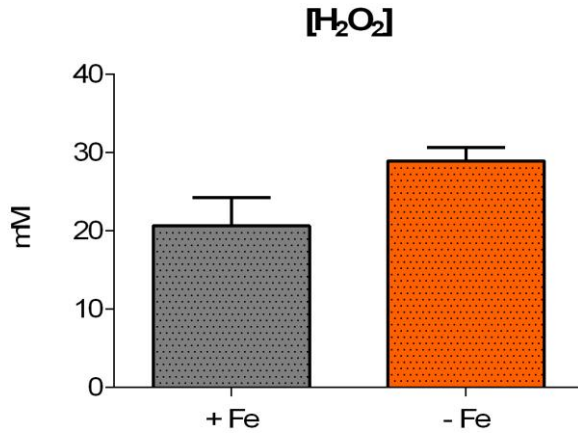


Figure 4.3. Quantification of hydrogen peroxide in leaves: plants grown in the presence or absence of Fe (50-0 mM Fe) for 10 d;

Discussion

Under our experimental conditions, reactive oxygen species accumulation detected in cucumber plants grown in the absence of Fe could be linked to an imbalance in the antioxidant machinery. More in detail, the lack of Fe could result in an accumulation of ROS due either to their increased synthesis or to their reduced degradation. To test this hypothesis, we have analysed the main enzymes involved in ROS metabolism. Among these activities, the SODs are involved in the responses to Fe deficiency stress, catalysing the dismutation into H₂O₂ of O₂⁻, formed to a high extent under this condition (Ranieri et al. 1999, Molassiotis et al. 2005). To determine whether differences between the individual SOD isoforms were present, we have also determined SOD activity by using non-denaturing gel staining (Figure 4.1). We observe a slight induction in the activity of Cu/Zn-SOD isoform whereas, in the same experimental conditions, we saw a reduction in Fe and also in Mn-SOD isoforms activity. These findings are quite in

accordance with studies already performed on plants grown in Fe-deprived conditions, which showed higher SOD activity, mainly due to increased Cu/Zn-SOD or Mn-SOD isoforms (Iturbe-Ormaeche et al. 1995, Molassiotis et al. 2006, Donnini et al., 2012).

At the same time, the concentration of hydrogen peroxide in the leaves of Fe-deficient plants, was significantly higher (+40%) in the absence of Fe, and this is in accordance with the measured reduction of catalase activity in Fe-deficient plants, determined by enzymatic activity assay (-35%) and activity staining on native PAGE. Nevertheless, it is remarkably that this increase of H₂O₂ could be also triggered by rise in other enzymatic activities, such as NAD(P)H oxidases (Romero-Puertas et al. 2004), pH-dependent PODs (Bestwick et al. 1998), as previously suggested by Donnini et al. (2012). In general, we can infer that though other activities could not be completely ruled out. In view of this, further investigation should be conducted, in particular the activities of PODs, the cellular distribution of H₂O₂ and the concentration of O₂⁻ should be determined. In particular, increase in the concentrations of hydrogen peroxide might play an important role in the Fe deficiency response signalling processes, which should be further investigated, also considering the increasingly important role of this molecule as a messenger involved in the processes of adjustment of cell expansion during leaf development (Lu et al., 2014), which is effectively reduced in Fe deficient plants.

Taken together, all the data obtained in these experiments allow us to speculate that Fe deficiency can induce in the leaves of cucumber plants imbalances in the metabolism of reactive oxygen species, either attributable to an increase in the activity of enzymes involved in the formation of these

species, or due to a simultaneous reduced activity of enzymes involved in their detoxification. This overproduction of reactive oxygen species, if not properly handled by the cell, could lead to an imbalance in the cellular homeostasis of the ROS, resulting in an onset of oxidative stress which, if not correctly managed, can lead to further cell damage at different levels, also with the involvement of the photosynthetic apparatus.

References

Alscher, R.G., N. Erturk and L.S. Heath, (2002). Role of superoxide dismutases (SODs) in controlling oxidative stress in plants. *J. Exp. Bot.* 53:1331–1341.

Arnesano F., Banci L., Bertini I., Martinelli M., Furukawa Y., O'Halloran T.V, The unusually stable quaternary structure of human Cu/Zn superoxide dismutase 1 is controlled by both metal occupancy and disulfide status, *J. Biol. Chem.* 279 (2004) 47998–48003.

Barondeau D.P., Kassmann C.J., Bruns C.K., Tainer J.A., Getzoff E.D., Nickel superoxide dismutase structure and mechanism, *Biochemistry* 43 (2004) 8038–8047.

Battistoni A., Rotilio G., Isolation of an active and heat-stable monomeric form of Cu/Zn superoxide dismutase from the periplasmic space of *Escherichia coli*, *FEBS Lett.* 374 (1995) 199–202.

Beauchamp, C. and I. Fridovich. 1971. Superoxide dismutase: improved assay and an assay applicable to acrylamide gels. *Anal. Biochem.* 44: 276–287.

Bertini I., Mangani S., Viezzoli M.S., Structure and properties of copper–zinc superoxide dismutases, *Adv. Inorg. Chem.* 45 (1998) 127–250.

Bestwick, C.S., I.R. Brown and J.W. Mansfield. 1998. Localized

changes in POD activity accompany hydrogen peroxide generation during the development of a non-host hypersensitive reaction in lettuce. *Plant Physiol.* 118: 1067–1078.

Beyer W.F., Fridovich I., *In vivo* competition between iron and manganese for occupancy of the active site region of the manganese-superoxide dismutase of *Escherichia coli*, *J. Biol. Chem.* 266 (1991) 303–308.

Blokhina, O., E. Virolainen and K.V. Fagerstedt. 2003. Antioxidants, oxidative damage and oxygen deprivation stress. *Ann. Bot.* 91:179–194.

Bordo D., Djinovic K., Bolognesi M., Conserved patterns in the Cu/Zn superoxide dismutase family, *J. Mol. Biol.* 238 (1994) 366–386.

Bradford, M.M. 1976. A rapid and sensitive method for the quantification of microgram quantities of protein utilising the principle of protein-dye binding. *Anal. Biochem.* 72:248–254.

Brouwer M., Hoexum Brouwer T., Grater W., Brown-Peterson N., Replacement of a cytosolic copper/zinc superoxide dismutase by a novel cytosolic manganese superoxide dismutase in crustaceans that use copper (haemocyanin) for oxygen transport, *Biochem. J.* 374 (2003) 219–228.

Brown N.M., Torres A.S., Doan P.E., O'Halloran T.V., Oxygen and the copper chaperone CCS regulate posttranslational activation of Cu, Zn superoxide dismutase, *Proc. Natl. Acad. Sci. U. S. A.* 101 (2004) 5518–5523.

Cadenas E., Davies K.J., Mitochondrial free radical generation, oxidative stress, and aging, *Free Radic. Biol. Med.* 29 (2000) 222–230.

Chang L.Y., Slot J.W, Geuze H.J., Crapo J.D., Molecular immunocytochemistry of the CuZn superoxide dismutase in rat hepatocytes, *J. Cell Biol.* 107 (1988) 2169–2179.

Changela A., Chen K., Xue Y., Holschen J., Outten C.E., O'Halloran T.V., Mondragon A., Molecular basis of metal-ion selectivity and zeptomolar sensitivity by CueR, *Science* 301 (2003) 1383–1387.

Chouliaras, V., K. Dimassi, I. Therios, A. Molassiotis and G. Diamantidis. 2004. Root-reducing capacity, rhizosphere acidification, peroxidase and catalase activities and nutrient levels of *C. taiwanica* and *C. volkameriana* seedlings, under Fe deprivation conditions. *Agronomie* 24: 1-6.

Clare D.A., Duong M.H., Darr D., Archibald F., Fridovich I., Effects of molecular oxygen on detection of superoxide radical with nitroblue tetrazolium and on activitu stains for catalase, (1984) *Anal. Biochem.* 140, 532-537.

Culotta V.C., Klomp L.W., Strain J., Casareno R.L., Krems B., Gitlin J.D., The copper chaperone for superoxide dismutase, *J. Biol. Chem.* 272 (1997) 23469-23472.

Culotta V.C., Yang M., O'Halloran T.V., Activation of superoxide dismutases: putting the metal to the pedal, *Biochimica et Biophysica Acta* 1763 (2006) 747-758.

Donnini S., Dell'Orto M., Zocchi G., Oxidative stress responses and root lignification induced by Fe deficiency conditions in pear and quince genotypes, *Tree Physiology* 31, 102-113, 2012

Duttaroy A., Paul, Kundu M., Belton A., A Sod2 null mutation confers severely reduced adult life span in *Drosophila*, *Genetics* 165 (2003) 2295-2299.

Field L.S., Furukawa Y., O'Halloran T.V., Culotta V.C., Factors controlling the uptake of yeast copper/zinc superoxide dismutase into mitochondria, *J. Biol. Chem.* 278 (2003) 28052-28059.

Finney L.A., O'Halloran T.V., Transition metal speciation in the cell: insights from the chemistry of metal ion receptors, *Science* 300 (2003) 931-936.

Foyer, C.H., H. Lopez-Delgado, J.F. Dat and I.M. Scott. 1997. Hydrogen peroxide and glutathione-associated mechanisms of acclamatory stress tolerance and signalling. *Physiol. Plant.* 100:241-254.

Furukawa Y., Torres A.S., O'Halloran T.V., Oxygen-induced maturation of SOD1: a key role for disulfide formation by the copper chaperone CCS, *EMBO J.* 23 (2004) 2872-2881.

Furukawa Y., O'Halloran T.V., Post-translational modifications in Cu, Zn-superoxide dismutase and mutations associated with ALS., *Antioxid. Redox Signal.* 8, 847–867 (2006).

Han D., Williams E., Cadenas E., Mitochondrial respiratory chain-dependent generation of superoxide anion and its release into the intermembrane space, *Biochem. J.* 353 (2001) 411–416

Halliwell, B. and J. Gutteridge. 1984. Oxygen toxicity, oxygen radicals, transition metals and disease. *Biochem. J.* 219:1–14.

Hottinger A.F., Fine E.G., Gurney M.E., Zurn A.D., Aebischer P., The copper chelator d-penicillamine delays onset of disease and extends survival in a transgenic mouse model of familial amyotrophic lateral sclerosis, *Eur. J. Neurosci.* 9 (1997) 1548–1551.

Immenschuh S., Baumgart-Vogt E., Peroxiredoxins, oxidative stress, and cell proliferation, *Antioxid. Redox Signal.* 7 (2005) 768–777.

Iturbe-Ormaeche, I., J.F. Moran, C. Arrese-Igor, Y. Gogorcena, R.V. Klucas and M. Becana. 1995. Activated oxygen and antioxidant defenses in iron deficient pea plants. *Plant Cell Environ.* 18:421–429.

Jbir, N., W. Chaïbi, S. Ammar, A. Jemmali and A. Ayadi. 2001. Root growth and lignification of two wheat species differing in their sensitivity to NaCl, in response to salt stress. *Compt. Rendus Acad. Sci. III Sci. Vie.* 324:863–868.

Keele B.B., McCord J.M., Fridovich I., Superoxide dismutase from *Escherichia coli* B: a new manganese containing enzyme, *J. Biol. Chem.* 245 (1970) 6176–6181

Kirby K., Hu J., Hilliker A.J., Phillips J.P., RNA interference-mediated silencing of Sod2 in *Drosophila* leads to early adult-onset mortality and elevated endogenous oxidative stress, *Proc. Natl. Acad. Sci. U. S. A.* 99 (2002) 16162–16167.

Lamarre C., LeMay J.D., Deslauriers N., Bourbonnais Y., *Candida albicans* expresses an unusual cytoplasmic manganese-containing superoxide dismutase (SOD3 gene product) upon the entry and during the stationary phase, *J. Biol. Chem.* 276 (2001)

Lebovitz R.M., Zhang H., Vogel H., Cartwright Jr J., Dionne L., Lu N., Huang S., Matzuk M.M., Neurodegeneration, myocardial injury, and perinatal death in mitochondrial superoxide dismutase-deficient mice, *Proc. Natl. Acad. Sci. U. S. A.* 93 (1996) 9782–9787.

Lee, B.R., K.Y. Kim, W.J. Jung, J.C. Avice, A. Ourry and T.H. Kim. 2007. Peroxidases and lignification in relation to the intensity of water-deficit stress in white clover (*Trifolium repens* L.). *J. Exp. Bot.* 58:1271–1279.

Leopold J.A., Loscalzo J., Oxidative enzymopathies and vascular disease, *Arterioscler. Thromb. Vasc. Biol.* 25 (2005) 1332–1340.

Lewis, N.G. and E. Yamamoto. 1990. Lignin: occurrence, biogenesis and biodegradation. *Annu. Rev. Plant Physiol. Plant Mol. Biol.* 41: 455–496.

Lindenau J., Noack H., Possel H., Asayama K., Wolf G., Cellular distribution of superoxide dismutases in the rat CNS, *Glia* 29 (2000) 25–34.

Lombardi, L., L. Sebastiani and C. Vitagliano. 2003. Physiological, biochemical, and molecular effects of in vitro induced iron deficiency in peach rootstock Mr.S 2/5. *J. Plant Nutr.* 26:2149–2163.

Lu D., Wang T., Persson S., Mueller-Roeber M. Schippers J.H.M.; Transcriptional control of ROS homeostasis by KUODA1 regulates cell expansion during leaf development, *NATURE COMMUNICATIONS* 5:3767

Luk E., Yang M., Jensen L.T., Bourbonnais Y., Culotta V.C., Manganese activation of superoxide dismutase 2 in the mitochondria of *Saccharomyces cerevisiae*, *J. Biol. Chem.* 280 (2005) 22715–22720.

McCord J.M., Fridovich I., Superoxide dismutase. An enzymic function for erythrocuprein (hemocuprein), *J. Biol. Chem.* 244 (1969) 6049–6055.

Mizuno K., Whittaker M.M., Bachinger H.P., Whittaker J.W., Calorimetric studies on the tight-binding metal interactions of *Escherichia coli* manganese superoxide dismutase, *J. Biol. Chem.*

Molassiotis, A., G. Diamantidis, I. Therios, V. Tsirakoglou and K. Dimassi. 2005. Oxidative stress, antioxidant activity and Fe(III)-chelate reductase activity of five *Prunus* rootstocks explants in response to Fe deficiency. *Plant Growth Regul.* 46:69–78.

Molassiotis, A., G. Tanou, G. Diamantidis, A. Patakas and I. Therios. 2006. Effects of 4-month Fe deficiency exposure on Fe reduction mechanism, photosynthetic gas exchange, chlorophyll fluorescence and antioxidant defense in two peach rootstocks differing in Fe deficiency tolerance. *J. Plant Physiol.* 163:176–185.

Moriwaki Y., Yamamoto T., Suda M., Nasako Y., Takahashi S., Agbedana O.E., Hada T., Higashino K., Purification and immunohistochemical tissue localization of human xanthine oxidase, *Biochim. Biophys. Acta* 1164 (1993) 327–330.

Napier I., Ponka P., Richardson D.R., Iron trafficking in the mitochondrion: novel pathways revealed by disease, *Blood* 105 (2005) 1867–1874.

Okado-Matsumoto A., Fridovich I., Amyotrophic lateral sclerosis: a proposed mechanism, *Proc. Natl. Acad. Sci. U. S. A.* 99 (2002) 9010–9014.

Outten C.E., O'Halloran T.V., Femtomolar sensitivity of metalloregulatory proteins controlling zinc homeostasis, *Science* 292 (2001) 2488–2492.

Pacello F., Langford P.R., Kroll J.S., Indiani C., Smulevich G., Desideri A., Rotilio G., Battistoni A., A novel heme protein, the Cu/Zn superoxide dismutase from *Haemophilus ducreyi*, *J. Biol. Chem.* 276 (2001) 30326–30334.

Passardi F., C. Cosio, C. Penel and C. Dunand. 2005. Peroxidases have more functions than a Swiss army knife. *Plant Cell Rep.* 24:255–265.

Privalle C.T., Fridovich I., Transcriptional and maturation effects of manganese and iron on the biosynthesis of manganese-superoxide dismutase in *Escherichia coli*, *J. Biol. Chem.* 267 (1992) 9140–9145.

Polle, A., T. Otter and F. Seifert. 1994. Apoplastic peroxidases and lignification in needles of Norway spruce (*Picea abies* L.). *Plant Physiol.* 106:53–60.

Rae T.D., Torres A.S., Pufahl R.A., O'Halloran T.V., Mechanism of Cu, Zn-superoxide dismutase activation by the human metallochaperone hCCS, *J. Biol. Chem.* 276 (2001) 5166–5176.

Ranieri, A., A. Castagna, B. Baldan and G.F. Soldatini. 2001. Iron deficiency differently affects peroxidase isoforms in sunflower. *J. Exp.Bot.* 52:25–35.

Romero-Puertas, M.C., M. Rodriguez-Serrano, F.J. Corpus, M. Gomez and L.A. del Rio. 2004. Cadmium-induced subcellular accumulation of O₂⁻ and H₂O₂ in pea leaves. *Plant Cell Environ.* 27:1122–1134.

Rouault T.A., Iron on the brain, *Nat. Genet.* 28 (2001) 299–300.

Scebba, F., I. Pucciarelli, G.F. Soldatini and A. Ranieri. 2003. O₃-induced changes in the antioxidant systems and their relationship to different degrees of susceptibility of two clover species. *Plant Sci.* 165:583–593.

Schweikert, C., A. Liszkai and P. Schopfer. 2000. Scission of polysaccharides by peroxidase-generated hydroxyl radicals. *Phytochemistry* 53: 562–570.

Spagnolo L., Toro I., D'Orazio M., O'Neill P., Pedersen J.Z., Carugo O., Rotilio G., Battistoni A., Djinovic-Carugo K., Unique features of the sodC-encoded superoxide dismutase from *Mycobacterium tuberculosis*, a fully functional copper-containing enzyme lacking zinc in the active site, *J. Biol. Chem.* 279 (2004) 33447–33455.

Srinivasan C., Liba A., Imlay J.A., Valentine J.S., Gralla E.B., Yeast lacking superoxide dismutase(s) show elevated levels of “free iron” as measured by whole cell electron paramagnetic resonance, *J. Biol. Chem.* 275 (2000) 29187–29192.

Strassburger M., Bloch W., Sulyok S., Schuller J., Keist A.F., Schmidt A., Wenk J., Peters T., Wlaschek M., Krieg T., Hafner M., Kumin A., Werner S., Muller W., Scharffetter-Kochanek K., Heterozygous deficiency of manganese superoxide dismutase results

in severe lipid peroxidation and spontaneous apoptosis in murine myocardium *in vivo*, *Free Radic. Biol. Med.* 38 (2005) 1458–1470.

St John G., Steinman H.M., Periplasmic copper–zinc superoxide dismutase of *Legionella pneumophila*: role in stationary-phase survival, *J. Bacteriol.* 178 (1996) 1578–1584.

Sturtz L.A., Diekert K., Jensen L.T., Lill R., Culotta V.C., A fraction of yeast Cu,Zn-superoxide dismutase and its metallochaperone, CCS, localize to the intermembrane space of mitochondria—A physiological role for SOD1 in guarding against mitochondrial oxidative damage, *J. Biol. Chem.* 276 (2001) 38084–38089.

Totter S., Harvie D.R., Robinson N.J., Understanding how cells allocate metals using metal sensors and metallochaperones, *Acc. Chem. Res.* 38 (2005) 775–783.

Tyler D.D., Polarographic assay and intracellular distribution of superoxide dismutase in rat liver, *Biochem. J.* 147 (1975) 493–504.

Weisiger R.A., Fridovich I., Mitochondrial superoxide dismutase, *J. Biol. Chem.* 248 (1973) 4793–4796.

Whittaker J.W., The irony of manganese superoxide dismutase, *Biochem. Soc. Trans.* 31 (2003) 11318–11321.

Whittaker M., Whittaker J., Thermally triggered metal binding by recombinant *Thermus thermophilus* manganese superoxide dismutase, expressed as the apo-enzyme, *J. Biol. Chem.* 274 (1999) 34751–34757.

Whittaker M.M., Mizuno K., Bachinger H.P., Whittaker J.M., Kinetic analysis of the metal binding mechanism of *Escherichia coli* manganese superoxide dismutase, *Biophys. J.* 274 (2005) 34751–34757.

Van Remmen H., Ikeno Y., Hamilton M., Pahlavani M., Wolf N., Thorpe S.R., Alderson N.L., Baynes J.W., Epstein C.J., Huang T.T., Nelson J., Strong R., Richardson A., Life-long reduction in MnSOD activity results in increased DNA damage and higher incidence of cancer but does not accelerate aging, *Physiol. Genomics* 16 (2003) 29–37.

Vijayvergiya C., Beal M.F., Buck J., Manfredi G., Mutant superoxide dismutase 1 forms aggregates in the brain mitochondrial matrix of amyotrophic lateral sclerosis mice, *J. Neurosci.* 25 (2005) 2463–2470.

Wintjens R., Noel C., May A.C., Gerbod D., Dufernez F., Capron M., Viscogliosi E., Rooman M., Specificity and phenetic relationships of iron- and manganese-containing superoxide dismutases on the basis of structure and sequence comparisons, *J. Biol. Chem.* 279 (2004) 9248–9254

Yost F.J., Fridovich I., An iron-containing superoxide dismutase from *Escherichia coli*, *J. Biol. Chem.* 248 (1973) 4905–4908.

CHAPTER V

Iron deficiency induces alterations in the photorespiratory peroxisome metabolism

Highlights

Fe deficiency induces alterations in peroxisomes at different levels indicating modifications in the photorespiratory metabolism. The complete lack of Fe results in a strong inhibition of catalase enzymatic activity (-35%). Nevertheless, we detect higher levels of catalase in Fe-deficient plants compared to control condition (plants grown in the presence of Fe). No significant changes in the glycolate oxidase activity in all the different experimental conditions verified were observed. In Fe sufficiency condition the total activity of hydroxypyruvate reductase was fully attributable to the peroxisomal isoform (HPR1), while we record an equal distribution of the activity between the two isoforms, peroxisomal and cytosolic (HPR2) in plants grown under conditions of Fe deficiency.

Abstract

Plant peroxisomes are small (about 0,5-1 μm diameter), ubiquitous eukaryotic organelles essential to several physiological processes such as lipid metabolism and plant hormone biosynthesis and metabolism (Olsen and Harada, 1995; Zolman et al., 2000; Hayashi and Nishimura, 2003; Nyathi and Baker, 2006; Reumann and Weber, 2006). A central function of plant peroxisomes is their contribution to photorespiration (Hu et al., 2012). This light-dependent pathway is linked to photosynthesis by the dual function of plastidic Rubisco. Low CO_2 concentrations favour the oxygenase reaction of Rubisco leading to an accumulation of toxic 2-phosphoglycolate (Reumann and Weber, 2006). This compound is efficiently degraded via the photorespiratory C2 cycle, converting 2-phosphoglycolate to 3-phosphoglycerate, which re-enters the Calvin-Benson cycle. Substantial energy costs are required for re-assimilation (Reumann and Weber,

2006). Peroxisomes also mediate a wide range of oxidative metabolic activities that vary among the species, cell type, and environmental conditions in which the organism lives (Beever, 1979; Van den Bosch et al., 1992). Under non-stress conditions ROS produced by peroxisomal metabolism are scavenged by the simultaneous action of the peroxisomal antioxidant systems catalase, ascorbate peroxidase and the ascorbate–glutathione cycle (del Rio et al., 2002). However, under oxidative stress conditions peroxisomal ROS generation is enhanced and ROS scavenging is insufficient (del Rio et al., 2002). The ability to cope with an increased ROS production is correlated with up-regulation of peroxisomal antioxidant systems in natural stress-tolerant plant species (Mittova et al., 2003; 2004).

Performed Western Blot analysis allowed us to observe that Fe deficiency induces a louder accumulation of catalase in Fe-deficient plants compared to control condition (plants grown in the presence of Fe). Curiously, the two treatments result in a different distribution of the immunochemical signal among the different fractions of our separation gradient. The complete lack of Fe results in a strong inhibition of catalase enzymatic activity (-35%). We were not able to observe any significant change in the glycolate oxidase enzyme activity in all the different experimental conditions verified. Moreover, we discriminate the activity of the two hydroxypyruvate reductase isoforms (cytosolic and peroxisomal). In Fe sufficiency condition the total activity was fully attributable to the peroxisomal isoform (HPR1), while we observe an equal distribution of the activity between the two isoforms in plants grown under conditions of Fe deficiency. However the total enzymatic activity was comparable to that of the control condition.

Taken together our data suggest that Fe deficiency induces alterations in peroxisomes at different levels, indicating modifications in the photorespiratory metabolism. Nevertheless, further analyses are required to complete the metabolic characterization of this organelle, in order to fill the complete form of the metabolic changes during Fe-starvation.

Introduction

Peroxisomes are metabolically diverse organelles with essential roles in plant development. Surrounded by single membranes, peroxisomes are small (about 0,5-1 μm diameter), ubiquitous eukaryotic organelles mediating a wide range of oxidative metabolic activities that vary among the species, cell type, and environmental conditions in which the organism lives (Beevers, 1979; Van den Bosch et al., 1992). Plant peroxisomes are essential to many physiological processes such as lipid metabolism, photorespiration, and plant hormone biosynthesis and metabolism (Olsen and Harada, 1995; Zolman et al., 2000; Hayashi and Nishimura, 2003; Nyathi and Baker, 2006; Reumann and Weber, 2006). They are also essential for embryogenesis and play pivotal roles in plant responses to abiotic and biotic stresses (Lin et al., 1999; Hu et al., 2002; Schumann et al., 2003; Sparkes et al., 2003; Fan et al., 2005; Lipka et al., 2005; Desai and Hu, 2008). Early models of peroxisome biogenesis invoked an origin from the endoplasmic reticulum (ER) (Beevers, 1979) and electron microscopic observations that peroxisomes were sometimes seen closely associated with ER (Frederick and Newcomb, 1969) were often used as an argument to support this concept. However whether such association also reflected luminal continuity and a biogenetic relationship was hotly debated, as was the significance of reports of glycoproteins in peroxisomes and similarities in membrane protein and

phospholipid composition between ER and peroxisomal membranes (reviewed in Kindl, 1982). Following the discovery of a specialised peroxisome protein import machinery and the ability of peroxisomes to divide, the field as a whole moved from the idea that peroxisomes derived from the ER to the concept that they imported proteins post translationally, but with the capacity to import some components, lipids certainly and possibly some membrane proteins from the ER (reviewed in Hu et al, 2012 and reference therein).

Electron microscopy fails to capture the dynamic nature of peroxisomes. With the advent of live cell imaging it has become apparent that plant peroxisomes move actively on the actin based cytoskeleton (Collings et al., 2002; Jedd et al. 2002) and undergo changes of shape, extending tubules termed peroxules (Scott et al., 2007) particularly under conditions of oxidative stress that generate hydroxyl radicals (Sinclair et al., 2009). Extension of peroxules often reflects underlying ER dynamics, with the peroxules appearing to extend along ER tubules (Sinclair et al., 2009). To address the question of whether there is direct physical connection between ER and peroxisomes in *Arabidopsis* cells, peroxisomes were labelled with the photo-switchable red-to green EosFP in the *apm1* mutant background. The mutants are defective in *DRP3a* required for peroxisome division (Mano et al., 2004) and display highly elongated peroxisomes that also mirror underlying RFP marked ER (Barton et al., 2013). However despite the close and frequent contact between peroxisomes and ER no evidence for luminal connection was observed (Barton et al., 2013). Nevertheless it seems possible that membrane contact sites between ER and peroxisomes could exist which might aid delivery of membrane lipids and potentially some membrane proteins. The machinery for sorting membrane proteins to peroxisomes comprises 3

peroxins, PEX3, PEX19 and PEX16. In *S. cerevisiae* mutants of *pex3* and *pex19* lack peroxisomes, and peroxisomal membrane proteins (PMPs) are either degraded or mis-localised. In mammalian cells an additional peroxin, PEX16, which is absent in *S. cerevisiae*, is also essential for PMP insertion and *pex3*, *pex16* and *pex19* mutants all lack peroxisomes. In both yeast and mammalian cells, transformation of these mutants with the corresponding wild type gene is sufficient to restore membrane and matrix protein import, and therefore to reconstitute functional peroxisomes. These observations are one of the strongest arguments for the formation of peroxisomes de novo from the ER, and indeed PEX3 and PEX19 in *Saccharomyces*, and PEX3, 19 and 16 in mammals all play a role in the formation of peroxisomes from the ER. However PEX3, PEX16 and PEX19 also have roles in direct targeting of membrane proteins to peroxisomes (reviewed in Kim and Hetterna, 2015). PEX3, PEX16 and PEX19 homologues can be found across the green plants, however PEX16 is absent in diatoms. A schematic diagram showing PMP targeting pathways based on composite data from different systems is shown in Fig. 5.1

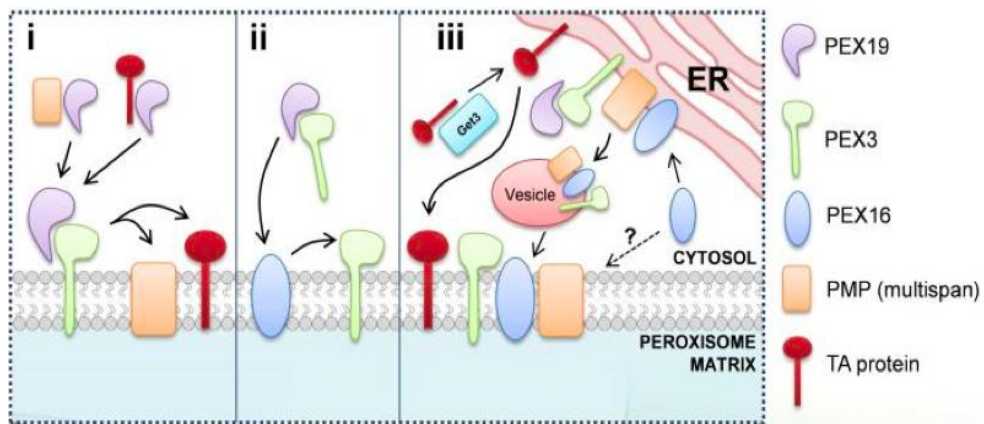


Figure 5.1 Schematic diagram of peroxisomal membrane protein trafficking. As information from studies from plant systems are very limited, the diagram incorporates information from studies on yeast and mammalian systems, which may not be identical. (i) Direct import pathway for both multispan and tail anchored PMPs. These interact with PEX19 via their mPTS in the cytosol; subsequently PEX19 docks with PEX3 on the peroxisome membrane leading to insertion of the PMP. *Arabidopsis* PMP22 inserts directly into peroxisomes in vitro and in vivo (Tugal et al., 1999; Murray et al., 2003) and *Arabidopsis* PEX19 binds multiple PMPs [22]. (ii). Direct insertion of PEX3 in a PEX19 and PEX16 dependent manner. This pathway has been described in mammalian cells (Matsuzaky et al., 2008) but has not been examined in any plant system. (iii) In humans and fungi some tail anchored (TA) proteins are inserted first in the R by the Get complex. PEX16 and PEX3 are delivered to the ER and are delivered to peroxisomes via vesicular traffic (from Cross et al., 2015).

PEX3

PEX3 is the membrane bound receptor for PEX19 (Fang et al., 2004; Schmidt et al., 2010; Sato et al., 2010) and is encoded by 2 isoforms in *Arabidopsis*. AtPEX3-2 is proposed to have both N and C termini in the peroxisome (Hunt et al., 2004) but it is difficult to see how that can be the case, given that in other systems the protein has a single membrane transmembrane segment with N terminal facing the peroxisome lumen while the C terminus is required to be exposed to the cytosol in order to interact with PEX19 (Cross et al., 2015). The deduced topology of AtPEX3-2 was based on

the inability to detect N and C terminal epitope tagged versions of AtPEX3-2 when cells were permeabilised with digitonin, which selectively permeabilises the plasma membrane (Banjoko et al. 1995) Although this method can be very useful in determining topology, it is prone to false negatives if the protein folds or interacts with other proteins such that the epitope tag is obscured.

PEX3 is considered to be one of the 'early' peroxins that is generally accepted to sort from the ER to peroxisomes in mammalian and yeast systems (Kim et al., 2015) (Fig. x iii). N terminally myc tagged AtPEX3-2 sorted rapidly to peroxisomes within 2 h when transiently expressed in either Arabidopsis or tobacco suspension cells and was not detected in ER or pER (peroxisomal ER subdomain). (Hunt et al., 2004). This was interpreted as evidence for direct transport of PEX3 to peroxisomes in plants (Fig. x ii). However 2 h may be too long a time frame to see ER intermediates as ScPex3p was completely localised to peroxisomes within a 45–60 min chase period (Fakieh et al., 2013). The 40 N terminal amino acids of AtPEX3-2 (including the conserved basic cluster and predicted N terminal transmembrane domain (TMD)) could target chloramphenicol acetyl transferase to peroxisomes in both Arabidopsis and tobacco. Deletion and substitution analysis showed the importance of these sequence features (Hunt et al., 2004). Similarly, the N terminal 45 residues of *S.cerevisiae* Pex3 were required for peroxisomal targeting (via the ER) (Tam et al., 2005; Halbach et al., 2009). More detailed analysis showed that the TMD and 6 charged residues of the cytosolic domain of ScPex3p are needed for ER targeting while the N terminal luminal part is needed to reach pER and peroxisomes, since removal leads to vacuolar localisation. Within this region the two positively charged regions act redundantly for peroxisomal sorting (Fackieh et al., 2013).

In the *Arabidopsis pex3i* mutant both PEX3 genes were simultaneously down regulated to < 20% of wild type expression level but the mutants were not dependent on sucrose for post germinative growth and remained sensitive to 2,4 dB. This compound is bio-activated to 2,4D (a herbicide) by β -oxidation, and so retention of sensitivity in mutants is an indication that the peroxisomes retain a functional beta oxidation pathway. The *pex3i* double knock down had large elongated peroxisomes, (Nito et al, 2007) which is very different to phenotypes of *pex3* mutants in mammals and plants. Given the differences in mutant phenotypes and possible difference in topology, the function of PEX3 in plant systems warrants further study.

PEX19

PEX19 isoforms are present in wheat, *Arabidopsis*, moss (*Physcomitrella patens*) and the diatom *Phaeodactylum tricorutum*. In *Arabidopsis* there are 2 isoforms of PEX19 (Hadden et al., 2006). Down regulation by RNAi gave different phenotypes compared to those seen in the equivalent mammalian or yeast mutants (Nito et al., 2007). In *pex19-1i* and *pex19-2i* plants where the individual genes were knocked down independently slightly enlarged peroxisomes that contained a matrix targeted GFP reporter were observed, but in each mutant the other isoform was expressed, which may explain why a severe phenotype was not observed. Biochemical characterisation of AtPEX19-1 showed that, like PEX19 in other systems, it is a predominantly soluble protein with only a small proportion associated with peroxisome membranes. Recombinant AtPEX19-1 could bind AtPEX10 in vitro, consistent with its proposed receptor/chaperone role in yeasts and mammals (Hadden et al., 2006). At PEX19-1 and At PEX19-2 could also bind the *Arabidopsis* peroxisomal ABC

transporter COMATOSE (Nyathi et al., 2010) which was correctly targeted to peroxisomes when expressed in *S. cerevisiae* (Nyathi et al., 2010, 2012). The human ABCD1-3 transporters ALDP, PMP70 and ALDPR were correctly targeted to peroxisomes in tobacco cells and could be mis-targeted to the nucleus by co-expression with Arabidopsis PEX19-1 to which a nuclear localisation signal had been appended (Zhang et al., 2011). Taken together the findings reported in those works suggest that despite the large evolutionary distance, recognition and delivery of PMPs is conserved. However AtPEX19 could not complement the *S. cerevisiae* pex19 Δ mutant, indicating that not all PEX19 functions are conserved (Nyathi 2012). Perhaps this is not surprising given that in *S. cerevisiae* PEX19 has multiple functions. As well as its role in direct import of membrane proteins, its interaction with PEX3 at the ER is important for the initiation of de novo peroxisome biogenesis (Fig. x). It is required for the formation of vesicles containing PEX3 from the ER, it interacts with the myosin myo2p and also with PEX14 of the docking translocation machinery (DTM) for matrix protein import (reviewed in Theodoulou et al., 2013).

AtPEX19 appears to form a disulphide bonded dimer both in vitro and in vivo, and in vivo cross-linking showed that it was the dimeric form of PEX19 that preferentially binds cargo proteins (Hadden et al., 2006). While this property has not been reported for PEX19 of other organisms, it is intriguing to note that the PTS1 receptor PEX5 has also been shown to form a disulphide bonded dimer and it was proposed that the disulphide bonded form had higher affinity for PTS1 cargo (Ma et al., 2013). A number of parallels can be drawn between the functions of PEX5 and PEX19. Both proteins shuttle between cytosol and peroxisomes. Both have a folded C terminal domain that binds to cargo proteins (Stanley et al., 2006;

Schueller et al., 2010) and an unstructured N terminal domain that interact with docking components; PEX14 in the case of PEX5 (Schliebs, 1999; Lanyon-Hogg, 2014) and PEX3 in the case of PEX19 (Fang et al., 2004; Schmidt et al., 2010; Sato 2010). Perhaps the redox regulation of both matrix and membrane protein import is one means by which peroxisomes can regulate their activities in concert with metabolism (Nordgren et al., 2014).

PEX16

In addition to targeting to the peroxisome via the ER in mammals, PEX3 can also insert directly into peroxisome membranes in a PEX19 and PEX16-dependent manner, with PEX16 proposed to function as the membrane receptor (Matsuzaki et al., 2008) (Fig. x ii). However PEX16 is not a universal peroxin as it is absent from *S. cerevisiae* and *P. tricornutum*. PEX16 itself traffics to peroxisomes via the ER (Fig. 5.1 iii) (reviewed in Kim, 2015). In Arabidopsis a PEX16 homologue (SSE1) was identified through the cloning of the gene defective in the ShrunkenSEed 1 (*sse1*) mutant (Lin et al., 1999). As the name suggests this mutant has shrunken seeds due to abnormal deposition of protein and oil bodies during seed development. Despite only low (26% identity) the corresponding SSE1 gene could partially complement the growth of *Yarrowia lipolytica* *pex16* mutant for growth on oleate (Lin et al., 1999). In homozygous *sse1* embryos the signal from a PTS1 fluorescent reporter was not detected, and a PTS2 reporter labelled small abnormal structures against a diffuse background suggesting normal peroxisomes were absent. SSE1 over expression caused formation of peroxisomal aggregates (Lin et al., 2004). As well as these effects on peroxisomes, the *sse1* mutant shows reduced fatty acid biosynthesis and production of oil bodies; both ER-

dependent processes. The mutant phenotype emphasises the close relationship between ER and peroxisomal metabolic processes, and how disruption of one can impact the other.

SEE1/AtPEX16 itself is targeted to peroxisomes (Lin et al, 2004) and peroxisomes and ER (Karnik et al, 2005) Transient expression of myc tagged AtPEX16 in Arabidopsis and tobacco suspension cells resulted in co-localisation with ER markers at early time points and with peroxisome markers at late time points. Cold treatment resulted in AtPEX16 accumulation in reticular structures and upon subsequent warming localisation in peroxisomes (Karnik et al., 2007) A recent study provides evidence that AtPEX16 like its human counterpart can act as a receptor for PMPs (Hua et al., 2015)

As additional functions are discovered for plant peroxisomes, a comprehensive inventory of peroxisomal proteins will be crucial to determine the under-lying mechanisms for the new roles. The major protein constituents of plant peroxisomes are well characterized, whereas only a few low-abundance and regulatory proteins have been reported to date.

Because peroxisomes lack DNA, all peroxisomal proteins are imported directly from the cytosol or via the endoplasmic reticulum (Purdue and Lazarow, 2001). With a few exceptions, proteins destined to the peroxisome matrix contain a conserved peroxisome targeting type 1 (PTS1) or type 2 (PTS2) signal. PTS1 is a tripeptide sequence located at the extreme C terminus of a majority of matrix proteins; it consists of SKL (Ser-Lys-Leu) or a variant of this canonical sequence. PTS2 is a nonapeptide sequence with the prototype RLx₅HL, which is present at or near the N terminus of some matrix proteins. After PTS2-containing proteins enter the peroxisome, the N-terminal domain is cleaved off in plants and animals (Purdue

and Lazarow, 2001). *In silico* searches of fungal, plant, and animal genomes for proteins containing putative C-terminal PTS1 sequences revealed that plants might contain the highest number of peroxisomal proteins (Emanuelsson et al., 2003). Screening the Arabidopsis genome for proteins carrying targeting signals specifically defined for higher plants (Hayashi et al., 1997; Reumann, 2004) has led to the identification of about 280 genes that encode proteins containing putative PTS1 (220) and PTS2 (60) peptides (Kamada et al., 2003; Reumann et al., 2004). Results from these *in silico* analyses suggest that, although only a few dozen proteins have annotated peroxisomal functions, the total number of proteins in plant peroxisomes may well exceed 300.

Fusion of either signal peptide to a heterologous protein results in direct targeting to peroxisomes. Thus, the enzymatic content of peroxisomes can be easily modified. In contrast to plastids and mitochondria, the peroxisomal protein import machinery is able to import fully folded proteins and stable protein complexes in a receptor-independent fashion (Hu et al. 2012). The import of heterologous protein complexes into peroxisomes depends on a mechanism called “piggybacking”, where a protein without a peroxisomal-targeting signal uses a PTS-carrying protein as shuttle (Mullen et al., 1997; Meyer et al., 2011). Therefore, coupling of a shuttle protein to other proteins might enable the targeting of even larger protein complexes to peroxisomes without modifying the import receptor machinery.

Novel plant PTS peptides are being discovered in the postgenomic era. The characterization of only three additional PTS1 tripeptides allowed the prediction of about 100 additional PTS1-containing proteins in Arabidopsis (Reumann et al., 2007). However, *in silico* predictions of peroxisomal

proteins also have limitations. We are still unable to predict proteins that are targeted to the membrane of peroxisomes or imported into the peroxisomal matrix by non-PTS1/2 pathways or “piggy-backing” mechanisms. In addition, some true peroxisomal proteins are currently missed by predictions, because of our insufficient knowledge of PTS variant sequences. Furthermore, amino acid residues located adjacent to PTSs can be crucial in some cases for PTS recognition and peroxisome targeting (Brocard and Hartig, 2006): for example, protein targeting to plant peroxisomes by weak PTS1 tripeptides such as SHL (where . indicates the stop codon) is dependent on the presence of basic residues upstream of PTS1 (Ma and Reumann, 2008); thus, plant proteins terminating with a weak PTS1 tripeptide and lacking essential targeting enhancer elements nearby are likely nonperoxisomal. In addition, proteins carrying strong PTS1s such as SKL can be nonperoxisomal if the PTS1 is preceded by several acidic residues (Ma and Reumann, 2008). Lastly, some predicted PTSs may not be surface exposed and/or can be overruled by other targeting signals (Brocard and Hartig, 2006).

Mass spectrometry (MS) analysis of proteins from purified peroxisomes is a powerful alternative approach to discover peroxisomal proteins, especially those unidentifiable by computational strategies. To date, researchers have generally used two-dimensional gel electrophoresis (2-DE) of purified plant peroxisomes followed by MS analysis to identify proteins from peroxisomes taken from *Arabidopsis* green cotyledons and leaves (Fukao et al., 2002; Reumann et al., 2007) or from etiolated *Arabidopsis* and soybean (*Glycine max*) cotyledons (Fukao et al., 2003; Arai et al., 2008). Initial proteome analyses of *Arabidopsis* peroxisomes identified a relatively small number of proteins, largely due to the great difficulty in

isolating highly pure peroxisomes, which is a bottleneck in organelle proteomics (Fukao et al., 2002, 2003). Leaf peroxisomes are generally very instable in aqueous solution due to the presence of a single membrane and (para-)crystalline inclusions in the matrix. Leaf peroxisomes from *Arabidopsis* are particularly fragile and, moreover, strongly physically adhere to chloroplasts and mitochondria for largely unknown reasons.

A proteome study with improved peroxisome purification methods significantly increased the number of peroxisomal matrix proteins identified from leaf peroxisomes (Reumann et al., 2007). However, some known matrix proteins and unknown regulatory proteins, most membrane proteins, and numerous novel proteins predicted to be peroxisome targeted with high probability by *in silico* PTS searches (Reumann et al., 2004) remained undetected. Eubel et al. (2008) purified peroxisomes from *Arabidopsis* cell suspension cultures by free-flow electrophoresis and detected about 20 novel proteins whose functions had not been associated with peroxisomes before. One of these putative novel proteins was confirmed to be peroxisomal by *in vivo* subcellular targeting analysis (Eubel et al., 2008).

Various abiotic and biotic stress conditions, such as salinity, heat, cold, drought, and pathogen infection induce oxidative stress in plants. This results in overproduction of ROS in chloroplasts, mitochondria, and peroxisomes, with highly oxidative metabolism (Halliwell et al., 2006; Mittler et al., 2002). Plants are unable to escape exposure to environmental stresses, thus they have developed a complex antioxidant defense system to control ROS levels and protect cells from oxidative injury (Palma et al., 2006). Under non-stress conditions ROS produced by peroxisomal metabolism are

scavenged by the simultaneous action of the peroxisomal antioxidant systems catalase, ascorbate peroxidase and the ascorbate–glutathione cycle (del Rio et al., 2002). However, under oxidative stress conditions peroxisomal ROS generation is enhanced and ROS scavenging is insufficient (del Rio et al., 2002). The ability to cope with an increased ROS production is correlated with up-regulation of peroxisomal antioxidant systems in natural stress-tolerant plant species (Mittova et al., 2003; 2004). One goal for engineering plants with wide-ranging stress resistance would be improving the peroxisomal ROS scavenging machinery (i.e. modulate the gene expression and enzymatic activity). Catalase as a prominent H₂O₂ scavenger is an important target. It is highly abundant in plant peroxisomes but has a low substrate affinity (Mhamdi et al., 2012). Modulation of its catalytic activity might be a starting-point to overcome this drawback, leading to more efficient ROS detoxification in plant peroxisomes. Because bacterial catalases offer higher H₂O₂ affinity, several studies have ectopically expressed the *Escherichia coli* catalase in plant species such as tobacco, tomato, and rice (Shikanai et al., 1998; Mohamed et al., 2003; Moriwaki et al., 2008). The resulting transgenic plants displayed an increased protection against oxidative stress. The same outcome was achieved by over-expression of the peroxisomal ascorbate peroxidase (APX), which acts in tandem with catalase to degrade H₂O₂ (Wang et al., 1999; Li et al., 2009;). Alternatively, an enhanced ascorbate–glutathione cycle in the peroxisomal matrix could reduce plant stress (del Rio et al., 2002). To accomplish this task various modifications are required simultaneously: (i) enlarging the peroxisomal glutathione and ascorbate pool by stimulating biosynthesis and uptake into peroxisomes, (ii) increasing the NADPH levels in peroxisomes by over-expressing the peroxisomal NAD kinase for NADPH production (Waller et al., 2010), and (iii) constitutive peroxisomal

targeting of glutathione reductase, which carries a weak peroxisomal targeting signal and is located in the cytosol and peroxisomes (Kataya et al., 2010). Previous studies have successfully induced the biosynthesis of glutathione and ascorbate, resulting in higher glutathione and ascorbate levels in the cytosol (Foyer et al., 1995; Chen et al., 2003). To increase peroxisomal import of glutathione and ascorbate, specific peroxisomal transport proteins remain to be identified. To date, modifying the redox state of peroxisomal ascorbate and glutathione pools is feasible (Waller et al., 2010; Kataya et al., 2010). Enhancing glutathione and ascorbate uptake remains to be achieved in future, since corresponding peroxisomal transporters have not been identified thus far.

Peroxisomes are an attractive target for metabolic engineering, to increase yield and quality of plant products. Manipulation of peroxisomal scavenging systems for reactive oxygen species (ROS) might enhance plant fitness under environmental stress conditions (Nielsen, 1998). Besides altering peroxisomal functions, novel pathways can be implemented in peroxisomes, enabling the synthesis of desired metabolites or degradation of toxic molecules. The following characteristics illustrate why peroxisomes are well suited for biotechnological purposes: (i) Peroxisomes are surrounded by a single bilayer lipid membrane (Hu et al., 2014). Novel reactions can be compartmentalized within peroxisomes. A peroxisomal compartmentation is favourable because end products or intermediates can be toxic for the cell. As peroxisomes are equipped with efficient ROS-detoxifying systems (Palma et al., 2006), ROS-producing reactions can be introduced in peroxisomes without deleterious effects. (ii) Peroxisomes allow an efficient targeting of heterologous proteins, since protein-targeting signals for the peroxisome are well established. However, several limitations have to be considered when

modifying or introducing pathways to peroxisomes. If fluxes through endogenous peroxisomal pathways are changed, overall cellular metabolism and substrate homeostasis could be negatively influenced. For example, changes in peroxisomal contributions to auxin synthesis or photorespiration were reported to create substantial reductions in fitness (Zolman et al., 2000; Igarashi et al., 2003)).

Peroxisomal bypass pathways to reduce photorespiration

A central function of plant peroxisomes is their contribution to photorespiration (Fig. 5.2) (Hu et al., 2012). This light-dependent pathway is linked to photosynthesis by the dual function of plastidic Rubisco. Low carbon dioxide concentrations favour the oxygenase reaction of Rubisco leading to an accumulation of toxic 2-phosphoglycolate (Reumann and Weber, 2006). This compound is efficiently degraded via the photorespiratory C₂ cycle, converting 2-phosphoglycolate to 3-phosphoglycerate, which re-enters the Calvin–Benson cycle. CO₂ and ammonia (NH₃) are released. Substantial energy costs are required for re-assimilation (Fig. 5.2) (Reumann and Weber, 2006). The goal is to optimize plant metabolism and to increase biomass production by minimizing energy losses in photorespiration. As photorespiration is required in all photosynthetic organisms, it cannot be eliminated completely, but bypassed (Maurino and Peterhansel, 2010). So far, three reactions have been tested in plants circumventing energy loss from photorespiration (Peterhansel et al., 2013). A reduction of the Rubisco oxygenase reaction was attempted by increasing CO₂ levels inside chloroplasts, utilizing carbon derived from 2-phosphoglycolate (Fig. 5.2, blue pathway) (Maier et al., 2012). Secondly, an alternative plastidic conversion route for 2-phosphoglycolate has been reported (Fig. 5.2, red pathway)

(Kebeish et al., 2007). Both approaches bypassing the mitochondrial CO₂ release led to an increase in biomass production under ambient CO₂ conditions (Kebeish et al., 2007; Maier et al., 2012). To avoid mitochondrial NH₃ production a short-circuit pathway of the photorespiratory nitrogen cycle was implemented into peroxisomes (Carvalho et al., 2011). Glyoxylate carboligase (GCL) and hydroxypyruvate isomerase (HYI) from *E. coli* were introduced into peroxisomes of transgenic tobacco leaves resulting in a peroxisomal conversion of glyoxylate to hydroxypyruvate (Fig. 5.2, green pathway). Unfortunately, this bypass did not show the benefits expected for biomass production (Carvalho et al., 2013). Instead, leaves of transgenic tobacco displayed chlorotic lesions under ambient CO₂ levels. Detailed analyses revealed that the GCL/HYI pathway introduced was not fully operating, due to silencing of the bacterial hydroxypyruvate isomerase gene (Carvalho et al., 2013). Thus, the functionality of this proposed pathway remains to be demonstrated. The use of RNA-silencing tobacco mutants might overcome this obstacle (Voinett et al., 2003). It might enable further analyses studying peroxisomes as tools to bypass photorespiration (Carvalho et al., 2013).

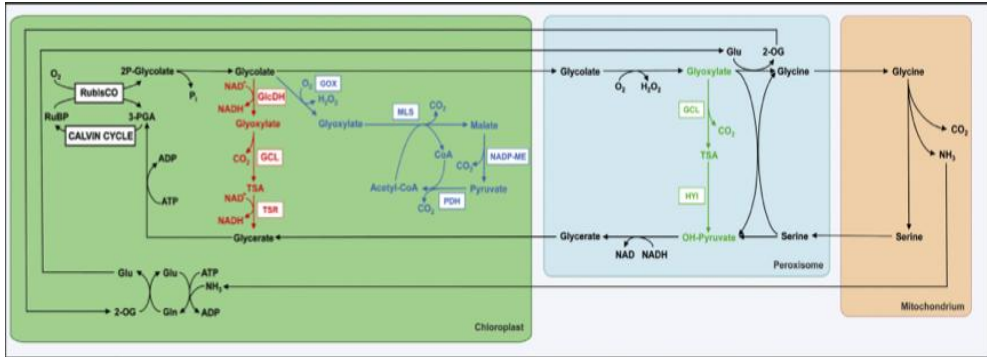


Fig. 5.2 The loss of ammonia during photorespiration can be bypassed. Ammonia and CO_2 are released in mitochondria during the conversion of glycine to serine. Ammonia can be re-assimilated in chloroplasts. The ammonia-consuming reactions can be bypassed by a photorespiratory short-circuit in peroxisomes (shown in green) by introducing two bacterial enzymes GCL and HYI. The plastidic bypasses introduced by Maier et al. and Kebeish et al. are presented in blue and red, respectively.

Materials and Methods.

Plant material and growth conditions

Seeds of cucumber (*Cucumis sativus* L. cv. Marketmore '76) were surface-sterilized and sown in Agriperlite, watered with 0.1 mm $CaSO_4$, allowed to germinate in the dark at $26^\circ C$ for 3 d, and then transferred to a nutrient solution with the following composition: 2 mm $Ca(NO_3)_3$, 0.75 mm K_2SO_4 , 0.65 mm $MgSO_4$, 0.5 mm KH_2PO_4 , 10 μm H_3BO_3 , 1 μm $MnSO_4$, 0.5 μm $CuSO_4$, 0.5 μm $ZnSO_4$, 0.05 μm $(NH_4)Mo_7O_{24}$ and 0.1 mm Fe(III)-EDTA (when added). The pH was adjusted to 6.2 with NaOH. Aerated hydroponic cultures were maintained in a growth chamber with a day:night regime of 16:8 h and a photosynthetic photon flux density (PPFD) of $200 \mu mol m^{-2} s^{-1}$ photosynthetically active radiation (PAR) at the plant level. The temperature was $18^\circ C$ in the dark and $24^\circ C$ in the light. For the time-course experiments, 3 d-old plants grown in the

nutrient solution were transferred, after removal of cotyledons, to 10 L of the same solution without Fe (Fe-deprived plants). Roots of these plants were carefully washed with 0.5 mM CaSO₄ and rinsed with distilled water before being transferred. Other 3-day-old plants grown in the nutrient solution without Fe were transferred of the complete solution (Fe-resupplied plants). Sampling was performed after 0, 1, 3 and 7 days following induction/removal of Fe deficiency and 4 h after onset of the photoperiod. For clarity, plants previously grown in the presence/absence of Fe for 3 d and then transferred to a Fe-free/complete solution are hereby referred to as 0 throughout the text.

Iron-deficient plants showed the typical Fe deficiency morphological responses (development of leaf Fe deficiency chlorosis, stunted growth and appearance of lateral roots) and the increase in the specific activities (Fe³⁺-chelate reductase and H⁺-ATPase) proper of Strategy I plants (data not shown).

Isolation of Peroxisomes from Mature Leaves in High Purity

To identify plant-specific peroxisomal proteins we follow a new purification method described by Reumann et al., (2007, 2009, 2014) for leaf peroxisomes with some modifications, established with the objectives of (i) increasing the stability of peroxisomes in aqueous solution, (ii) reducing the physical interaction of peroxisomes with mitochondria and chloroplasts, and (iii) increasing the specificity of peroxisome enrichment by a combination of Percoll and sucrose density gradient centrifugation. 10-d-old leaves from cucumber plants were harvested at the end of the dark period, stored in a ice bag during the lagging time, and then gently ground in a buffer of high osmolarity (GB: 170 mM Tricine-KOH, pH 7.5, 1.0 M sucrose, 1% [w/v] BSA, 2 mM EDTA, 5 mM DTT, 10 mM KCl, and 1 mM MgCl₂) in the presence of protease inhibitors

cocktail (0,1 mM PMSF, 0,2 mM benzamide and 0,2 mM ϵ -amminocaproic acid) using a mortar and a pestle. The suspension was filtered, and chloroplasts were sedimented at 5000g (1 min, SS34 rotor). Approximately 20 mL of supernatant was loaded onto a Percoll density gradient prepared in TE buffer (20 mM Tricine-KOH, pH 7.5, and 1 mM EDTA) supplemented with 0.75 M sucrose and 0.2% (w/v) BSA underlaid by 36% sucrose (w/w) in TE buffer (top to bottom gradient composition: 3 mL of 15% Percoll, 9 mL of 38% Percoll, 2 mL each of a mixture of 38% Percoll, and 36% [w/w] sucrose at a ratio of 2:1 and 1:2, and 3 mL of 36% (w/w) sucrose in TE buffer). The mixed Percoll-sucrose gradients were centrifuged for 12 min at 10,500 rpm and then 10 to 20 min at 15,000 rpm (SS34 rotor). Co-sedimentation of peroxisomes along with mitochondria and thylakoid membranes by differential centrifugation prior to isopycnic organelle separation increased irreversibly interorganellar adhesion and peroxisome contamination. Whereas chloroplasts, thylakoid membranes, and mitochondria were largely retained in the 15 and 38% (v/v) Percoll fraction near the top of the gradient, intact leaf peroxisomes crossed the Percoll layer and were recovered at the bottom, visible as a whitish diffuse organelle sediment (Figure 5.3). The peroxisome fractions at the bottom of the gradient of several Percoll gradients were combined, diluted in 36% (w/w) sucrose in TE buffer, washed several times in TE buffer and finally sedimented by centrifugation (30 min, 15,000 rpm, SS34 rotor), supplemented with protease inhibitors, and stored in appropriate aliquots, yielding the leaf peroxisomal fraction LP-P1. The enrichment in leaf peroxisomes was high, as determined by western blot analysis using catalase and glyoxilate oxidase as marker. Contaminating chloroplasts and mitochondria were estimated to comprise only 0.1 and 1.7% of the total, respectively (Reumann et al., 2007 (Table 5.1).

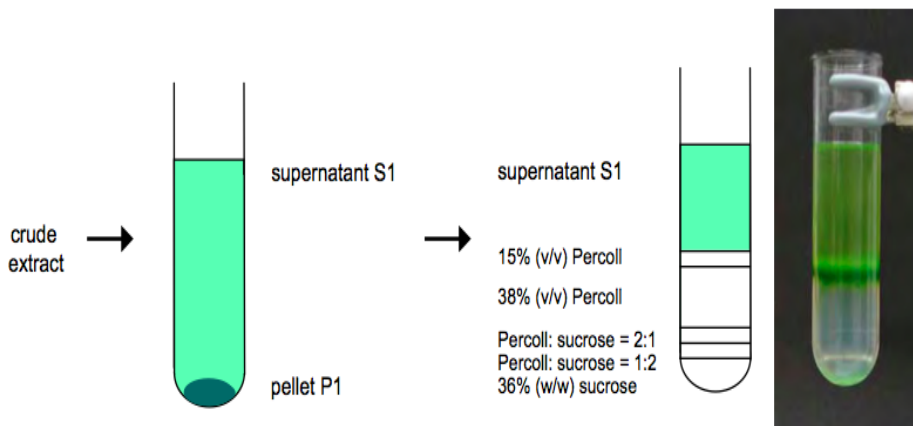


Figure 5.3 Work flow of the isolation of leaf peroxisomes from mature leaves of *Cucumis sativus* L. by a mixed Percoll and sucrose density gradient centrifugation. The green colour at the bottom of the Percoll gradient is due to light reflection from the thylakoid fraction rather than plastid contamination (see also table 5.1)

Biochemical Analysis of Peroxisome Purity								
	HPR		NADP-Dependent GAPDH			Fumarase		
	Activity (nkat)	Percentage of CE	Activity (nkat)	Percentage of CE	Contamination (%)	Activity (nkat)	Percentage of CE	Contamination (%)
Crude extract	1240 ± 70	100	1500 ± 500	100		167 ± 35	100	
Leaf peroxisome fraction LP-P1	89.5 ± 27.5	7.2	0.39 ± 0.14	0.026	0.36	0.56 ± 0.32	0.33	4.6
Leaf peroxisome fraction LP-P2	45.8 ± 17.5	3.7	0.065 ± 0.029	0.0043	0.12	0.10 ± 0.04	0.062	1.7

Table 5.1 Peroxisome purity was determined on the basis of the activity of specific marker enzyme for leaf peroxisome (HPR), chloroplasts (NADP-dependent GAPDH) and mitochondria (fumarase). CE, crude extract.

Western blot analysis

Purified peroxisomes isolated from leaf of cucumber plants grown in the presence and the absence of Fe were loaded on a discontinuous SDS-polyacrylamide gel, (3.75% (w/v) acrylamide stacking gel, and 10–15% (w/v) acrylamide separating gel) (according to the method of Laemmli, 1970).

Electrophoretic transfer to nitrocellulose membrane filters (Sigma, Milan, Italy) was performed in 48 mM Tris, 39 mM glycine, 0.0375% SDS and 20% (v/v) methanol for 1.5 h at room temperature at 0.8 mA cm⁻². After blotting, the membrane was incubated for 1 h in PBS-TB blocking buffer (phosphate-buffered saline, 0.1% Tween-20, 1% BSA, (for monoclonal antibodies)) or TBS-TM blocking buffer (Tris-buffered saline, 0.1% Tween-20, 5% commercial dried skimmed milk, (for polyclonal antibodies)). Different antibodies were used, and the dilution ratios were: 1:6000 for α -CAT (Yamaguchi et al., 1984), 1:3000 for α -GOX (Nishimura et al., 1983), 1:3000 for α -PEX14 (Hayashi et al., 2000). All these antibodies were a kind gift from Dr. Shoji Mano from the department of Cell Biology, National Institute for Basic Biology, Okazaki, Japan. The incubation in primary antibody, diluted in blocking buffer, was carried out for 2 h at room temperature. After rinsing with TBS-TM or PBS-TB, nitrocellulose membranes were incubated at room temperature for 2 h with a 1:10000 diluted secondary antibody (alkaline phosphatase-conjugated anti-rabbit (for polyclonals) or anti-mouse (for monoclonals) IgG, Sigma). After rinsing in TBS-T (Tris-buffered saline, 0.1% Tween-20) or PBS-T (phosphate-buffered saline, 0.1% Tween-20), filters were incubated in 5-bromo-4-chloro-3-indolylphosphate and nitroblue tetrazolium (FAST BCIP/ NBT, Sigma) for detection.

Assay of Catalase (enzymatic) activity

Catalase activity assay was performed according to the method described by Luck et al. (1965). 10-days-old leaves of cucumber plant were grounded in a mortar with the addition of liquid nitrogen (N₂), polyvinyl pyrrolidone (PVPP) 10% (w/w leaves), and buffer in a ratio 1: 2.5 (w:v) (Buffer composition: Tris-HCl 220 mM- pH 7.4; MgCl₂ 1mM; KCl 50 mM; Sucrose 250 mM; DTT 1mM (P.M.154,3); PMSF (50 mg/ml DMSO). The suspension was filtered and then centrifugated at 12000 g for 30 minutes at 4° C. Supernatant was recovered and then dialyzed overnight against diluted extraction buffer (approximately 1:50). Degradation of H₂O₂, which reflects the catalytic activity of catalase was monitored by spectrophotometric analysis at 240 nm, 25° C ($\epsilon_{m\ 240} = 39,4\text{ mM}^{-1}\text{ cm}^{-1}$) using Na-phosphate buffer 65 mM pH 7.2 as assay buffer.

Assay of Glycolate oxidase activity

Glycolate oxidase activity was measured according to Macheroaux et al (1991) in an enzyme-coupled assay using horseradish peroxidase and *o*-dianisidine to remove hydrogen peroxide generated during oxidation of glycolate. A typical assay mixture contained μ 10 L of horseradish peroxidase (1 mg/mL), 50 μ L of *o*-dianisidine solution (8 mM, 20% Triton X-100), 10 μ L of sodium glycolate (1 M), and 930 μ L of 0.1 M potassium phosphate buffer, pH 8.3. The reaction was started by adding 10 μ L of the glycolate oxidase sample. Formation of the *o*-dianisidine radical cation, which reflects the catalytic activity of glycolate oxidase was monitored by spectrophotometric analysis at 440 nm and at 25° C ($\epsilon_{m\ 440} = 11600\text{ M}^{-1}\text{ cm}^{-1}$).

Assay of Hydroxypyruvate reductase activity

Hydroxypyruvate activity assay was measured as described previously by Schwizguebel and Seigenthaler (1984) in a reaction medium containing 50mm phosphate buffer (pH 6.2); 0.025%(v/v) TritonX-100; 1 mM KCN 0.2mm NADH. The reaction was started by the addition of 2mm hydroxypyruvate and the oxidation of NADH was followed at 340 nm ($\epsilon_{m\ 340} = 6,22\ M^{-1}\ cm^{-1}$).

Protein determination

Protein content was determined by the Bradford (1976) procedure using the Bio-Rad reagent and bovine serum albumin as a protein standard.

Results

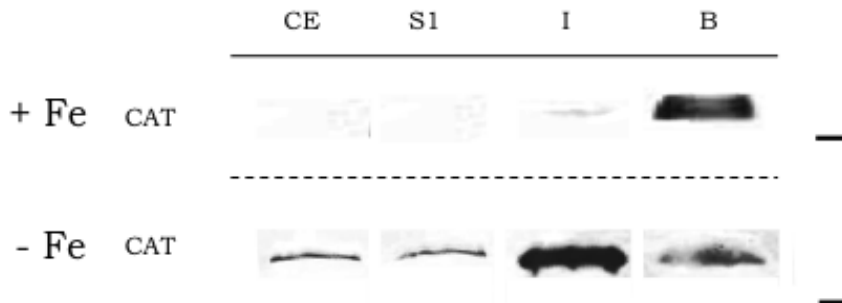


Figure 5.4. Western blot analysis of different fraction of the mixed Percoll-Sucrose gradient on + Fe and - Fe cucumber leaves. For each sample, 10 μ g of protein was used. Antibody used was against catalase. CAT catalase; CE crude extract; S1 supernatant 1; I Percoll-Sucrose interface; B bottom of the centrifugation tubes.

In order to assess the efficiency of the protocol used for peroxisome isolation, we firstly perform western blot analysis on our samples, using catalase as a marker. The results of this experiment are shown in figure 5.4. As shown by the image, Fe deficiency induces a louder immunochemical signal compared to control condition (plants grown in the presence of Fe). Curiously, the two treatments result in a different distribution of the immunochemical signal among the different fractions of the mixed Percoll-sucrose separation gradient. To fill the complete form of catalase behaviour under Fe deficiency, we decide to determine the activity of this enzyme at different bioavailability conditions of this element. As reported in figure 5.5 (left), the complete lack of Fe results in a strong inhibition of catalase activity (-35%) after 10d of growth in the leaves of cucumber plants. This result was consistent to our previous observation of reduced activity determined through activity staining assay on native PAGE (see chapter IV). Deprivation of Fe to Fe-sufficient plants determines no significant variation in the activity of this enzyme, whereas Fe resupply to Fe-deficient plants results in a restoration of the activity to level similar to the Fe-sufficient plants after 24 h (fig. 5.5 (centre)). Iron deprivation of Fe-sufficient plants seems to induce a gradually and constant increase in the catalase activity with the proceedings of Fe deficiency during the time. Nevertheless, this variation was not significant.

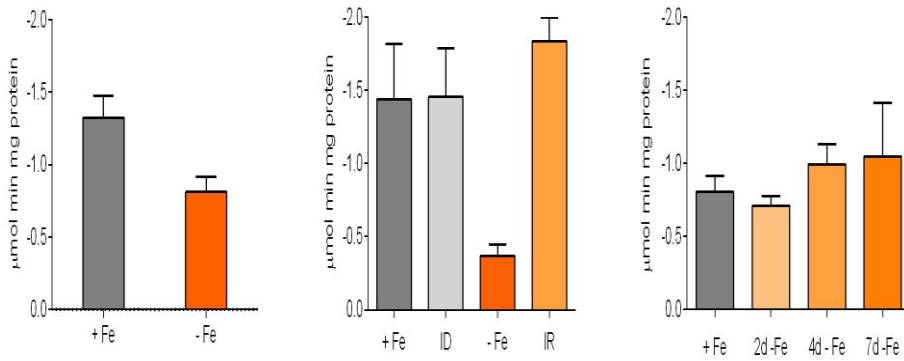


Figure 5.5 Enzymatic activity of catalase in different experimental conditions: (left) plants grown in the presence or absence of Fe (50-0 mM Fe); (centre) plants grown for 6 g in the presence/absence of Fe and subsequently deprived/replenished with Fe, sampling after 1 d; (right) plants grown under Fe sufficiency to 6 d subsequently deprived of Fe, samples after 2, 4 and 7 d of treatment.

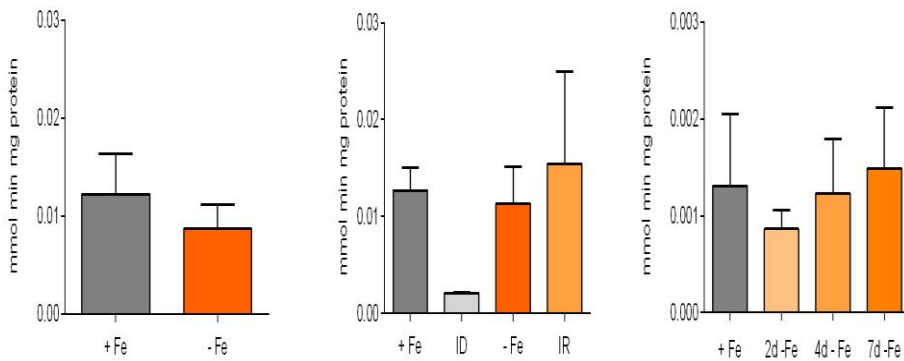


Figure 5.6 Enzymatic activity of glycolate oxidase in different experimental conditions: (left) plants grown in the presence or absence of Fe (50-0 mM Fe); (centre) plants grown for 6 g in the presence/absence of Fe and subsequently deprived/replenished with Fe, sampling after 1 d; (right) plants grown under Fe sufficiency to 6 d subsequently deprived of Fe, samples after 2, 4 and 7 d of treatment.

To check if the Fe deficiency also affects the activity of enzymes that do not use Fe as a cofactor, we then determinate the activity of another peroxisomal enzyme, glycolate oxidase, which catalyze the first reaction of photorespiration into peroxisome, the conversion of glycolate to glyoxilate. During this reaction, H₂O₂ is normally generated as byproduct and then scavenged by catalase. As shown in figure 5.6, Fe deficiency does not result in significant variation in the activity of this enzyme. Due to the great variability inherent in the method, we were not able to observe any significant change in the enzyme activity in all the different experimental conditions verified, with the sole exception of a strong reduction in the enzymatic activity after 24 h from the deprivation of Fe in Fe-sufficient plants. In any case, it would appear that the deprivation of Fe to Fe-sufficient plants might result in a gradual increase in the activity of glycolate oxidase. Furthermore, western blot analysis on peroxisomal purified fraction LP-P1 against glycolate oxidase, allow us to observe no difference in the immunochemical signal, as showed in figure 5.7.

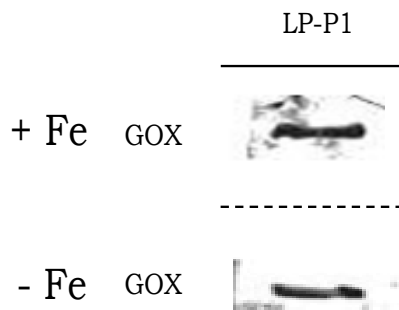


Figure 5.7 Western blot analysis of + Fe and - Fe cucumber leaves. For each sample, 12 µg of protein was used. Antibody used was against Glycolate oxidase. GOX catalase; LP-P1 Leaf peroxisome purified fraction.

The activity of another Fe-independent peroxisomal enzyme, the hydroxypyruvate reductase, has been investigated. The lack of Fe during growth does not induce significant alterations in the total activity of this enzyme in the leaves of cucumber plants (figure 5.8 left). Moreover, we discriminate the activity of the two hydroxypyruvate reductase isoforms (cytosolic and peroxisomal), using NADPH or NADH, according to the selective substrate affinity of the two different isoform. As shown in figure 5.8, right, in Fe sufficiency condition the total hydroxypyruvate reductase activity was fully attributable to the peroxisomal isoform (HPR1), while we can not observe any cytosolic isoform (HPR2) activity. Conversely, in plants grown under conditions of Fe deficiency the total enzymatic activity was comparable to that of the control condition, whereas there was an equal distribution of the activity between the two isoforms.

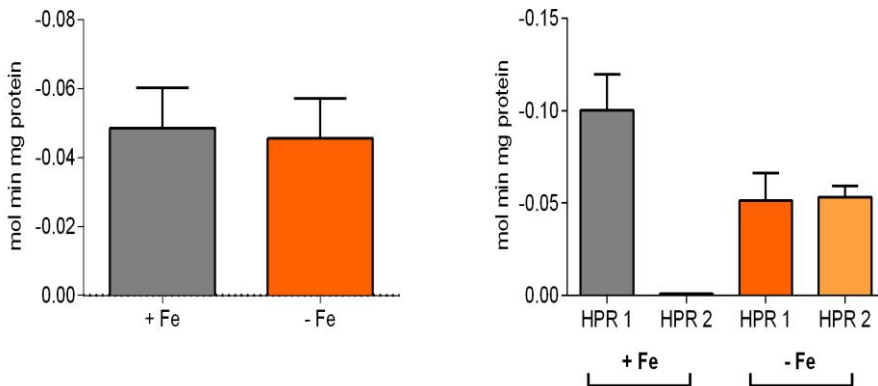


Figure 5.8 Enzymatic activity of hydroxypyruvate reductase. Plants grown in the presence or absence of Fe (50-0 mM Fe); (left) total hydroxypyruvate activity; (right) discrimination of isoform activity achieved using NADPH or NADH as substrate, according to the selective affinity of the two different isoform. Hydroxypyruvate reductase activity 1 (peroxisomal isoform); HPR2 Hydroxypyruvate reductase activity 2 (cytosolic isoform).

Discussion

The conducted western blot analysis on catalase allowed us to verify the efficiency of the protocol used for the isolation of peroxisomes. In the Fe-deficient plants it was observed an increase in the immunochemical signal, index of a greater accumulation of this enzyme compared to control conditions. However, in the two different experimental conditions tested, a different distribution of the induced signal within the separation gradient was observed. In Fe deficiency conditions peroxisomes accumulate mainly in the interface between the mixed Percoll-sucrose 1: 2 and 36% sucrose (w/v) fractions on the bottom of the tube. In conditions of Fe sufficiency, peroxisomes instead accumulate on the bottom of the separation gradient. Some variability was still seen among the various biological repetitions. This behaviour is in agreement with what reported by the authors of the method (Reumann et al., 2007). For this reason, we decided to collect the mixed Percoll-sucrose 1: 2 and 36% sucrose (w/v) fractions and name them LP-P1, in order to isolate the largest possible amount of peroxisomes. We then started the biochemical characterization of the peroxisome on these purified fractions. Instead the greater accumulation of the protein in the leaves, the activity of one of the principal enzymes of the peroxisomal metabolism, catalase, which is involved in the photorespiratory process since it catalyses the detoxification of hydrogen peroxide produced by the reaction catalysed by glycolate oxidase, results to be greatly compromised (-35%), in conditions of Fe deficiency. This is probably due to the lack of the element in the tissues, since catalase uses it as a cofactor (Fe is contained in the heme group).

Recent studies (Shibata et al., 2013; Sinclair et al., 2009) report that the accumulation of inactive catalase in

peroxisomes triggers an aggregation process that mediate their subsequent degradation through autophagy, in a process mediated by the consequent accumulation of H₂O₂. More in detail, in peroxisomes of photosynthetic organs, hydrogen peroxide is excessively produced, mainly from photorespiratory metabolism. Catalase is the main scavenging enzyme for hydrogen peroxide, but this enzyme is irreversibly inactivated by its substrate (Williams, 1928). Thus, H₂O₂ accumulates in response to catalase inactivation in the peroxisomes, and the peroxisomes gradually exhibit oxidative conditions. When plant leaves are treated with hydrogen peroxide, peroxisomes change their morphology, forming extended structures termed peroxules (Sinclair et al., 2009). In addition, data reported by Shibata et al. (2013) reveal that peroxisome aggregates observed in the Arabidopsis *peup1* mutant consist of peroxisomes that were oxidized by an excess of hydrogen peroxide. The aggregated peroxisomes in the *peup1* mutant actually sometimes formed extended structures similar to peroxules, suggesting that the accumulation of hydrogen peroxide induces peroxisome aggregation through the production of peroxule-like structures (Shibata et al., 2013). In this respect, a peroxisome aggregate can be considered to be a cluster of damaged peroxisomes. Because hydrogen peroxide also functions as a signalling molecule in processes such as programmed cell death (Alvarez et al., 1998; Gechev and Hille, 2005; del Rio and Pusso, 2009), damaged peroxisomes with un-controllable hydrogen peroxide levels preclude optimal plant growth. These damaged peroxisomes were accumulated in the *peup1* mutant, suggesting that autophagic processes in the wild type must degrade the peroxisomes. However, the factors that hold the peroxisomes together in the aggregates are still not completely understood (Shibata et al., 2013).

This phenomenon may also partly explain the different distribution of the catalase immunochemical signal within the different fractions of the separation gradient. This accumulation of inactive catalase in conditions of Fe deficiency could then induce a different density of peroxisomes. However, further investigation should be conducted to validate this hypothesis.

The activity of Fe-independent enzyme glycolate oxidase does not show significant changes in the various experimental conditions tested, probably this was due to the great variability inherent in the analytical method. No variation in quantity of the protein was also observed in the western blot analysis conducted.

The hydroxypyruvate reductase however, while not changing its total activity, sharing it equally between the peroxisomal and the cytosolic isoform under Fe-deficiency. This behaviour could be due to an alteration of the reducing state of the peroxisome. The data we obtained in rice (see also chapter VI) show that in Fe-deficiency was observed a strong reduction of malic acid in the tissues: this may result in a slowing of the reaction of malate dehydrogenase, which recycle NADH inside the peroxisome. NADH is the intermediate required by hydroxypyruvate reductase in the reduction reaction of hydroxypyruvate. The Fe-deficient plants could then bypass this lack of reducing power by a major activation of the cytosolic isoform to reduce hydroxypyruvate present. Up to date, however, the membrane transporters responsible for the movement of the photorespiratory intermediate among the different cellular compartments involved in photorespiration have not yet been identified and characterized, so we can not exclude that this different distribution of tasks between the two isoforms is attributable to an increased activity of the

transporter that moves the hydroxypyruvate outside peroxisomes.

Taken together, our data suggest that Fe deficiency induces alterations in peroxisomes, indicating alterations in the photorespiratory metabolism at different levels. However, further analysis are required to complete the metabolic characterization of this organelle, in order to fill the complete form of the metabolic changes of these organelles during Fe-starvation.

References

Arai Y., Hayashi M., Nishimura M. (2008) Proteomic analysis of highly purified peroxisomes from etiolated soybean cotyledons. *Plant Cell Physiol* 49: 526–539

Barton K., Mathur N., Mathur J., Simultaneous live-imaging of peroxisomes and the ER in plant cells suggests contiguity but no luminal continuity between the two organelles, *Frontiers in Physiology*, 4 (2013).

Banjoko A., Trelease R.N., Development and Application of an *in-Vivo* Plant Peroxisome Import System, *Plant Physiology*, 107 (1995) 1201-1208

Beever H., Microbodies in higher plants, *Annual Review of Plant Physiology*, 30 (1979) 159-193.

Bradford, M.M. 1976. A rapid and sensitive method for the quantification of microgram quantities of protein utilising the principle of protein-dye binding. *Anal. Biochem.* 72:248–254.

Brocard C., Hartig A. (2006) Peroxisome targeting signal 1: is it really a simple tripeptide? *Biochim Biophys Acta* 1763: 1565–1573

Carvalho J.d.F.C., et al., An engineered pathway for glyoxylate metabolism in tobacco plants aimed to avoid the release of ammonia in photorespiration, *BMC Biotechnol.* 11 (2011) 111.

Chen Z., Young T.E., Ling J., Chang S.C., Gallie D.R., Increasing vitamin C content of plants through enhanced ascorbate recycling, *Proc. Natl. Acad. Sci. USA* 100 (2003) 3525–3530.

Collings D.A., Harper J.D.I., Marc J., Overall R.L., Mullen R.T., Life in the fast lane: actin-based motility of plant peroxisomes, *Canadian Journal of Botany-Revue Canadienne De Botanique*, 80 (2002) 430-441.

Cross L.L., Ebeed H.T., Baker A., Peroxisome biogenesis, protein targeting mechanisms and PEX gene functions in plants, *BBA - Molecular Cell Research* (2015).

del Rio L.A., et al., Reactive oxygen species, antioxidant systems and nitric oxide in peroxisomes, *J. Exp. Bot.* 53 (2002) 1255–1272.

Eubel H., Meyer E.H., Taylor N.L., Bussell J.D., O'Toole N., Heazlewood J.L., Castleden I., Small I., Smith S.M., Millar A.H. (2008) Novel proteins, putative membrane transporters, and an integrated metabolic network are revealed by quantitative proteomic analysis of Arabidopsis cell culture peroxisomes. *Plant Physiol* 148: 1809–1829

Emanuelsson O., Elofsson A., von Heijne G., Cristobal S. (2003) In silico prediction of the peroxisomal proteome in fungi, plants and animals. *J Mol Biol* 330: 443–456

Fakieh MH, Drake PJM, Lacey J, Munck JM, Motley AM, Hettema EH, Intra-ER sorting of the peroxisomal membrane protein Pex3 relies on its luminal domain, *Biology Open*, 2 (2013) 829-837.

Fang Y., Morrell J.C., Jones J.M., Gould S.J., PEX3 functions as a PEX19 docking factor in the import of class I peroxisomal membrane proteins, *J Cell Biol*, 164 (2004) 863-875.

Frederick S.E., Newcomb E.H., Cytochemical localisation of catalase in leaf microbodies (peroxisomes), *J Cell Biol*, 43 (1969) 343-353.

Fukao Y., Hayashi M., Nishimura M. (2002) Proteomic analysis of leaf peroxisomal proteins in greening cotyledons of *Arabidopsis thaliana*. *Plant Cell Physiol* 43: 689–696

Fukao Y., Hayashi M., Hara-Nishimura I., Nishimura M. (2003)

Novel glyoxysomal protein kinase, GPK1, identified by proteomic analysis of glyoxysomes in etiolated cotyledons of *Arabidopsis thaliana*. *Plant Cell Physiol* 44: 1002–1012

Hadden D.A., Phillipson B.A., Johnston K.A., Brown L.-A., Manfield I.W., El-Shami M., Sparkes I.A., Baker A., Arabidopsis PEX19 is a dimeric protein that binds the peroxin PEX10, *Mol Membr Biol*, 23 (2006) 325-336.

Halbach A., Rucktaeschel R., Rottensteiner H., Erdmann R., The N-domain of Pex22p Can Functionally Replace the Pex3p N-domain in Targeting and Peroxisome Formation, *J Biol Chem*, 284 (2009) 3906-3916

Halliwell B., Reactive species and antioxidants. Redox biology is a fundamental theme of aerobic life, *Plant Physiol.* 141 (2006) 312–322.

Hayashi M., Aoki M., Kondo M., Nishimura M. (1997) Changes in targeting efficiencies of proteins to plant microbodies caused by amino acid substitutions in the carboxy-terminal tripeptide. *Plant Cell Physiol* 38: 759–768

Hayashi, M., Nito, K., Toriyama-Kato, K., Kondo, M., Yamaya, T., and Nishimura, M. (2000). AtPex14p maintains peroxisomal functions by determining protein targeting to three kinds of plant peroxisomes. *EMBO J.* 19: 5701–5710.

Hu J., Baker A., Bartel B., Linka N., Mullen R.T., Reumann S., Zolman B.K., Plant, Peroxisomes: Biogenesis and Function, *The Plant Cell* 24 (2012) 2279-2303.

Hua R., Gidda S.K., Aranovich A., Mullen R.T., Kim P.K., Multiple Domains in PEX16 Mediate Its Trafficking and Recruitment of Peroxisomal Proteins to the ER, *Traffic*, 16 (2015) 832-852.

Hunt J.E., Trelease R.N., Sorting pathway and molecular targeting signals for the Arabidopsis peroxin 3, *Biochem Biophys Res Commun*, 314 (2004) 586-596.

Igarashi D., et al., Identification of photorespiratory glutamate:glyoxylate aminotransferase (GGAT) gene in Arabidopsis, *Plant J.* 33 (2003) 975–987.

Jedd G., Chua N.-H., Visualization of Peroxisomes in Living Plant Cells Reveals Acto-Myosin-Dependent Cytoplasmic Streaming and Peroxisome Budding, *Plant Cell Physiol*, 43 (2002) 384-392.

Karnik S.K., Trelease R.N., Arabidopsis Peroxin 16 Coexists at Steady State in Peroxisomes and Endoplasmic Reticulum, *Plant Physiol.*, 138 (2005) 1967-1981.

Karnik S.K., Trelease R.N., Arabidopsis peroxin 16 trafficks through the ER and an intermediate compartment to pre-existing peroxisomes via overlapping molecular targeting signals, *J Exp Bot*, 58 (2007) 1677-1693.

Kamada T., Nito K., Hayashi H., Mano S., Hayashi M., Nishimura M. (2003) Functional differentiation of peroxisomes revealed by expression profiles of peroxisomal genes in *Arabidopsis thaliana*. *Plant Cell Physiol* 44:1275–1289

Kataya A.R., Reumann S., Arabidopsis glutathione reductase 1 is dually targeted to peroxisomes and the cytosol, *Plant Signal. Behav.* 5 (2010).

Kebeish R., et al., Chloroplastic photorespiratory bypass increases photosynthesis and biomass production in *Arabidopsis thaliana*, *Nat. Biotechnol.* 25 (2007) 593–599.

Kindl H., The biosynthesis of microbodies (peroxisomes and glyoxysomes). *International Review of Cytology-a Survey of Cell Biology*, 80 (1982) 193-229.

Kim P.K., Hettema E.H., Multiple Pathways for Protein Transport to Peroxisomes, *J Mol Biol*, 427 (2015) 1176-1190.

Lanyon-Hogg T., Hooper J., Gunn S., Warriner S.L., Baker A., PEX14 binding to Arabidopsis PEX5 has differential effects on PTS1 and PTS2 cargo occupancy of the receptor, *FEBS Lett*, 588 (2014) 2223-2229.

Laemmli U.K. 1970. Cleavage of structural proteins during the assembly of the head of bacteriophage T4. *Nature* 227: 680–685.

Li Y.-J., Hai R.-L., Du H.-X., Jiang H.-N., Lu H., Over-expression of

a *Populus* peroxisomal ascorbate peroxidase (PpAPX) gene in tobacco plants enhances stress tolerance, *Plant Breeding* 128 (2009) 404–410.

Lin Y., Sun L., Nguyen L.V., Rachubinski R.A., Goodman H.M., The pex16p homolog SSE1 and storage organelle formation in *Arabidopsis* seeds, *Science*, 284 (1999) 328-330.

Lin Y., Cluette-Brown J.E., Goodman H.M., The Peroxisome Deficient *Arabidopsis* Mutant sse1 Exhibits Impaired Fatty Acid Synthesis, *Plant Physiol.*, 135 (2004) 814-827

Ma C., Reumann S. (2008) Improved prediction of peroxisomal PTS1 proteins from genome sequences based on experimental subcellular targeting analyses as exemplified for protein kinases from *Arabidopsis*. *J Exp Bot* 59: 3767–3779

Ma C., Hagstrom D., Polley S.G., Subramani S., Redox-regulated Cargo Binding and Release by the Peroxisomal Targeting Signal Receptor, Pex5, *J Biol Chem*, 288 (2013) 27220-27231.

Maier A., et al., Transgenic introduction of a glycolate oxidative cycle into *A. thaliana* chloroplasts leads to growth improvement, *Front. Plant Sci.* 3 (2012) 38.

Mano S., Nakamori C., Kondo M., Hayashi M., Nishimura M., An *Arabidopsis* dynamin-related protein, DRP3A, controls both peroxisomal and mitochondrial division, *Plant J*, 38 (2004) 487-498.

Matsuzaki T., Fujiki Y., The peroxisomal membrane protein import receptor Pex3p is directly transported to peroxisomes by a novel Pex19p- and Pex16p-dependent pathway, *J Cell Biol*, 183 (2008) 1275-1286

Maurino V.G., Peterhansel C., Photorespiration: current status and approaches for metabolic engineering, *Curr. Opin. Plant Biol.* 2010 (2010) 23.

Mhamdi A., Noctor G., Baker A., Plant catalases: peroxisomal redox guardians, *Arch. Biochem. Biophys.* 61 (2012) 4197–4220.

Mittler R., Oxidative stress, antioxidants and stress tolerance, *Trends Plant Sci.* 7 (2002) 405–410.

Mittova V., Guy M., Tal M., Volokita M., Salinity up-regulates the antioxidative system in root mitochondria and peroxisomes of the wild salt-tolerant tomato species *Lycopersicon pennellii*, *J. Exp. Bot.* 55 (2004) 1105–1113.

Mittova V., Tal M., Volokita M., Guy M., Up-regulation of the leaf mitochondrial and peroxisomal antioxidative systems in response to salt-induced oxidative stress in the wild salt-tolerant tomato species *Lycopersicon pennellii*, *Plant Cell Environ.* 26 (2003) 845–856.

Mohamed E.A., et al., Overexpression of bacterial catalase in tomato leaf chloroplasts enhances photo-oxidative stress tolerance, *Plant Cell Environ.* 26 (2003) 2037–2046.

Moriwaki T., et al., Overexpression of the *Escherichia coli* catalase gene, katE, enhances tolerance to salinity stress in the transgenic indica rice cultivar, BR5, *Plant Biotechnol. Rep.* 2 (2008) 41–46.

Mullen R.T., Lee M.S., Flynn C.R., Trelease R.N. (1997) Diverse amino acid residues function within the type 1 peroxisomal targeting signal: implications for the role of accessory residues upstream of the type 1 peroxisomal targeting signal. *Plant Physiol* 115: 881–889

Nielsen J., Metabolic engineering: techniques for analysis of targets for genetic manipulations, *Biotechnol. Bioeng.* 58 (1998) 125–132.

Nishimura, M., Akhmedov, Y.D., Strzalka, K., and Akazawa, T. (1983). Purification and characterization of glycolate oxidase from pumpkin cotyledons. *Arch. Biochem. Biophys.* 222: 397–402.

Nito K., Kamigaki A., Kondo M., Hayashi M., Nishimura M., Functional classification of Arabidopsis peroxisome biogenesis factors proposed from analyses of knockdown mutants, *Plant Cell Physiol*, 48 (2007) 763-774.

Nyathi Y., Lousa C.D,M., van Roermund C.W., Wanders R.J.A.,

Johnson B., Baldwin S.A., Theodoulou F.L., Baker A., The Arabidopsis Peroxisomal ABC Transporter, Comatose, Complements the *Saccharomyces cerevisiae* pxa1 pxa2 Delta Mutant for Metabolism of Long-chain Fatty Acids and Exhibits Fatty Acyl-CoA-stimulated ATPase Activity, *J Biol Chem*, 285 (2010) 29892-29902

Nyathi Y., Zhang X., Baldwin J.M., Bernhardt K., Johnson B., Baldwin S.A., Theodoulou F.L., Baker A., Pseudo half-molecules of the ABC transporter, COMATOSE, bind Pex19 and target to peroxisomes independently but are both required for activity, *FEBS Lett*, 586 (2012) 2280-2286.

Nordgren M., Fransen M., Peroxisomal metabolism and oxidative stress, *Biochimie*, 98C (2014) 56-62.

Palma J.M., et al., Antioxidative enzymes from chloroplasts, mitochondria, and peroxisomes during leaf senescence of nodulated pea plants, *J. Exp. Bot.* 57 (2006) 1747-1758.

Purdue P.E., Lazarow P.B. (2001) Peroxisome biogenesis. *Annu Rev Cell Dev Biol* 17: 701-752

Reumann S. (2004) Specification of the peroxisome targeting signals type 1 and type 2 of plant peroxisomes by bioinformatics analyses. *Plant Physiol* 135: 783-800

Reumann S., Ma C., Lemke S., Babujee L. (2004) AraPeroX: a database of putative Arabidopsis proteins from plant peroxisomes. *Plant Physiol* 136: 2587-2608

Reumann S., Weber A.P., Plant peroxisomes respire in the light: some gaps of the photorespiratory C2 cycle have become filled – others remain, *Biochim. Biophys. Acta* 1763 (2006) 1496-1510.

Reumann S., Babujee L., Ma C., Wienkoop S., Siemsen T., Antonicelli G.E., Rasche N., Luder F., Weckwerth W., Jahn O. (2007) Proteome analysis of Arabidopsis leaf peroxisomes reveals novel targeting peptides, metabolic pathways, and defense mechanisms. *Plant Cell* 19: 3170-3193

Reumann S., Singhal R., Isolation of leaf peroxisomes from Arabidopsis for organelle proteome analysis, in: Jorriin-Novo J.V. et al. (eds.), Plant Proteomics: Methods and Protocols, *Methods in*

Molecular Biology, vol. 1072, (2014)

Peterhansel C., Blume C., Offermann S., Photorespiratory bypasses: how can they work? *J. Exp. Bot.* 64 (2013) 709–715.

Sato Y., Shibata H., Nakatsu T., Nakano H., Kashiwayama Y., Imanaka T., Kato H., Structural basis for docking of peroxisomal membrane protein carrier Pex19p onto its receptor Pex3p, *Embo Journal*, 29 (2010) 4083-4093.

Scott I., Sparkes I.A., Logan D.C., The missing link: inter-organellar connections in mitochondria and peroxisomes?, *Trends Plant Sci*, 12 (2007) 380-381.

Schliebs W., Saidowsky J., Agianian B., Dodt G., Herberg F.W., Kunau W.H., Recombinant human peroxisomal targeting signal receptor PEX5 - Structural basis for interaction of PEX5 with PEX14, *J Biol Chem*, 274 (1999) 5666-5673.

Schmidt F., Treiber N., Zocher G., Bjelic S., Steinmetz M.O., Kalbacher H., Stehle T., Dodt G., Insights into Peroxisome Function from the Structure of PEX3 in Complex with a Soluble Fragment of PEX19, *J Biol Chem*, 285 (2010) 25410-25417.

Schueller N., Holton S.J., Fodor K., Milewski M., Konarev P., Stanley W.A., Wolf J., Erdmann R., Schliebs W., SongY.-H., Wilmanns M., The peroxisomal receptor Pex19p forms a helical mPTS recognition domain, *Embo Journal*, 29 (2010) 2491-2500.

Shibata M., Oikawa K., Yoshimoto K., Kondo M., Mano S., Yamada K., Hayashi M., Sakamoto W., Oshumi Y., Nishimura M., Highly oxidized peroxisomes are selectively degraded via autophagy in *Arabidopsis*, *The Plant Cell* Vol. 25:4967-4983 (2013)

Shikanai T., et al., Inhibition of ascorbate peroxidase under oxidative stress in tobacco having bacterial catalase in chloroplasts, *FEBS Lett.* 428 (1998) 47–51.

Sinclair A.M., Trobacher C.P., Mathur N., Greenwood J.S., Mathur J., Peroxule extension over ER-defined paths constitutes a rapid subcellular response to hydroxyl stress, *Plant J*, 59 (2009) 231-242.

Stanley W.A., Filipp F.V., Kursula P., Schueller N., Erdmann R., Schliebs W., Sattler M., Wilmanns M., Recognition of a functional peroxisome type 1 target by the dynamic import receptor Pex5p, *Mol Cell*, 24 (2006) 653-663.

Tam Y.Y.C., Fagarasanu A., Fagarasanu M., Rachubinski R.A., Pex3p initiates the formation of a preperoxisomal compartment from a subdomain of the endoplasmic reticulum in *Saccharomyces cerevisiae*, *J Biol Chem*, 280 (2005) 34933-34939.

Theodoulou F.L., Bernhardt K., Linka N., Baker A., Peroxisome membrane proteins: multiple trafficking routes and multiple functions?, *Biochem J*, 451 (2013) 345-352.

Tugal H.B., Pool M., Baker A., Arabidopsis 22-kilodalton peroxisomal membrane protein. Nucleotide sequence analysis and biochemical characterization, *Plant Physiology*, 120 (1999) 309-320.

Voinnet O., Rivas S., Mestre P., Baulcombe D., An enhanced transient expression system in plants based on suppression of gene silencing by the p19 protein of tomato bushy stunt virus, *Plant J*. 33 (2003) 949-956.

Waller J.C., Dhanoa P.K., Schumann U., Mullen R.T., Snedden W.A., Subcellular and tissue localization of NAD kinases from Arabidopsis: compartmentalization of de novo NADP biosynthesis, *Planta* 231 (2010) 305-317.

Wang J., Zhang H., Allen R.D., Overexpression of an Arabidopsis peroxisomal ascorbate peroxidase gene in tobacco increases protection against oxidative stress, *Plant Cell Physiol.* 40 (1999) 725-732.

Yamaguchi, J., Nishimura, M., and Akazawa, T. (1984). Maturation of catalase precursor proceeds to a different extent in glyoxysomes and leaf peroxisomes of pumpkin cotyledons. *Proc. Natl. Acad. Sci. USA* 81: 4809-4813.

Zhang X., Lousa C.D.M., Schutte-Lensink N., Ofman R., Wanders R.J., Baldwin S.A., Baker A., Kemp S., Theodoulou F.L.,

Conservation of targeting but divergence in function and quality control of peroxisomal ABC transporters: an analysis using crosskingdom expression, *Biochem J*, 436 (2011) 547-557.

Zolman B.K., Yoder A., Bartel B., Genetic analysis of indole-3-butyric acid responses in *Arabidopsis thaliana* reveals four mutant classes, *Genetics* 156 (2000) 1323–1337.

**Knocking down Mitochondrial Iron Transporter (MIT)
reprograms
primary and secondary metabolism in rice plants(*)**

Gianpiero Vigani, Khurram Bashir, Yasuhiro Ishimaru, Martin Lehmann, **Fabio Marco Casiraghi**, Hiromi Nakanishi, Motoaki Seki, Peter Geigenberger, Graziano Zocchi and Naoko K Nishizawa.

(*) In press: Journal of Experimental Botany

Highlights

The partial loss of function of MIT (*mit-2*) affects the mitochondrial functionality by decreasing the respiratory chain activity. Furthermore, the transcriptome and the metabolome strongly change in rice mutant plants, in a different way (at a different extent) in roots and shoot. Such changes were different in roots and in shoot of *mit-2* rice plant.

Abstract

Iron is an essential micronutrient for plant growth and development and its reduced bioavailability strongly impairs mitochondrial functionality. In this work, the metabolic adjustment in rice (*Oryza sativa*) mitochondrial Fe transporter knockdown mutant (*mit-2*) was analyzed. Biochemical characterization of purified mitochondria from rice roots showed alteration in the respiratory chain of *mit-2* compared to wild type plants. In particular, proteins belonging to the type II alternative NAD(P)H dehydrogenases strongly accumulated in *mit-2* plants, indicating that *mit-2* mitochondria activate alternative pathways to keep the respiratory chain working.

Analyzing transcriptomic data of the *mit-2* plants, a strong alteration (up/down regulation) in the expression of genes encoding enzymes of both primary and secondary metabolism was found. In line with these changes, the metabolite profiles significantly changed both in roots and shoots of *mit-2* plants, e.g. leading to alterations in the levels of amino acids belonging to the aspartate-related pathways (aspartate, lysine, threonine in roots and aspartate, ornithine in shoots) that are strictly connected to the Krebs cycle. Furthermore, some metabolites (for instance pyruvate, fumarate, ornithine and oligosaccharides of the raffinose family) accumulated only in

shoot of mit-2 plant, indicating possible hypoxic responses. These findings suggest that the induction of local Fe deficiency in mitochondrial compartment of mit-2 plants differentially affects the transcriptome as well as the metabolite profile in root and shoot tissues.

Keywords: *Oryza sativa*, iron, iron deficiency, mitochondria, metabolomics, transcriptomics.

Abbreviations: Fe: Iron, MIT: mitochondrial Fe transporter

Introduction

Iron (Fe) is an essential element for plants, as it is part of the prosthetic group of different proteins directly involved in photosynthesis and respiration (heme or Fe-sulfur [Fe-S] clusters) as well as in other key metabolic pathways, such as nitrogen assimilation and scavenging of Reactive Oxygen Species (ROS) (Balk and Schaedler, 2014; Couturier et al., 2013).

Despite its abundance in soils, Fe is scarcely soluble especially under alkaline and aerobic conditions (Guerinot and Ying, 1994). Plants growing under low Fe availability, such as in calcareous soils, often suffer from Fe deficiency, which reduces growth, crop yield and quality (Marschner, 1995). The molecular mechanisms of Fe uptake from the rhizosphere have been extensively studied and two strategies have been identified in the plant kingdom: Strategy I, i. e. the reduction strategy and Strategy II, i.e. the chelation strategy (Bashir et al., 2010; Bashir et al., 2013; Kobayashi and Nishizawa, 2012a). Dicots and non-graminaceous monocots utilize Strategy I, whereas graminaceous plants utilize the Strategy II and possess a specific ability to synthesize the so-called phytosiderophores, Fe(III) chelators belonging to the mugineic acid family (Marschner and Romheld, 1994). These strategies have been previously considered mutually exclusive,

but some exceptions were recently reported in which Strategy II plants possess partial Strategy I uptake systems (Bashir et al., 2011b; Bashir et al., 2013; Bughio et al., 2002; Ishimaru et al., 2011; Kobayashi and Nishizawa, 2012b).

Despite the wealth of knowledge that has been gained concerning the processes by which plants can respond to Fe deficiency, the mechanisms of Fe sensing and signaling are not fully understood yet. It has been recently reviewed that some transcription factors involved in the Fe deficiency-induced responses might play a role as Fe sensors in the cell, while several molecules might be good candidates as Fe signals (Kobayashi and Nishizawa, 2014). At the cellular level, the regulation of Fe deficiency-mediated responses in plants is a complex mechanism that requires the orchestration of all compartments. It has been suggested that cellular organelles such as mitochondria might regulate Fe deficiency-induced responses through retrograde signaling pathways that are still undiscovered in plants (Vigani et al., 2013a; Vigani et al., 2013b). Plant mitochondria are central hubs in energy conversion and redox homeostasis and are connected to metabolic pathways residing in different subcellular compartments. Hence, mitochondria are ideally placed to act as sensors of the energetic and metabolic status of the cell (Millar et al., 2011; Sweetlove et al., 2007). Perturbations of the cellular energy status can lead to a re-configuration of mitochondrial activities which in turn have profound effects on other cellular compartments, including major changes in the nuclear gene expression (NGE) and photosynthetic activity (Schwarzländer et al., 2012).

The Mitochondrial Fe Transporter (MIT) is an essential gene for rice with mit knockdown mutants (mit-2) exhibiting a slow growth phenotype and a reduced chlorophyll concentration. Moreover, the mit-2 mutation significantly alters the cellular Fe homeostasis.

Indeed, in *mit-2* plants, the mitochondrial Fe concentration is low while the total Fe concentration is high compared to wild-type (WT) plants (Bashir et al., 2011c). Beside the mitochondrial Fe transport, the *mit-2* mutation affects Fe-S cluster assembly, in agreement with previous observations in other organisms. In yeast and mammals, the loss of mitochondrial Fe transport affects heme and Fe-S cluster synthesis (Shaw et al., 2006; Zhang et al., 2005; Zhang et al., 2006). In rice, partial loss of MIT results in a decrease in total and mitochondrial aconitase activity, therefore it has been suggested that Fe-S cluster synthesis might be affected at both mitochondrial and cytosolic levels. The MIT protein seems to act as a high affinity Fe uptake system in plant mitochondria in analogy with the yeast MRS3/4 homologous transporters, that are thought to serve as high affinity ferrous ion transporters which are essential in the absence of other low affinity mitochondrial Fe transporters (Froschauer et al., 2009).

In this work, we have characterized the effect of mitochondrial impairments of Fe transport on the overall metabolism of the cell, using mutant rice plants knocked down in the Mitochondrial Fe Transporter (MIT) (Bashir et al., 2011a; Bashir et al., 2011c). Combined transcriptomics and GC-MS based metabolomics approaches were used to provide evidence that specific Fe deficiency localized in mitochondria in response to a partial loss of MIT leads to global changes in metabolism.

Material and Methods

Plant growing conditions

Rice seeds (*Oryza sativa* L. cv. Dongjing) of WT and mit-2 were germinated for one

week on paper towels soaked with distilled water at room temperature. After one week, seedlings were transferred to a nutrient solution with the following composition: 0.7 mM K₂SO₄, 0.1 mM KCl, 0.1 mM KH₂PO₄, 2.0 mM Ca(NO₃)₂, 0.5 mM MgSO₄, 10 μM H₃BO₃, 0.5 μM MnSO₄, 0.2 μM CuSO₄, 0.5 μM ZnSO₄, 0.05 μM Na₂MoO₄, and 100 μM Fe-EDTA as described previously (Suzuki et al., 2006) and grown for three weeks. Plants were grown with a day/night regime of 16/8 h and 25°/20° C and a photon path-length probability density function of 200 μmol photons m⁻²s⁻¹ at the plant level. The pH of nutrient solution was adjusted daily to 5.5 with 1 M HCl. The solution was renewed every 5 days. Plants were harvested at noon.

Root oxygen consumption rate, mitochondrial purification and Western blot analyses

Oxygen consumption rate of rice root tips was measured as described previously (Vigani et al., 2009). To determine the contribution of mitochondrial respiration to the O₂ consumption rate of root tissues, specific inhibitors of the respiratory chain were used (Vigani et al., 2009).

Mitochondria were isolated from rice roots as described previously (Vigani et al., 2009). Roots of three-week-old rice plants were homogenized with a mortar and pestle in 0.4 M mannitol, 25 mM MOPS, pH 7.8, 1 mM EGTA, 8 mM cysteine and 0.1% (w/v) bovine serum albumin (BSA). Cell debris was pelleted by a brief centrifugation at 4000 g. The supernatant was re-centrifuged at 12000 g for 15 min to pellet mitochondria. The crude mitochondrial pellet was resuspended in 0.4 M mannitol, 10 mM Tricine, pH 7.2, 1 mM

EGTA (resuspension buffer, RB) and lightly homogenized with a potter and mitochondria were purified on a 40, 28 and 13.5% (v/v) percoll (Pharmacia, Uppsala, Sweden) step gradient in RB. The buff-coloured fraction (purified mitochondria) at the interface between 28 and 40% percoll was collected and washed by differential centrifugation in RB. The purified mitochondria were frozen and stored at -80°C until use. Iron content in purified mitochondria was determined by ICP-MS spectroscopy (Varian, Fort Collins, CO, USA) after mineralization in HNO₃ at 100-120°C as described previously (Vigani et al., 2009).

Mitochondrial proteins were loaded on a discontinuous SDS-polyacrylamide gel and processed as described previously (Vigani et al., 2009). Western blot analysis was performed as described previously (Vigani et al., 2009), using six different antibodies, corresponding to: NAD9 polyclonal antibody from wheat; NDB1 and NDA1 polyclonal antibodies from potato (Svensson and Rasmusson, 2001), Rieske (polyclonal antibody) from yeast (Balk and Leaver, 2001), the alternative oxidase (AOX) and the porin maize proteins (monoclonal antibodies).

Analysis of microarray data

The microarray data have been already described briefly (Bashir et al., 2011c). We reanalyzed the data with a particular focus on genes related to metabolism. For MapMan analysis, the average log₂ value was calculated for individual annotations in roots and shoots. This log₂ value was then used to compare the transcriptomic changes in metabolism-related genes using MapMan 3.5.1R2 (Kim et al., 2012).

Metabolomic analysis of root and leaf tissues of mit-2 and WT plants

Leaf and root tissues were frozen and homogenized in liquid nitrogen. For extraction, 50 mg ground material was mixed with methanol containing ribitol and C13-sorbitol as internal standards. After mixing and incubating at 70°C, water and chloroform were added to force a phase separation by centrifugation. Only the upper polar phase was dried in vacuum and used for further analysis. The pellet was derivatized using methoxyaminehydrochloride (20 mg ml in pyridine) for methoxyamination and N,O-Bis(trimethylsilyl)trifluoroacetamide (BSTFA) for silylation. To perform a retention time alignment later on, a mixture of alkanes (C10, C12, C15, C19, C22, C28, C32) was added to the derivatization mix.

Metabolites were analyzed using a GC-TOF-MS system (Pegasus HT, Leco, St Joseph, USA). Baseline correction was done by ChromaTOF software (Leco). For peak alignment and peak annotation the TagFinder software tool (MPIMP Golm, Luedemann et al. 2008) was used in combination with the Golm Metabolome Database (GMD, Kopka et al. 2005). The metabolites were normalized using the internal standard and the fresh weight. Statistical analysis was performed using Excel and the Multi Experiment Viewer (MEV). Data for the HCL tree are log₂ transformed. PCA analysis was performed using MetaGeneAlyse platform (www.metagenealyse.mpimp-golm.mpg.de, Daub et al. 2003). Data for the PCA were median centered and log₁₀ transformed.

Statistical analysis

Student's t-tests were performed using the algorithm embedded in Microsoft EXCEL (Microsoft, <http://www.microsoft.com>). The term significant is used in the text only when the change in question has been confirmed

to be significant ($P < 0.05$) by Student's t-test. All experiments were conducted independently at least three times (metabolomics experiments were conducted independently five times).

Results

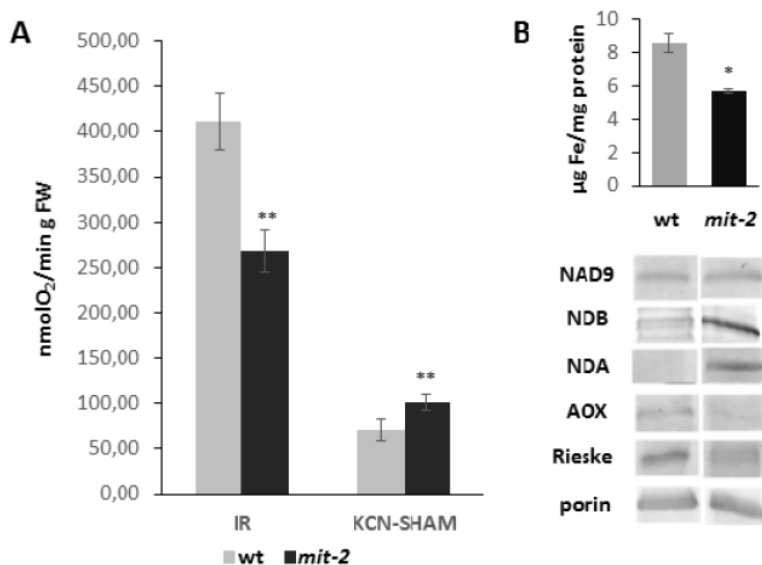


Figure 1. **Biochemical characterization of purified mitochondria from roots of mit-2 and WT plants** showed alterations in the respiratory chain in mit-2. A). O₂ consumption of root tips. The specific inhibitors of respiratory chain (KCN for cytochrome c oxidase and SHAM for alternative oxidase) were added after recording the initial O₂ consumption rate (IR). The difference between IR and the O₂ consumption recorded after addition of KCN/SHAM provides the contribution of mitochondrial O₂ consumption rate. B). Mitochondrial Fe concentration in roots. C) Western blot analysis of mit-2 and WT roots. For each sample, 10 µg of protein was used. The antibodies used were for: NAD9 (a subunit of complex I), NAD(P)H dehydrogenases (NDB and NDA), AOX (alternative oxidase), Rieske (a subunit of complex III), and porin. mit-2 Error bars represent S.D. Column bars followed by asterisk are significantly different from WT according to Student's t-test (n=3, * means p<0.01 and ** means p<0.001).

Knocking down MIT gene affects mitochondrial functionality in rice plant roots.

The partial loss of function of MIT affects mitochondria functionality in root tissues. In vivo O₂ consumption rate (Initial Rate; IR), determined on root tips, were significantly lower in mit-2 compared to WT plants (Figure 1A). By using

inhibitors of the respiratory chain activity (KCN, specific inhibitor of complex IV activity and salicylhydroxamic acid (SHAM), specific inhibitor of alternative oxidase (AOX)), the contribution of mitochondrial respiration to the total O₂ consumption by tissue was also found to be significantly reduced in mit-2 compared to WT plants (Fig. 1A). The possible explanation for these results is that they may be due to the significantly reduced Fe concentration of mitochondria purified from mit-2 roots compared to WT ones (Fig. 1B). Accordingly, some proteins belonging to the electron transport chain were affected in mit-2 compared to WT plants (Fig. 1C): NDB1 (external alternative NAD(P) dehydrogenases) and NDA1 (internal alternative NAD(P) dehydrogenases) strongly accumulated in mit-2 roots compared to WT plants; Fe-containing proteins such as Rieske and alternative oxidase (AOX) decreased in mit-2 plants (Fig. 1C).

Transcriptional changes in mit-2 roots

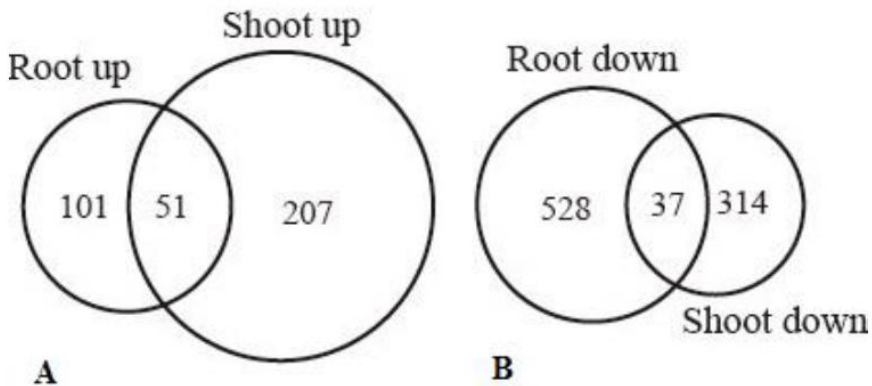


Figure 2. Summary of transcriptomic changes in mit-2 plants grown under control conditions. a) Numbers of up regulated genes identified in root and shoot tissues in mit-2 respect to WT plants. B) Numbers of down regulated genes identified in root and shoot tissues in mit-2 respect to WT plants

We reanalyzed the microarray data to identify genes related to metabolic changes in mit-2 roots. The expression of 152 genes was significantly upregulated in mit-2 roots compared to WT ones and among these, the expression of 51 genes was also upregulated in shoots. On the contrary, the expression of 663 genes was significantly down-regulated (Fig. 2). We particularly focused our attention on changes of genes related to the metabolism.

MapMan analysis clearly indicated that the metabolism is significantly reprogrammed in mit-2 roots compared to WT ones (Fig. 3A). The expression of genes belonging to the primary mitochondrial metabolism was affected in mit-2 plants. The expression of *Os01g0226600* and *Os02g0530100* (C4-dicarboxylate transporter/malic acid transport protein family proteins) was down-regulated in roots, while the expression of *Os09g0508900* (a member of mitochondrial substrate transporter family) was significantly upregulated. The expression of this gene is reported to be regulated by an excess of Fe in shoot (Bashir et al., 2014). Furthermore, genes related to TCA cycle, such as *PEPCK1* (*Os10g0204400*) showed a significant down regulation in mit-2 plants as well as the gene encoding for a pyruvate orthophosphate dikinase (*PPDK*). The expression of two pyruvate orthophosphate dikinase genes (*Os05g0405000* and *Os03g0432100*) was significantly down-regulated also in mit-2 roots. A strong induction of genes belonging to the fructose-2,6-bisphosphatase (*Os08g0367300*; *Os07g0212400*; *Os02g012900*) was observed in mit-2 roots and shoots while other glycolytic genes showed a significant down-regulation. A total of 44 genes belonging to the secondary metabolism were affected in mit-2 plants.

The majority of those (31 genes) showed a significant down-regulation while the expression of 13 genes was upregulated. The down-regulated genes are mainly grouped in the

phenylpropanoid and flavonoid pathways while the upregulated genes belong to the pathways of terpene biosynthesis.

Transcriptional changes in mit-2 shoots

In shoots the expression of 258 genes was significantly upregulated in mit-2 plants compared to WT plants, while the expression of 351 genes was significantly down-regulated (Fig.2). MapMan analysis clearly indicated that the metabolism significantly changed in mit-2 shoots compared to WT ones (Fig. 3B). As observed in roots, few genes encoding proteins participating in the mitochondrial metabolism were differentially expressed in mit-2 plants compared to WT plants. Five genes were upregulated and two of them encode for the alternative pathways of the respiratory chain (Os08g0141400, NDB3, putatively related to the ND II type internal; Os04g0600300, AOX1B). Os05g0331200, encoding for external type II alternative NDs was down regulated. Additionally, two S-type anion channel genes related to mitochondrial transport were up-regulated: Os01g0385400, SLAH3, and Os01g0623200, SLAH2. These genes are homologues to SLAC1 which is required for plant guard cell S-type anion channel function in stomatal signaling (Vahisalu et al., 2008). Three genes encoding proteins of TCA pathway were up-regulated in mit-2 plants (Os05g0405000, PPDK; Os07g0529000, isocitrate lyase, ICL; Os01g0743500, NADPH malic enzyme3), while the expression of two genes was down-regulated (Os10g0204400, PCK1 phosphoenolpyruvate carboxykinase1; Os01g0829800, malate dehydrogenase MDL). Similarly to the changes observed in roots, genes encoding fructose2,6-bisphosphatase (Os08g0367300; Os07g0212400; Os02g012900) were upregulated in mit-2 shoots together with the gene encoding for HEXOKINASE1 (HXK, Os01g0722700), while other glycolytic genes showed a significant down-

regulation.

Expression of 53 genes belonging to the secondary metabolism was significantly affected in mit-2 shoots. In contrast to what was observed in roots, the majority (85%) of differentially expressed genes were upregulated while expression of 8 genes (15%) was down-regulated. The upregulated genes are mainly grouped in the terpenoid, phenylpropanoid and flavonoid pathways, suggesting a strong induction of such pathways in the mutant when compared to WT plants. The down-regulated genes were: Os10g0108700 and Os07g0179300 (transferase family proteins), Os10g0118000 (o-methyltransferase), Os11g0708100 (laccase7), Os07g0526400 (narigerin-chalcone synthase), Os02g713900 (HMGR2, 3-hydroxy-3-methylgluraryl-CoA reductase 2), Os10g0533500 (Beta-hydroxylase 1), and Os07g0179300 (2 methyl-6-phytyl-1,4-benzoquinone).

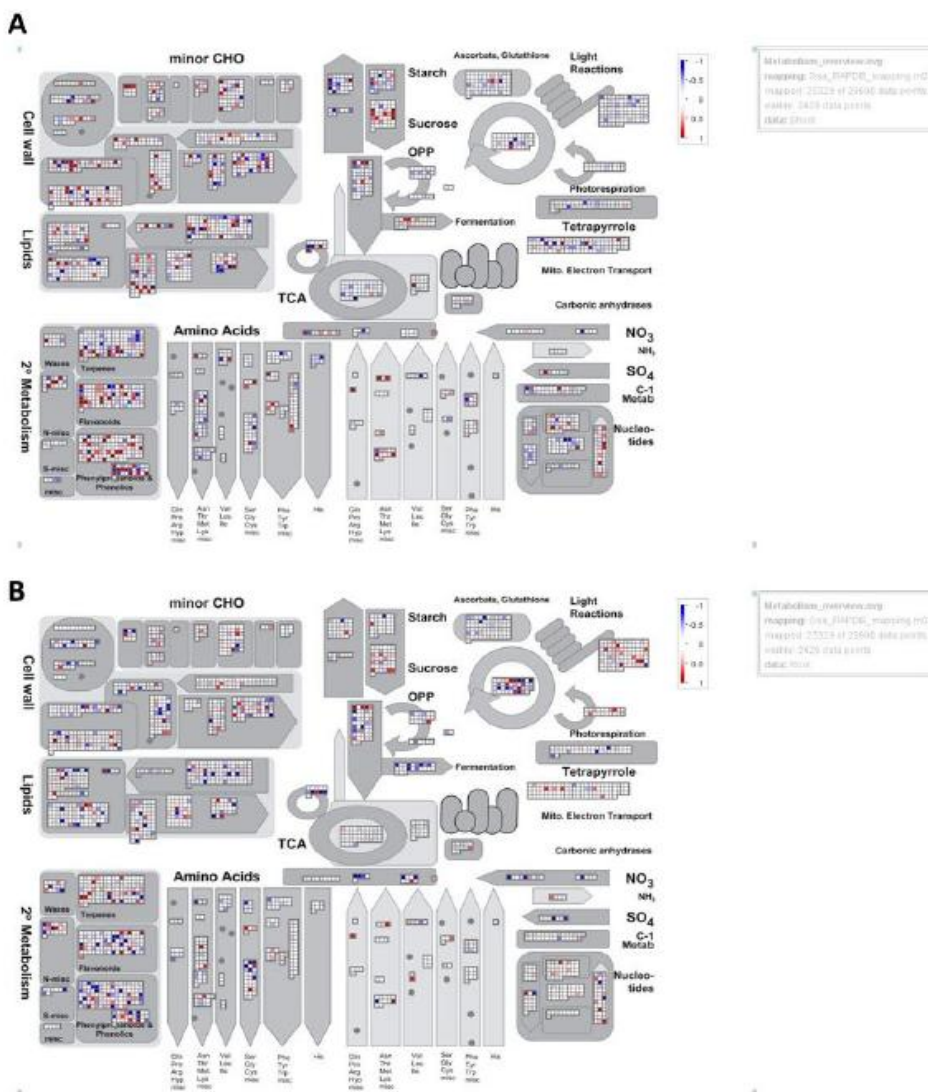


Figure3. Overview of transcriptomic changes in shoots and roots of mit-2 mutant as indicated by microarray analysis and visualized with Mapman 3.5.1R2 (values expressed as log₂ mit-2/WTWT ratio). Various components of primary and secondary metabolism 23 including CHO metabolism, cell wall synthesis, lipid metabolism, Calvin cycle etc. were up- and down regulated as indicated by microarray analysis. a) overview of changes in gene.

Metabolomic changes in mit-2 plants

To further investigate the role of MIT-2 in global metabolism, we performed a metabolomic analysis in both root and shoot tissues of mit-2 and WT rice plants (Table 1; Fig 4A, B). A total of 159 metabolites were detected by GS-TOF-MS analysis and 68 of them were identified. Among the metabolites identified, 23 (32%) significantly changed their amount in mit-2 compared to the WT tissues. To get an overview of the metabolic changes a PCA analysis was performed. The variance of the metabolomic data was mainly between the different tissues analyzed (root and shoot) as explained by the PC1. Urea, galactaric acid showed higher amounts in roots than in shoots (galactaric acid was not detected in shoots), while malonic acid and raffinose mainly accumulated in shoots. The separation of the genotypes contributed to the variance along PC2 (Fig 4A). Thereby the mutant plants are characterized by a higher content of an unknown metabolite (probably sugar) and a lower amount of urea (not detected in the mutant shoots) and malonic acid (not detected in the mutant roots). Interestingly, the separation of the genotypes is stronger in shoots than in roots (Fig 4B).

Generally, there is mainly an upregulation of metabolite levels in shoots of mit-2 plants, compared to WT. 36 metabolites increased more than 2-fold (22 of them being significantly changed), while five metabolites decreased to half of WT level (one of them changed significantly). On the other hand, the metabolite levels in roots are generally down-regulated.

Overall, 26 metabolites decreased with less than 0.5-fold change, 13 of these changes are significant, but only 13 metabolites increased with more than 2-fold in the root tissue and only two of these increases were significant.

Specifically, 13 amino acid related compounds were significantly affected in the mutant plants. In roots, a decreased content (expressed as fold change mit-2/WT ratio)

of several metabolites such as alanine, glycine, guanidine, homoserine, was observed. Additionally, the concentration of other metabolites such as citric acid was significantly decreased in roots of the mutant plants as well as a decrease in fructose and sucrose content.

By contrast, in *mit-2* shoots a significant accumulation of eight different metabolites was observed in comparison to WT shoots, These comprised amino acid related metabolites (ornithine and ethanolamine), organic acids such as fumaric acid, pyruvic acid, ribonic acid, and some carbohydrates, such as galactose, raffinose, mannose.

metabolites	Root		Shoot	
	<i>mit-2</i> /WT ratio	<i>p</i> -value	<i>mit-2</i> /WT ratio	<i>p</i> -value
<i>Amino acids (and related compounds)</i>				
Alanine	0.321*	<i>0.0002</i>	1.053	<i>0.0121</i>
Arginine	0.444	<i>0.3260</i>	1.409	<i>0.1595</i>
Aspartic acid	0.695*	<i>0.0114</i>	0.527*	<i>0.0346</i>
Butanoic acid, 2-amino-	0.010	<i>0.0876</i>	1.396	<i>0.3535</i>
diethanolamine	0.968	<i>0.3535</i>	0.963	<i>0.8709</i>
ethanolamine	1.340	<i>0.9743</i>	1.752*	<i>0.0185</i>
Glutamic acid	1.120	<i>0.0185</i>	0.763	<i>0.1481</i>
glutamine	1.000	<i>0.0701</i>	15.655	<i>0.1516</i>
glycine	0.479*	<i>0.0065</i>	0.763	<i>0.0065</i>
guanidine	0.447*	<i>0.0065</i>	2.125	<i>0.0065</i>
homoserine	0.414*	<i>0.0008</i>	2.618	<i>0.0629</i>
isoleucine	0.845	<i>0.0807</i>	1.193	<i>0.5858</i>
leucine	1.423	<i>0.1310</i>	1.464	<i>0.4236</i>
leucine, cyclo	0.322*	<i>0.0023</i>	0.644	<i>0.5934</i>
lysine	0.667*	<i>0.0208</i>	0.793	<i>0.5589</i>
ornithine	68.746	<i>0.2300</i>	4.418*	<i>0.0155</i>
octopamine	1.302	<i>0.3048</i>	0.690	<i>0.1960</i>
Phenylalanine	0.702*	<i>0.0088</i>	2.125	<i>0.0661</i>
Pyroglutamic acid	0.660*	<i>0.0073</i>	1.493	<i>0.0073</i>
Proline	0.529	<i>0.0903</i>	1.427	<i>0.4096</i>
Serine	0.906*	<i>0.0441</i>	1.172	<i>0.6675</i>
Serine, O-acetyl	0.823	<i>0.0717</i>	2.156	<i>0.1682</i>
Threonine	0.458*	<i>0.0013</i>	1.626	<i>0.0013</i>
tyrosine	1.129	<i>0.2055</i>	0.743	<i>0.5265</i>
Urea	0.472	<i>0.0854</i>	0.000	<i>0.3466</i>
Valine	0.656	<i>0.1226</i>	1.228	<i>0.3969</i>
<i>Carbohydrates (and related compounds)</i>				
Glucose	0.921*	<i>0.0446</i>	1.081	<i>0.8886</i>
Glucose-6-phosphate	2.074	<i>0.4729</i>	1.909*	<i>0.0436</i>
Fructose	0.495*	<i>0.0063</i>	0.487	<i>0.4485</i>
Fructose-1-phosphate	1.000	<i>0.0825</i>	1.655	<i>0.0752</i>
Sucrose	0.563*	<i>0.0034</i>	0.837	<i>0.5371</i>
Raffinose	1.000	<i>0.1999</i>	4.228*	<i>0.0066</i>
Rhamnose	0.555	<i>0.0901</i>	1.583	<i>0.1555</i>
Ribonic acid	1.315	<i>0.4038</i>	2.974*	<i>0.0227</i>
Ribose	0.713	<i>0.0749</i>	1.227	<i>0.6517</i>
Mannose	1.123	<i>0.1411</i>	4.436*	<i>0.0079</i>
Arabinose	0.978	<i>0.0851</i>	1.313	<i>0.3126</i>
Melezitose	1.000	<i>0.0610</i>	1.436	<i>0.0981</i>
Fucose	1.417*	<i>0.0331</i>	1.290	<i>0.3600</i>
Galactaric acid	1.113	<i>0.3409</i>	1	<i>0.000</i>
Galactinol	0.676	<i>0.9945</i>	1.466	<i>0.1781</i>
Galactosamine, N-acetyl-	1.014	<i>0.0755</i>	0.813	<i>0.2831</i>
Galactose	0.704*	<i>0.0248</i>	2.247*	<i>0.0078</i>
Glucosheptonic acid-1,4-lactone	1.091	<i>0.0698</i>	0.726	<i>0.1776</i>
Beta-galactopyranosyl-1,3-arabinoseD	1.000	<i>0.4677</i>	1.525	<i>0.1660</i>
<i>Organic acids (and related compounds)</i>				
Citric acid	0.309*	<i>0.0035</i>	0.740	<i>0.2464</i>
Fumaric acid	1.022	<i>0.0906</i>	6.663*	<i>0.0250</i>
Glutaric acid, 2-oxo-	1.530	<i>0.0716</i>	1.887	<i>0.0887</i>
Malic acid	0.590	<i>0.6898</i>	0.970	<i>0.9430</i>
Malonic acid	0.011	<i>0.0941</i>	0.998	<i>0.9960</i>
Succinic acid	1.000	<i>0.1112</i>	0.837	<i>0.6528</i>
Shikimic acid	0.983	<i>0.1482</i>	1.180	<i>0.6661</i>
Pyruvic acid	1.758	<i>0.9149</i>	3.249*	<i>0.0472</i>
Phosphoric acid monomethyl ester	1.590*	<i>0.0466</i>	1.053	<i>0.8588</i>
Phosphoric acid	2.198	<i>0.5017</i>	1.229	<i>0.4907</i>
Isocaproic acid, 2-oxo-	1.000	<i>0.1517</i>	0.882	<i>0.8198</i>
<i>Others metabolites</i>				
Inositol, myo	0.939*	<i>0.0423</i>	1.140	<i>0.4266</i>
Diethyleneglycol	0.935	<i>0.0603</i>	1.916	<i>0.0748</i>
Lyxonic acid-1,4-lactone	0.781*	<i>0.0120</i>	1.299	<i>0.3070</i>
Mannosamine, N-acetyl-	0.949	<i>0.0626</i>	1.090	<i>0.7844</i>
Sphingosine	0.961	<i>0.1919</i>	1.307	<i>0.2223</i>

Table 1. Metabolite contents in roots and shoot tissues of *mit-2* and WT rice plants. Metabolite changes are expressed as fold changes (*mit-2*/WT ratio). The metabolites in bold and followed by * changes significantly in its content in *mit-2* with respect to WT samples ($p < 0.05$)

Discussion

Mitochondria were previously suggested to be involved in Fe sensing and signaling pathways in plant cells (Vigani et al., 2009). The characterization of mutant plants defective in mitochondrial Fe importer therefore represents a useful tool to investigate the specific involvement of impaired mitochondria in the regulation of nuclear gene expression under Fe deficiency. Indeed, recently the characterization of the rice oligopeptide 7 mutant (*opt7-1*) showed that such mutant plants display similar phenotype to that observed in *mit-2* mutant plants: i) accumulation of Fe in plant tissues and ii) symptoms of Fe deficiency (Bashir et al., 2015). However, *opt7-1* mutant plants showed different transcriptomic changes compared to what was observed in *mit-2* plant in the present work, highlighting the specific changes with regard to mitochondrial function. To investigate the effect of such mutation on the expression of nuclear genes as well as overall cellular metabolism, a transcriptomic and metabolomic analysis of both root and leaf tissues was performed. Here we show in *mit-2* plants global changes in gene expression and metabolite profiles in different metabolic pathways.

In *mit-2* plants the affected mitochondrial functionality in both root (as shown in this work) and shoot (Bashir et al., 2011c), is associated to an impairment of the glycolytic pathway.

Indeed, only genes encoding the fructose-2,6-bisphosphatase (F2,6BPase) are strongly up-regulated when compared to WT plants, while other genes belonging to the glycolytic pathway are down-regulated. In Fe-deficient Strategy I plants, mitochondrial impairment was associated with an induction of glycolytic flux as well as fermentative pathways (Vigani et al., 2012). The increase in glucose-6 phosphate (G6P) and pyruvic acid in the shoot of the mutant could be indicative for a stimulation of fermentative pathways. Accordingly, the shoot

transcript profiles also show a clear induction of transcripts encoding genes involved in fermentation. However, a Fe deficiency localized in mitochondria might also have led to a glycolysis slowdown, as mitochondria may not be able to metabolize pyruvate supplied by glycolysis. Indeed, despite mit-2 plants were chlorotic, Fe content in shoot was higher than in WT plants (Bashir et al., 2011c). Therefore, Fe supply to the chloroplast does not seem to be significantly affected by MIT mutation and thereby chloroplasts would be working, and consequently supplying energy to the mit-2 plants. Moreover, genes belonging to secondary metabolism were generally upregulated in shoots of mutant plants, which is in agreement with phenylalanine accumulation occurring. By contrast, in roots of mutant plants the down-regulation of genes belonging to secondary metabolism suggests that knocking down MIT determines a deficit in the energy supply to the cell, slowing down cellular metabolism. Similar changes were observed at the metabolite level. The majority of metabolites decreased their content in roots, while the content of only few increased. In shoots the response was the opposite: most of the metabolites had increased levels and only few metabolites showed a decrease. These findings suggest that the shoots can compensate the impaired mitochondrial activity to some extent by photosynthetic activity and possibly by additional upregulation of fermentative pathways.

In mit-2 plants a significant decrease in citrate content was observed in root tissues. Citrate is a Fe(III) chelator and is thought to play a relevant role in xylem Fe transport (Inoue et al., 2004; Rellan-Alvarez et al., 2010; Yokosho et al., 2009). As a higher concentration of Fe was observed in mit-2 shoots (Bashir et al., 2011) we suggest that the partial loss of MIT might channel more citrate to chelate Fe and translocate it to the shoot. To enhance citrate synthesis TCA should operate at high rate. Apart from glycolysis, one of the pathways feeding

the TCA cycle is the aspartate-family pathway (Kirma et al., 2012). Such pathway synthesizes, through several different metabolic branches, five amino acids (lysine, threonine, methionine, isoleucine and glycine); all of them can be catabolised in the TCA cycle in order to contribute to cellular energy supply (Kirma et al., 2012). In roots of mit-2 plant, a decrease in energy supply to the cell by mitochondria, as well as a decrease of glycolysis, occurred (Fig 1, 2), therefore a need to supply substrates for the TCA cycle by alternative pathways (i.e. aspartate-family pathway) should be expected (Fig 5). Indeed, in mit-2 plants the content of aspartate decreased in both roots and shoots, while the aspartate-related compounds (lysine, homoserine, threonine, isoleucine) decreased only in roots. The decreased content of aspartate in shoot might be due to the concomitant accumulation of ornithine: indeed, aspartate could generate ornithine through the arginino-succinate lyase which converts arginino-succinate to fumarate and arginine which in turn is converted to ornithine (Fig 5). Ornithine is a non-protein amino acid playing a central role in the polyamine (PA)-amino acid biosynthetic pathway (Majumdar et al., 2013). Indeed, it has been suggested that ornithine might be involved in monitoring and/or signalling pathway for the biosynthesis of metabolites such as proline, putrescine, GABA, and perhaps also arginine (Majumdar et al., 2013). Interestingly, an additional product of such biosynthetic pathway is nitric oxide (NO), whose role in various developmental and physiological processes in plants is well documented (Mur et al., 2013; Tanou et al., 2014; Tun et al., 2006). The production of NO also increases under abiotic stress conditions (Wimalasekera et al., 2011) such as Fe and oxygen deficiency (Graziano and Lamattina, 2007; Murgia et al., 2002). Therefore, considering the importance of such pathway, the existence of a mechanism to control cellular ornithine, has been proposed (Minocha et al., 2014). However,

ornithine can also be synthesized, along with urea, from arginine through the reaction catalysed by arginase which, in plants, localizes in mitochondria (Taylor et al., 2010). A significant accumulation of ornithine occurred in shoot of mit-2 plants, suggesting that in this mutant, the arginase-dependent pathway would be responsible for the ornithine accumulation. Accordingly, a strong accumulation of fumarate occurred in shoots. Fumarate is an intermediate of TCA cycle and its accumulation might be due to TCA cycle impairment. However it could be synthesized from the reaction catalysed by arginino-succinate lyase which converts arginino-succinate to arginine and fumarate (Fig 5). The slight accumulation of arginine, together with the significant accumulation of ornithine occurring at the shoot level in mutant plants suggests that fumarate accumulation might derive from such a pathway, although we cannot sort out other possible sources (Fig 5).

Recently, a strong accumulation of ornithine, together with arginine, in rice embryos germinated under anaerobic condition has been observed, suggesting an enhanced amino acid metabolism involving these compounds under anaerobic conditions. Therefore, we might suggest that mit-2 mutation induces accumulation of compounds related to the arginine metabolism accordingly to what occurs in anaerobic-germinated seeds of rice plants (Taylor et al., 2010). These findings suggest that knocking down MIT expression might mimic some hypoxia-induced responses in rice plants. Under anaerobic condition NAD(P)H oxidation and ATP synthesis are insensitive to rotenone, suggesting that complex I is not working (Stoimenova et al., 2007). In fact, the activation of alternative NAD(P) dehydrogenases (ND- DHs) mediates such anaerobic NAD(P)H oxidation in mitochondria (Igamberdiev and Hill, 2009). Here, NDB1 and NDA proteins, belonging to the ND-DHs, accumulate in mit-2 purified mitochondria compared to WT plants. It has been demonstrated that the induction of ND-DHs activities is required to bypass a decreased activity of complex I occurring in Fe-deficient Strategy I plants (Higa et al., 2010; Vigani and Zocchi, 2010). Therefore, such adaptation of the respiratory chain activity occurring under Fe deficiency seems to be similar to what occurs under hypoxia. In graminaceous plants, the responses to Fe deficiency and hypoxia are intimately related: Fe deficiency causes physiological hypoxia (Mori et al., 1991), whereas submergence and hypoxia induce enzymes involved in phytosiderophore and ethylene biosynthesis (Sauter et al., 2005; Suzuki et al., 1998). The possible role of O₂ as signal molecule for Fe-responsive gene in rice has been recently suggested (Kobayashi and Nishizawa, 2014). Furthermore, knocking down MIT gene, a decline in ATP synthesis would be expected as the respiratory chain activity is decreased (compared to WT plants). Interestingly, several genes encoding

enzymes of fermentative pathways were up-regulated in shoots of mit-2 plants, suggesting that such mutation could indeed simulate a hypoxia-induced response. This however was not the case in roots.

Furthermore, changes in the leaf sugar concentration were also observed in mit-2 plants.

Partial loss of MIT leads to the accumulation of some oligosaccharides of the raffinose family (RFO) such as galactose and raffinose. Interestingly, such changes have also been observed in Fe-deficient *Beta vulgaris* plants (Rellan-Alvarez et al., 2010). As raffinose has hydroxyl radical scavenging activity similar to other soluble antioxidants such as glutathione and ascorbic acid, it has been suggested that a strong increase in the relative amounts of RFOs could play a role in the antioxidant defence (Nishizawa et al., 2008; Rellan-Alvarez et al., 2010; Van den Ende and Valluru, 2009). Indeed, the increase in RFO concentration could help to alleviate ROS damage produced under Fe deficiency (Rellan-Alvarez et al., 2010). Furthermore, the increase in RFOs could also act as a long distance Fe deficiency signal via phloem sap transport.

Considering that RFOs accumulate in mit-2 plants, such accumulation might depend on the Fe deficiency perception by mitochondria (Fig 5).

All together these results suggest that i) localized Fe deficiency perceived specifically in mitochondria affects genomic responses in plants; ii) partial loss of MIT differentially regulates root and shoot transcriptomes and in turn iii) it differentially reprograms the whole metabolism in root and shoot tissues. The metabolites significantly affected in their content both in root and shoot of mit-2 plants mainly belong to the aspartate-related pathways (aspartate, lysine and threonine in roots; aspartate and ornithine in shoot) that are strictly connected to TCA cycle. It has been suggested that the

biological function of the connection between aspartate-family pathways and TCA cycle might have a major role in the physiological response of plants to various abiotic stresses causing energy deprivation (Kirma et al., 2012).

Indeed, mit-2 deficiency led to changes in gene expression and metabolite levels in shoots that resemble hypoxic responses in plants.

Furthermore, the mitochondria-plastids cross-talk occurring in the roots might differentially influence nuclear gene expression with respect to the mitochondria-chloroplast cross-talk occurring in the shoot. Such cross-talk might be responsible for the accumulation in leaf of some metabolites (for instance ornithine, and RFOs) which are considered as signal molecules acting under various stress conditions.

In conclusion, this work provides in-planta evidence that Fe-deficient mitochondria affect overall metabolism in plants. Whether such changes are due to the impaired activity of Fe-S cluster-containing enzymes in cell or to a still unknown retrograde signaling pathway, it is to be elucidated. Therefore, further work is required to decipher the role of mitochondria in the regulation of Fe homeostasis in plants.

References

Balk J, Schaedler TA. 2014. Iron cofactor assembly in plants. *Annual Review of Plant Biology* 65, 125-153.

Bashir K, Hanada K, Shimizu M, Seki M, Nakanishi H, Nishizawa N. 2014. Transcriptomic analysis of rice in response to iron deficiency and excess. *Rice* 7, 18.

Bashir K, Ishimaru Y, Itai RN, Senoura T, Takahashi M, An G, Oikawa T, Ueda M, Sato A, Uozumi N, Nakanishi H, Nishizawa N. 2015. Iron deficiency regulated OsOPT7 is essential for iron homeostasis in rice. *Plant Molecular Biology* 87, Accepted.

Bashir K, Ishimaru Y, Nishizawa N. 2010. Iron uptake and loading into rice grains. *Rice* 3, 122 - 130.

Bashir K, Ishimaru Y, Nishizawa NK. 2011a. Identification and characterization of the major mitochondrial Fe transporter in rice. *Plant Signaling & Behavior* 6, 1591-1593.

Bashir K, Ishimaru Y, Shimo H, Kakei Y, Senoura T, Takahashi R, Sato Y, Sato Y, Uozumi N, Nakanishi H, Nishizawa NK. 2011b. Rice phenolics efflux transporter 2 (PEZ2) plays an important role in solubilizing apoplasmic iron. *Soil Science and Plant Nutrition* 57, 803-812.

Bashir K, Ishimaru Y, Shimo H, Nagasaka S, Fujimoto M, Takanashi H, Tsutsumi N, An G, Nakanishi H, Nishizawa NK. 2011c. The rice mitochondrial iron transporter is essential for plant growth. *Nature Communications* 2, 322.

Bashir K, Nozoye T, Ishimaru Y, Nakanishi H, nishizawa NK. 2013. Exploiting new tools for iron bio-fortification of rice. *Biotechnology Advances* 31, 1624-1633.

Bughio N, Yamaguchi H, Nishizawa NK, Nakanishi H, Mori S. 2002. Cloning an iron- regulated metal transporter from rice. *Journal of Experimental Botany* 53, 1677-1682.

Couturier J, Touraine B, BRIAT J-F, Gaymard F, Rouhier N. 2013. The iron-sulfur cluster assembly machineries in plants: current knowledge and open questions. *Frontiers in Plant Science* 4.

Froschauer EM, Schweyen RJ, Wiesenberger G. 2009. The yeast mitochondrial carrier proteins Mrs3p/Mrs4p mediate iron transport across the inner mitochondrial membrane. *Biochimica et Biophysica Acta (BBA) - Biomembranes* 1788, 1044-1050.

Graziano M, Lamattina L. 2007. Nitric oxide accumulation is required for molecular and physiological responses to iron deficiency in tomato roots. *The Plant Journal* 52, 949-960.

Guerinot M, Ying Y. 1994. Iron: nutritious, noxious, and not readily

available. *Plant Physiol* 104, 815 - 820.

Higa A, Mori Y, Kitamura Y. 2010. Iron deficiency induces changes in riboflavin secretion and the mitochondrial electron transport chain in hairy roots of *Hyoscyamus albus*. *Journal of Plant Physiology* 167, 870-878.

Igamberdiev AU, Hill RD. 2009. Plant mitochondrial function during anaerobiosis. *Annals of Botany* 103, 259-268.

Inoue H, Mizuno D, Takahashi M, Nakanishi H, Mori S, Nishizawa NK. 2004. A rice FRD3-Like (OsRFDL1) gene is expressed in the cells involved in long-distance transport. *Soil Science and Plant Nutrition* 50, 1133-1140.

Ishimaru Y, Kakei Y, Shimo H, Bashir K, Sato Y, Sato Y, Uozumi N, Nakanishi H, Nishizawa NK. 2011. A rice phenolic efflux transporter is essential for solubilizing precipitated apoplasmic iron in the plant stele. *JOURNAL OF BIOLOGICAL CHEMISTRY* 286, 24649-24655.

Kim S, Song M, Lee K, Hwang S, Jang C, Kim J, Kim S, Ha B, Kang S, Kim D. 2012. Genome-wide transcriptome profiling of ROS scavenging and signal transduction pathways in rice (*Oryza sativa* L.) in response to different types of ionizing radiation. *Mol Biol Rep* 39, 11231 - 11248.

Kirma M, Araújo WL, Fernie AR, Galili G. 2012. The multifaceted role of aspartate-family amino acids in plant metabolism. *Journal of Experimental Botany*.

Kopka J, Schauer N, Krueger S, et al. 2005. GMD@CSB.DB: the *Golm Metabolome Database*. *Bioinformatics* 21 , 1635–1638.

Kobayashi T, Nishizawa N. 2012a. Iron uptake, translocation, and regulation in higher plants. *Ann Rev Plant Biol* 63, 131 - 152.

Kobayashi T, Nishizawa NK. 2012b. Iron Uptake, translocation, and regulation in higher plants. *Annual Review of Plant Biology* 63, 131-152.

Kobayashi T, Nishizawa NK. 2014. Iron sensors and signals in response to iron deficiency. *Plant Science* 224, 36-43.

Majumdar R, Shao L, Minocha R, Long S, Minocha SC. 2013. Ornithine: The overlooked molecule in the regulation of polyamine metabolism. *Plant and Cell Physiology* 54, 990-1004.

Marschner H. 1995. Mineral nutrition of higher plants. London: Academic Press.

Marschner H, Romheld V. 1994. Strategies of plants for acquisition of iron. *Plant Soil* 165, 261 - 274.

Millar AH, Whelan J, Soole KL, Day DA. 2011. Organization and regulation of mitochondrial respiration in plants. *Annual Review of Plant Biology* 62, 79-104.

Minocha R, Majumdar R, Minocha SC. 2014. Polyamines and abiotic stress in plants: A complex relationship. *Frontiers in Plant Science* 5.

Mori S, Nishizawa NK, Hayashi H, Chino M, Yoshimura E, Ishihara J. 1991. Why are young rice plants highly susceptible to iron deficiency? *Plant and Soil* 130, 143-156.

Mur LAJ, Mandon J, Persijn S, Cristescu SM, Moshkov IE, Novikova GV, Hall MA, Harren FJM, Hebelstrup KH, Gupta KJ. 2013. Nitric oxide in plants: an assessment of the current state of knowledge. *AoB Plants* 5.

Murgia I, Delledonne M, Soave C. 2002. Nitric oxide mediates iron-induced ferritin accumulation in Arabidopsis. *The Plant Journal* 30, 521-528.

Nishizawa A, Yabuta Y, Shigeoka S. 2008. Galactinol and raffinose constitute a novel function to protect plants from oxidative damage. *Plant Physiology* 147, 1251-1263.

Rellan-Alvarez R, Andaluz S, Rodriguez-Celma J, Wohlgemuth G, Zocchi G, Alvarez-Fernandez A, Fiehn O, Lopez-Millan A, Abadia J. 2010. Changes in the proteomic and metabolic profiles of *Beta vulgaris* root tips in response to iron deficiency and resupply. *BMC*

Plant Biology 10, 120.

Sauter M, Lorbiecke R, OuYang B, Pochapsky TC, Rzewuski G. 2005. The immediate-early ethylene response gene OsARD1 encodes an acireductone dioxygenase involved in recycling of the ethylene precursor S-adenosylmethionine. *The Plant Journal* 44, 718-729.

Schwarzländer M, König A-C, Sweetlove LJ, Finkemeier I. 2012. The impact of impaired mitochondrial function on retrograde signalling: a meta-analysis of transcriptomic responses. *Journal of Experimental Botany* 63, 1735-1750.

Shaw GC, Cope JJ, Li L, Corson K, Hersey C, Ackermann GE, Gwynn B, Lambert AJ, Wingert RA, Traver D, Trede NS, Barut BA, Zhou Y, Minet E, Donovan A, Brownlie A, Balzan R, Weiss MJ, Peters LL, Kaplan J, Zon LI, Paw BH. 2006. Mitoferrin is essential for erythroid iron assimilation. *Nature* 440, 96-100.

Stoimenova M, Igamberdiev A, Gupta K, Hill R. 2007. Nitrite-driven anaerobic ATP synthesis in barley and rice root mitochondria. *Planta* 226, 465-474.

Suzuki K, Itai R, Suzuki K, Nakanishi H, Nishizawa N-K, Yoshimura E, Mori S. 1998. Formate dehydrogenase, an enzyme of anaerobic metabolism, is induced by iron deficiency in barley roots. *Plant Physiology* 116, 725-732.

Suzuki M, Takahashi M, Tsukamoto T, Watanabe S, Matsushashi S, Yazaki J, Kishimoto N, Kikuchi S, Nakanishi H, Mori S, Nishizawa NK. 2006. Biosynthesis and secretion of mugineic acid family phytosiderophores in zinc-deficient barley. *The Plant Journal* 48, 85-97.

Svensson ÅS, Rasmusson AG. 2001. Light-dependent gene expression for proteins in the respiratory chain of potato leaves. *The Plant Journal* 28, 73-82.

Sweetlove LJ, Fait A, Nunes-Nesi A, Williams T, Fernie AR. 2007. The Mitochondrion: An integration point of cellular metabolism and signaling. *Critical Reviews in Plant Sciences* 26, 17-43.

Tanou G, Ziogas V, Belghazi M, Christou A, Filippou P, Job D,

Fotopoulos V, Molassiotis A. 2014. Polyamines reprogram oxidative and nitrosative status and the proteome of citrus plants exposed to salinity stress. *Plant, Cell & Environment* 37, 864-885.

Taylor NL, Howell KA, Heazlewood JL, Tan TYW, Narsai R, Huang S, Whelan J, Millar AH. 2010. Analysis of the rice mitochondrial carrier family reveals anaerobic accumulation of a basic amino acid carrier involved in arginine metabolism during seed germination. *Plant Physiology* 154, 691-704.

Tun NN, Santa-Catarina C, Begum T, Silveira V, Handro W, Floh EIS, Scherer GFE. 2006. Polyamines induce rapid biosynthesis of nitric oxide (NO) in *Arabidopsis thaliana* seedlings. *Plant and Cell Physiology* 47, 346-354.

Vahisalu T, Kollist H, Wang Y-F, Nishimura N, Chan W-Y, Valerio G, Lamminmaki A, Brosche M, Moldau H, Desikan R, Schroeder JI, Kangasjarvi J. 2008. SLAC1 is required for plant guard cell S-type anion channel function in stomatal signalling. *Nature* 452, 487-491.

Van den Ende W, Valluru R. 2009. Sucrose, sucrosyl oligosaccharides, and oxidative stress: scavenging and salvaging? *Journal of Experimental Botany* 60, 9-18.

Vigani G, Donnini S, Zocchi G. 2012. Metabolic adjustment under Fe deficiency in roots of dicotyledonous plants. Iron deficiency and its complications: *Nova publisher*, 1-27.

Vigani G, Maffi D, Zocchi G. 2009. Iron availability affects the function of mitochondria in cucumber roots. *New Phytologist* 182, 127-136.

Vigani G, Morandini P, Murgia I. 2013a. Searching iron sensors in plants by exploring the link among 2'-OG-dependent dioxygenases, the iron deficiency response and metabolic adjustments occurring under iron deficiency. *Frontiers in Plant Science* 4.

Vigani G, Zocchi G. 2010. Effect of Fe deficiency on mitochondrial alternative NAD(P)H dehydrogenases in cucumber roots. *Journal of Plant Physiology* 167, 666-669.

Vigani G, Zocchi G, Bashir K, Philippar K, Briat J-F. 2013b. Signals from chloroplasts and mitochondria for iron homeostasis regulation. *Trends in Plant Science* 18, 305-311.

Wimalasekera R, Tebartz F, Scherer GFE. 2011. Polyamines, polyamine oxidases and nitric oxide in development, abiotic and biotic stresses. *Plant Science* 181, 593-603.

Yokosho K, Yamaji N, Ueno D, Mitani N, Ma JF. 2009. OsFRDL1 Is a citrate transporter required for efficient translocation of iron in rice. *Plant Physiology* 149, 297-305.

Zhang Y, Lyver ER, Knight SAB, Lesuisse E, Dancis A. 2005. Frataxin and mitochondrial carrier proteins, Ms3p and Mrs4p, cooperate in providing iron for heme synthesis. *JOURNAL OF BIOLOGICAL CHEMISTRY* 280, 19794-19807.

Zhang Y, Lyver ER, Knight SAB, Pain D, Lesuisse E, Dancis A. 2006. Mrs3p, Mrs4p, and frataxin provide iron for Fe-s cluster synthesis in mitochondria. *JOURNAL OF BIOLOGICAL CHEMISTRY* 281, 22493-22502.

CHAPTER VII

General Conclusions

One of the greatest challenges in modern agriculture is increasing biomass production, while improving plant product quality, in a sustainable way. This requires increasing productivity and improving product quality within the confines of a changing global climate with increasing average CO₂ concentrations and temperatures. Mineral nutrients are major actors in this new scenario. They are essential both for plant productivity and for the quality of their products, and they can affect the environment through the application of fertilizers. Among minerals, iron (Fe) plays a major role in this process because it is essential for plant life and productivity, and also for the quality of production. Clearly, the properties of Fe are unique and irreplaceable, and cells spend a large amount of energy to acquire Fe from the environment and handle it safely inside the cell. Due to all these reasons Fe is an essential element readily incorporated for use in biological processes where Fe ions play a key role in metabolic pathways such as DNA synthesis, nitrogen and hormone production. A wide number of cellular enzymes depend also on Fe for their biological function, (Curie and Briat, 2003; Briat et al., 2007). (Thomine and Vert, 2013). Furthermore, Fe is required for the proper functionality of the photosynthetic and the respiratory chain, which are respectively located in chloroplasts and mitochondria. These processes are responsible for the energetic support of the cell and therefore of the whole plant life. Despite its geologic abundance (it is the second most abundant metal in the earth's crust after aluminium) Fe is often a growth-limiting factor in the environment (Quintero-Gutiérrez et al., 2008). According to FAO 39% of rural land areas are affected by mineral deficiency and low fertility that constrain crop production (Cramer et al., 2011). Fe deficiency is a problem in crop production worldwide but particularly in plants grown on calcareous soils (Vose, 1982). Calcareous soils represent almost the 30% of the earth land surface. Their

total extent has been estimated by FAO at 800 million hectares worldwide, 57 million of which in Europe. In the near future to cope with the increasing demand of food caused by a strong increase in world's population (FAO estimates in 10 billion people by 2050), agriculture must be extended to marginal areas, many of which include calcareous soils.

The data obtained and exposed in this doctorate thesis, in agreement with what widely previously reported in literature, allow us to state that the absence or the low Fe bioavailability during the growth of the plants results in several alterations more or less reversible at different levels of the overall metabolic plant system. The observations reported in many works regarding the influence of Fe deficiency on the general metabolism of plants prompted us to perform various analysis on the pathways more involved in the response processes to Fe deficiency. In particular, in this thesis, we have focused our attention on the possible induction of alterations in the photorespiratory metabolism, investigating some alterations in the metabolism of reactive oxygen species and on the enzymatic activity in peroxisomes and mitochondria.

It is well acknowledged that under Fe deficiency leaves generally have low photosynthetic activity due to several reasons discussed in the introduction of this work, but they absorb more light energy per chlorophyll molecule than required for photosynthesis, especially under high radiation (Abadía *et al.*, 1999). This results in a high risk for photo-inhibitory and photo-oxidative damages and may also cause a reduction in CO₂ assimilation rate in Fe-deficient leaves, leading to substantial agricultural losses and decreases in nutritional quality of many crops of great economic interest. In addition, under these conditions of supra-optimal light, photoinhibition of photosynthesis occurs due to over-excitation on chloroplast membranes, generation of reactive

oxygen species (ROS) which may induce an alteration in the cellular redox state with the onset of oxidative stress and further damage of photosystem II (PSII) and sometimes photosystem I (PSI) (Andersson and Aro, 2001).

In this, it was widely reported that the photorespiratory cycle can be considered as an energy dissipating cycle, operating between chloroplasts, peroxisomes, mitochondria and cytosol, which helps to protect chloroplasts from photoinhibition and plants from excessive accumulation of reactive oxygen species (Tolbert 1985, Wingler et al. 2000). Photorespiration, as well, might be an important protective mechanism to prevent photoinhibition.

From the data obtained in our experiments, it appears clear that Fe-deficiency strongly impairs the photosynthetic machinery at different levels: the reaction centers of PS-II are largely inactive. A general increase in non-photochemical quenching (qNP) in chlorotic leaves was also observed, indicating the activation of photoprotective mechanisms which, however, are not sufficient to prevent photoinhibition, as indicated by a significant reduction in the maximal PSII photochemistry (Fv/Fm) and photochemical quenching (qp). These findings are in agreement with previous researches performed in other species, pear (Morales et al., 2000), tomato (Donnini et al., 2003), peach (Molassiotis et al., 2006), and pea (Jelali et al., 2011). Under Fe deficiency condition we recorded an increase in the rate of CO₂ assimilation rate in many biological repetition (+29%), suggesting a possible induction of photorespiratory metabolism. However, the variation was not significant and so further analyses are strictly required to reduce the variability among the repetitions in order to get a more reliable result. In addition, in these plants the reduction in stomatal aperture restricts the entry of CO₂. However, the increase in the level indicates that

there was a mesophyll-reduced utilization of CO₂. On the other hand the V_{Cmax} was significantly reduced, indicating a reduced activity of this carboxylative enzyme (-70%).

Metabolite content analysis performed allowed us to suggest that Fe deficiency strongly affected aa metabolism. Among all aa variations, we focus our attention mainly on the changes showed by Gly and Ser, due to their involvement in the photorespiratory metabolism. In particular, the strong accumulation of these two aa in leaves (+94% Ser and +160% Gly) might suggest an alteration in the mitochondrial activity of the Glycine decarboxylase complex-Serine hydroxymethyltransferase cycle (GDC-SHMT1 cycle), that converts glycine into serine within the mitochondria, with the involvement of methylene tetrahydrofolate and complex I of the respiratory chain, in a process uncoupled from the ATP synthesis. Under Fe deficiency root and leaf showed some important differences: the aa content in root decreased while in leaf it increased. It has been proposed that it occurs by a limited NR activity and by an increase in GS/GOGAT in both root and leaf (Borlotti et al., 2012). Additionally, the different aa distribution in Fe-deficient plants might be due the a major translocation (together with other metabolites) via xylem from root to leaf (Borlotti et al., 2012). Thus, under Fe deficiency, root seems to respond more efficiently sustaining the whole plant by furnishing metabolites (i.e. aa, organic acids) to the leaves, in which the whole metabolism is inferred by the decreased photosynthetic activity. The observed alterations in the concentrations of metals suggest that Fe deficiency induces a metabolic imbalance in which other divalent cations are absorbed by (unspecific) transporters, due to their similar characteristics to Fe, this can affect the metabolism of the plant at different levels.

We can also infer that the lack of iron can induce in the leaves of cucumber plants imbalances in the metabolism of reactive oxygen species, either attributable to an increase in the activity of enzymes involved in the formation of these species, or due to a simultaneous reduced activity of enzymes involved in their detoxification. This overproduction of reactive oxygen species, if not properly handled by the cell, could lead to an imbalance in the cellular homeostasis of the ROS, resulting in an onset of oxidative stress which, if not correctly managed, can lead to further cell damage at different levels, also with the involvement of the photosynthetic apparatus. In fact the concentration of H₂O₂ in the leaves of Fe-deficient plants, was significantly higher (+40%) with respect to the control, and this is in accordance with the measured reduction of the catalase activity in Fe-deficient plants, determined by enzymatic activity assay (-35%) and activity staining on native PAGE. Nevertheless, it is remarkable that this increase of H₂O₂ could be also triggered by rise in other enzymatic activities, such as NAD(P)H oxidases (Romero-Puertas et al. 2004), pH-dependent PODs (Bestwick et al. 1998), as previously suggested by Donnini et al. (2012). Hydrogen peroxide might play an important role in the iron deficiency response signalling processes, which should be further investigated, also considering the increasingly important role of this molecule as a messenger involved in the processes of adjustment of cell expansion during leaf development (Lu et al., 2014), which is effectively reduced in Fe-deficient plants.

We also observed a slight induction in the activity of Cu/Zn-SOD isoform whereas, in the same experimental conditions, we saw a reduction in Fe- and also in Mn-SOD isoform activity. These findings are quite in accordance with studies already performed on plants grown in Fe-deprived conditions, which showed higher SOD activity, mainly due to increased

Cu/Zn-SOD or Mn-SOD isoforms (Iturbe-Ormaeche et al. 1995, Molassiotis et al. 2006, Donnini et al., 2012).

Fe deficiency also induces alterations in peroxisomes, indicating alterations in the photorespiratory metabolism at different levels. Using a new purification method described by Reumann et al., (2007, 2009, 2014) for leaf peroxisomes with some modifications, we were able to isolate peroxisomes from mature leaves in high purity in order to perform the biochemical characterization of these organelles. The activity of one of the principal enzymes of the peroxisomal metabolism, catalase, results to be greatly compromised (-35%) in condition of Fe deficiency: this is probably due to the lack of the element in the tissues, since catalase uses it as a cofactor (Fe is contained in the heme group). Recent studies (Shibata et al., 2013; Sinclair et al., 2009) report that the accumulation of inactive catalase in peroxisomes triggers an aggregation process that mediates their subsequent degradation through autophagy, in a process mediated by the consequent accumulation of H₂O₂ which was observed in the leaves of cucumber Fe-deficient plants. On the contrary, the activity of Fe-independent enzyme glycolate oxidase does not show significant changes in the various experimental conditions tested, probably this was due to the great variability inherent in the analytical method. No variation in quantity of the protein was also observed in the western blot analysis conducted. Furthermore, the hydroxypyruvate reductase do not change its total activity, sharing its equally distribution between the peroxisomal and the cytosolic isoform under Fe-deficiency. This behaviour could be the consequence of an alteration of the redox state of the peroxisome caused by a slowdown in the reaction of malate dehydrogenase, due to a reduction in the malic acid content, which recycles NADH inside the peroxisome. NADH is the

intermediate required by hydroxypyruvate reductase in the reduction reaction of hydroxypyruvate. The Fe-deficient plants could then bypass this lack of reducing power by a major activation of the cytosolic isoform to reduce hydroxypyruvate present. Up to date, however, the membrane transporters responsible for the movement of the photorespiratory intermediate among the different cellular compartments involved in photorespiration have not yet been identified and characterized, so we can not exclude that this different distribution of tasks between the two isoforms is attributable to an increased activity of the transporter that moves the hydroxypyruvate outside peroxisomes.

Moreover, the characterization of rice mutant plants defective in mitochondrial Fe importer may represents a useful tool to investigate their specific involvement in the regulation of nuclear gene expression and the involvement of this organelle in the photorespiratory metabolism during Fe deficiency, also considering the previously suggested role of these organelle in Fe sensing and signaling pathways in plant cells (Vigani et al., 2009; 2013). The partial loss of function of MIT (*mit-2*) affects the mitochondrial functionality by decreasing the respiratory chain activity. Furthermore, the transcriptome and the metabolome patterns strongly change in rice mutant plants, in a different way (at a different extent) in root and shoot. In particular, proteins belonging to the type II alternative NAD(P)H dehydrogenases strongly accumulated in *mit-2* plants, indicating that *mit-2* mitochondria activate alternative pathways to keep the respiratory chain working.

Analyzing the transcriptomic data of the *mit-2* plants, a strong alteration (up/down regulation) in the expression of genes encoding enzymes of both primary and secondary metabolism was found. In line with these changes, the metabolite profiles significantly changed both in roots and shoots of *mit-2* plants,

e.g. leading to alterations in the levels of amino acids belonging to the aspartate-related pathways (aspartate, lysine, threonine in roots and aspartate, ornithine in shoots) that are strictly connected to the Krebs cycle. Furthermore, some metabolites (for instance pyruvate, fumarate, ornithine and oligosaccharides of the raffinose family) accumulated only in shoot of mit-2 plant, indicating possible hypoxic responses. These findings suggest that the induction of local Fe deficiency in mitochondrial compartment of mit-2 plants differentially affects the transcriptome as well as the metabolite profile in root and shoot tissues.

References.

Abadía, J., Morales, F., Abadía, A. (1999): Photosystem II efficiency in low chlorophyll, iron-deficient leaves. *Plant Soil* 215, 183–192.

Andersson B., Aro E.M., Photodamage and D1 Protein Turnover in Photosystem II, *Advances in Photosynthesis and Respiration* Vol 11 pp 377-393

Bestwick, C.S., I.R. Brown and J.W. Mansfield. 1998. Localized changes in POD activity accompany hydrogen peroxide generation during the development of a non-host hypersensitive reaction in lettuce. *Plant Physiol.* 118:1067–1078.

Borlotti et al.: Iron deficiency affects nitrogen metabolism in cucumber (*Cucumis sativus* L.) plants. *BMC Plant Biology* 2012 12:189.

Briat, J.F., Curie C., Gaymard F., Iron utilization and metabolism in plant, *Current Opinion in Plant Biology* (2007), 10:276–282

Donnini S., Castagna, A., Guidi, L., Zocchi, G., Ranieri, A. (2003): Leaf responses to reduced iron availability in two tomato genotypes: T3238FER (iron efficient) and T3238fer (iron inefficient). *J. Plant Nutr.* 26, 2137–2148.

Donnini S., Dell'Orto M., Zocchi G., (2012) Oxidative stress responses and root lignification induced by Fe deficiency conditions in pear and quince genotypes, *Tree Physiology* 31, 102–113,

Houtz R.L., Stanley K. Ries and N. E. Tolbert, Effect of Triaccontanol on *Chlamydomonas* II. Specific Activity of Ribulose-Bisphosphate Carboxylase/Oxygenase, Ribulose-Bisphosphate Concentration, and Characteristics of Photorespiration; *Plant Physiology* (1985) vol. 79 no. 2 365-370.

Iturbe-Ormaeche, I., J.F. Moran, C. Arrese-Igor, Y. Gogorcena, R.V. Klucas and M. Becana. 1995. Activated oxygen and antioxidant defenses in iron deficient pea plants. *Plant Cell Environ.* 18:421–429.

Jelali, N., Salah, I. B., M'sehli, W., Donnini, S., Zocchi, G.,

Gharsalli, M. (2011): Comparison of three pea cultivars (*Pisum sativum*) regarding their responses to direct and bicarbonate-induced iron deficiency. *Sci. Hort.* 129, 548–553.

Lu D., Wang T., Persson S., Mueller-Roeber M. Schippers J.H.M.; Transcriptional control of ROS homeostasis by KUODA1 regulates cell expansion during leaf development, *NATURE COMMUNICATIONS* 5:3767

Molassiotis, A., Tanou, G., Diamantidis, G., Patakas, A., Therios, I. (2006): Effects of 4-month Fe deficiency exposure on Fe reduction mechanism, photosynthetic gas exchange, chlorophyll fluorescence and antioxidant defense in two peach rootstocks differing in Fe deficiency tolerance. *J. Plant Physiol.* 163, 176–185.

Morales, F., Belkhodja, R., Abadia, A., Abadia, J. (2000): Photosystem II efficiency and mechanisms of energy dissipation in iron deficient, field grown pear trees (*Pyrus communis* L.). *Photosynth. Res.* 63, 9–21.

Quintero-Gutiérrez A.G., González-Rosendo G., Sánchez-Muñoz J., Polo-Pozo J., Rodríguez-Jerez J.J. Bioavailability of heme iron in biscuit filling using piglets as an animal model for humans. *Int J Biol Sci.* (2008); 4:58–62.

Reumann S., Babujee L., Ma C. et al. (2007) Proteome analysis of Arabidopsis leaf peroxisomes reveals novel targeting peptides, metabolic pathways, and defense mechanisms. *Plant Cell* 19:3170–3193

Reumann S., Quan S., Aung K. et al. (2009) In-depth proteome analysis of Arabidopsis leaf peroxisomes combined with in vivo subcellular targeting verification indicates novel metabolic and regulatory functions of peroxisomes. *Plant Physiol* 150:125–143

Reumann S. and Singhal R., Isolation of Leaf Peroxisomes from Arabidopsis for Organelle Proteome Analyses, in Jorriñ-Novo J.V. et al. (eds.), *Plant Proteomics: Methods and Protocols, Methods in Molecular Biology*, vol. 1072,

Romero-Puertas, M.C., M. Rodríguez-Serrano, F.J. Corpus, M. Gomez and L.A. del Rio. 2004. Cadmium-induced subcellular accumulation of O₂⁻ and H₂O₂ in pea leaves. *Plant Cell Environ.*

Shibata M., Oikawa K., Yoshimoto K., Kondo M., Mano S., Yamada K., Hayashi M., Sakamoto W., Ohsumi Y., and Nishimura M., Highly Oxidized Peroxisomes Are Selectively Degraded via Autophagy in *Arabidopsis*; *The Plant Cell*, Vol. 25: 4967–4983, December 2013

Sinclair A.M., Trobacher C.P., Mathur N., Greenwood J.S., Mathur J., Peroxule extension over ER-defined paths constitutes a rapid subcellular response to hydroxyl stress, *Plant J*, 59 (2009) 231-242.

Thomine, S.; Vert G., Iron transport in plants: better be safe than sorry, *Current Opinion in Plant Biology* 2013, 6:322–327

Vose P.B., Iron nutrition in plants: a world overview, *Journal of Plant Nutrition*, Volume 5, issue 4-7, 1082

Vigani G, Maffi D, Zocchi G. 2009. Iron availability affects the function of mitochondria in cucumber roots. *New Phytologist* 182, 127-136.

Vigani G, Zocchi G, Bashir K, Philippar K, Briat J-F. 2013. Signals from chloroplasts and mitochondria for iron homeostasis regulation. *Trends in Plant Science* 18, 305-311.

Wingler A., Lea P.J. , Quick P.W. and Leegood R.C.; Photorespiration: metabolic pathways and their role in stress protection, *Phil. Trans. R. Soc. Lond. B* (2000) 355, 1517-1529

APPENDIX A

Trascriptomic investigation data

Introduction

One of the achievements of these three years doctorate course was also the investigation of the transcriptomical changes induced in the photorespiratory metabolism in plants under different iron (Fe) bioavailability during their growth. However, a research thorough specific literature allowed us to find several information and data concerning these alterations. For this reason, during the Ph.D. we gathered, crossed and revised the data found in different papers to develop a series of charts on transcriptomic changes induced by Fe deficiency. We grouped the genes on the basis of their presumed physiological function. The most interesting results are illustrated in the graphs below.

Results

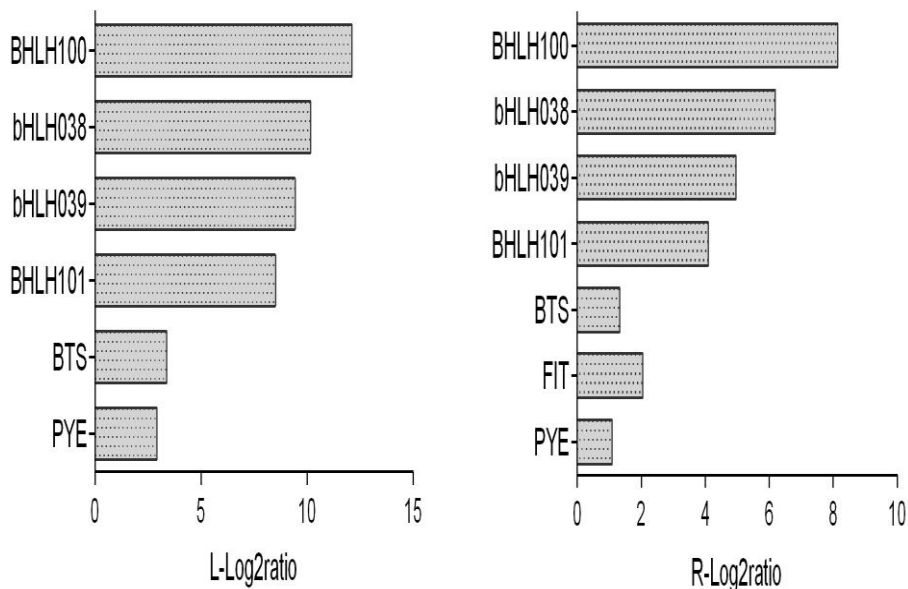


Figure A.1 Variation in the expression of transcription factors (TF) involved in the response to Fe deficiency that vary in leaves (left) or roots (right) of Fe-deficient *Arabidopsis thaliana*. (Yang et al., 2010; Schuler et al. 2011; Rodriguez-Celma et al., 2013). bHLH100 basic helix-loop-helix DNA-binding superfamily protein 100; bHLH038 basic helix-loop-helix DNA-binding superfamily protein 038; bHLH039 basic helix-loop-helix DNA-binding superfamily protein 039; bHLH101 basic helix-loop-helix DNA-binding superfamily protein 101; BTS zinc-finger protein-related BRUTUS; FIT FER-like regulator of Fe uptake. PYE basic helix-loop-helix (bHLH) DNA-binding superfamily protein POPEYE.

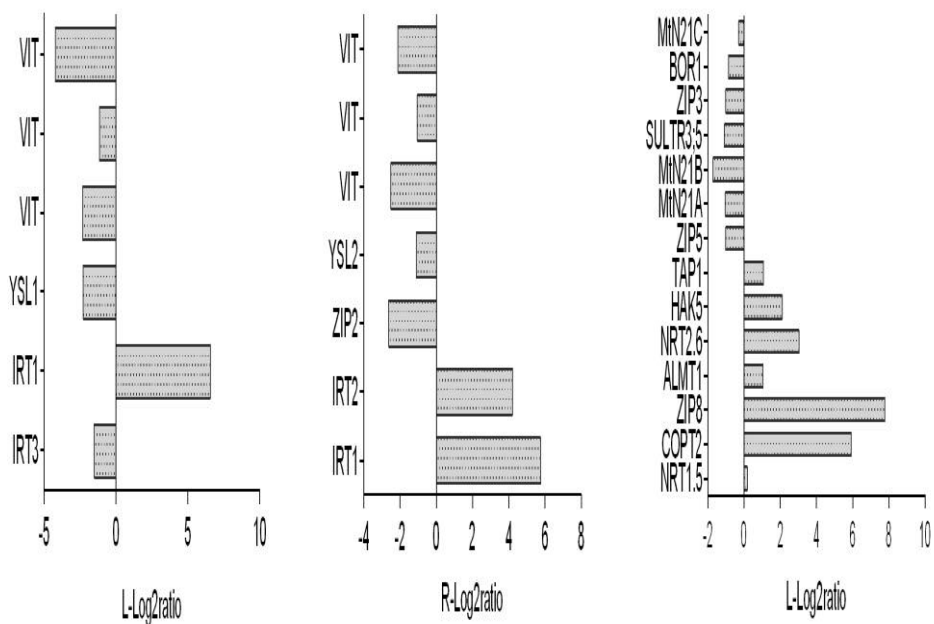


Figure A.2 Variation in the expression of mineral transporters involved in the response to Fe deficiency that vary in leaves (left); variation in the roots of the same transporter showed on the left sheets (center); variation of transporters in the roots (right) of Fe-deficient *Arabidopsis thaliana*. (Yang et al., 2010; Schuler et al. 2011; Rodriguez-Celma et al., 2013). IRT1; IRT3: Iron-Regulated-Transporter, YSL1; YSL2 yellow-strip-like transporter. VIT Vacuolar iron transporter family protein. NRT1.5 nitrate transporter; COPT2 copper transporter; ZIP8 Zinc transporter precursor; ALMT1 Aluminium activated malate transporter family protein; NRT2.6 high affinity nitrate transporter; HAK5 high affinity potassium transporter; TAP1 transporter associated with antigen processing protein 1; ZIP5 zinc transporter 5 precursor; MtN21 A; MtN21B; MtN21C nodulin MtN21 /EamA-like transporter family protein; SULTR3:5 sulfate transporter 3;5; ZIP3 zinc transporter 3 precursor; BOR1 HCO_3^- transporter family.

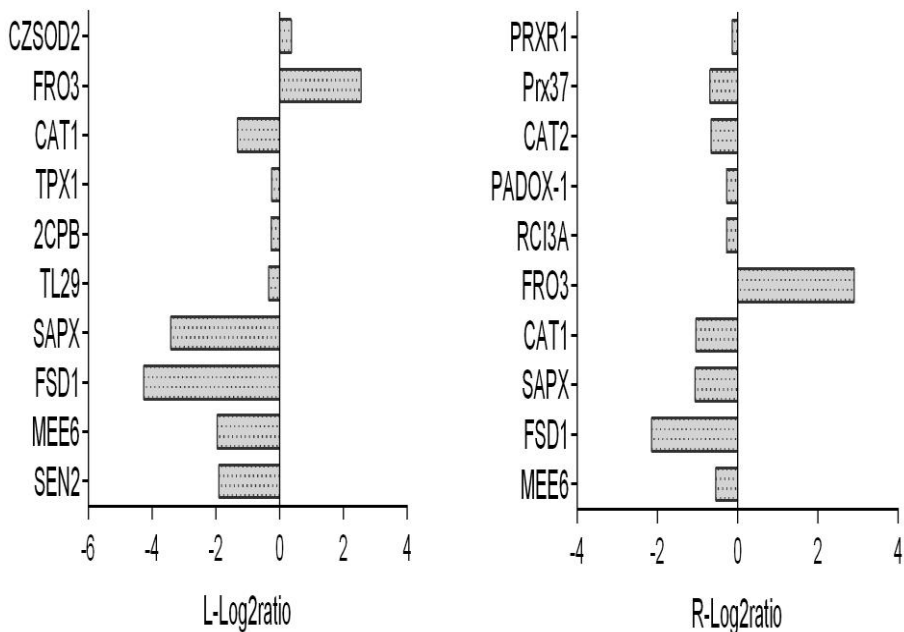


Figure A.3 Variation in the expression of genes involved in the response to oxidative stress that changes under Fe-deficient condition. Variation in the leaves (left) or in the roots (right) of *Arabidopsis thaliana* (Yang et al., 2010; Schuler et al. 2011; Rodriguez-Celma et al., 2013). SEN2 catalase 3; MEE6 ascorbate peroxidase 1; FSD1 Fe superoxide dismutase 1; SAPX stromal ascorbate peroxidase; TL29 ascorbate peroxidase 4; 2CPB 2-cysteine peroxiredoxin B; TPX1 thioredoxin-dependent peroxidase 1; CAT1 catalase 1; FRO3 ferric reduction oxidase; 3CZSOD2 Cu/Zn superoxide dismutase 2.

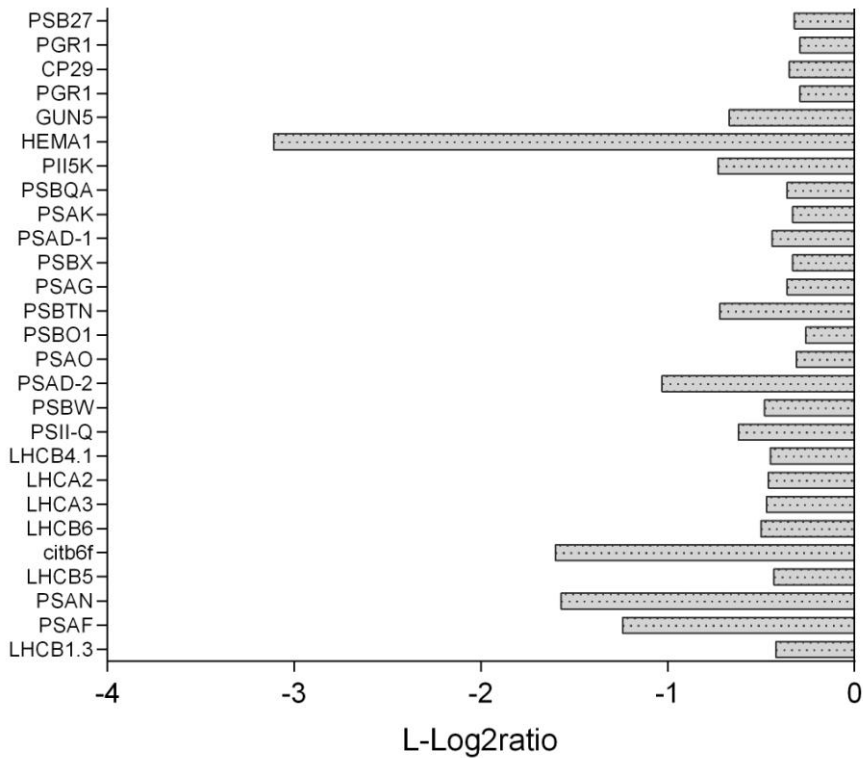


Figure A.4 Variation in the expression of genes belonging to the photosynthetic machinery that changes under Fe-deficient condition that vary in leaves of *Arabidopsis thaliana* (Yang et al., 2010; Schuler et al. 2011; Rodriguez-Celma et al., 2013). LHCB1.3 chlorophyll A/B binding protein 1; PSAF photosystem I subunit F; PSAN photosystem I reaction center subunit; PSI-N chloroplast, putative/ PSI-N, putative (PSAN); LHCB5 light harvesting complex of photosystem II 5; CITB6F cytochrome b6f complex subunit (petM), putative; LHCB6 light harvesting complex photosystem II subunit 6; LHCA3 photosystem I light harvesting complex gene 3; LHCA2 photosystem I light harvesting complex gene 2; LHCB4.1 light harvesting complex photosystem II; PSII-Q photosystem II subunit Q-2; PSBW photosystem II reaction center W; PSAD-2 photosystem I subunit D-2; PSAO photosystem I subunit O; PSBO1 PS II oxygen-evolving complex 1; PSBTN photosystem II subunit T; PSAG photosystem I subunit G; PSBX photosystem II subunit X; PSAD-1 photosystem I subunit D-1; PSAK; photosystem I subunit K; PSBQA photosystem II subunit QA; PII5K Photosystem II 5 kD protein; EMA1 Glutamyl-tRNA reductase family protein; GUN5 magnesium-chelatase subunit chlH, chloroplast, putative /

Mg-protoporphyrin IX chelatase, putative (CHLH); PGR1 photosynthetic electron transfer C; CP29 chloroplast RNA-binding protein 29; PGR1 photosynthetic electron transfer C; PSB27photosystem II family protein.

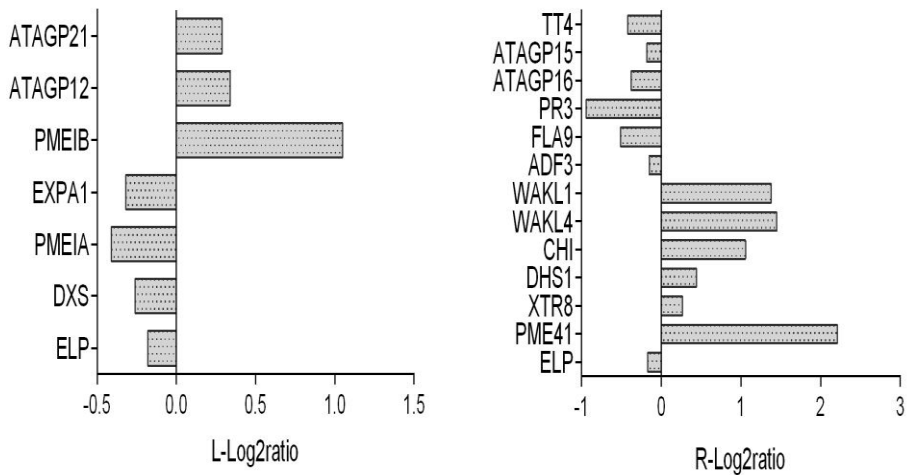


Figure A.5 Variation of the expression of genes related to secondary and cell wall metabolism in leaves (left) and roots (right) of Fe-deficient Arabidopsis. (Yang et al., 2010; Schuler et al. 2011; Rodriguez-Celma et al., 2013). ELP extensin-like protein; DXS Deoxyxylulose-5-phosphate synthase; PMEIA Plant invertase/pectin methylesterase inhibitor superfamily protein; EXPA1 expansin A1; PMEIB Plant invertase/pectin methylesterase inhibitor superfamily; ATAGP12 arabinogalactan protein 12; ATAGP21 arabinogalactan protein 21; PME41 Plant invertase/pectin methylesterase inhibitor superfamily.

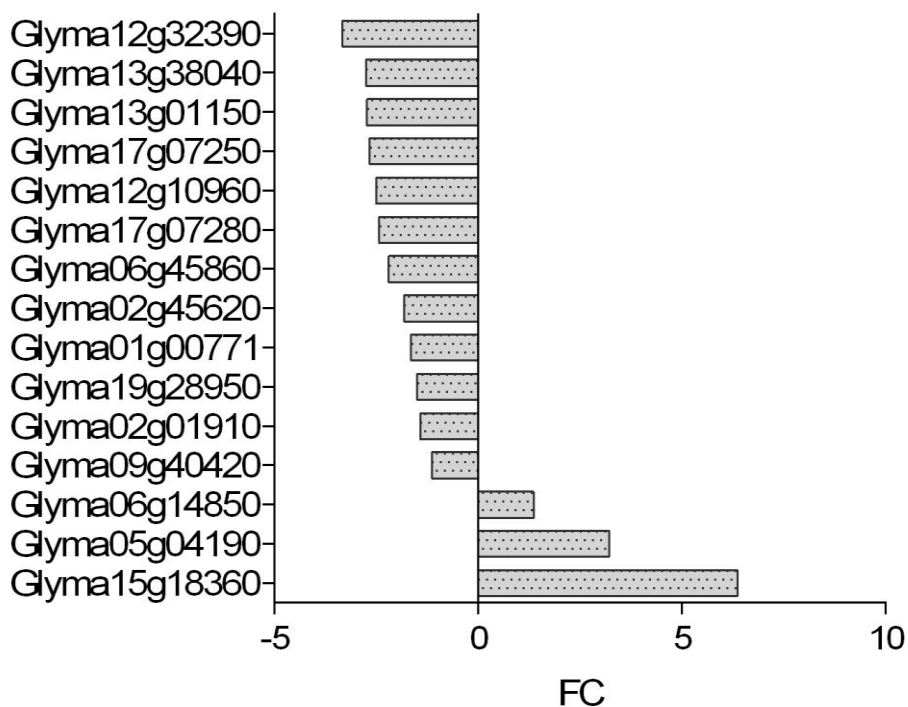


Figure A.6 Variation of the expression of genes related to secondary and cell wall metabolism in leaves of *Glycine max* after 6h of Fe-deficiency. (Moran-Lauter et al., 2014). Glyma15g18360 Xyloglucan endotransglycosylase; Glyma05g04190 Pectinesterase; Glyma06g14850 Expansin 2 (Fragment); Glyma09g40420 Fasciclin-like arabinogalactan protein; Glyma02g01910 Polygalacturonase, putative; Glyma19g28950 Arabinogalactan peptide 14; Glyma01g00771 Arabinogalactan peptide 20; Glyma02g45620 Pectinesterase; Glyma06g45860, Glyma17g07280, Glyma12g10960, Glyma17g07250, Glyma13g01150, Glyma13g38040, Glyma12g32390 Xyloglucan endotransglucosylase/hydrolase protein.

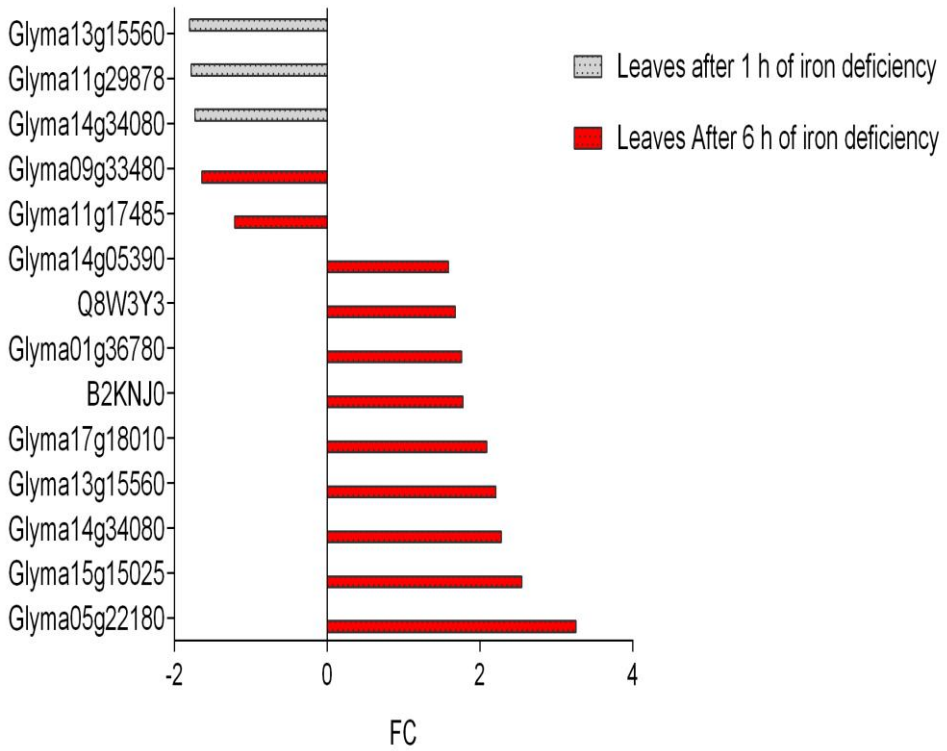


Figure A.7 Variation of the expression of genes in leaves of *Glycine max* after 1h (grey) or after 6h (red) of Fe-deficiency. (Moran-Lauter et al., 2014). Glyma05g22180 Peroxidase2 Glyma15g150254 Fe-4S ferredoxin, iron-sulfur binding; Glyma14g34080 Photosystem II D1 protein; Glyma13g15560 Photosystem Q(B) protein; Glyma17g18010 Ferrous ion membrane transport protein; B2KNJ0 S-adenosylmethionine decarboxylase; Glyma01g36780 Peroxidase (Fragment); Q8W3Y3 1-aminocyclopropane-1-carboxylic acid oxidase; Glyma14g05390 1-aminocyclopropane-1-carboxylic acid oxidase; Glyma11g17485 Photosystem II protein I; Glyma09g33480 Serine hydroxymethyltransferase; Glyma14g34080 Photosystem II D1 protein (Fragment); Glyma11g29878; PsbA (Fragment); Glyma13g15560 Photosystem Q(B) protein.

References

Moran Lauter A.N., Peiffer G.A., Yin T., Whitham S.A., D. Cook,^[ORCID] Shoemaker R.C. and Graham M.A.; Identification of candidate genes involved in early iron deficiency chlorosis signaling in soybean (*Glycine max*) roots and leaves; *BMC Genomics* 2014, 15:702

Schmutz J., Cannon S.B., Schlueter J., Ma J., Mitros T., Nelson W., Hyten D.L., Song Q., Thelen J.J., Cheng J., Xu D., Hellsten U., May G.D., Yu Y., Sakurai T., Umezawa T., Bhattacharyya M.K., Sandhu D., Valliyodan B., Lindquist E., Peto M., Grant D., Shu S., Goodstein D., Barry K., Futrell-Griggs M., Abernathy B., Du J., Tian Z., Zhu L., Gill N., Joshi T., Libault M., Sethuraman A., Zhang X.C., Shinozaki K., Nguyen H.T., Wing R.A., Cregan P., Specht J., Grimwood J., Rokhsar D., Stacey G., Shoemaker R.C., Jackson S.A., Genome sequence of the palaeopolyploid soybean., *Nature*. 2010 Jan 14; 463 7278 178-83

Schuler M., Andreas Keller A., Backes C., Philippar K., Lenhof H.-P. and Bauer P.; Transcriptome analysis by GeneTrail revealed regulation of functional categories in response to alterations of iron homeostasis in *Arabidopsis thaliana*; *BMC Plant Biology* 2011, 11:87

A.-F., and Schmidt W.; Mutually Exclusive Alterations in Secondary Metabolism Are Critical for the Uptake of Insoluble Iron Compounds by *Arabidopsis* and *Medicago truncatula*; *Plant Physiology*, July 2013, Vol. 162, pp. 1473–1485,

Yang T.J.W., Lin W.-D., and Schmidt W.; Transcriptional Profiling of the *Arabidopsis* Iron Deficiency Response Reveals Conserved Transition Metal Homeostasis Networks; *Plant Physiology*, April 2010, Vol. 152, pp. 2130–2141